PROPERTIES AND APPLICATIONS OF POLYETHER SALT COMPLEXES

by

E.G. HARRISON

Supervisor: Dr. R.E. Wetton

A doctoral thesis submitted in partial fulfilment of the requirements for the award of the Degree of Doctor of Philosophy of Loughborough University of Technology.

September 1984

Department of Chemistry

To Kathleen for showing more patience and understanding than I would ever have thought possible in one person.

ACKNOWLEDGEMENTS

The author would like to thank Dr. R.E. Wetton for his supervision and ideas throughout this work. Thanks are also due to Professor F.W. Wilkinson for the use of laboratory facilities, and to the Science and Engineering Research Council and Polymer Laboratories Limited for the award of a C.A.S.E. studentship.

Thanks are due to the technical staff of this Department for practical assistance, and in particular to Mr. A.F. Bower and Mr. A.G. Stevens for their help.

Finally I would like to thank Mrs. B. Macfarlane for her efficient, speedy and accurate typing of this thesis.

ORIGINALITY

The work presented in this thesis has been carried out by the author, except where otherwise acknowledged, and has not previously been submitted to this University or any other institution for a higher degree.

ABSTRACT

The physical properties of polyethers have been modified by complexation with inorganic salts. The cation is bound to the polyether oxygen atoms to produce a single phase polymer-salt solution. The salts chosen were generally from the alkali and alkaline earth metals but other salt systems were investigated.

It was observed, using the technique of differential thermal analysis, that the complexes gave single, well defined, glass transitions which occurred at temperatures higher than the uncomplexed polymer.

High dielectric losses and constants were observed in dielectric measurements at audio and low radio frequencies. Conventional dielectric theories have been applied to these complexes and were found to be consistent with the formation of a complex between the polymer and the inorganic salt. Ionic conduction was observed above the glass transition temperature.

Viscosity measurements were obtained using a cone and plate viscometer. The results obtained revealed similar trends to those observed in the glass transition results above an initial concentration of salt.

The data obtained has been explained in terms of two models. When it is energetically favourable the inorganic salts are coordinated to the polyether in chelate structures involving two or three adjacent oxygen atoms. When steric hindrance or the formation of energetically unfavourable seven-membered rings are involved, a cage structure involving several oxygen atoms is proposed.

The polyether complexes prepared were blended with low dielectric

constant material with the intention of improving their dielectric heating capability. Although some improvement was recorded, insufficient dielectric enhancement by the salt complexes in highly active dielectric heating systems (EVA, PVC) were recorded. However polymers that do not normally dielectric heat seal have been converted to heat sealable materials upon blending with salt complexes.

Future commercial developments including applications as capacitors, solid electrolytes and electrets have been discussed.

CONTENTS

CONTENTS (Continued)

CONTENTS (Continued)

LIST OF TABLES

1.0 INTRODUCTION

1.1 The study of the electrical properties of polymers is well-established. Figure 1.1 illustrates succinctly the position polymers generally have in the scale of conductivity of materials. However, this image is changing. For many years conductive fillers have been added to polymers to improve their electrical conductivity. Most polymers are inherently insulating in character resulting in the build-up of static charge on surfaces. This is potentially an explosive situation which has led to the incorporation of a heterogenous conductive filler[1] or chemical antistatic agents[2] to alleviate the risk. Obviously materials to be used as conductive fillers have come from the highly conductive materials in general; metal powders, carbon blacks and graphites. The shape and size of such inclusions together with the degree of inter-particle spacing and the nature of the substrate/filler contact, and/or particle-particle contact, all influence the overall conductivity.[3]

As fillers influence the electrical properties so they also affect the mechanical properties, often to the detriment of the designed polymer system, resulting in the need for an inherently conductive material that is lightweight, cheap, easy to process and flexible. For a system to conduct electricity either ions or electrons must move. In the latter case, for this situation to exist, sufficient overlap of the molecular orbitals must exist between neighbouring molecules which themselves have delocalised electronic molecular orbitals. The following examples indicate possible schematic solutions to meet these requirements.

(a) Conjugated Chains

By far the most studied of the specified solutions are the alternately saturated, unsaturated, backbone chains as illustrated below.

Figure 1,1

Chart of typical conductivities

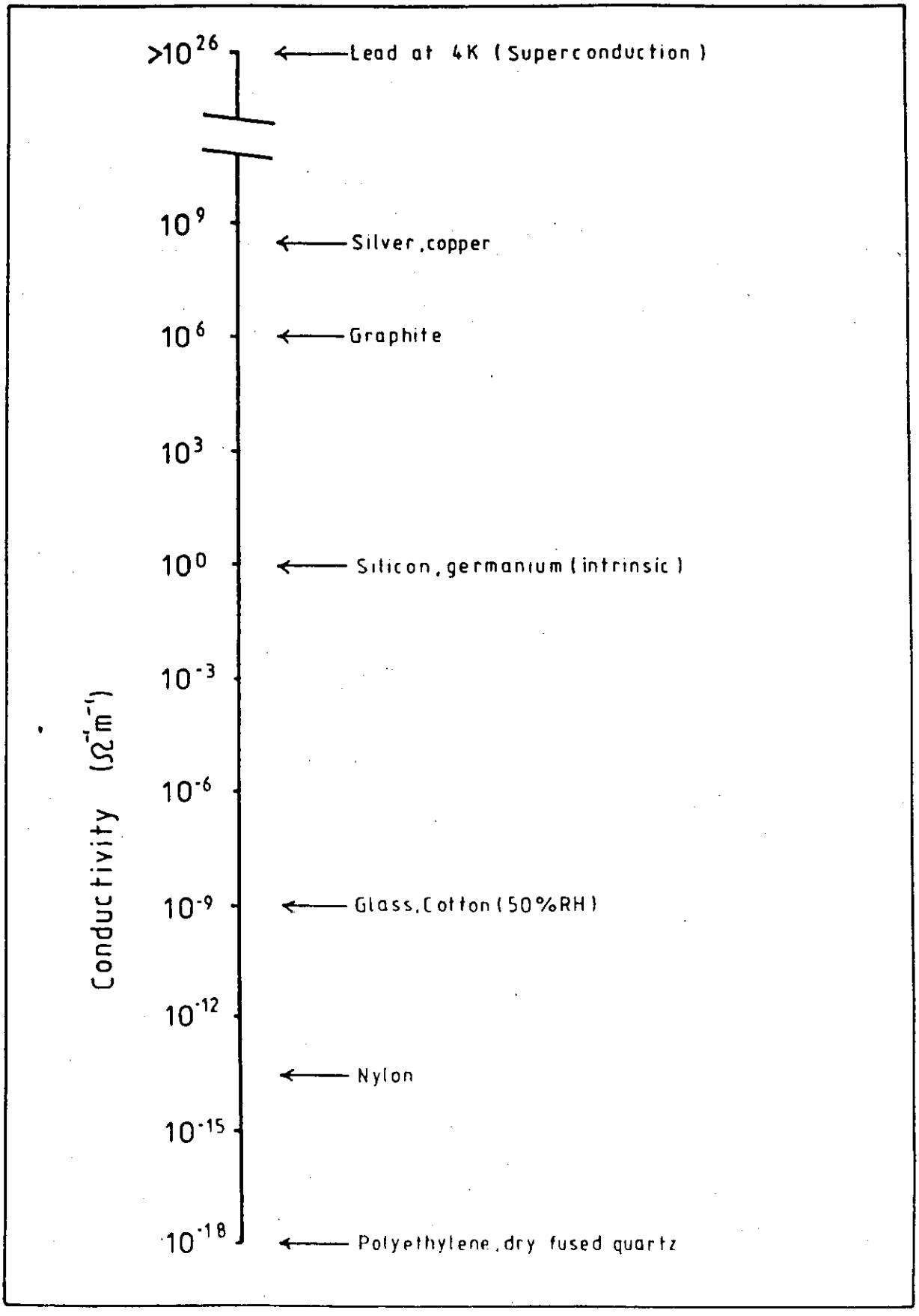

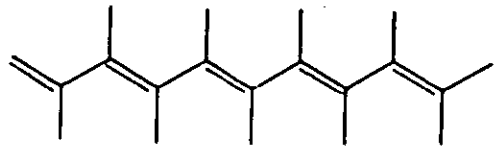

The π-orbitals can be delocalised along the whole backbone (cf the π-orbitals in a benzene ring) to form a 'valence band' capable of metallic conduction. Although the activation energy of conduction is low in such systems and thus the conductivities should be high, this is not always achieved. To achieve the theoretical high conductivities stereoregular highly crystalline polymers must be made. As will be seen later planar molecules present their own set of mechanical problems. Depressing the theoretically possible high conductivities are two factors. Firstly, Jahn-Teller stabilisation, which produces a system of alternating long and short bonds and thus a variation of delocalisation distance and activation energy. Secondly, rotation about any of the bonds reduces overlap and breaks the conjugation; for conjugation to exist over a long range the molecules must remain planar. Shirakawa and Ikeda[4] observed values of resistivities up to 10 $(\Omega\,cm)^{-1}$ with thin films of trans poly(acetylene) as opposed to values less than 10^{-10} $(\Omega\,cm)^{-1}$ for poly (phenyl acetylene) in which steric hindrance prevents adoption of a planar conformation.

To overcome the problem of maintaining a planar configuration 'ladder-type' polymers have been developed. Characteristic of these are the poly (acene quinone radical) (PAQR) polymers[5,6] which have the general structure

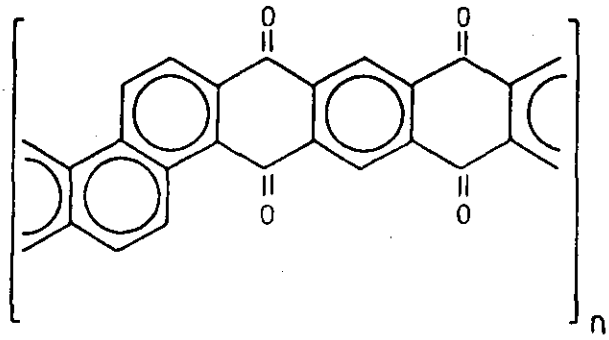

Conductivities in the range 10^{2} to 10^{-5} $(\Omega\,cm)^{-1}$ have been noted but as with many of these planar compounds are intractable and suffer from imperfect bonding. Theoretically large sheets of fused rings should produce the ultimate in such systems as in the case of 'Black Orlon'[7]. This is a pyrolised poly(acrylonitrile).

desired shape resulting in conductivities of ≈ 10 $(\Omega cm)^{-1}$.

(b). Charge Transfer Complexes

A charge-transfer complex is formed when an electron is partially transferred from a donor molecule of low ionisation potential to an acceptor molecule of high affinity.

$$D + A \longrightarrow D^{\delta+} \; A^{\delta-}$$

A radical ion (i.e. an ion carrying an odd number of electrons) would result if an electron were completely transferred.

Pyrene and iodine, conductivities 10^{-10} $(\Omega\,cm)^{-1}$ and $10^{-5}(\Omega\,cm)^{-1}$ respectively, react to form a complex with a conductivity of $10^{2}(\Omega cm)^{-1}$

The conduction is very directional, being greatest along the direction of the stacks. The stacks are formed by the way the complex packs. Charge transfer complexes having the donating species attached to the polymer backbone have been reported, for example poly(phenylene)-iodine[8] ($10^4(\Omega\ cm)^{-1}$) and poly(vinyl-anthracene)-iodine[9] ($10^6(\Omega\ cm)^{-1}$). Much of the research directed towards obtaining a conductive material from a charge transfer complex has been centred on the compound 7,7,8,8 tetra cyano quinodimethane (TCNQ)[10], a very strong electron acceptor, capable of firstly forming a radical anion and then the dianion.

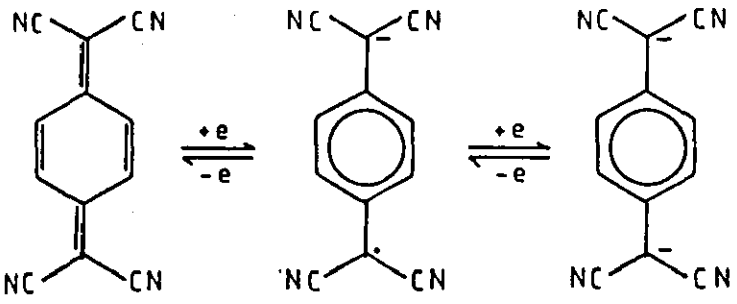

TCNQ is capable of forming either a charge transfer complex or a radical -ion salt. The lithium salt Li^+ TCNQ shows conductivity of $10^{-1}\ (\Omega\ cm)^{-1}$, even higher values have been observed with some organic cations[3], e.g.

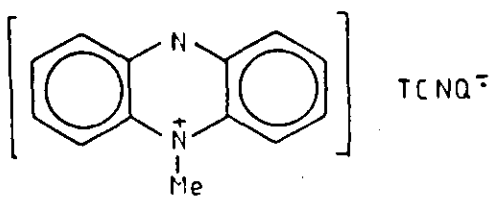

N-methyl phenazinium TCNQ, conductivity $\approx 10^{6}(\Omega\,\mathrm{cm})^{-1}$.

Under certain conditions TCNQ may form both simple and complex salts, the latter containing an extra equivalent of neutral TCNQ and showing greater conductivity.

The success in obtaining polymeric versions of TCNQ complexes has been limited. The simplest approach utilising polymeric cations (ideally with some aromatic nature). Examples [11,12] include poly(2-vinyl pyridine), poly(vinyl methyl imadazole) and poly(1-methyl 2-vinyl pyridine). To obtain the correct conformation in the solid state to allow the necessary face to face stacks for electron transfer between the associated TCNQ units has only found limited success. Conductivities of $10^{2}(\Omega\mathrm{cm})^{-1}$ have, however, been reported.[4]

Examples of radical cation systems also exist; these have been based on a family of heterocyclic compounds known as violenes. An example is tetrathiafulvalene (TTF)

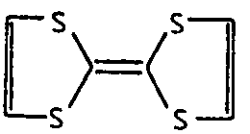

whose compound with TCNQ shows very high conductivities ($10^{7}(\Omega\,\mathrm{cm})^{-1}$).

Rosseinsky et al.[13] have grown single crystals by anodic electrocrystallisation of adducts containing tetrathiafulvalene with inorganic and organic anions. The crystals are unidimensionally metallic non-stoichiometric adducts. Conductivities between 10^{-3} and 20 $(\Omega\,\mathrm{cm})^{-1}$ have been recorded. Further work by Rosseinsky et al.[14] using galvonostatic control (constant current) rather than electrocrystallisation has produced even higher conductivities, up to 500 $(\Omega\,\mathrm{cm})^{-1}$ for a tetrathiatetracene nitrate adduct.

Similar adducts [15] have been grown by cathodic electrocrystallisation from tetracyanoquino-dimethane (TCNQ) in the presence of metal salts. Conductivities of copper TCNQ adducts varied from 10^{-5} to 800 $(\Omega\,cm)^{-1}$.

(c) Organometallic Compounds

When an organometallic group is introduced into polymers electronic conduction is enhanced. The metal d orbitals can overlap with the π orbitals of the organic structure, extend the delocalisation and act as bridges to adjacent molecules. Dewar and Talata[16] obtained conductivities up to 1 $(\Omega\,cm)^{-1}$ for the polymeric complex of Cu II with 1, 5 diformyl - 2, 6 - dihydroxy naphthalene dioxime.

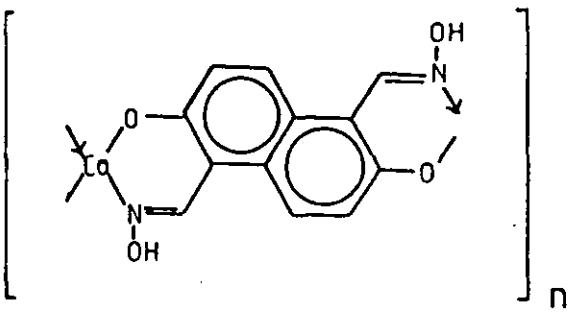

They are similar to compounds previously described in that they have poor mechanical properties.

1.2 Objectives and Scope of Present Work

It has been shown in the previous section that donor/acceptor complexes although rendering high conductivity, in general, showed poor mechanical properties.

The donation of electrons from a non-bonding orbital, containing electrons on a suitable atom, e.g. oxygen, sulphur or nitrogen to a

vacant orbital on the metal atom (normally a hybrid of the available s, p and d orbitals) occurs commonly in organic chemistry. Examples are the interaction between anions of acetyl acetone and salicyl-aldehyde and metal compounds.[17,18] Such coordination compounds are often used in organic synthetic routes.[19]

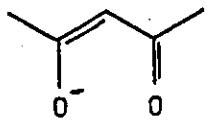

acetyl acetone I

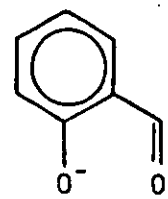

salicylaldehyde II

The bonds formed are essentially covalent showing some ionic character, the degree of which is a reflection on the difference in electronegativity between the metal and the ligand atoms. The ability of a liquid to bestow covalent character to a bond which it forms with a metal is frequently termed the donor strength and reflects the ability to increase the electron density on the metal. Very few references exist for such analogous complexes in which a polymer or part thereof acts as the donor.[20]

Davydova[21] has considered the parameters involved in complex formation by polymers, concluding that the efficiency of complex formation is affected by the distribution of ligands along, and their position relative to the main chain. Also, that the conformation of the ligand will also be a limiting factor. If a conformational difference occurs between the metal ion and the ligand then a conformational change must take place if complexation is to occur. Davydova also noted that as in the case of low molecular weight substances chelation enhances complexation especially so if the energetically favourable 5 or 6 membered ring is formed. Suitable donors may be found in O, S and N containing polymers such as poly(ethers), poly(thio ethers), poly (amides), poly(vinyl pyridines), etc.

The work presented in this thesis is a study of the complexation of inorganic salts with poly(ethers). It is a continuation of two research projects undertaken at Loughborough University. D.B. James[22] studied the physical properties of metal salt complexes of low and high molecular weight poly(propylene oxide). Using techniques such as DTA and X-ray scattering he found a large positive shift in the values of Tg and that the complexes were amorphous single phase elastomers. Dielectric measurements revealed high values for dielectric loss and storage. He concluded that the results could be interpreted in the form of a chelate ring involving the coordination of two adjacent oxygens in the polymer backbone to the metal salt. Such a model could be regarded as a copolymer of complexed and uncomplexed monomer units.

A.M. Rowe[23] investigated the properties of salt complexes of poly(vinyl alcohol), poly(methyl vinyl ether) and poly(ethyl vinyl ether). Two models were proposed, depending on the steric hindrance of the side groups and the ability of the salt to accept donor electrons. For systems where the steric hindrance is low and the acceptor power of the salt is high, a model similar to that of James[19] was proposed. When the converse occurred a cage structure was proposed whereby the cation is surrounded by four ethereal oxygen atoms.

Principally the series poly(formaldehyde), $(CH_2 - O)_n$; poly (ethylene oxide), $(CH_2 - CH_2 - O)_n$, poly(propylene oxide), $\{ CH_2 - \underset{\displaystyle CH_3}{\underset{|}{CH}} - O)_n$; poly(tetramethylene oxide, $-(CH_2 - CH_2 - CH_2 - CH_2 - O)_n$; together with two vinyl ethers poly(methyl vinyl ether) $-(CH_2 - \underset{\displaystyle O-CH_3}{\underset{|}{CH}} -)_n$

$-(CH_2 - \underset{\displaystyle O - CH_2 - CH_3}{\underset{|}{CH}} ----------)_n$

The variation in distance between ethereal oxygens and the degree of steric hindrance were the underlying reasons for the choice of polymers. All the polymers are commercially available and readily soluble in polar organic solvents.

The choice of salts was determined primarily for their solubility in polar organic solvents, such as ketones, ethers and alcohols and being known to form stable complexes with a wide range of ligands.[17,18] As will be described later the solubility in such solvents was a pre-requisite of the method of preparation employed. Other salts were chosen in an effort to improve the conductivity of the resulting systems.

Careful consideration of both cation and anion was required to prevent degradation of the polymer and to ensure no self-degradation of it would occur in experimental conditions used. All salts, polymers and solvents used were either anhydrous or rendered anhydrous before processing. This was considered necessary for several reasons most poignant being the necessity for the energetically unfavourable displacement of water molecules hydrated to the salt by ether oxygens.

1.3 Modification of Polymers by the Inclusion of Metal Ions

There have been several reviews of late[19,22,24] discussing the modification of polymers by metal salts therefore extensive discussion will not take place here. However, where pertinent, some studies will be discussed.

1.3.1 Poly(ethers)

(a) Crown Ethers

Crown ethers are ring structures containing between 3 and 20 oxygen atoms. The repeat unit is that of poly(ethylene oxide), i.e.

$-(CH_2 - CH_2 - O -)$. Several studies have been carried out on these macrocyclic structures notably by Pederson[25,26], Kopolow[27,28,29], Dale[30] and Alev[31]. An informal nomenclature has arisen concerning the naming of such compounds as their I.U.P.A.C. names are long and complex.

Crown ethers act as a strong chelating agent to cations, e.g. potassium ion forms a complex with a crown ether 18-crown-6 which has a stability complex of $10^{6.1}$ in methanol compared with $10^{2.2}$ for the equivalent potassium ion complex with the chelating ligand $Me(OCH_2CH_2)_5OMe$. Due to this powerful interaction with crown ethers inorganic salts can be dissolved in aromatic solvents, a phenomenon which is being exploited in organic synthetic routes.

In crown ether complexes the ligand oxygens bond solely by electrostatic forces and are located at distinct points on the coordination sphere of the cation. It has also been shown that the size of the macrocyclic ring and the cationic radius govern the stability of the complex. The tighter the fit the more stable the complex. This can be illustrated by considering the three crown ethers:

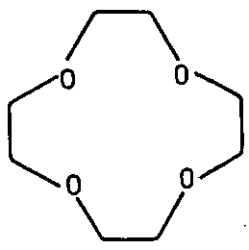

1

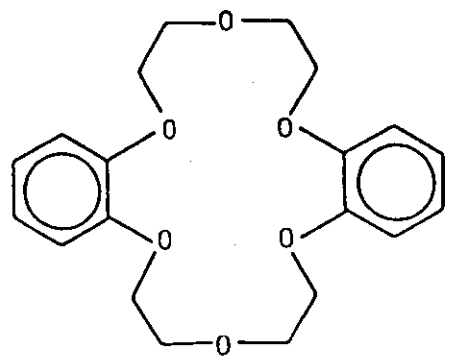

2

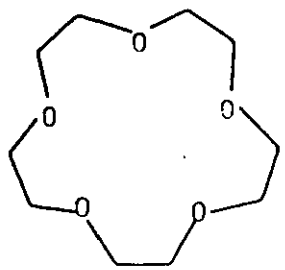

3

1 binds with Li^+ and not K^+ [32] whereas 2 binds with K^+ and not Li^+ or Na^+ [33]. Similarly 3 binds with Hg^{2+} and not Cd^{2+} or Zn^{2+}.

(b) Poly(ethylene oxide)

The formation of crystalline adducts of Hg (II) Cl_2 and poly (ethylene oxide) have been reported by several workers. [34-37] As is shown in Figure 1.2, two adducts were formed. Type 1 with the empirical formula $(CH_2CH_2O)_4$ Hg Cl_2, and (CH_2CH_2O) Hg Cl_2 for Type II. In Type I, interaction between ether oxygens and the mercury atoms in the salt was thought to be unilateral, resulting in the distortion of the normally linear Cl-Hg-Cl to an angle of 176°, where in Type II it was thought that each ethereal oxygen atom was complexed with two mercury atoms.

Iwamoto[38] obtained further information from X-ray difraction studies of single crystals of oligomers of ethylene oxide coordinated to Hg (II) Cl_2. He suggested that the complexes were formed by electrostatic forces acting between the positively charged metal ion and the negatively charged oxygen forming a coordination between a mercury atom and several coplanar oxygen atoms. Iwamoto postulated that the metal oxygen bonds contained some covalent character.

Wright et al.[39] prepared complexes of poly(ethylene oxide) and various alkali metal salts with a molar ratio of salt to polymer of 1:4. Sodium iodide, sodium thiocyanate and potassium thiocyanate formed the most stable complexes with poly(ethylene oxide) having melting points of 205°, 160° and 100°C respectively. These complexes were spheralitic as results from X-ray diffraction and IR spectroscopy indicated. The structure of the complex is totally different from the parent polymer and at concentrations in excess of 20 mole% result in recrystallisation of the pure salt as shown by the presence of characteristic peaks for the salts in X-ray spectrum of the complex.

In further studies Wright[40,41] measured the electrical conductivity

Figure 1,2

Poly(ethylene oxide)-Mercuric Chloride Complexes

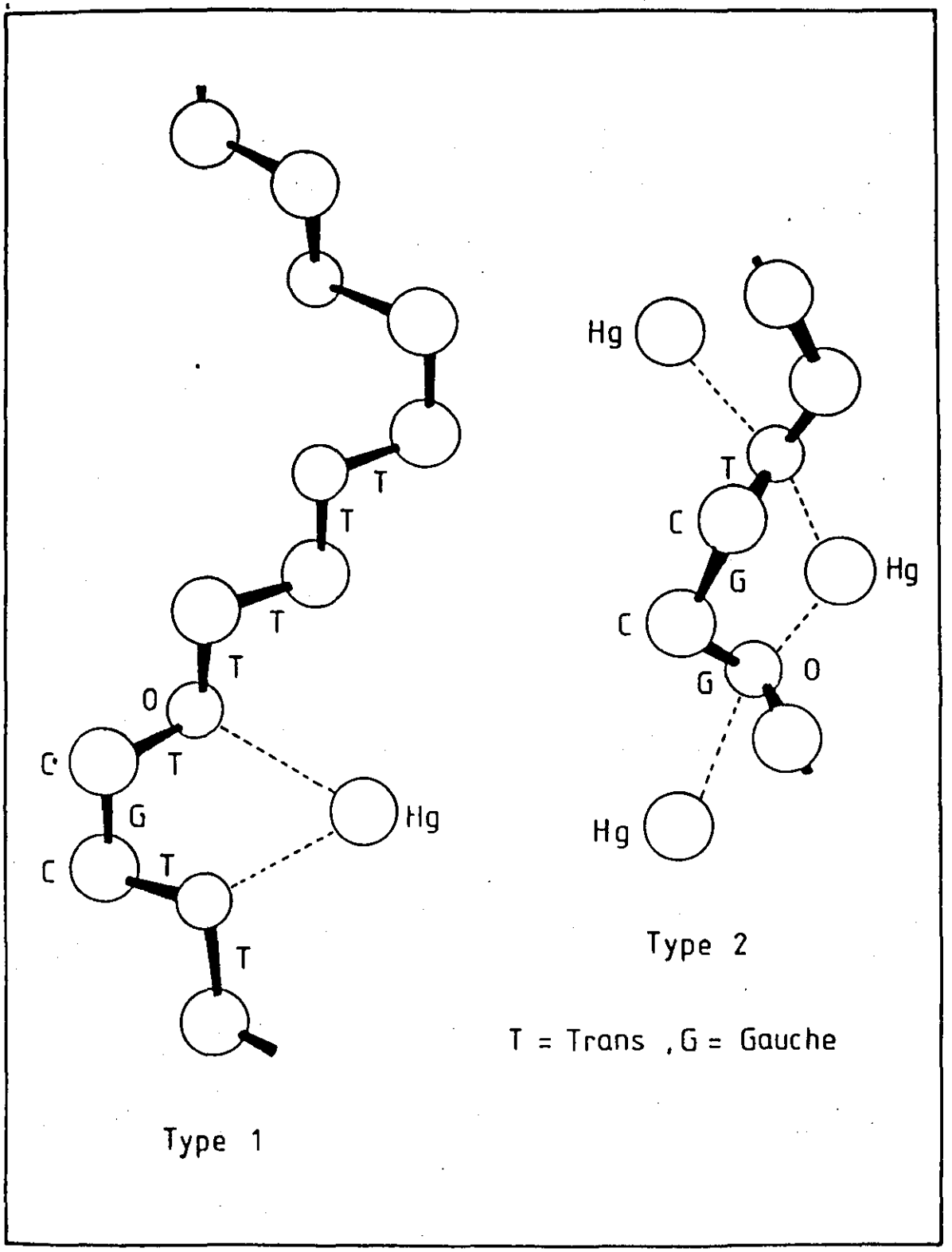

of these complexes. He found a transition zone from high to low activation energy for conduction was observed (which for the sodium complexes was situated at approximately 55°C). The transition was attributed to the thermal breakdown of the complexes in the amorphous regions. Infra red spectra of these samples show similarities to those of complexed cyclic ethers, suggesting a similar coordination of cation to the backbone ether oxygens as shown in Figure 1.3. Wright et al.[42] also claims that the anion has no effect on the principal crystalline lamellar melt temperature. The use of such complexes has recently been highlighted by Armand[43] for use as solid electrolytes. He has indicated that the conductivity of such complexes was dependent upon several parameters including cation size, salt concentration and crystallinity.

Finally, of interest are the studies of Lundberg et al.[44] concerning the complexes of alkali metal halides and poly(ethylene oxide). The results obtained showed a depression of melting point and crystallinity of the polymer and no new crystalline complexes of the type described by Wright. The results were interpreted in terms of ion-dipole interaction. It is pertinent to consider the method of preparation of complexes as proposed by Lundberg. In this mode of preparation the salt is milled directly into the polymer. This allows for less intimate mixing and consequentially the formation of new crystalline phases would not be favoured.

(c) Poly(propylene oxide)

Moacanin and Cuddihy[45] were the first to study the effect of salts in poly(propylene oxide). They studied the viscoelastic properties of lithium perchlorate. They noticed an elevation in Tg of up to 110°C (at 25 wt.% salt loading) above that of the parent polymer for low

Figure 1,3

Coordination of poly(ethylene oxide) segments with alkali metal cations

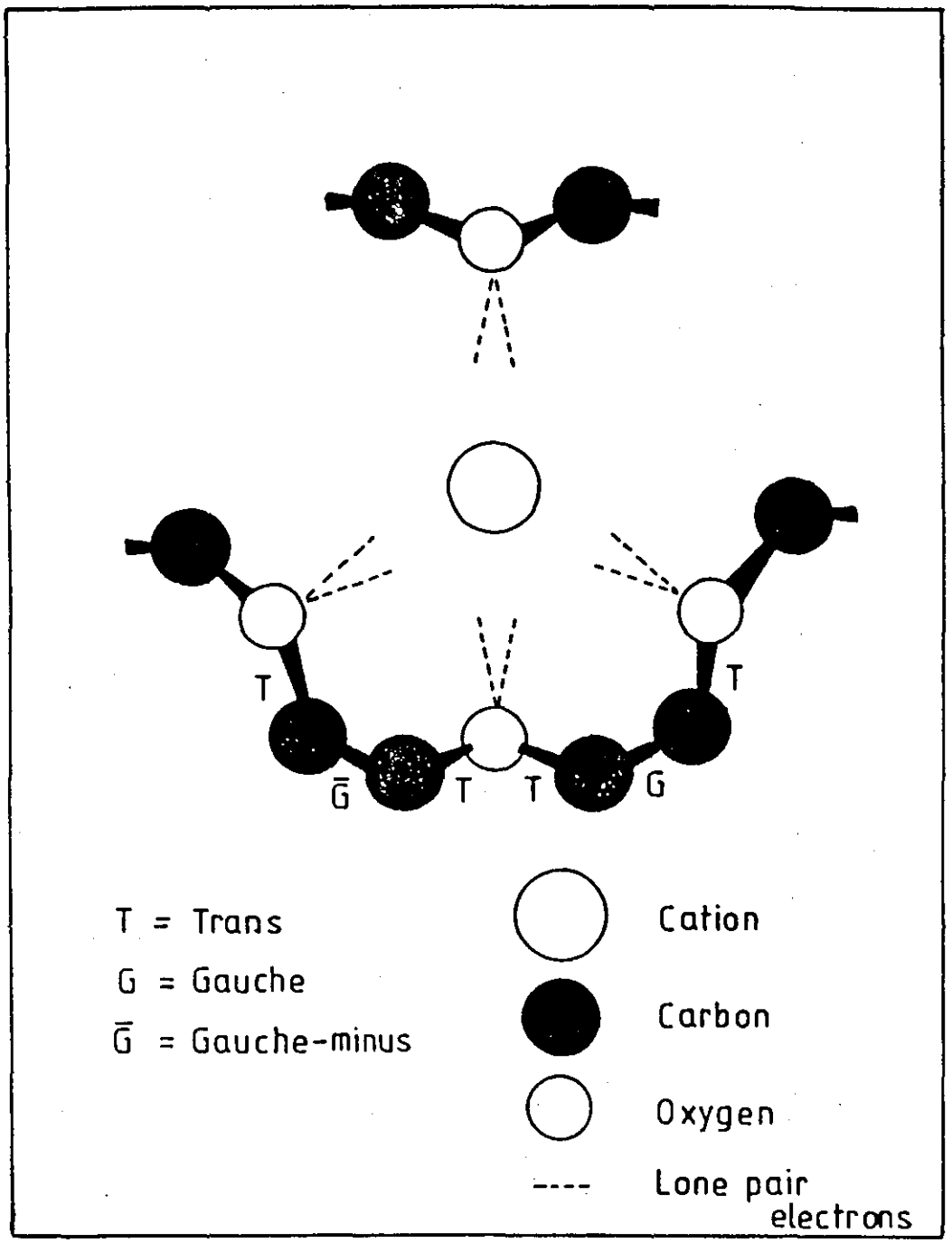

molecular weight polymer. Large elevation of Tg was also noted for high molecular weight polymer, however below 16 wt.% salt loading two transitions were oberved. The first transition occurred at a temperature slightly greater than that of the homopolymer (-65°C) whilst the second, at -10°C, was interpreted as a stabilisation by the salt of the polymer helices, the salt being situated in the helical core. The elevation of Tg was explained in terms of strong interaction forces between the cation and the ethereal oxygen atoms analogous to those observed in low molecular weight oxygen containing compounds.

In recent studies, James and Wetton[46,47] have investigated the glass transition behaviour of poly(propylene oxide) of high and low molecular weight complexed with zinc chloride. An elevation in Tg of up to 140°C above that of the parent polymer was recorded. A plot of Tg versus salt concentration gave a sigmoidal curve which levelled off at high salt concentrations. The results were interpreted in terms of the coordination of two adjacent ethereal oxygen atoms in the polymer backbone coordinating to the metal salt forming a stable five-membered chelate ring as can be seen in Figure 1.4.

The electrical properties of inorganic salt complexes of polyethers have aroused interest in several workers. Delduca et al.[48] have reviewed the formation of complexes between poly(alkyleneoxy) and inorganic salts. Their investigation centred mainly around the group 1 and 2 metal tetraphenylborates complexed with poly(ethylene glycol) and poly(propylene glycol). Using IR and NMR spectroscopy they found that for a given alkylene oxide a cation ratio of 8.5:1 was indicated for group 1 complexes and 12:1 for group 2 complexes. Cheradame et al.[49] noted that the electrical conductivity of poly(propylene oxide) complexed to sodium tetraphenylborate followed an apparent Arrhenius Law over the temperature range 50-150°C.

Figure 1,4

Coordination of poly(propylene oxide) segments with transition metal halides

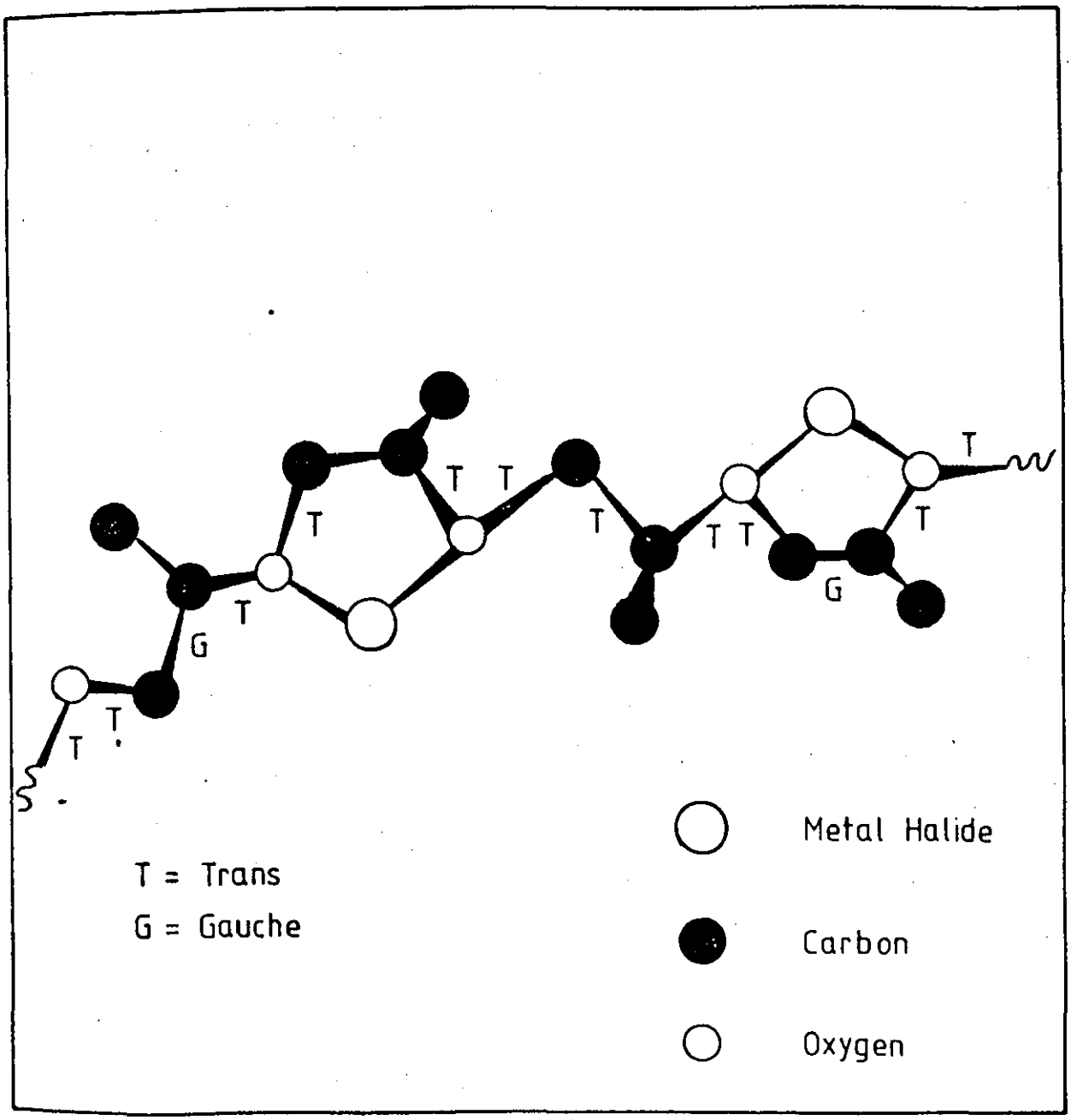

(d) Poly(vinyl alcohol)

Hannon and Wissbrun[50] have studied the interactions of inorganic nitrates with several polymers including poly(vinyl alcohol). Using IR spectroscopy they noted shifts both in the inorganic nitrate and polymer absorption frequencies. Together with Tg measurements they interpreted the results in terms of the formation of a complex between the polymer and the salt in the solid state. However, the solvent was an integral part of the complex. It is also worth noting that the oxidising nature of the salts used may have led to polymer degradation and misleading results.

Higashi[51] has reported a semi-conducting polymer based upon a poly(vinyl alcohol)/Cu II salt/I_2 complex. The resistivity was found to be a variable of both salt and I_2 concentration. A surface resistivity of $\approx 10^3$ Ω cm^{-2} was reported corresponding to a salt concentration of 15% and I_2 concentration of 4%.

1.3.2 Poly(amides)

Dunn and Sansom[52,53] investigated the stress cracking of poly(amides), mainly nylon 6 and nylon 66, by metal salts in aqueous and non-aqueous solutions. Several halides were found to be active stress-cracking agents, but could be sub-divided into type I or type II depending on the mechanism by which they caused stress cracking. These are illustrated in Figure 1.5. The first involved the coordination of the metal atom to the carbonyl oxygen atom of the amide group and is preferred by transition metal salts. The resultant stress cracking was a consequence of interference in the polyamide's hydrogen bonding. The second type of complex was due to the ability of group I and II metal salts when solvated to form proton donating species which act as direct solvents for the polyamide. Similar effects were observed with metal thiocyanates and nitrates.[55]

Figure 1,5

Structure of complexes of Polyamides

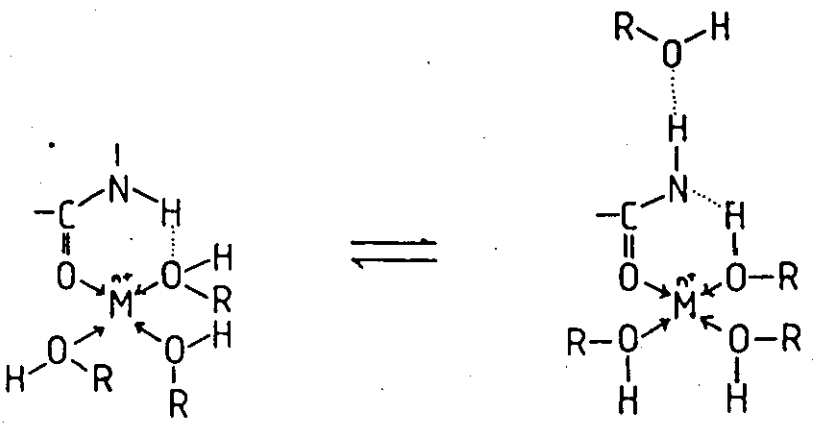

Cis

Trans

(a) with Type 1 metal halides

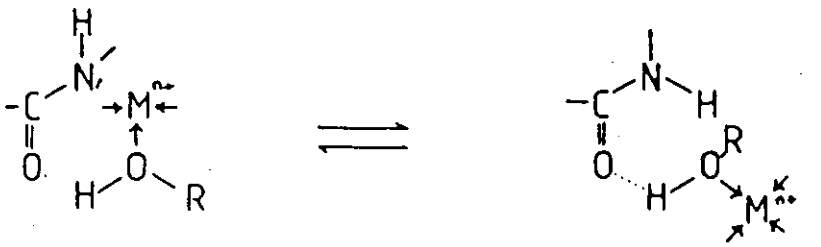

Trans

Cis

(b) with Type 2 metal halides

Andrews[56,57] measured the dynamic mechanical properties of nylon 6 treated with zinc and cobalt, chlorides, and cobalt thiocyanate. The absorbed salt was found to shift the tan δ peak associated with the α - relaxation to higher temperatures. Associated with this was a significant increase in the magnitude of the relaxation. The original properties were restored (except for a small residual shift due to irreversible morphological changes) on extraction of the zinc chloride or cobalt chloride. However on extraction of cobalt thiocyanate permanent structural changes occurred. There was no explanation proferred for this behaviour.

Ciferri[58-60] and Frasci et al.[61] have studied the effects of alkali metal halides, especially lithium chloride and lithium bromide upon nylon 6. They found a continuous depression of the melt temperature of the polymer with increasing salt content. The degree of crystallinity and the rate of crystallisation were also depressed with the addition of salt. As in the work by Andrews[56] they found a restoration of the original polymer characteristics on removal of the salts with hot water. The results were attributed to a strong interaction between the amide group in the amorphous region of the polymer and the halides, resulting in the observed specific volume reductions which were not consistent with a pure addition of polymer and salt. However Acierno et al.[62] found that the Tg of the polymer seemed unaffected by the type and concentration of the alkali metal salts in the polymer.

In subsequent work by Kim and Harget[63] and Siegmann and Baraam[64] the Tg of the nylons were found to be dependent on both the type and the concentration of salt. Kim and Harget found that the ratio of oxidation number (Q) to ionic radius (R) was related to the observed increase in Tg.

Kakinoki[65] treated poly(acrylamide)-copper II chelates with iodine pressed into films. He recorded surface resistivity of $10^3\ \Omega\ cm^{-2}$.

Reich and Michaeli[66,67] polymerised acrylonitrite in the presence

of various hydrated metal perchlorates to form solid solutions. A decrease in Tg with increasing salt concentration was noted. The solution showed high conductivities of $10^{-2}(\Omega\text{cm})^{-1}$. The obervations have been attributed to plasticisation by the salt of the polymer network. Dewsberry[68] has proposed a mechanism for conduction to account for the observed variation of activation energy with temperature.

1.3.3 Poly(vinyl pyridine)

That first row transition metal salts coordinate to poly(2-vinyl pyridine)[69] and poly(4-vinyl pyridine)[70-73] has been known for some time. Kopylova[74] and Agnew[75] discussed the general features of coordination including the stereochemistry of the coordinated ion, the stoichometry of the complexes formed, and the inter and intramolecular forms of complexation.

Complexation was attributed to the nitrogen atom of the pyridine ring. The isomer chosen governed the type of coordination occurring (i.e. either intra or intermolecular). For poly(4-vinyl pyridine) polymers, the coordination was predominantly intermolecular, with the metal salt forming a cross-link between chains. However in the poly(2-vinyl pyridine) intramolecular coordination predominates since the nitrogen atoms are more favourably situated for such a process. The two structures are illustrated in Figure 1.6.

1.3.4 Ionomers

Ionomers may be defined as a copolymer containing an organic monomer and an ionisable copolymer. The most common is a copolymer of ethylene containing a small amount of methacrylic acid. Reviews by Otocka[76] and Eisenberg[77,20] have attempted to coalesce the differing opinions on the morphology of these compounds.

Two structural models have been developed to explain the observed changes in tensile properties, impact resistance and melt viscosity[78] which occur when some of the acid groups are neutralised. The first[79]

Figure 1,6

Metal salt complexes of Poly(vinyl pyridines)

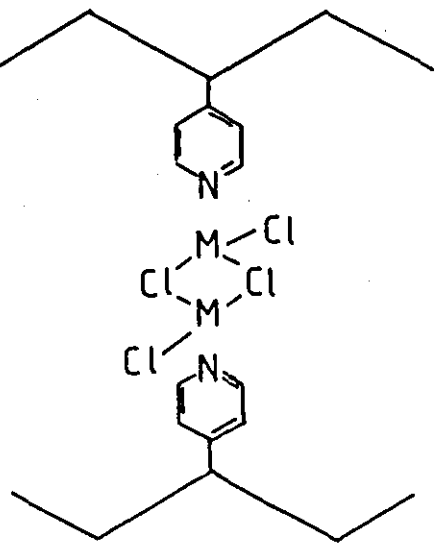

(a) Intermolecular Coordination [Poly(4-Vpy)]

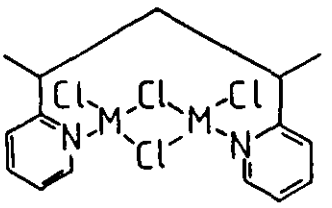

(b) Intramolecular Coordination [Poly(2-Vpy)]

describes a three-phase model, consisting of an amorphous hydrocarbon phase, a poly(ethylene) crystal phase and a phase consisting of microphase separated clusters of salt groups. The second model describes an even distribution of salt groups throughout the amorphous phase[80-82] in which the salt groups form dimers as opposed to any significant clustering.

Strong evidence for the first model comes from several experimental techniques, X-ray diffraction[78,83,84], electron microscopy[78,85,86], mechanical and dielectric measurements[87-90], and thermodynamic parameters[91]. The model is illustrated in Figure 1.7.

Evidence for the second model is not as well documented, and it has been argued[20] that much of the experimental data supporting the model can be used to support the Macknight proposal[79].

The interpretation of much of the morphological data has been hindered by the inherent crystallinity. Eisenberg and Navratil[92-94] have studied ionomers of styrene-methacrylic acid. They found, using X-ray diffraction, that below 6% of ionic comonomer simple ion multiplets occurred but that above this level ion-clustering was found

PNVC doped with a charge transfer acceptor, particularly 2,4,7 trinitroflurenone, has been used as an electro-imager in a commercial photocopying machine[95-98]. Similar systems have been employed by Schaffert[99] in electrophotography.

Cummins et al.[100] have constructed a photoconductor consisting of poly(vinyl carbazole) doped with $Bi_4Ti_3O_{12}$.

Shigahara et al.[101] describe a semi-dry photogalvanic cell consisting of a polymer gel such as PVA or poly(ethylimine) as a carrier for the redox couple thionine (TH^+) and ferrous ion (Fe^{2+}):

$$\underset{\text{(violet)}}{TH^+} + Fe^{2+} + H^+ \underset{\text{dark}}{\overset{h\nu}{\rightleftharpoons}} \underset{\text{(colourless)}}{TH^+_2} + Fe^{3+}$$

Figure 1,7

Ion cluster model for ionomeric systems

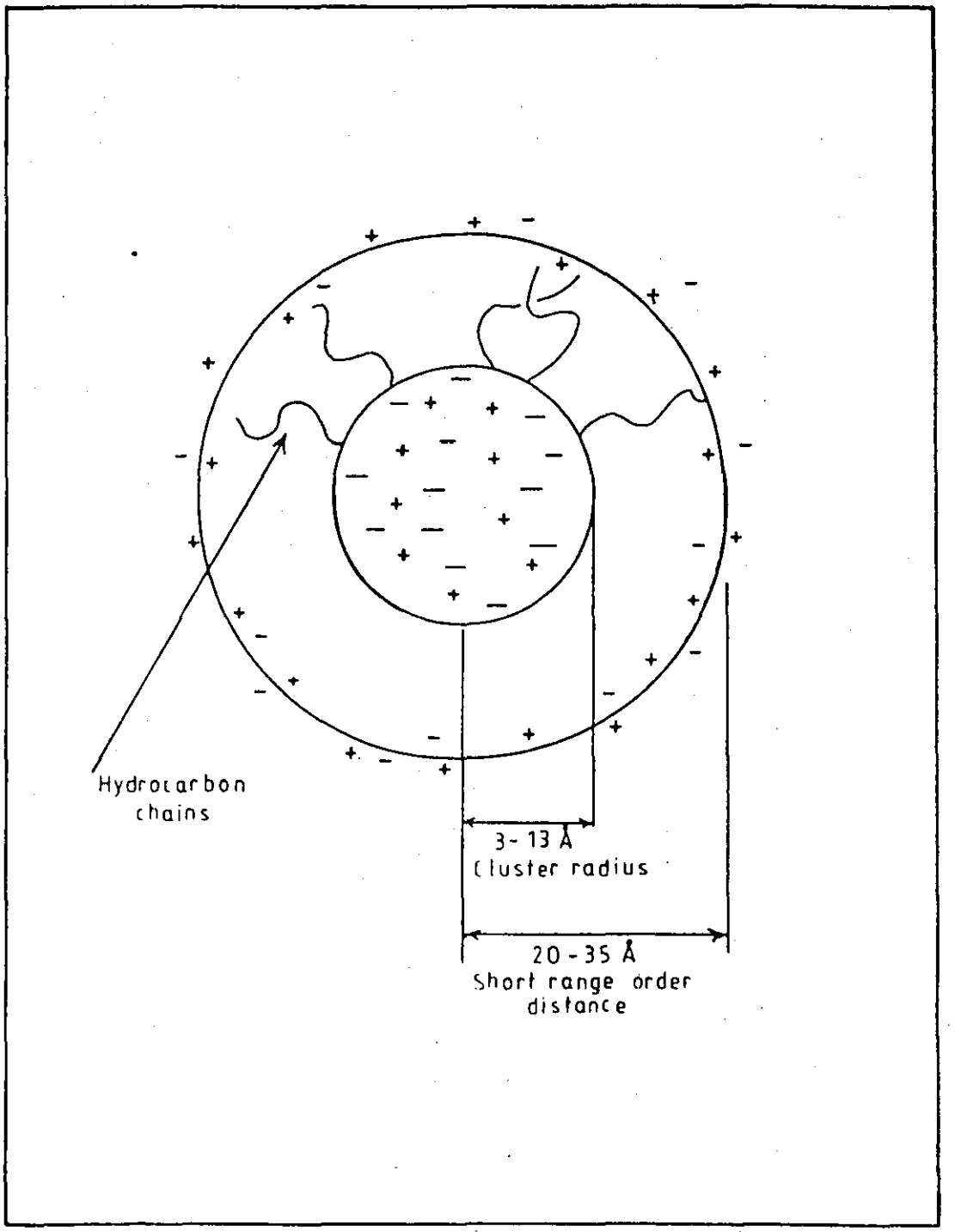

The TH^+ polymer gel from poly(epichlorohydrin) TH^+, and trimethylamine had an output efficiency sixty times greater than the monomeric $TH^+ - Fe^{2+}$ system.

A dry photochemical cell[102] was constructed from two layers of cation and anion exchange resins adsorbing TH^+ and ascorbic acid respectively.

A photomechanical model transducer[103] consisting of water swollen membranes of poly(2-hydroxyethyl methacrylate) crosslinked with ethylene glycol dimethacrylate (1.1 wt.%) in the presence of sulphonated bis-azostilbene dye (chrysophenine G), the ratio of chrysophenine G/2-hydroxyethyl methacrylate being 1/400. On irradiation the t-t-t dye is isomerised to its c-t-c isomer, this confirmational change causes a decrease of dye-polymer interactions resulting in a gel contraction of 1.2%, i.e. a change in volume of about 3.6%. In the dark the gel recovers its original dimensions.

Chiang et al.[104] discussed the use of p and n-type doped polyacetylenes as polymeric film solar cells. Using a p-type doped polyacetylene and a single crystalline n-Si wafer a solar cell was constructed[105] with a conversion efficiency of 4.3% (comparable to a maximum conversion efficiency of 8% so far achieved with an inorganic system). To further improve efficiencies of solar cells it is necessary to increase the light flux. A solar concentrator containing poly(methacrylic acid) doped with luminescent dye molecules has been described[106].

Kaneko et al.[107] describe the use of a system which incorporates a ruthenium (II) bis (2,2'-bipyridyl) salt, $Ru(bpy)_2^{2+}$ complexed with two pyridinium rings (linked aliphatically) which are formed as a pendant group on polystyrene. This complex is used in conjunction with 1,1'-dimethyl 4,4'-dipyridinium dichloride and EDTA to give a

system that photolyses water to hydrogen and oxygen.

Further work by Kaneko et al. using $Ru(bpy)_3^{2+}$ has been described[108]. A photodiode is produced by coating a platinum electrode with an anionic polystyrene-sulphonate on to which $Ru(bpy)_3^{2+}$ is electrostatically absorbed. This electrode together with an untreated platinum counter electrode is dipped into a solution of methyl violet (mV^+). Kaneko et al.[109] made a similar photodiode using nafion instead of polystyrene-sulphonate.

Anionic TCNQ associated with polymeric cations in the presence of neutral TCNQ have been developed[110,111] for use as conductive coatings on glass and plastics in printed circuits and as adhesives to replace solder in electric circuits.

A Dutch patent[112] describes the use in electrical circuitry of a system containing quaternised poly(2-vinyl pyridine) doped with TCNQ.

A battery consisting of poly(acetylene) electrodes dipped in propylene carbonate containing tetra-alkyl ammonium salt as dopant has been developed:[113]

$$(CH)_n + 0.06\ n\ (ClO_4^-) \underset{\text{discharge}}{\overset{\text{charge}}{\rightleftharpoons}} (CH^{+0.06})(ClO_4^-)\ 0.06_n + 0.06_{ne}^-$$

$$(CH)_n + 0.06\ n\ (n\text{-}Bu_4N^+) + 0.06_{ne}^- \underset{\text{discharge}}{\overset{\text{charge}}{\rightleftharpoons}} (n\text{-}Bu_4N^+)\ 0.06\ (CH^{-0.06})_n$$

The power density (kW/kg) of the battery was estimated to be more than ten times that of a conventional lead dioxide battery.

Similar power densities have been achieved from a lithium perchlorate/ poly(ethylene oxide) system. A rechargeable lithium battery is being

developed at Harwell for a battery-powered electric vehicle[114]. The cell is

$$Li(s) \mid LiF_3\ CSO_3 \quad (PEO)_s \mid V_6\ O_{13}(s),\ C(s)$$

with reactions

$$x\ Li\ (s) + V_6\ O_{13}\ (s) \underset{\text{charge}}{\overset{\text{discharge}}{\rightleftharpoons}} Li_x\ V_6\ O_{13}\ (s)$$

The active cathode material $V_6\ O_{13}$ is known as an 'insertion host' ; it can accommodate lithium on a reversible basis. The battery is designed to operate at 100-140^{o}C and it is claimed that practical energy densities will be of the order of 400 Wh kg^{-1}.

A Japanese patent[115] describes a high fidelity coaxial cable consisting of a semi-conducting sleeve of a condensation product of nylon-6 formaldehyde and 4-vinyl pyridine complexed with boron trifluoride. The sleeve lies between the braiding and core-insulation to improve screening and eliminate electrical noise caused by flexing of the cable.

Higashi et al.[116,117] have succeeded in preparing new semi-conductors from Cu^{2+} chelates of poly(vinyl alcohol) and poly(acrylamide) by charge transfer complexation with iodine.

A novel use for polymer complexes has been found by Melsungen and Alsdorf of Germany. Water soluble iodine complexes with poly(1-vinyl pyrrolidone) are commercially available as disinfecting agents under the trade names of Polyvidon and PVP-Jod respectively.

M. Mutter and E. Bayer[118] have discussed the highly selective binding of certain polymers to inorganic salts with regard to waste water treatment.

Sulphonated and carboxylated ionomers are used as thermoplastic

elastomers[119], and are finding use in solution applications[120] and related uses[121].

2.0 THEORY

2.1 The Glass Transition

2.1.1 Definition of the Glass Transition

A prominent change in the macroscopic behaviour of amorphous polymers occurs at the glass transition where the rigid glassy solid material becomes a viscoelastic fluid. The glass transition may be defined[122] as the narrow temperature region over which the temperature and pressure derivatives of thermodynamic parameters such as energy E, heat content H and volume V suffer a discontinuity, and below which configurational rearrangements of the polymer chain are extremely slow. Because this transition occurs over a relatively small temperature range any reasonable measurement which attempts to define the temperature at which the material becomes brittle will be a fair indication of the glass transition temperature Tg. However even this definition is somewhat ambiguous since a Tg thus defined is found to be lower for a slowly cooled material than for a rapidly cooled material[122]. The final value for Tg is also very dependent on the heating rate of the experiment involved being highest for greater heating rates.

Flory[123] has described an amorphous polymer whether or not as a glass below or rubber above Tg as being a random tangled network. Kargin[124] and Yeh[125] have proposed models consisting of bundles of ordered polymer chains in a random matrix . However Flory's description has found experimental support[126] from Neutron, light, electron and X-ray scattering indicating the adoption of a random configuration in the glassy state which is comparable to those of dilute solutions of polymers in theta solvents[123]. The glass transition can however be explained independently of the basic element involved in the morphology of the polymer.

2.1.2 Theories of the Glass Transition

There are several theories concerning the glass transition. However there are two of prominence, the kinetic Free Volume Theory[127,128] and the Statistical Mechanical Theory of Gibbs and Di Marzio[129-136] which considers a thermodynamic viewpoint.

(a) Free Volume Theory

The presence of a substantial degree of free volume is found in both liquids and polymers. In an elementary way if segments of a polymer chain may be regarded as rigid bodies, the free volume may be envisaged as holes between the segments due to packing irregularities. The coefficient of expansion can thus be regarded as the increase in free volume with temperature. As temperature decreases a corresponding decrease in free volume occurs down to a temperature (Tg) when the large scale configurational rearrangements cannot occur within experimental times. This corresponds to a critical value in free volume of approximately 0.025. Figure 2.1 illustrates this effect.

Doolittle[137,138] applied the principle of free volume to the shear viscosity of simple liquids and has derived the equation

$$\ln \eta = \ln A + B(V - V_f) / V_f \qquad (2.1)$$

Where η is the viscosity of a system of total volume V, free volume V_f, A and B are constants. If the fractional free volume f is defined as V_f/V then equation (2.1) becomes

$$\ln \eta = \ln A + B(1/f - 1) \qquad (2.2)$$

Above the glass transition temperature the fractional free volume increases linearly as shown in Figure 2.1. It may now be represented as

Figure 2,1

Schematic variation total specific volume, occupied volume, and free volume with temperature for a supercooled liquid

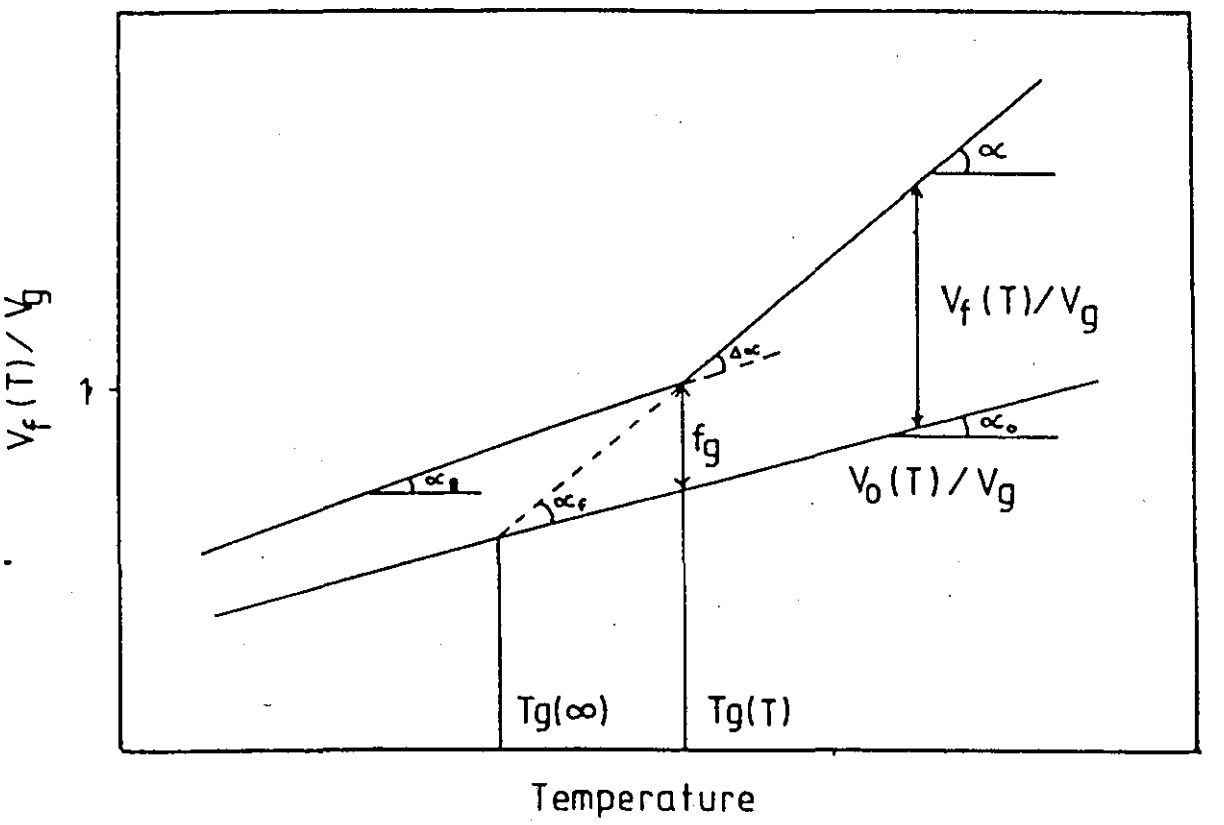

$$f = fg + \Delta\alpha(T - Tg) \qquad (2.3)$$

Where f is the fractional free volume at temperature T ($T > Tg$), fg is the fractional free volume at temperature Tg and $\Delta\alpha$ is the difference between the thermal coefficients of expansion above and below Tg. Substitution of equation (2.3) into equation (2.2) produces

$$\ln\eta_T = \ln A + B\left(\frac{1}{fg + \Delta\alpha(T - Tg)}\right) - 1 \qquad \text{for } T > Tg \qquad (2.4)$$

$$\ln\eta_{Tg} = \ln A + B\left(\frac{1}{fg} - 1\right) \qquad \text{for } T = Tg \qquad (2.5)$$

Subtraction and simplification of equations (2.4) and (2.5) produces

$$\log\frac{\eta_T}{\eta_{Tg}} = \log a_T = \frac{-B}{2{\cdot}303fg}\left(\frac{T - Tg}{fg(\alpha) + (T - Tg)}\right) \qquad (2.6)$$

Equation (2.6) has the same form as the Williams, Landel and Ferry equation for amorphous polymers which, if Tg is taken as the reference temperature may be written as

$$\log a_T = \frac{C_1(T - Tg)}{C_2 + (T - Tg)} \qquad (2.7)$$

Where C_1 and C_2 are constants. A comparison of equations (2.7) and (2.6) produces values of C_1 and C_2 as

$$C_1 = \frac{B}{2{\cdot}303fg} \qquad C_2 = fg/\alpha \qquad (2.8)$$

In practice B approximates to unity and the values of and fg can be calculated given the values of C_1 and C_2.

The values of C_1 and C_2 were erroneously taken as 17.44 and 51.6 respectively for all amorphous polymers. Although C_1 is indeed approximately constant, C_2 is dependent upon $\Delta\alpha$.

(b) Statistical Mechanical Theory

The statistical mechanical theory developed by Gibbs and Di Marzio depends upon the assumption that the glass transition observed is a manifestation of a true equilibrium second order transition. A lattice model was proposed upon which the polymer chain was fitted. The lattice sites could contain one chain segment only and vacant sites allowed for polymer configurational changes.

Chemical bonds of the backbone restrict internal rotation thus under normal conditions several conformations may be adopted. As the molecule cools, a reduction in energy available for conformational changes occurs and thus low conformational energy structures predominate. Consequently the number of ways in which a molecule may pack a lattice is reduced and the number of alternative conformations rapidly approaches zero. A point T_2 is reached on further temperature reduction at which a level of lowest energy is reached. At this temperature the configurational entropy becomes zero as illustrated in Figure 2.2. No further changes in packing arrangement from that adopted at T_2 can occur because there is no available energy to give lower energy rearrangements on the lattice.

The temperature T_2 is referred to as the second order transition temperature. T_2 may be derived from the relationship

$$\frac{\Delta E}{k\,T_2} = \text{const.} \qquad (2.9)$$

Figure 2, 2

Variation of configurational entropy with temperature for a glass forming liquid

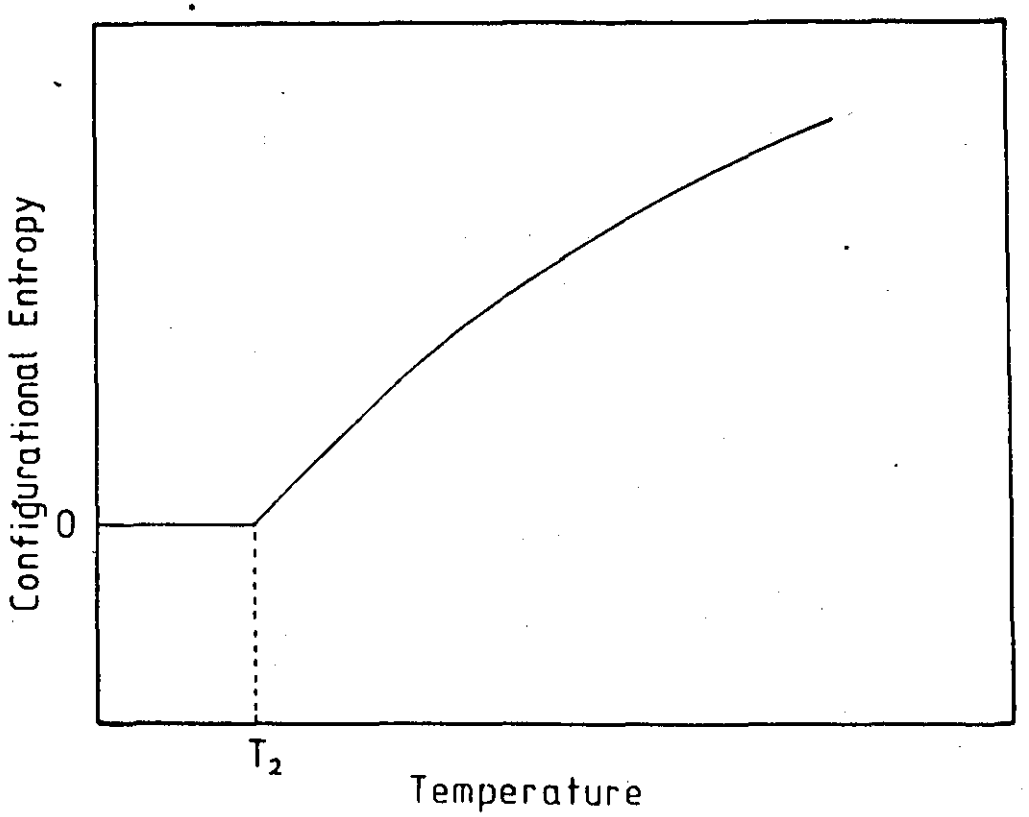

Where ΔE is a function of the flex energy.

At temperatures near to T_2 the free energy barrier which restricts configurational change from one ground state to another is very high. This is a consequence of the limited number of states available and their wide separation within the phase which would require extensive alterations in spatial arrangements of molecular entanglements. A slow response would thus be expected to any external forces applied. Dielectric and viscoelastic relaxation times have been shown to increase as the temperature falls toward T_2. T_2 has thus been substantiated in practice but is of little use as it can only be deduced from experiments of infinite time scale. The entities Tg and T_2 are very similar in character, such that postulations made about T_2 equally apply to Tg.

A molecular kinetic theory of Adams and Gibb[135] has extended the original Gibbs and Di Marzio concept, to include non-equilibrium conditions.

Their theory considers the temperature dependence of the relaxation behaviour and explains it in terms of the variation of the size of the cooperatively rearranging body. The size of this region is determined by restraints on the configuration which can be adopted with amorphous packing. As a consequence a relationship similar to the WLF equation (shown in equation (2.7)) was derived. From a consideration of both theoretical and empirical values they found that $Tg/T_2 = 1.30 \pm 8.4\%$ for many glass forming liquids. They concluded that the kinetic properties of glass-forming liquids within approximately $100^{\circ}C$ of the glass temperature could be satisfactorily explained in terms of the thermodynamic properties of the equilibrium melt. Thus they have gone some way towards resolving the essentially kinetic or essentially

thermodynamic approach in a theory that takes elements from both.

2.1.3 Factors Influencing the Glass Transition Temperature

Several factors influence the position of the glass transition temperature and those of relevance to this thesis (namely the chemical structure of the polymer, the degree of cross-linking, the consequences of cross-linking and the addition of fillers) will be discussed.

(a) Chemical Structure

The glass transition temperature of a polymer is dependent upon both the intra and intermolecular aspects of chemical structure.

Intramolecular forces involve purely structural parameters involving the stiffness of the polymer backbone. They can be clearly illustrated by consideration of the glass transition temperature of a series of polymers in which a hydrogen atom of a poly(ethylene) molecule is replaced by other substituents. When a methyl group replaces a hydrogen atom the Tg is raised by a 100° and even more dramatically raised by 200° when the substituent is a benzene ring. The increase can be explained in pure statistical mechanical terms as an increase in flex energy[130]. This is the difference between the potential energy minima, the favoured rotational positions, of the backbone bonds with respect to their neighbours. In general the greater the steric hindrance, i.e. the bulkier the side groups the larger the increase in Tg for mono-substituted polymer chains.

However if the polymer is symmetrically substituted a lower Tg will be recorded than for a mono-substituted polymer, e.g. poly(propylene) has a Tg of $-20^{\circ}C$ whereas poly(isobutylene) has a Tg of $-70^{\circ}C$. Even though the second substituent increases the hindrance the potential energy minima are reduced as a consequence of the chain symmetry.

Increasing the intermolecular forces between polymer chains will increase Tg, this can be illustrated by the effect of differing the polarity of the substituent side groups. Poly(propylene) has a Tg of -20°C; poly(vinyl chloride), which has a much more polar side group, has a Tg of +85°C. Bueche[91] interprets these observations in terms of the degree of expansion. A polymer with strong intermolecular forces needs to be raised to a higher temperature before sufficient free volume is acquired for a glass transition.

(b) Crosslinking Effects

The effect of crosslinking by polymers upon the Tg of a polymer have been reviewed by Nielson[140,141], as predicted both by free volume and statistical mechanical theories, the Tg is increased by crosslinking. Crosslinking effectively decreases the free volume of the system and therefore a higher temperature is required before the necessary free volume for a glass transition is attained. In statistical mechanical terms crosslinking effectively decreases the configurational entropy.

Changes in the chemical structure occur as the degree of crosslinking increases. The crosslinking agent can be described as a comonomer, resulting in a shift in Tg which is dependent on both the crosslinking effect and the copolymerisation effect (which itself may either depress or elevate Tg depending on the nature of the crosslinking agent).

From a review of the literature Nielson[141] has produced the empirical relationship

$$Tg - Tg_o = \frac{3.9 \times 10^4}{Mc} \qquad (2.10)$$

Where Tg and Tg_o are the glass transition temperatures of crosslinked and uncrosslinked polymers respectively and Mc is the molecular weight

between crosslinks. However, it does not account for shifts due to the copolymerisation effect.

In accordance with statistical mechanical theory Di Marzio[134] has derived a relationship between the Tg shift and the degree of crosslinking.

$$\frac{Tg - Tg_o}{Tg_o} = \frac{KX_c}{1 - X_c} \simeq \frac{2K}{n_c} \qquad (2.11)$$

Where Tg_o is the glass transition temperature of a polymer of equivalent composition in the absence of crosslinks, X_c is the mole fraction of crosslinked monomer units and n_c is the average number of atoms between crosslinks in the backbone. K is a function of segmental mobility and the cohesive energy density of crosslinked and uncrosslinked polymer having a value of $1 \leqslant K \leqslant 1.2$.

Equation (2.11) describes the Tg shift due to crosslinking only because Tg_o is inclusive of a term for the copolymerisation effect.

(c) Copolymerisation

Fox [142] has derived a relationship for the glass transition temperature of an amorphous random copolymer

$$\frac{1}{T_g} = \frac{W_A}{Tg_A} + \frac{W_B}{Tg_B} \qquad (2.12)$$

Alternatively Gordon and Taylor[143] derived the equation

$$Tg = \frac{Tg_A + K\ (Tg_B - Tg_A)\ W_B}{1 - (1-K)\ W_B} \qquad (2.13)$$

Where Tg is the copolymer glass transition temperature of a polymer consisting of two monomers A and B, weight fractions W_A and W_B respectively and whose homopolymers have glass transition temperatures Tg_A and Tg_B respectively, K is a constant.

Using both the free volume[144] and statistical mechanical [132] theories equation (2.13) can be derived . In the free volume approach by Fox[142] and others it was incorrectly assumed that the free volume contributed by the monomer unit was identical for both homopolymer and copolymer. In practice the free volume is affected by near neighbour groups on the polymer backbone as a consequence of steric and energetic considerations. In practice it is found that K has a lower value than that predicted which would suggest incorrect assumptions in the derivations.

An average stiffness energy for the copolymer may be derived from statistical mechanical theory in the form of

$$\varepsilon = B_A \varepsilon_A + B_B \varepsilon_B \qquad (2.14)$$

Where B_A and B_B are the fraction of rotatable bonds of two homopolymers A and B, and ε_A ε_B are the stiffness energies of rotatable chemical bonds of A and B respectively.

An equation has been derived from (2.13) such that

$$W_a \left(\frac{\sim_A}{M_A}\right)\left(T_2 - T_{2A}\right) + W_b \left(\frac{\sim_B}{M_B}\right)\left(T_2 - T_{2B}\right) = 0 \qquad (2.15)$$

Where W_A and W_B are weight fractions of A and B monomer units $\sim_A$ and $\sim_B$ are the number of flexible bonds per monomer; M_A and M_B are the molecular weight of monomers A and B; T_{2A} and T_{2B} are the second order transition temperatures for A and B homopolymers respectively; T_2 is the second order transition temperature for the copolymer.

This equation has the same form as equation (2.13) with $\sim_A/M_A$ and $\sim_B/M_B$ replacing K. These coefficients may be derived from the chemical structures for the homopolymers. Equation (2.15) is related to the second order transition temperature as opposed to the experimentally determined glass transition temperature. Within certain

limits equation (2.15) can be applied to the glass transition.

The copolymerisation of A and B will produce A-A, A-B and B-B bonds. Therefore the theory cannot be exact for all the polymers as the stiffness energy of A-B bonds will bear no unique relationship to the stiffness energies of the A-A, B-B bonds. Even if ε_A and ε_B do not differ greatly the assumptions made in equation (2.14) need not be valid. Therefore equation (2.15) cannot give accurate predictions of Tg if the proportion of A-B bonds is large.

Thus the significance attached to K in the Gordon-Taylor-Wood equation in free volume terms differs from that in statistical mechanical terms. Illers[145], Kanig[146] and Johnson[147] have discussed deviations from the equation. Johnson[147] has considered the sequence distribution of the polymer whose sequence length is dependent upon the reactivity ratios r_A and r_B of the monomers A and B if r_A and r_B are small. He argues that for a copolymer, the A-A and B-B sequences will retain their homopolymer Tg values since both will experience essentially the same interactions as in their respective homopolymers. Obviously the formation of A-B sequences results in new interactions, therefore predictions can be made for the Tg of the copolymers if the A-B sequences are assigned a Tg.

(d) Fillers

Manson[148] has reviewed the effect of fillers on the glass transition of polymers. Normally the addition of inorganic fillers results in a dispersed second phase where a weak interaction, due to polymer adsorption on the filler surface, causes a slight increase in Tg. The magnitude of the Tg elevation will be determined by the type, concentration and surface area of the filler as well as the type of polymer. The absolute magnitude of the Tg elevation defies generalisation.

This is well illustrated by comparing a study by Landel[149] on a glass bead filled poly(isobutylene) and a study by Kumins et al.[150] on TiO_2 filled poly(vinyl chloride-vinyl acetate) copolymer. Landel reported a Tg elevation of 7°C at 36.7 vol.% loading which he explained in terms of the crosslinking effect from polymer adsorption at the glass surface. Kumins however recorded a Tg depression which he explained in terms of adsorption of the acetate groups on the filler surface with a resulting disruption of the existing hydrogen bonded network.

2.2 Dielectric Relaxation

2.2.1 Molecular Polarizability

There are three components of molecular polarization:-

(a) Electronic Polarization. An electric field will slightly displace the electrons of an atom with respect to the positive nucleus. The shift is quite small because the applied electric field is usually quite weak relative to the intra-atomic field at an electron due to the nucleus. Electronic polarization can react, however, to very high frequencies and is responsible for the refraction of light. The dielectric permittivity at such frequencies is related to the refractive index via the following relationship.

$$\varepsilon_u = n^2 \qquad (2.16)$$

(b) Atomic Polarization. An electric field can distort the arrangement of atomic nuclei in a molecule or lattice. The movement of heavy nuclei is more sluggish than electrons so that atomic polarization cannot occur at such high frequencies as electronic polarization, and it is not observed above infra-red frequencies. In the case of molecular solids, it is known from vibrational spectroscopy that the force constants for bending or twisting of molecules, involving

changes in angles between bonds, are generally much lower than those for bond stretching, so bending modes are the major contribution to atomic polarization. The magnitude of atomic polarization is usually quite small, often only one-tenth of that of electronic polarization, although exceptions do occur, especially in ionic compounds, due to relative shifts of all the positive ions with respect to the negative ions.

(c) Orientational Polarization. If the molecules already possess permanent dipole moments, there is a tendency for these to be aligned by the applied force to give a net polarization in that direction. This effect is further discussed later in the chapter. The rate of dipolar orientation which is highly dependent on molecule-molecule interaction can make a large contribution, but which may be slow to develop, to the total polarization of a material in an applied field. Figure 2.3 depicts the characteristic stepwise fall-in polarization of a material as the measurement frequency is raised. The dielectric constant follows a similar pattern.

2.2.2 Dielectric Dispersion

Dielectric relaxation is a rate dependent effect. When an alternating field is applied to a polar material, it produces an alternating electrical polarization. If ample time is allowed, then the observed dielectric constant is called the static dielectric constant ε_r. If the polarization is measured immediately after the field is applied, allowing no time for dipole orientation, then the instantaneous (or unrelaxed) dielectric constant εu will be low and due to deformational effects only.

An alternating electric field E, amplitude E_o and angular frequency w can be defined as

FIGURE 2·3 FREQUENCY DEPENDENCE OF POLARIZATION

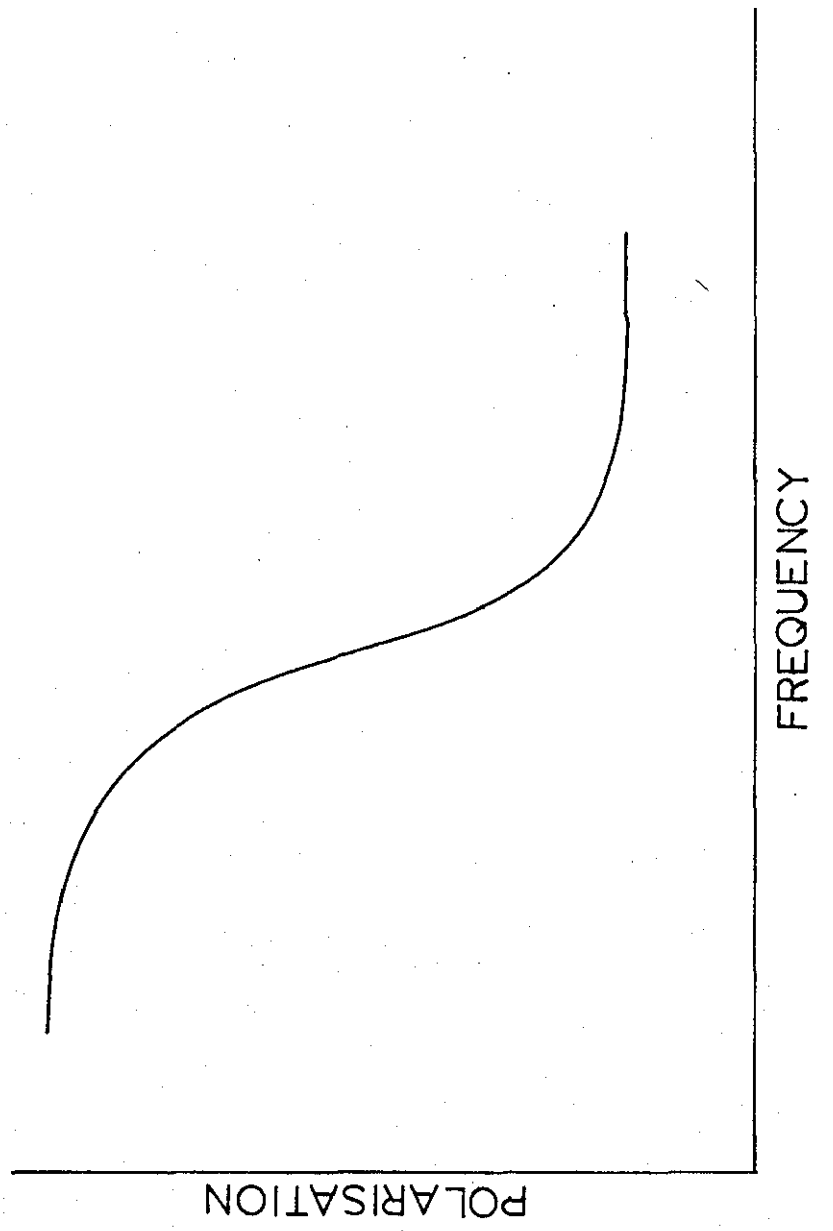

$$E = E_o \cos wt \tag{2.17}$$

Where t is time.

This will produce an alternating polarization in a dielectric material, and, if the frequency is high enough, the orientation of any dipoles which are present will lag behind by a phase angle in the dielectric displacement D where

$$D = D_o \cos (wt - \delta) \tag{2.18}$$

which may be written as

$$D = D_1 \cos wt + D_2 \sin wt \tag{2.19}$$

where $$D_1 = D_o \cos\delta \tag{2.20}$$

and $$D_2 = D_o \sin\delta \tag{2.21}$$

Two dielectric constants can thus be defined as

$$\varepsilon' = \frac{D_1}{\varepsilon_o E_o} \quad \text{and} \quad \varepsilon'' = \frac{D_2}{\varepsilon_o E_o} \tag{2.22}$$

linked by the relationship

$$\tan\delta = \frac{\varepsilon''}{\varepsilon'} \tag{2.23}$$

The current I^* which flows in the external circuit (see Figure 2.4) after application of an alternating voltage given by the real part of

$$V^* = V_o \, e^{iwt} \tag{2.24}$$

may be calculated as

$$I^* = \varepsilon^* C_o \frac{dV}{dt} = iw \, \varepsilon^* C_o V^*$$

$$= w C_o (\varepsilon'' + i\varepsilon') V^* \tag{2.25}$$

This means that there is a capacitive component of the current

$$I_c = iw C_o \varepsilon' V^* \tag{2.26}$$

which leads the voltage by 90^o, and a resistive component

FIGURE 2·4 VECTOR DIAGRAM FOR A CAPACITOR WITH DIELECTRIC EXHIBITING RELAXATION

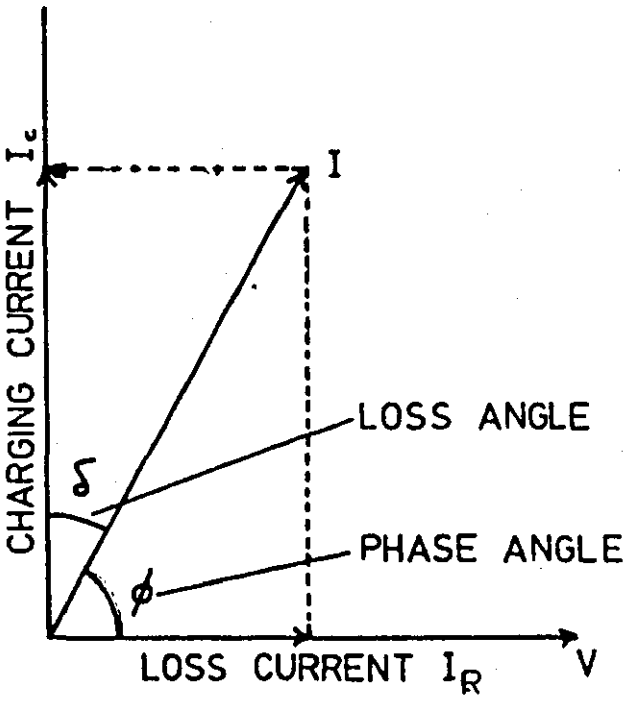

$$I_R = w C_o \varepsilon'' V^* \qquad (2.27$$

which is in phase with the voltage. Thus the equation becomes apparent:

$$\tan \delta = \frac{\varepsilon''}{\varepsilon'} = \frac{\text{energy dissipated per cycle}}{\text{energy stored per cycle}}$$

ε'' is known as the dielectric loss factor, $\tan \delta$ the dielectric loss tangent or dissipation factor and ε' the dielectric 'constant' (or permittivity).

The resultant effect of applying an alternating electric field may as above be described in terms of complex permittivity and also in terms of complex polarizability or susceptibility

$$\chi^* = \frac{P^*}{E^*} = \chi' - i\chi'' \qquad (2.28)$$

The natural response may be considered[151, 152] in terms of a complex electrical modulus $M^*_{(w)}$ also referred to as the complex inverse permittivity and is defined as

$$M^*_{(w)} = M'_{(w)} + iM''_{(w)} \qquad (2.29)$$

and is related to $\varepsilon^*_{(w)}$ by the expression

$$\varepsilon^* = \frac{1}{M^*_{(w)}} \qquad (2.30)$$

Therefore

$$M'_{(w)} = \frac{\varepsilon'_{(w)}}{(\varepsilon'_{(w)})^2 + (\varepsilon''_{(w)})^2} \qquad (2.31)$$

$$M''_{(w)} = \frac{\varepsilon''_{(w)}}{(\varepsilon'_{(w)})^2 + (\varepsilon''_{(w)})^2} \qquad (2.32)$$

The loss tangent, $\tan \delta$, is expressed as

$$\tan \delta = M''_{(w)} / M'_{(w)} = \varepsilon''_{(w)} / \varepsilon'_{(w)} \qquad (2.33)$$

As shown in Figure 2.3 the dipolar polarization decreases with frequency, in the frequency region of decreasing polarization the

loss tangent passes through a maximum. At high frequencies there is insufficient time for the dipoles to orientate to the rapidly alternating field because the period of oscillation is much less than the retardation time τ_R. At low frequencies the converse is true and the period is large in comparison to the retardation time τ_R of the dipoles and consequently orientational polarization is maximised. Therefore at both low and high frequencies power loss is low. Between the two extremities the orientation polarization is out of phase with the applied field and power losses occur. This is maximised when

$$W_{max} = \frac{1}{\tau_R} \tag{2.34}$$

For a system having a single retardation time Debye[153] derived expressions for the frequency dependence of ε' and ε'' in the form

$$\varepsilon^*_{(w)} = \varepsilon_u + \frac{\varepsilon_r - \varepsilon_u}{1 + iw\tau_R} \tag{2.35}$$

$$\varepsilon'_{(w)} = \varepsilon_u + \frac{\varepsilon_r - \varepsilon_u}{1 + w^2\tau_R^2} \tag{2.36}$$

$$\varepsilon''_{(w)} = \frac{\varepsilon_r - \varepsilon_u}{1 + w^2\tau_R^2} \tag{2.37}$$

where w is the angular frequency.

Simple liquids may show single retardation times[154]; however it has never been observed in polymers. This is because the orientation of dipoles in polymers is a complex process with a spectrum of relaxation times, and the observed $\varepsilon''/\varepsilon_r - \varepsilon_u$ versus w curve is considerably broader and of less magnitude than that for a Debye model as shown in Figure 2.5.

For a single retardation time model the retardation time may be

FIGURE 2·5 CONTRASTS IN DIELECTRIC BEHAVIOUR

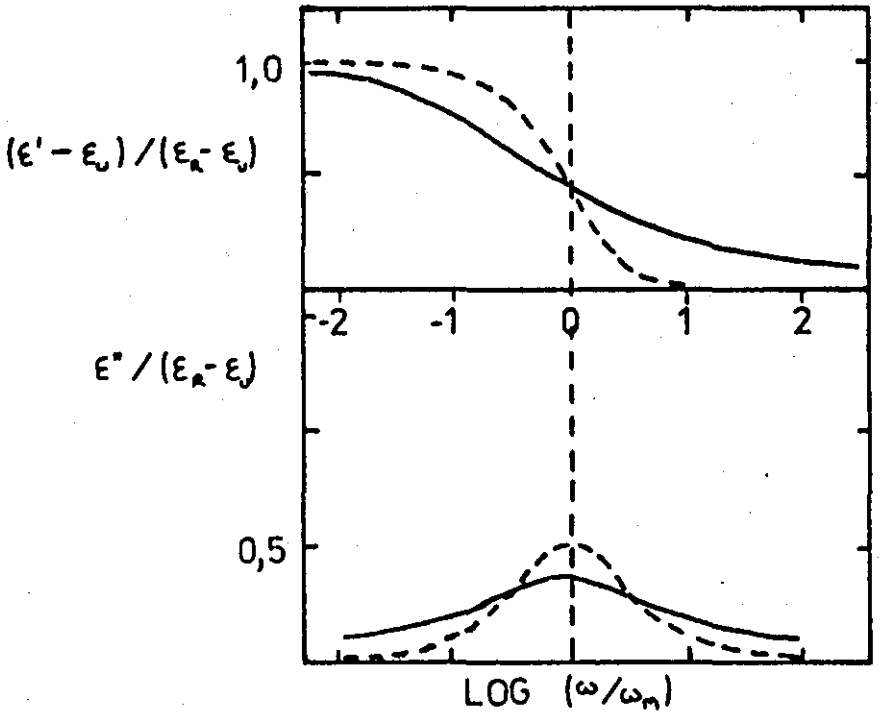

approximately regarded as the reciprocal of the rate constant for dipole orientation. Therefore over a limited temperature range it is possible to plot the temperature dependence of retardation time using an Arrhenius plot of the form

$$\tau_R = \tau_o \exp\ (\Delta E/RT) \qquad (2,38)$$

Where ΔE is the activation energy of dipolar orientation.

As a result, the dispersion regions move to shorter retardation times and consequently to higher frequencies with increasing temperature.

2.2.3 Distribution of Retardation Times

A distribution of retardation times may be the result of either a distribution of τ_o or a distribution of ΔE or both causing a broadening and depression of magnitude of the experimental retardation curves. This has led to the development of several empirical distributions to fit these curves, three of which are discussed below.

(a) Cole-Cole Distribution

The most familiar empirical distribution is that of Cole and Cole[155]. They proposed a more generalised form of $\varepsilon^*_{(w)}$ than defined by Debye, to account for the relaxation time distributions. They proposed the formula

$$\varepsilon^*_{(w)} = \varepsilon'_{(w)} - i\varepsilon''_{(w)} = \varepsilon_u + \frac{\varepsilon_r - \varepsilon_u}{(1 + iw\tau_o)^{1-\alpha}} \qquad (2.39)$$

Equation (2.39) may be divided into its real and imaginary parts as follows:

$$\varepsilon'_{(w)} = \varepsilon_u + \frac{1}{2}(\varepsilon_r - \varepsilon_u)\left(1 - \frac{\sinh(1-\alpha)X}{\cosh(1-\alpha)X + \cos\frac{1}{2}\alpha\pi}\right) \quad (2.40)$$

$$\varepsilon''_{(w)} = \frac{\frac{1}{2}(\varepsilon_r - \varepsilon_u)\cos\frac{1}{2}\alpha\pi}{\cosh(1-\alpha)X + \sin\frac{1}{2}\alpha\pi} \quad (2.41)$$

where $X = \ln w\tau_o$

combination and simplification of (2.40) and (2.41) produces

$$\left(\varepsilon''_{(w)} + \frac{(\varepsilon_r - \varepsilon_u)}{2}\tan\frac{\alpha\pi}{2}\right)^2 + \left(\varepsilon'_{(w)} - \frac{(\varepsilon_r + \varepsilon_u)}{2}\right)^2 = \left(\frac{(\varepsilon_r - \varepsilon_u)}{2}\sec\frac{\alpha\pi}{2}\right)^2 \quad (2.42)$$

This is in the form of a circle having centre

$$\left(\frac{(\varepsilon_r + \varepsilon_u)}{2} - \frac{(\varepsilon_r - \varepsilon_u)}{2}\tan\frac{\alpha\pi}{2}\right) \quad \text{and radius}$$

$$\frac{(\varepsilon_r - \varepsilon_u)}{2}\sec\frac{\alpha\pi}{2} \quad .$$

When $\varepsilon''_{(w)} = 0$ the curve bisects the $\varepsilon'_{(w)}$ axis at ε_r and ε_u.

It is pertinent to note that when $\alpha = 0$ the Cole-Cole equations retreat back to the Debye equations. However if $\alpha > 0$ there is a broadening and depression in magnitude of the dispersion region but it is symmetrical around $w\tau_o = 1$, the maximum value of $\varepsilon''_{(w)}$. Figure 2.6 shows a typical Cole-Cole plot . The data is represented in the form of a plot of $\varepsilon''_{(w)}$ at a certain frequency versus $\varepsilon'_{(w)}$ at the same frequency. The angle of depression $\frac{\alpha\pi}{2}$ permits a determination of the distribution of retardation times, whilst ε_r and ε_u may be determined from the intercepts at the $\varepsilon'_{(w)}$ axis.

(b) Fuoss-Kirkwood Distribution

Fuoss and Kirkwood [156] rearranged the dielectric loss expression

Figure 2·6 TYPICAL COLE-COLE DIAGRAM

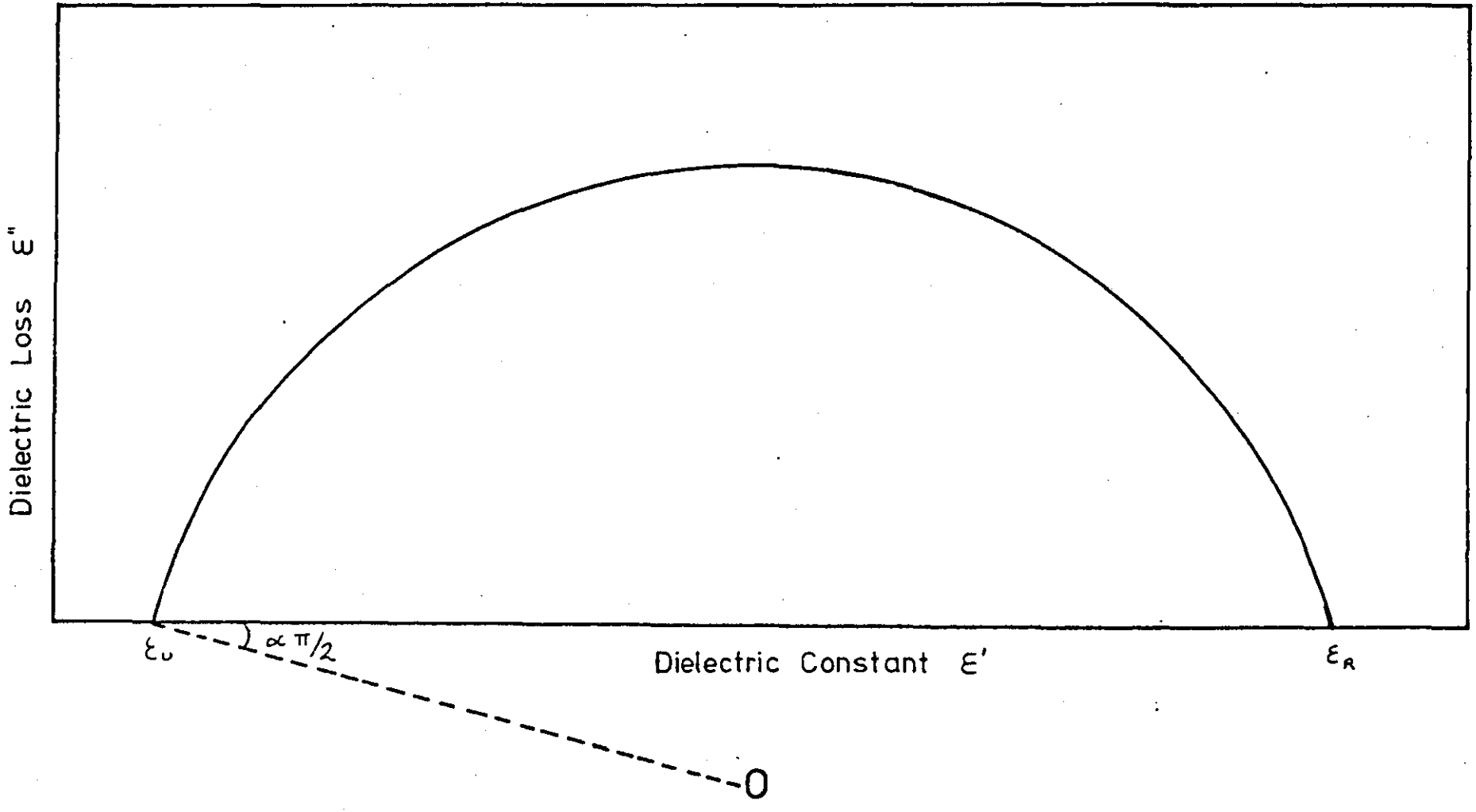

for a single retardation time such that

$$\varepsilon''_{(w)} = \varepsilon''_{max} \text{ sech } (\ln w \tau_R) \qquad (2.43)$$

and further extended this for a distribution of relaxation times by an inclusion of parameter β into equation (2.41) such that

$$\varepsilon''_{(w)} = \varepsilon''_{max} \text{ sech } (\beta \ln w \tau_{AV}) \qquad (2.44)$$

where β measures the breadth of the distribution and τ_{AV} is the most probable retardation time defined by $1/w_{max}$, where w_{max} is the angular frequency of maximum loss.

Methods for the evaluation of β from the experimental data have been discussed by several workers including McCrum et al.[157] and Wetton and Allen[158]. Three of these methods are discussed below.

(i) From the equation

$$\beta = \frac{2 \varepsilon''_{max}}{\varepsilon_r - \varepsilon_u} \qquad (2.45)$$

β may be found if a sufficient frequency range is examined from values of ε_r and ε_u, alternatively $\varepsilon_r - \varepsilon_u$ may be determined from Cole-Cole diagrams.

(ii) From the equation

$$\cosh^{-1} (\varepsilon''_{max} / \varepsilon''_{(w)}) = \beta \ln w \tau_{AV} \qquad (2.46)$$

A plot of $\cosh^{-1} (\varepsilon''_{max} / \varepsilon''_{(w)})$ versus logw, produce a straight line of slope 0.2303β.

(iii) From the equation

$$\cosh^{-1} 2 = \beta \ln (w_1 / w_{max}) \qquad (2.47)$$

where w_1 is the angular frequency at which $\varepsilon''_{(w)}$ has dropped to a half of its magnitude together with a measure of the half-width of the loss peak.

With a fair knowledge of β a plot of the experimental $\varepsilon''_{(w)}$

versus w curve may be compared to a theoretical curve calculated from equation (2.44). The resultant loss curves of similar but not identical to those of Cole-Cole may be produced.

(c) Davidson-Cole Distribution

Both the Cole-Cole and Fuoss-Kirkwood empirical equations relate only to dispersion and adsorption curves that are symmetrical about $w\tau = 1$. However it is often found that dielectric loss curves have a high frequency broadening resulting in the Cole-Cole arcs for such systems being 'skewed'. Davidson and Cole [159,160] attempted to fit experimental results to the following function

$$\frac{\varepsilon^*_{(w)} - \varepsilon_u}{\varepsilon_r - \varepsilon_u} = \frac{1}{(1 + iw\tau_1)^\gamma} \qquad 0 < \gamma \leq 1 \qquad (2.48)$$

where τ_1 is a characteristic relaxation time.

Equation (2.48) may be split into its real and imaginary components as follows

$$\frac{\varepsilon'_{(w)} - \varepsilon_u}{\varepsilon_r - \varepsilon_u} = (\cos \phi)^\gamma \cos \gamma \phi \qquad (2.49)$$

$$\frac{\varepsilon''_{(w)}}{\varepsilon_r - \varepsilon_u} = (\cos \phi)^\gamma \sin \gamma \phi \qquad (2.50)$$

$$\text{where } \tan \phi = w\tau_1 \qquad (2.51)$$

At the maximum loss $w\tau_1 \neq 1$ but is given by

$$w_{max}\,\tau_1 = \tan\left(\frac{1}{\gamma + 1} \cdot \frac{\pi}{2}\right) \qquad (2.52)$$

A typical Davidson-Cole plot is shown in Figure 2.7. The curve is circular at low frequencies but as the frequency increases the curve becomes a straight line of slope $\frac{\gamma\pi}{2}$ up to the abscissa.

Figure 2·7 TYPICAL COLE-DAVIDSON DIAGRAM

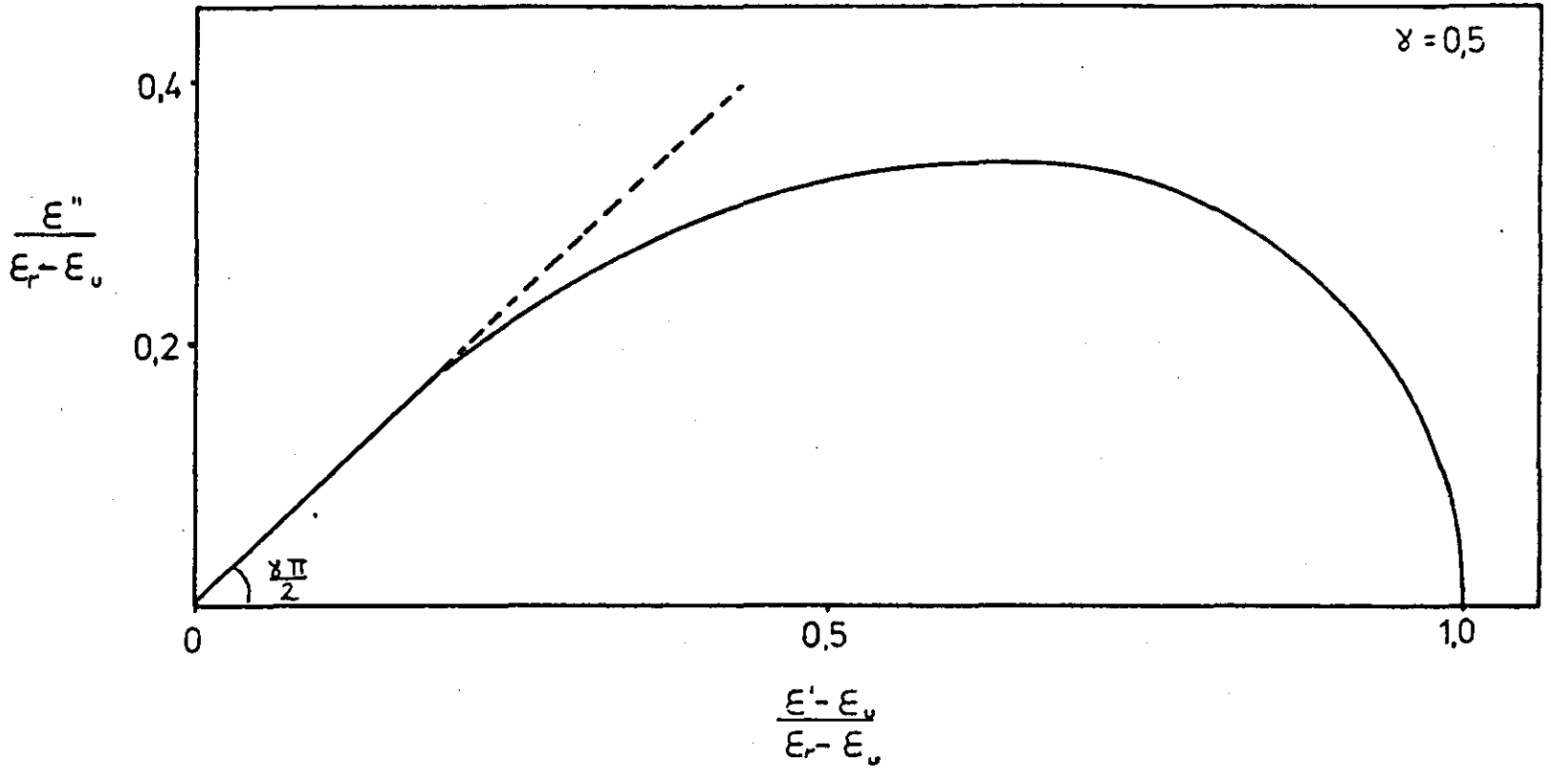

(d) Williams-Watts Approach

Use of the 'skewed' arc approach has been common in the presentation of experimental data[161]. However Williams and Watts[162] found it to be inadequate to explain the observed non-symmetrical behaviour associated with the primary or α relaxation of many polymers. Williams and Watts applied the superposition principle to the complex dielectric constant and produced

$$\frac{\varepsilon^*_{(w)} - \varepsilon_u}{\varepsilon_r - \varepsilon_u} = \int_0^\infty \left(- \frac{d\gamma_{(t)}}{dt} \right) \exp - iwdt \qquad (2.53)$$

where $\gamma_{(t)}$ is the normalised decay function obtained upon removal of a steady electric field from a sample.

A simple empirical decay function

$$\gamma_{(t)} = \exp - (t/\tau_o)^\beta \qquad 0 < \beta \leqslant 1 \qquad (2.54)$$

where τ_o is some effective retardation time, was proposed which when inserted into equation (2.53) produced

$$\frac{\varepsilon^*_{(w)} - \varepsilon_u}{\varepsilon_r - \varepsilon_u} = \mathcal{L} (\beta \lambda t^{\beta-1} \exp - \lambda t^\beta) \qquad (2.55)$$

where $\mathcal{L}$ represents the Laplace transform and $\lambda = \tau_o^{-\beta}$

By choosing suitable values of β, Williams and Watts[163] were able to represent the α-relaxations of many amorphous polymers. The dielectric loss curves drawn from the Williams-Watts empirical functions showed similar trends to those of Davidson-Cole as shown in Figure 2.7 but had marked deviations at higher frequencies.

Where conduction processes mask the underlying dielectric relaxation the Williams-Watts equations have been applied with success.Using this method the conduction relaxation of alkali silicate glasses[151] and

poly(arylene vinylenes)[152] have been studied. A broadening of the imaginary part of the dielectric loss peak was shown for both systems in comparison to a single relaxation peak. It was also noted that the curves were asymmetric and were skewed toward the high frequency end of the spectrum. Application of the simple empirical decay function (equation (2.54)) showed a good simulation of the observed data.

(e) Grant Complex Conductivity

The imaginary component of the complex dielectric constant may be resolved into the linear sum of a relaxation and conduction component for low conduction materials giving

$$\varepsilon^*_{(w)} = \varepsilon'_{(w)} - i\,(\varepsilon''_r + \sigma_o/w\,\varepsilon_o) \qquad (2.56)$$

where ε_o is the permittivity of free space and σ_o is the d.c. conductivity.

However in materials where conduction is significant it is not always found straightforward to analyse the complex dielectric constant. In such cases it has previously been shown that the complex dielectric modulus may be more convenient. Grant[164] has introduced a parameter Y, defined as

$$Y = iw\varepsilon^* = \sigma^* \qquad (2.57)$$

therefore

$$\sigma'_{(w)} + i\,\sigma''_{(w)} = iw\,(\varepsilon'_{(w)} - i\,\varepsilon''_{(w)}) \qquad (2.58)$$

and

$$\sigma' = w\varepsilon'' \qquad (2.59)$$

$$\sigma'' = w\varepsilon' \qquad (2.60)$$

Figure 2.8 shows the different conductivity and permittivity plots for four equivalent circuits. The presence of ε_u distorts the conductivity plots but may be removed by using $\varepsilon'_{(w)} - \varepsilon_u$ to find $\sigma''_{(w)}$.

2.2.4 Effects of Temperature on the Distribution of Relaxation Times

In the previous section the empirical distribution functions were discussed as a function of frequency at constant temperature. Temperature itself has a marked effect on the distribution of relaxation times. The effect is reflected in the temperature dependence of the parameters α, β, γ, previously defined, if either or both τ_o and ΔE are temperature dependent.

It has been shown that Eyring's general theory of rate processes[165] could be applied to many transitons such that the temperature dependence was shown in the form of an Arrhenius plot

$$\tau_R = \tau_o \exp (\Delta E/RT) \qquad (2.38)$$

If the distribution of relaxation times is not temperature dependent then it is possible to superimpose the normalised experimental $\varepsilon''_{(w)} / \varepsilon''_{max}$ versus w, and $\dfrac{\varepsilon'_{(w)} - \varepsilon_u}{\varepsilon_r - \varepsilon_u}$ versus w plots at different temperatures to produce a master curve. The principle of Time-Temperature superimposition is described by the semi-empirical Williams-Landel-Ferry (WLF) [139,166] equation (2.7) which is derived from

Figure 2,8

Complex conductivity and permittivity plots
for some equivalent circuits

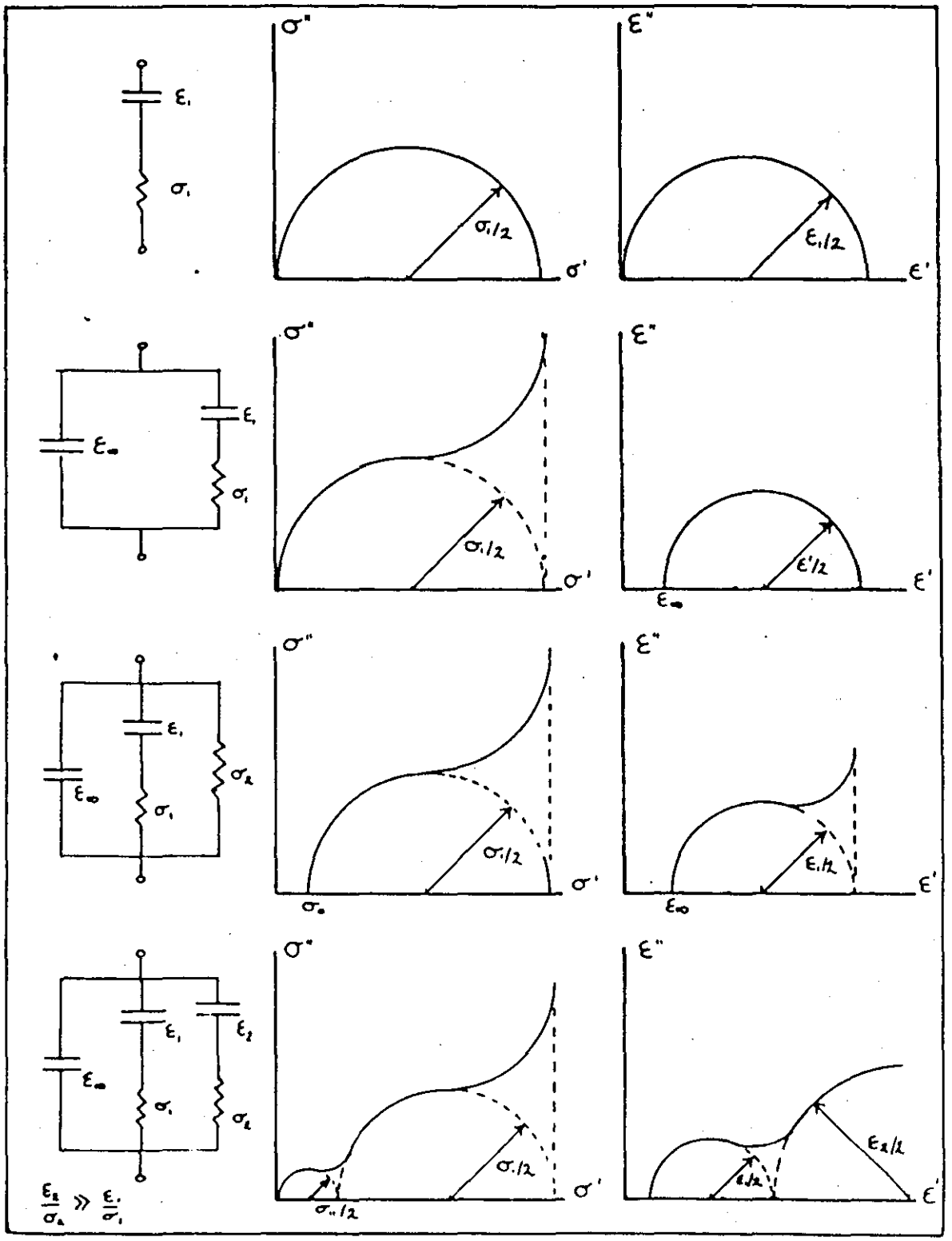

Leaderman's [167] general principle whilst measuring polymer creep-temperature relationships. The shift in ln a_τ can be represented in terms of an Arrhenius equation

$$\ln a_\tau = \frac{\Delta E}{R}\left(\frac{1}{T} - \frac{1}{Tg}\right) \qquad (2.61)$$

At temperatures greater than Tg the WLF equation holds true but temperatures lower than Tg produces significant variations. However the WLF equation has been used if an effective temperature is incorporated to account for the non-equilibrium state of the glass[168], down to temperatures of Tg - 100°C.

McCrum and Morris[169] have extended the WLF to incorporate the effect of temperature upon the relaxed and unrelaxed moduli (permittivity) of polymers.

2.2.5 Relationships Between Dielectric Constant and Dipole Moment

It has previously been stated that dipolar molecules align themselves in the direction of the applied field. The static dielectric constant inclusive of all contributing orientation processes, was related by Debye [153] to the dipole moment of the molecule such that

$$\frac{\varepsilon_r - 1}{\varepsilon_r + 2} = \frac{4}{3}\pi N\left(\alpha_e + \frac{\mu_o^2}{3kT}\right) \qquad (2.62)$$

where ε_r is the static dielectric constant, μ_o is the dipole moment of the molecule, N is the number of molecules per unit volume, k is the Boltzmann constant, T is the absolute temperature and α_e is the deformation polarizability due to molecular displacement and is given by the Clausius-Mosotti equation

$$\frac{\varepsilon_u - 1}{\varepsilon_u + 2} = \frac{4}{3}\pi N \alpha_e \qquad (2.63)$$

where ε_u is the dielectric constant measured at frequencies so high that any contribution from dipole orientation is absent.

Equation (2.63) is however limited to gases and extremely dilute polar molecules dissolved in non-polar solvents.

Onsager [170] has extended equation (2.62) to include effects due to the deformation polarizability caused by the surrounding medium of a condensed dipolar phase such that

$$\mu_o^2 = \frac{3kT}{4N}\left(\frac{2\varepsilon_r + \varepsilon_u}{3\varepsilon_r}\right)\left(\frac{3}{\varepsilon_u + 2}\right)(\varepsilon_r - \varepsilon_u) \qquad (2.64)$$

There is however no allowance made for orientation correlation between dipoles.

Kirkwood [171] has extended the Onsager equation to include short range interactions between molecules in the liquid state. However he omitted to include the effect of deformation polarizability on the molecules, consequently a term was empirically included into the final equation:

$$\frac{(\varepsilon_r - 1)(2\varepsilon_r + 1)}{9\varepsilon_r} = \frac{4}{3}\pi N\left(\alpha_e + \frac{g\mu^2}{3kT}\right) \qquad (2.65)$$

where μ is the 'liquid dipole moment'. It is the effective dipole moment of a molecule in the liquid state as opposed to μ_o, the effective moment of a molecule in vacuo. g is the Kirkwood Correlation Function and refers to the effect of short range orientation between a reference molecule and its nearest neighbours. For a molecule surrounded by 2 nearest neighbours the

$$g = 1 + z \overline{\cos\gamma} \tag{2.66}$$

where $\overline{\cos\gamma}$ is the average cosine of the angle between the reference molecule and one of its nearest neighbours, when there is no orientation correlation g = 1.

Frölich[172] has further extended Kirkwood's studies to include orientation processes in terms of statistical mechanics. He analysed a small region surrounding the reference molecule in an infinite matrix of the dipole. By averaging the dipoles inside the region and regarding the region as a continuum of dielectric constant ε_u he expressed the dielectric permittivity as

$$(\varepsilon_r - \varepsilon_u) = \left(\frac{3\varepsilon_r}{2\varepsilon_r + \varepsilon_u} \right) \frac{4\pi N}{3kT} \left(\frac{\varepsilon_u + 2}{3} \right) g\mu_o^2 \tag{2.67}$$

where g is the orientation correlation function given by

$$g = 1 + \sum_{i \neq j} \overline{\cos \gamma_{ij}} \tag{2.68}$$

and $\cos\gamma_{ij}$ is the average of the cosine of the angles γ_{ij} made between the reference molecule and a molecule j. If there is no orientation correlation between molecules g = 1, and the Frölich equation reverts to the Onsager equation.

Frölich's theory satisfactorily explains the behaviour of small molecules which possess intermolecular dipole orientation correlation such as water or alcohols. Together with the Onsager equation the

behaviour of rigid dipoler molecules may be predicted.

Unfortunately the Onsager theory is inapplicable to polymers. The dipole moment of a polymer chain is a vector sum of the component moments. The resultant moment will vary with time due to the continued Brownian motion of the chain. Additionally a strong correlation in orientations between the components of the chain would need consideration. For Frölich's theory to be applied to polymers the basic dipole unit cannot be taken as a single polymer chain but as the chemical repeat unit. Since a true liquid polymer consists of an intermingled network.

2.2.6 Dielectric Relaxation Processes

A systematic nomenclature is used to indicate the positions of the various relaxation processes. Deutsch et al.[173] proposed the system most commonly used whereby each process is labelled α, β, γ ..... in order of decreasing temperature at constant frequency and were subscripted to indicate the polymeric phase in which the transition was occurring.

There are normally three transitions in an amorphous polymer referred to as α_a, β_a and γ_a. α_a is associated with the glass transition involving large segmental motion due to equilibrium conformational changes (micro-Brownian motion). The β_a transition occurs in the glassy state and is associated with side group or limited segmental motion. There have been two mechanisms proposed for the latter, crankshaft motion[174], or local mode motions[175]. γ_a has been observed in certain substituted polymers[176], the mechanism of which is associated with the independent motion of side groups.

Crystalline polymers show a series of transitions labelled α_m, α_c, β_c, γ_c, attributed to the crystalline melting and crystal - crystal transitions[3].

James, Wetton and Brown[43] have noted two further transitions at higher temperatures than the α_a relaxation when metal salts are added to polymers. To sidestep the problem of nomenclature the transitions were designated α' and β'. Conventional theories of dielectric relaxation[157] were found to be unable to explain the greatly enhanced magnitude of these relaxations. The results may be explained in several ways, three of which will be presented here.

2.2.7 Maxwell-Wagner-Sillars Interfacial Polarization

If an otherwise loss-free dielectric contains a second trapped phase, usually of higher conductivity, this will produce an effect known as Maxwell-Wagner-Sillars Interfacial Polarization[177,179]. Charge migration through the conducting phase to the interface results in an increase in the apparent dielectric constant. The dielectric loss is also affected at certain frequencies because ohmic conduction takes place as current flows in the conducting phase producing changes in polarization at the interface.

The magnitude and position in the frequency plane of this effect is dependent upon the dielectric constants of the two phases, the volume ratio of each, and the size and geometry of the conducting phase.

Knowledge of these parameters allows calculation of the relaxation times. Van Beek[180] has reviewed these effects and derived equations for several phase geometries such as spheres, spheroids, rods, cylinders and lamellae. Application of these equations to dispersed ellipsoidal particles gave very high predicted values of permittivity and loss, especially if the ratio of the major and minor axes were large. The Maxwell-Wagner-Sillars relaxation is narrow and only slightly wider than that predicted for a single relaxation time model[181,182].

2.2.8 Colloidal Dispersions in Electrolyte Solutions

Schwarz et al.[183] observed unusually high dielectric constants in suspensions of non-conductive colloid particles in aqueous electrolytes. He further developed a theory[184] to explain this phenomenon.

Colloidal particles will be charged by fixed or adsorbed ions from the electrolytic solution. These ions will attract a layer of counter ions, which will be strongly bound by electrostatic attraction to the ions adsorbed and will have to overcome a large potential barrier to escape. However movement along the surface is less restricted therefore upon application of an external field they are moved tangentially and the ion atmosphere is polarized and a dipole results. The extent of counter-ion polarization within the double layer will depend upon the surface concentration and mobility of the ions and be opposed by the tendency of the ion to diffuse back and nullify the surface gradient.

Depending on the system the polarization may lead to an increase in the dielectric constant which is in excess of that contributed by the bulk phases.

Schwarz equated the magnitude of the relaxation as follows:

$$\varepsilon_r - \varepsilon_u = \frac{9}{4}\left(\frac{P}{(1 + P/2)^2}\right)\left(\frac{e_o^2 R \sigma_o}{\varepsilon_o kT}\right) \qquad (2.69)$$

where P is the volume fraction of dispersed spheres, e_o is the electrical charge of the counter ion, R is the sphere radius, σ_o is the counter ion density in the double layer, ε_o is the permittivity of free space, k is the Boltzmann constant and T is the absolute temperature.

The characteristic frequency of the relaxation is defined by

$$f = \frac{1}{2\pi\tau_R} = \frac{ukT}{\pi R^2} \qquad (2.70)$$

where τ_R is the characteristic retardation time, u is the counter ion surface mobility.

The surface mobility was shown to be governed by an exponential relationship involving an additional activation energy α of electrostatic origin as

$$u = u_o \exp(-\alpha/kT) \qquad (2.71)$$

where u_o is the free solution mobility from equations (2.70) and (2.71) it can be shown that

$$\tau_R = \tau_o \exp(\alpha/kT) \qquad (2.72)$$

where $$\tau_o = \frac{R^2}{2 u_o kT} \qquad (2.73)$$

Thus the theory predicts Debye-type behaviour for a system of spheres of equal size. However, if the spheres are not uniform then a spectrum of relaxations will result.

The primary requirements for the dielectric behaviour as described above are:

(a) A structure of mobile ions associated electrostatically with counter ions.

(b) Isolated regions containing the mobile ions.

(c) A continuous matrix having a sufficiently high conductivity and/or a dielectric constant of sufficiently low nature to ensure an adequate potential gradient across the ion-containing region to induce ion displacement.

The theory has been successfully applied to the anomalous dielectric behaviour of several systems. Examples of such are poly (styrene) spheres dispersed in potassium chloride solutions [183], and

of polysalts, poly(vinyl benzyl trimethyl ammonium) - poly (styrene sulfonate) containing water and sodium bromide[184].

Since the colloidal particles are suspended in an electrolyte form a heterogenous system, a Maxwell-Wagner-Sillars type relaxation might be expected. Calculations for both systems[183,185] did not substantiate this, as the relaxations observed were of several orders of magnitude higher than those calculated for MWS-type polarizations and occurred at much lower frequencies.

2.2.9 Pohl's Theory of Hyperelectronic Polarization

Pohl et al.[186,187] observed very high dielectric constants (between 50 and 900) in a system of highly conjugated macromolecules of the polyacene radical quinone type. They found that they were highly dependent upon frequency, field strength and temperature but only slightly dependent on pressure.

They accounted for the results by postulating a new type of electronic polarization by the field applied of groups of highly mobile charges in a region of very low resistance (e.g. π orbitals). A series of calculations were able to predict the observed frequency, field strength, temperature and pressure dependencies.

The dependence of dielectric constant upon field strength in the Pohl effect in contrast to MWS and Schwarz type relaxations allows it to be used to decide which mechanism is operating.

2.3 Electrical Conduction in Polymers

2.3.1 General Features

The electrical properties of the majority of plastic materials,

low conductivity, low dielectric loss and high breakdown strength, are usually exploited in their use as insulators[188]. However, recent research has observed conductances of sufficient magnitude to class them in the metallic range. It has been shown previously that special consideration must be used when applying the conventional theories of dielectric dispersion for low molecular weight compounds to high molecular weight substances. Similarly special care must be used when using conventional conduction theories to macromolecules.

The electrical conductivity σ of any substance is dependent upon the absolute temperature T, and direction, X, as shown in the general relationship

$$\sigma_{(T,X)} = \sum_j \cdot |q_j| n_{j(T)} \psi_{j\ (T,X)} \qquad (2.74)$$

where q_j is the charge on a carrier j whose mobility is ψ_j and number n_j.

It has been found empirically that conductivity frequently varies with temperature such that

$$\sigma = \sigma_o \exp\ (-E_a/kT) \qquad (2.75)$$

where σ_o is a constant, E_a is the thermal activation energy and k is the Boltzmann constant. E_a may thus be calculated from the slopes of a plot of log σ versus 1/T, which is usually linear.

A series of intersecting lines of differing slopes may exist for some systems, reflecting the different activation energies for individual regions (such as below and above the Tg)[41].

The effect of temperature upon the number of carriers is given by

$$n_{(T)} = n_o \exp\ (-E_n/2kT) \qquad (2.76)$$

where n_o is a constant and E_n is the carrier generation ionization energy.

Conduction in polymers can take the form of either, electronic due to the formation of electron-hole pairs in an energy band structure, or thermally activated electron or ion hopping. The primary mechanisms for polymer conduction are listed in Table 2.1.

TABLE 2.1 Mechanisms for Polymeric Conduction

Electronic Processes	Ionic Processes
(1) Conduction by electrons (a) Intrinsic (b) Extrinsic (impurities donate electrons) (2) Conduction by holes (a) Intrinsic (b) Extrinsic (impurities other than electrons) (3) Metallic conduction, e.g. poly(acetylenes)	(1) Electrolytic(cationic,anionic) (a) Intrinsic (self-dissociating) (b) Extrinsic (impurities or dopants) (2) Protonic

2.3.2 Charge Carriers

Conduction in an ordered system can result via an energy band structure due to the formation of electron-hole pairs. Holes will arise when a vacancy in the valence band occurs due to the promotion of an electron to a conduction band as a result of thermal energy.[189] Figure 2.9a illustrates this phenomenon.

When electronic conduction takes place without traps the parameter E_n (2.76) corresponds to the forbidden energy gap of the band theory and the observed activation energy has the value $E_n/2$. When the mass is effectively small the mobility $\Psi_{(T)}$ will be high. $\Psi_{(T)}$ becomes inversely proportional to temperature because of scattering. Therefore deviations from equation (2.75) occur as a consequence of the domineering exponential term in equation (2.76).

Figure 2,9

Band formation in ordered and disordered structures

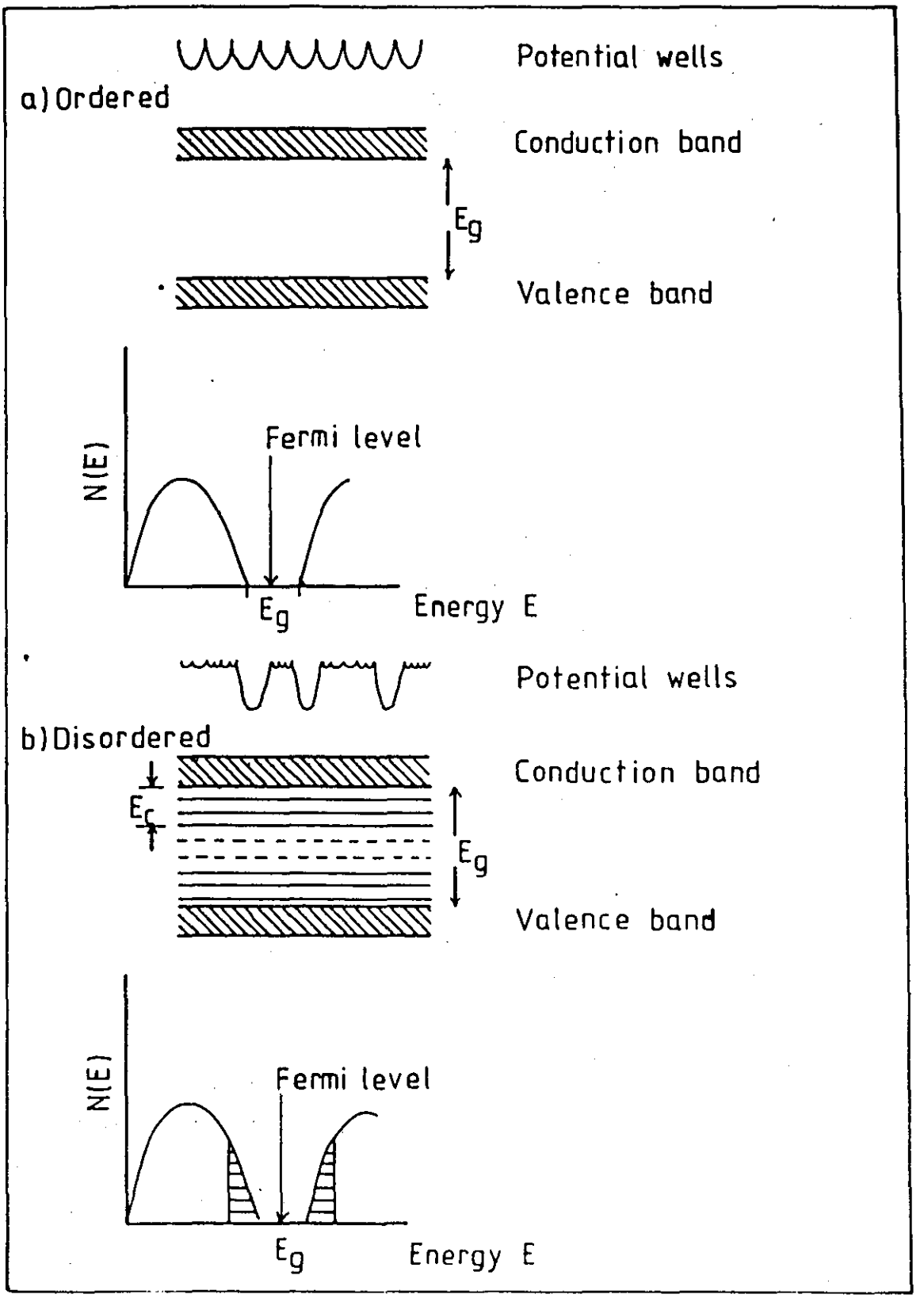

Figure 2,9

Band formation in ordered and disordered structures

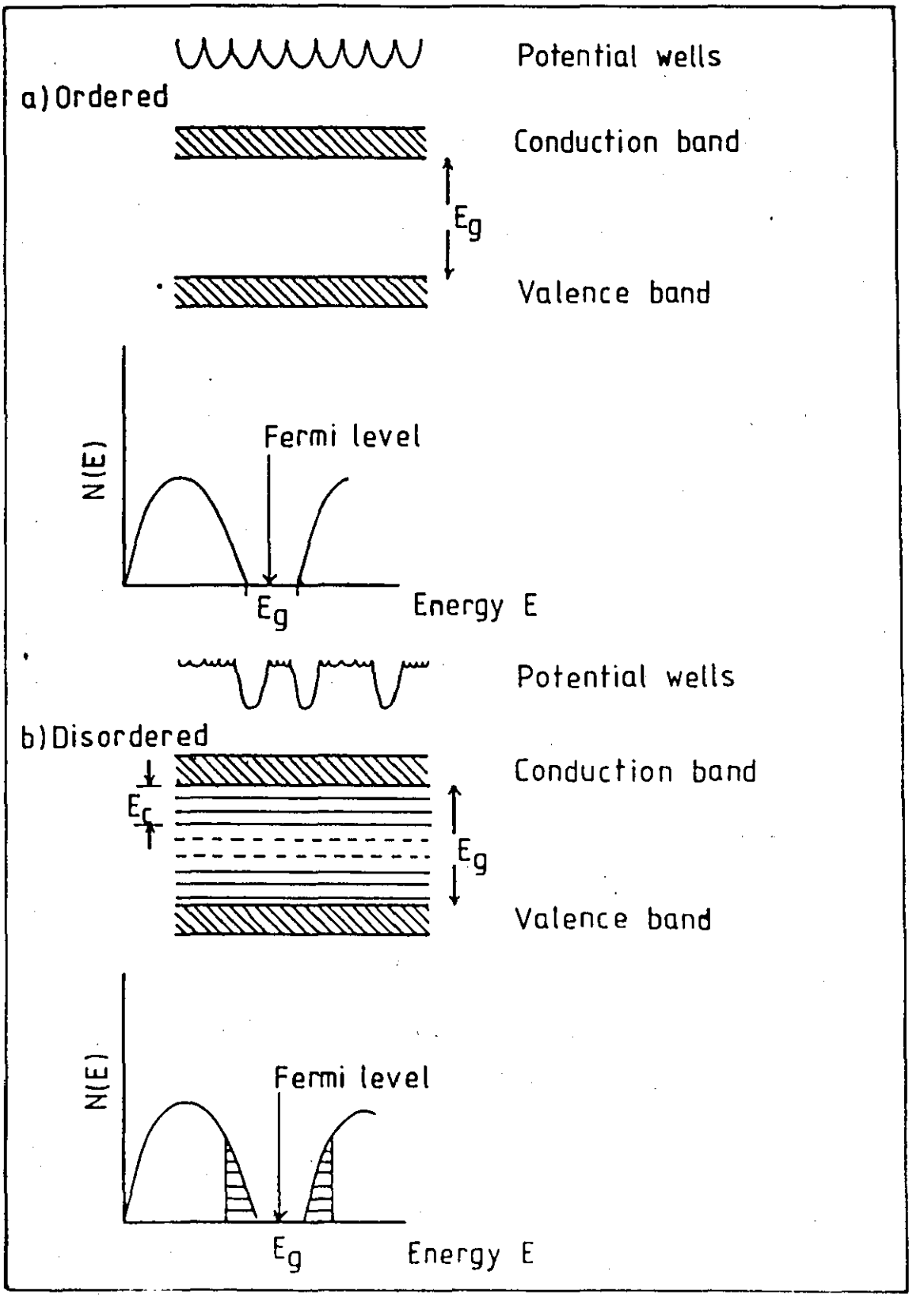

Mobility in the presence of traps is prescribed by

$$\psi_{(T)} \propto \exp(-E_\psi/kT) \tag{2.77}$$

where E_ψ is the activation energy for mobility. The conductivity becomes

$$\sigma \propto \exp - (E_n/2 + E_\psi)/kT \tag{2.78}$$

Comparison with equation (2.75) gives

$$E_a = E_\psi + E_n/2 \tag{2.79}$$

A similar approach may be made for electronic hopping processes which result in conduction. If ionic conduction occurs then E_n corresponds to the production and dissociation of ions. The mobility will be activated similarly and E_ψ will be of the same order of magnitude to those for ionic diffusion and so equation (2.79) will remain valid.

A disordered system requires a rather complex analysis. However Mott[190] has suggested a few qualitative generalisations which may be applied and are illustrated in Figure 2.9b. (i) The states of lowest energy will normally be localised, above which, some critical energy E_c, where there are no localised states. Electrons in a localised state may move either by hopping to another localised state or by thermal excitation to energy levels above E_c. (ii) Localised states may occur in the forbidden energy band.

Where intermolecular charge transfer occurs band conduction will not usually exist because of discontinuities between molecules. When a constant electric field is applied it is often difficult to differentiate between band-type conduction and hopping-type conduction. However, it has been observed[191] that for band-type conductors the conductivity is inversely proportional to frequency, whereas conductivity is proportional to frequency for hopping-type conduction.

Despite the frequency dependence the nature and source of charge carriers in many of the most insulating of polymers remains indistinct. Although ionic conduction has been observed in several polymers[188], it has been proven in relatively few[192,193]. In several examples electronic conduction processes have been equally postulated[194] such that the arguments for both are equally strong, e.g. poly(ethylene terephthalate), PET. Amborski[195] proposed that the non-linear relationship between current, field strength and temperature in PET was indicative of ionic conduction; whereas Fowler[194] suggested an electronic conduction process for PET supporting this idea with a calculation of the trap distribution required to produce the results obtained. Seanor[192] subsequently proposed a mechanism which involved both ionic and electronic conduction but where the former predominated at higher temperatures.

2.3.3 Carrier Injection

In low conducting polymers a charge carrier may be injected from the electrodes. If the carriers have to pass over a potential barrier U to enter or leave the polymer then the current I is given by

$$I \propto \exp(-U/kT) \tag{2.80}$$

The polymer-electrode interface is critical as a small variation will alter the potential barrier U and consequently produce a large variation in the conductivity. As a consequence of the Schottky effect, the effective potential barrier at the electrode will be reduced if a higher electric field is applied, the current is then given by

$$I \propto \exp \frac{-(U - e\beta E^{\frac{1}{2}})}{kT} \tag{2.81}$$

where $\beta = (e/4\pi\varepsilon'\varepsilon_o)^{\frac{1}{2}}$

ε' is the relative permittivity of the polymers, ε_o is the permittivity of face space and e is the electronic charge.

The currents in polymers may be space-charge limited. For a material with a well-defined band system without traps and with electrodes making ohmic contacts, the current density is proportional to the applied voltage V (ohmic) at low voltages (where injection is minimal), at higher voltages the current density J is given by Child's Law (a quadratic equation)

$$J = 9 \varepsilon_R \frac{\psi V^2}{8t^3} \qquad (2.82)$$

where ε_R is the static dielectric constant of the material, t is its thickness and ψ its drift mobility. Generally the current lies within a triangle as shown in Figure 2.10.

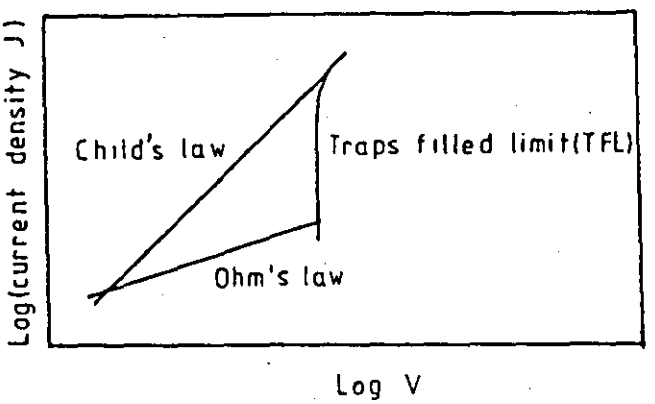

Figure 2.10 Behaviour of dielectrics with space charge limited currents

For a solid free of traps the restraints set by Child's Law (equation(2.82)) are shown in the upper curve. Similarly the restraints set by Ohm's Law are shown in the lower curve for the neutral solid (normal volume conductivity). The curve on the right represents the situation where all the traps in the solid have been filled before the voltage is applied (the traps filled limit or TFL).

2.3.4 The Effect of Structural Features

(a) Molecular Weight.

A brief review of the parameters necessary for electronic conduction have been discussed earlier. For electronic conduction to occur it has been shown that a continuum of alternating single and double bonds were necessary to provide a delocalised path for electrons. Therefore any increase in the degree of delocalisation will increase the conductivity thus higher conductivity is observed in higher molecular weight macromolecules.

The effect of molecular weight is minimal for ionic conductors up to a lower limit of approximately 10,000 where due to the plasticisation as a result of the increased number of chain ends (producing an increase in free volume and thus ion mobility) may increase conductivity. This behaviour is observed in, e.g. poly(ethylene terephthalate). No essential change in conductivity was observed in the solid polymer at 170°C [195] upon increasing molecular weight from 13,000 to 22,000. However, in the molten state at 283°C[196] by increasing the molecular weight from 9,000 to 18,000 it was observed that almost an order of magnitude fall occurred in (ionic) conductivity.

(b) Morphology and Crystallinity.

The mobility of the ions for conduction is dependent upon the free volume available therefore any process which increases the order of a system such as crystallisation is expected to decrease the ionic mobility. A reduction in ionic conduction has been noted in poly (ethylene terephthalate)[195,196] with increasing order (both crystalline and orientational). An increase in crystallinity from 10 to 50% resulted in a reduction in conductivity by a factor between 10 and 1000.

However, little is known about the effect of morphological changes with, e.g. polyacetylene [197] an increase in conductivity was observed with increasing crystallinity. This was explained in terms of a lengthening of the conjugated system thus an increase in intermolecular transfer of electrons. In contrast poly (vinyl anthracene)-iodine complexes[10] show little dependence on crystallinity.

(c) Crosslinking.

It has previously been stated that crosslinking results in a reduction of free volume thus causing a reduction in ion mobility. A decrease in conductivity has been observed [198] at the onset of crosslinking in thermosetting polymers and has been exploited as a means of determining structural parameters and the glass transition in such polymers.

(d) Ionising Radiation.

If a polymer is exposed to high energy radiation (α , X or γ) of sufficient dosage permanent changes may be induced[199].

A reduction in resistivity of nearly 4 orders of magnitude at room temperature was observed[200] when poly(ethylene) was irradiated with X-rays of dose rate 8 R/min. The current induced was found to be proportional to I^n where I is the radiation intensity and $0.5 < n < 1$. The induced current was not instantaneous upon irradiation but rose gradually.

The results were explained [194] as a production of free electrons and holes through the volume of the dielectric and the consequential formation of conduction bands whose energy distribution was governed by n.

(e) The Effect of Relative Permittivity.

The conductivity of a polymer may be markedly affected by its relative permittivity. Plasticiser, fillers or moisture may increase conduction either by increasing the relative permittivity of the mass or by self-dissociation[188]. The degree of dissociation of ion-pairs is proportional to $\exp(-V_o/\varepsilon' kT)$ where V_o is the energy required to separate ions, T is the absolute temperature, k is the Boltzmann constant and ε' is the relative permittivity. It can be shown that the volume resistivity ρ is given by

$$\log \rho = B + \frac{A}{\varepsilon'} \qquad (2.83)$$

where A + B are constants.

A similar relationship has been derived and proven for a system of cellulose acetate doped with alkali metal halides[201]. In this study it was postulated that water acted as charge carriers and consequently the theory of weak electrolytes could be applied to solid polymers containing ionic salts and water.

The creation of mobile electrons may also be affected by an increase in dielectric constant, and the effect of water absorption on charge carrier generation has been evaluated[202] and a general expression derived:

$$\sigma_{(T,\varepsilon')} = \sigma_o \exp\left(-\frac{E_d}{2kT} \exp\left(\frac{k}{T}\left(\frac{1}{\varepsilon'} - \frac{1}{\varepsilon_1'}\right)\right)\right) \qquad (2.84)$$

where E_d is the work required to separate the electron and hole in the dry material, k is a constant, ε' and ε_1' are the dielectric constants of the dry and wet materials respectively. At constant temperature equation (2.84) becomes (2.83).

Rosenberg[202] has further predicted

$$\log \sigma = Cm + D \qquad (2.85)$$

where m is the water content and C and D are constants. Good agreement has been found when applying equation (2.83) to the experimental data.

Eley and Leslie[203] have shown that water may act as an electron donor such that

$$\log_{10} \sigma = F + \log_{10}(m^{\frac{1}{2}}) + km^{x} \qquad (2.86)$$

where F and k are constants and x is a constant dependent upon the distribution of water molecules.

The difficulty in determining conduction processes in polymers was again highlighted by Eley and Leslie[203] using Rosenberg's[202] data. Equation (2.86) gave almost as good a fit when $X = {}^{1}/3$ as equation (2.85).

2.4 Dielectric Heating Theory

It was shown in section 2.2.2 that when a sinusoidally oscillating voltage is applied to a capacitor a complex alternating field I^{*} results where

$$I^{*} = I_R + jI_c \qquad (2.87)$$

The current I_c which leads the voltage by 90^{o} is given by

$$I_c = wCV \qquad (2.88)$$

The capacitance (C in picofarads) of a parallel plate capacitor is given by

$$C = 0.0884\varepsilon' \cdot \frac{A}{d}$$

where A and d are the area and thickness of the capacitor respectively.

The electrical power in the dielectric loss component is given by

$$P = VI_R \tag{2.89}$$

$$= 0.0884w \cdot \varepsilon' \cdot \frac{A}{d} \tan\delta V^2 \text{ watts}$$

$$= 0.555 \left(\frac{V}{d}\right)^2 \cdot f \cdot \varepsilon' \cdot \tan\delta \text{ watts/unit volume} \tag{2.90}$$

Hence if the density of the dielectric is ρ and its specific heat C_p, it can be shown that the rate of heating will be

$$\frac{\Delta T}{t} = 0.133 \cdot \frac{f}{\rho C_p} \cdot \left(\frac{V}{d}\right)^2 \cdot \varepsilon' \tan\delta \ ^\circ C/\text{sec} \tag{2.91}$$

The dielectric properties of a blended material may be described in terms of a predominantly series model described by a three-layer structure.

The dielectric properties of a 3-layer sandwich are shown below

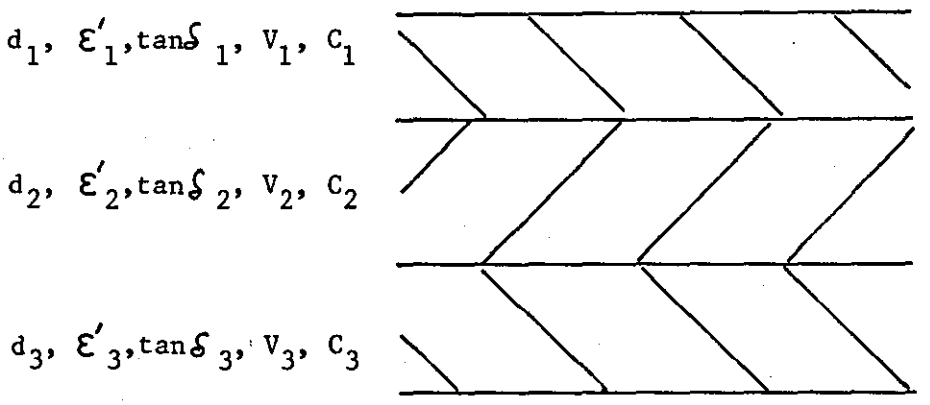

where d_1 V_1, d_2 V_2, d_3 V_3 are the thicknesses and voltages across each layer.

The instantaneous charge across each layer will be the same

$$Q = Q_1 = Q_2 = Q_3 \tag{2.92}$$

but $Q = CV$

therefore $Q_1 = V_1C_1$ $Q_2 = V_2C_2$ and $Q_3 = V_3C_3$ (2.93)

hence $V_1 : V_2 : V_3 = \frac{1}{C_1} : \frac{1}{C_2} : \frac{1}{C_3}$ (2.94)

which for parallel plate capacitors of the same area gives

$$V_1 : V_2 : V_3 = \frac{d_1}{\varepsilon'_1} : \frac{d_2}{\varepsilon'_2} : \frac{d_3}{\varepsilon'_3} \qquad (2.95)$$

From equation (2.91) the heating rate in each layer is given by

$$\left(\frac{\Delta T}{t}\right)_1 = 0.133 \cdot \frac{f}{\rho_1 C_{p1}} \cdot \left(\frac{V_1}{d_1}\right)^2 \cdot \varepsilon'_1 \cdot \tan\delta_1 \ ^{o}C/sec$$

The heating effects per unit volume in each layer will be related as follows:

$$\left(\frac{\Delta T}{t}\right)_1 : \left(\frac{\Delta T}{t}\right)_2 : \left(\frac{\Delta T}{t}\right)_3 = \frac{\tan\delta_1}{\varepsilon'_1 \cdot \rho_1 \cdot C_{p1}} : \frac{\tan\delta_2}{\varepsilon'_2 \cdot \rho_2 C_{p2}} : \frac{\tan\delta_3}{\varepsilon'_3 \cdot \rho_3 C_{p3}} \qquad (2.96)$$

Therefore the rate of energy up-take (H) by each layer per unit volume is related as follows

$$H_1 : H_2 : H_3 = \frac{d_1 \tan\delta_1}{\varepsilon'_1 \cdot \rho_1 \cdot C_{p1}} : \frac{d_2 \tan\delta_2}{\varepsilon'_2 \cdot \rho_2 \cdot C_{p2}} : \frac{d_3 \tan\delta_3}{\varepsilon'_3 \cdot \rho_3 \cdot C_{p3}} \qquad (2.97)$$

It can be seen from equation (2.96) that the governing parameter for dielectric heating is $(\tan\delta / \varepsilon')$.

3.0 EXPERIMENTAL

3.1 Purification and Characterisation of Polymers Studied

3.1.1 Poly(ethylene glycol)

Low molecular weight poly(ethylene glycol) (supplied by Shell Ltd.) was heated to above its melting point and degassed at 70°C under vacuum until required.

3.1.2 Poly(propylene glycol)

Several poly(propylene glycols), trade names PPG1500, PPG2000, PPG6000, PPG10,000 (obtained from Shell Ltd.) were degassed at 50°C under vacuum until required.

3.1.3 Poly(tetramethylene glycol)

Two low molecular weight poly(tetramethylene glycols), Polymeg's 1040 and 2010 (supplied by Quaker Oats Co.) were degassed at 50°C under vacuum until required.

3.1.4 Poly(tetramethylene oxide)

Poly(tetramethylene oxide), $\overline{M}n$ 10,000, was supplied courtesy of Polymer Laboratories Ltd. It was degassed at 70°C under vacuum and stored until required.

3.1.5 Poly(methyl vinyl ether)

Low molecular weight poly(methyl vinyl ether) (obtained from Polysciences Inc.) was degassed under vacuum at 50°C until required.

3.1.6 Poly(ethyl vinyl ether)

Poly(ethyl vinyl ether),(was supplied courtesy of B.A.S.F. Ltd.)

under the trade name Lutonal A50, was dissolved in dry methanol to give a 5% wt./vol. solution. During the commercial polymerisation cross-linking processes may occur forming insoluble particles. The 5% solution was therefore filtered and the solvent evaporated off and the polymer subsequently stored under vacuum at 50°C until required.

Two other copolymers containing polyethylene and propylene oxides were also investigated. These were supplied by Lankro and were stored at 50°C under vaccum until required.

3.2 Preparation of Polymer - Inorganic Salt Complexes

All the complexes were prepared in essentially the same manner. The salt and polymer were dissolved separately in a mutual solvent and the two solutions thoroughly mixed together. The solvent was then removed to leave the complex.

Evidently the solvent chosen must be a good solvent for both the polymer and the salt, and should have a relatively low boiling point to facilitate its subsequent removal. Acetone, methanol and ethanol were found to be suitable for the above requirements. The solvent chosen depending upon the particular complex being prepared.

All salts used were anhydrous; to remove any possible hydration they were stored for some time under vacuum prior to use.

Three specific methods for the production of complexes were employed and will be described in detail below.

3.2.1 Poly(tetramethylene oxide)

A known amount of vacuum dried poly(tetramethylene oxide) was dissolved in A.R. ethanol (dried over 3Å molecular sieve). An approximately 5% w/v solution of anhydrous salt and dry ethanol was prepared.

An aliquot of the salt solution was added to the polymer solution and thoroughly mixed to give the desired molar ratio of salt to monomer units. The resultant polymer/salt solution was then poured into a crystallisation dish and placed in a vacuum dessicator. The solvent was slowly removed by periodically applying a partial vacuum to the dessicator. When the solution became viscous, the crystallisation dish was transferred to a vacuum oven, and tbe remaining solvent was removed under vacuum at 70°C.

3.2.2 Poly(ethyl vinyl ether)

A solution of known concentration of poly(ethyl vinyl ether) was prepared by dissolving the polymer in A.R. grade ethanol (dried over 3Å molecular sieve). A salt solution was prepared as described in 3.2.1. An aliquot of salt solution was added to an aliquot of the polymer solution to produce the required molar ratio of salt to monomer units. The resultant solution was stirred to ensure good mixing, and poured into a circular glass mould which had a detachable tin base. Dry nitrogen/air was passed over the solution at ambient temperature until the majority of solvent was removed. The sample was then placed under vacuum at 70°C to remove the final traces of solvent.

Both poly(ethyl vinyl ether) and poly(methyl vinyl ether) are very tacky and hence precluded the methods described in 3.2.1 or 3.2.3. The size of the mould was dictated by the size of the dielectric cell described later.

3.2.3 Poly(propylene glycol)

A third method was employed for the preparation of all the low viscosity glycols. 50g of poly(propylene glycol) was dissolved in 250 mls of dry acetone (dried over 3Å molecular sieve) in a rotary-evaporator flask. The flask was placed on a rotary-evaporator in a

water bath and rotated until the polymer had dissolved. A quantity of anhydrous salt was dissolved in the polymer solution to give the desired molar ratio of salt to monomer units. A small partial vacuum was then periodically applied to the rotating flask and subsequently the solvent condensed into a collecting flask on the rotary-evaporator. As the viscosity of the polymer-salt solution increased, the temperature of the water bath was increased. After removing the majority of the solvent the flask was left to rotate under constant vacuum at 80°C for several hours. The resulting polymer/salt complex was stored under vacuum until required.

3.2.4 Polymer Blend Preparation

Polymer blends of inorganic salt complexes and low dielectric constant polymers were prepared using a Brabender internal mixer. The blends were prepared at temperatures above the softening point of the low dielectric constant polymers. Upon blending, the observed torque is seen to fall as the friction between blending components reduces. For all blends the torque reached a minimum value at which point the mixer was allowed to continue blending for a further few minutes to ensure thorough blending.

3.3 Differential Thermal Analysis

(a) Apparatus

The glass transition temperatures (Tg) of the polymer-salt complexes were determined using a Du Pont 900 Differential Thermal Analyser equipped with the Differential Scanning Calorimetry Accessory (Catalogue No. 900600). A diagram of the cell is shown in Figure 3.1. A sample pan and a reference pan were positioned on the two raised platforms on the constantan disc as shown. A constant heating rate is maintained within the cell by the single heating block. In the calorimetric mode

Figure 3,1

Calorimetry Cell

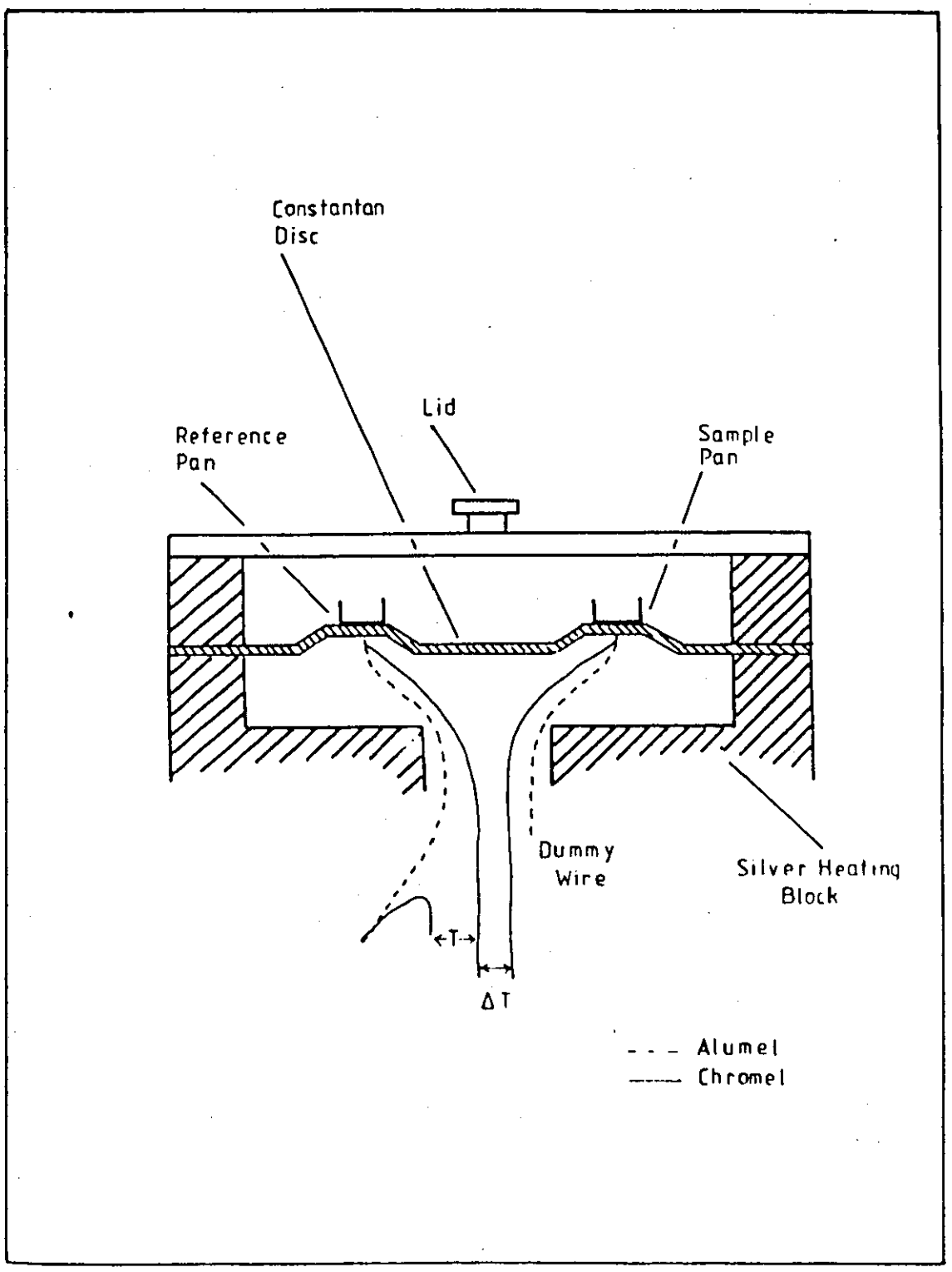

the temperature difference (ΔT) between the sample pan and the reference junction was plotted against the reference pan temperature. The instrument was calibrated using mercury and benzoic acid which melt at $-39^{o}C$ and $122^{o}C$ respectively.

Figure 3.2 shows a characteristic thermograph of a step response glass-rubber transition. For this work Tg has been defined such that:

$$Tg = \tfrac{1}{2} (T_H + T_J) \qquad (3.1)$$

where T_H and T_J are as shown in the diagram.

(b) Experimental Technique

Samples of the polymer-salt complex ($\sim$ 5-10 mg) were accurately weighed into aluminium pans and sealed to prevent the absorption of water. An empty aluminium pan was used as a reference. From the known sample weights a correlation with the Tg step as measured by the baseline shift was determined. Liquid nitrogen was used to cool the calorimetry cell down to $-100^{o}C$. The samples were then heated at $15^{o}C$/min to a temperature of $150^{o}C$.

3.4 Dielectric Measurements

(a) Apparatus

Low frequency dielectric measurements were undertaken using a Wayne Kerr B221 Universal Bridge, a Wayne Kerr A321 waveform analyser and an Advance Instruments low frequency oscillator. Each piece of equipment was operated as described in their respective instruction manuals.

The Wayne Kerr Bridge is a transformer ratio arm bridge designed for the measurement of high loss systems. The bridge regards the sample as equivalent to a capacitance C in parallel with a resistance

Figure 3,2

An Idealized Glass Transition

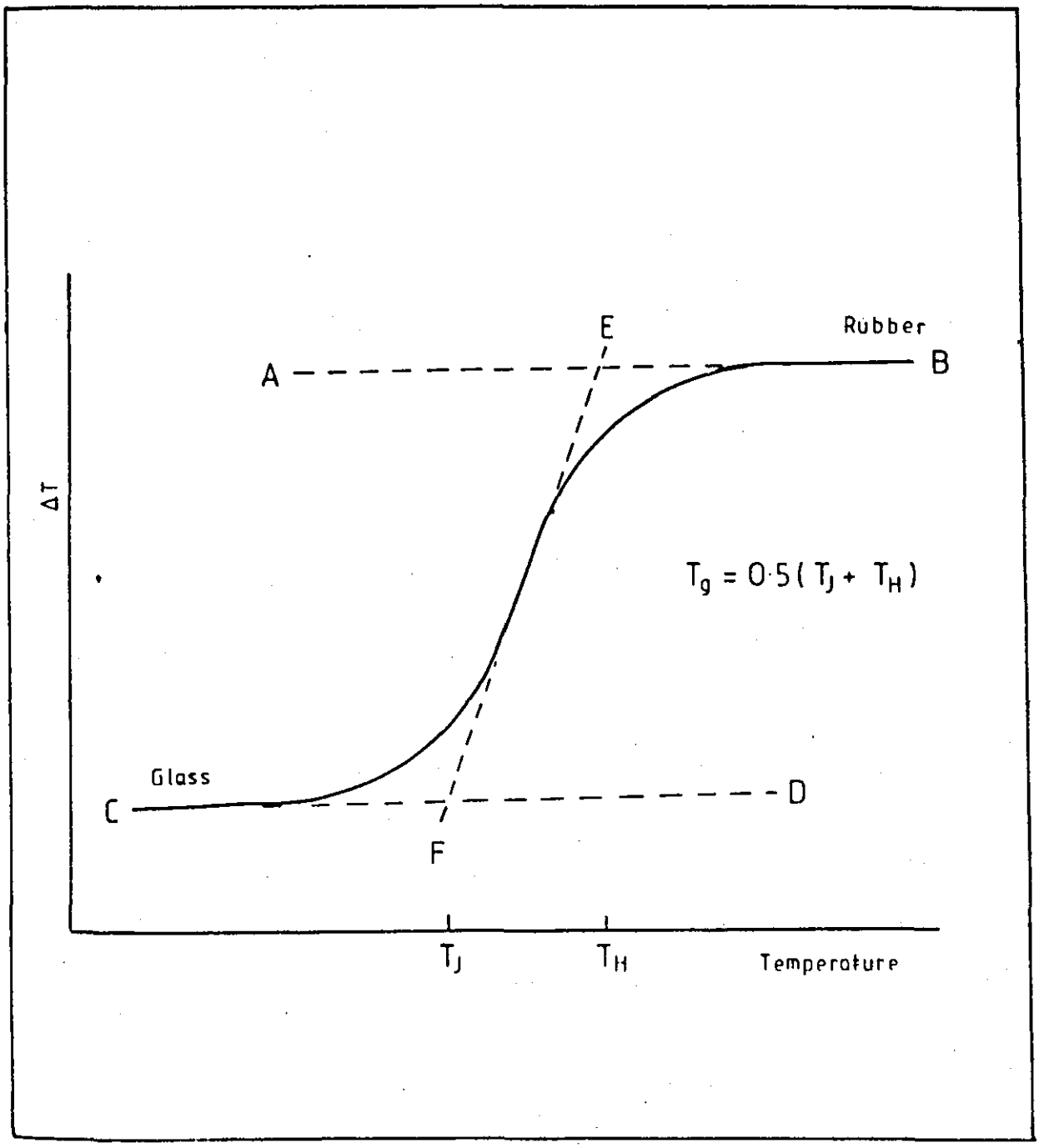

R. It can be shown[155] for such a system that:

$$\varepsilon' = \frac{C}{C_o} \tag{3.2}$$

$$\varepsilon'' = \frac{1}{R w C_o} \tag{3.3}$$

$$\tan\delta = \frac{1}{RCw} \tag{3.4}$$

where C_o, ε', ε'', $\tan\delta$ and w are as previously defined. Values for capacitance C and conductance G, where $G = R^{-1}$ are read directly from the bridge.

ε' could be calculated from equation (3.2) and ε'' was calculated from:

$$\varepsilon'' = \frac{10^6 G}{2\pi f C_o} \tag{3.5}$$

where G is in μ Mho, C_o in pf and f is in Hz.

From values of ε' and ε'', $\tan\delta$ may be calculated from:

$$\tan\delta = \frac{\varepsilon''}{\varepsilon'} \tag{3.6}$$

Capacitance and conductance measurements could be made to within $\pm$ 0.1% and $\pm$ 1% respectively.

Measurements were made in the frequency range 10^2 to 10^5 Hz and in the temperature range -60°C to +100°C. A solid sample in the form of a flat disc was positioned in a three terminal cell which was essentially a modified Wayne Kerr Solid Dielectric Permittivity Jig (Model D321) as described previously by Fielding Russell[204]. The cell is shown in Figure 3.3. The three terminal cell eliminated fringing fields and surface conduction across the edge of the sample. Electrode E_1 was shielded by a guard ring G separated by a 0.23 mm wall of epoxy resin. The field thus acts over an area given by:

$$A = \pi (r + \delta r/2)^2 \tag{3.7}$$

Figure 3,3

A Three-terminal Dielectric Cell

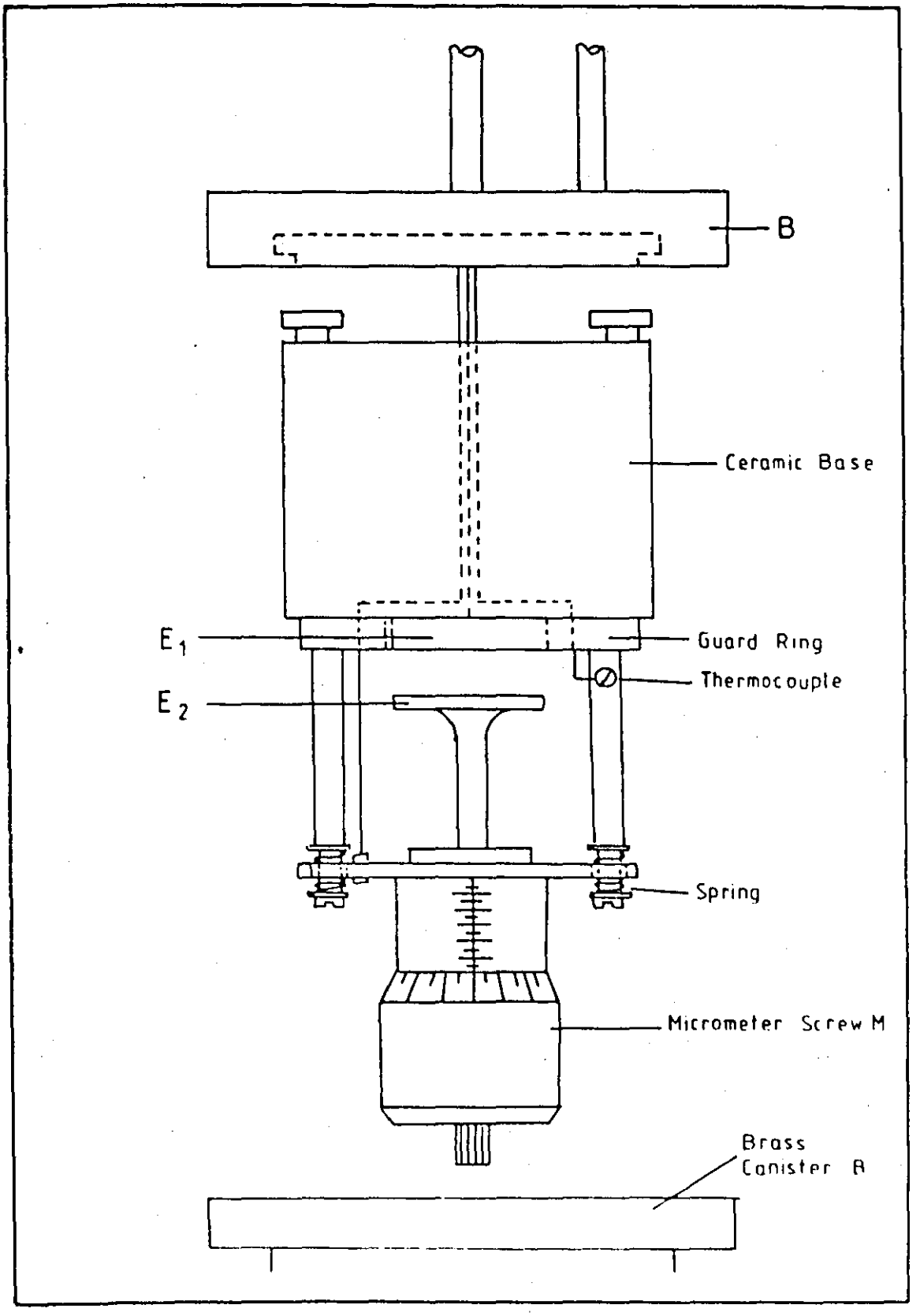

where r is the radius of electrode E_1 and δr is the thickness of the epoxy resin wall. Electrode E_2 could be moved up or down using the micrometer screw M. A copper/constantan thermocouple adjacent to the sample monitored the cell temperature. The whole assembly fitted into a vacuum tight brass canister.

The capacitance of the dielectric cell with space between the electrodes evacuated was given by:

$$C_o = \frac{A}{3.6 \pi d} \text{ pf} \qquad (3.8)$$

where A is the effective area as previously defined and d is the thickness of the sample.

High frequency dielectric measurements, i.e. greater than 20 kHz were taken using a Marconi Dielectric Test Set 704C. It is a development of the original high frequency dielectric test set designed by Hartshorn and Ward[203]. A simplified circuit is shown in Figure 3.4. The circuit is composed of two plug-in oscillators covering the frequency ranges 0.05 M Hz to 20 MHz and 10 MHz to 100 MHz. The amplitude of the oscillator output is controlled by an arrangement of coarse and fine resistors. The oscillator circuit was loosely coupled to a tuned circuit of various interchangeable coils L and two precision parallel plate capacitors with micrometer adjustment.

The principle of the apparatus was to equate the capacitance of the dielectric with that of a measured air gap. This was achieved by tuning for resonance at a particular frequency with the dielectric in place, removing the dielectric and re-establishing resonance with a measured air gap. Resonance was detected by a square law voltmeter V.

The instrument is tuned for resonance when the galvanometer is showing a maximum deflection. The half-width of the resonance

HIGH FREQUENCY CIRCUIT

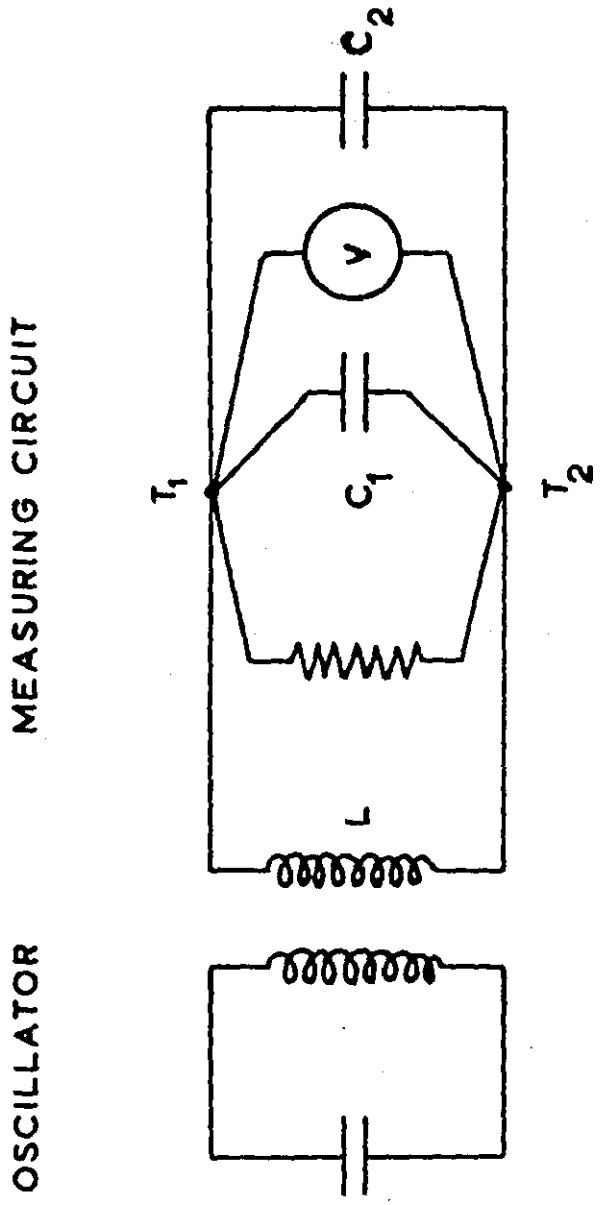

FIGURE 3·4

curve was determined by adjusting the micrometer until a galvanometer reading of $2^{-\frac{1}{2}}$ either side of the resonance peak.

This process was used to obtain the resonance peaks and half widths of both the 'dielectric in' and 'dielectric out' (air gap). The dielectric constant was calculated from:

$$\varepsilon = \frac{C_s}{C_o} \qquad (3.9)$$

where C_s is the sample capacitance obtained from the reading of the large micrometer at resonance with an air gap minus the reading of the capacitor at resonance with the sample connected, C_o is derived from (3.8). Micrometer readings can be converted to capacitance by:

$$\text{Capacitance pf} = \frac{1850}{R-0.6-0.02(T-23)} + (C_m-C_c) \qquad (3.10)$$

where R is the 'head' reading expressed as hundredths of a mm, T is the temperature in Celsius, (C_m-C_c) are given in the manufacturer's manual.

Tan δ is given by:

$$\tan\delta = \frac{\Delta C_i - \Delta C_o}{2C_s} \qquad (3.11)$$

where ΔC_i and ΔC_o are the differences in half widths between the dielectric in and out respectively.

is given by:

$$\varepsilon'' = \varepsilon' \tan\delta \qquad (3.12)$$

(b) Experimental Technique

Samples of poly(vinyl ethers) containing metal salts were cast directly onto tin foil as previously stated. These samples were loaded into the dielectric cell previously described, placed inside the brass container, sealed and evacuated.

The other samples were either highly viscous liquids or low melting point solids. These obviously would not remain in the cell described above so a new cell was made to contain these. Figure 3.5 shows the cell used for the dielectric measurements of all samples except the poly(vinyl ethers).

Two polished stainless steel electrodes were separated by macor ceramic rods. The upper electrode was attached to a micrometer screw which facilitated variation of the gap between the electrodes. Measurement of the gap size could be read directly from the micrometer. A copper-constantan thermocouple placed close to the electrodes enabled accurate measurement of the sample temperature.

The polymer-salt complexes are deliquescent, therefore, to ensure a water-free atmosphere was maintained, dry nitrogen was blown over the system for the duration of the experiment.

Both of the cells described were cooled and heated in the same manner. To cool the cells the cell containers were placed in a methanol bath and solid carbon dioxide was added to bring the temperature gradually down to -50°C. The temperature could be controlled to within $\pm$ 0.5°C using this method. Above ambient temperatures were achieved by immersing the cells in oil baths thermostated to $\pm$ 0.1°C. Readings were taken at approximately 5°C intervals over the entire temperature range studied. To ensure that steady state conditions prevailed, the heating/cooling rate was slow, approximately 10°C $hr.^{-1}$ and the required temperature was kept constant for twenty minutes before a reading was taken. From the data it was possible to obtain values of ε', ε'' and tan δ for each temperature and frequency.

LIQUID DIELECTRIC CELL

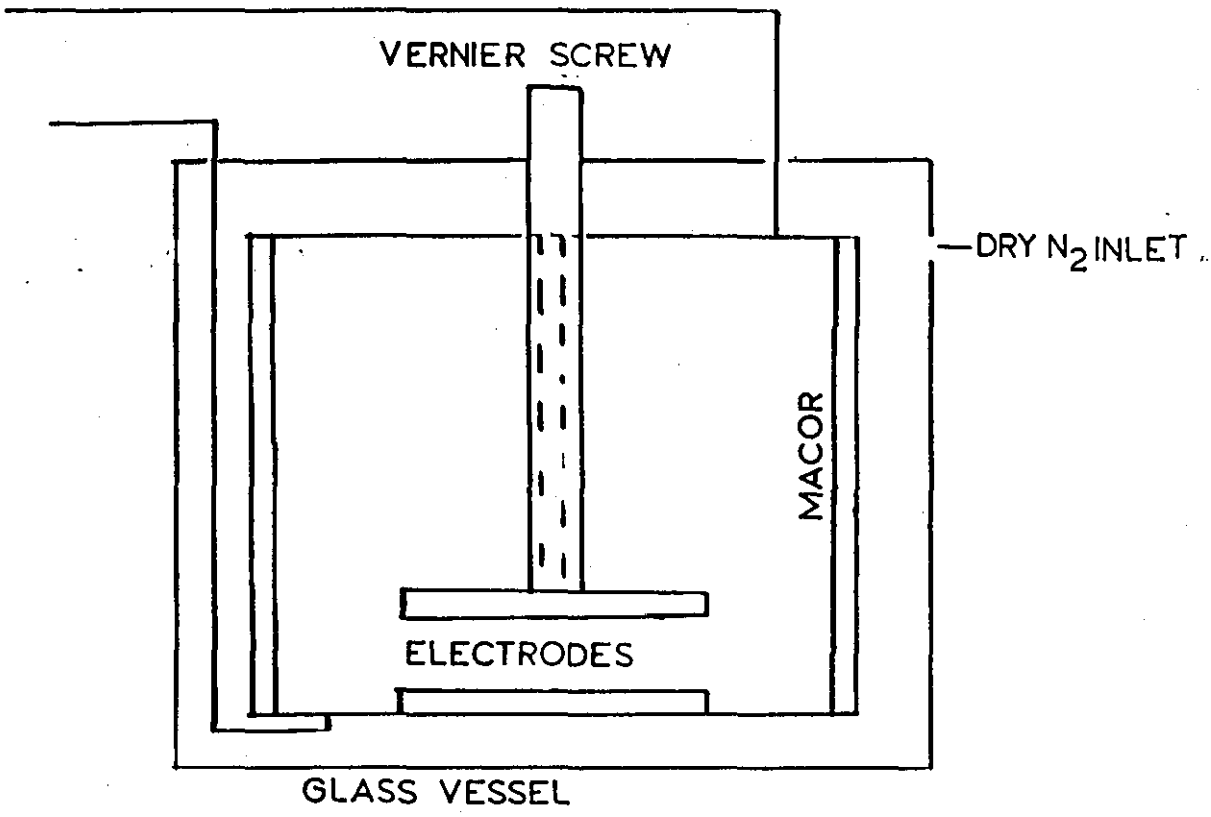

FIGURE 3·5

3.5 Viscosity Measurements

(a) Apparatus

Viscosities of several samples were obtained using a Contraves Rheomat 15T-FC cone and plate viscometer. A diagram of the cone and plate is shown in Figure 3.6. The instrument was operated as described in the instrument manual.

The Rheomat consists of a stainless steel cone and plate. The liquid to be measured is placed between the cone and plate. The cone makes a very small angle to the plate. The plate is fixed and the cone rotates at a fixed angular velocity the resulting torque is derived as follows from a form of the Navier[206a] - Stokes[206b] equation for Newtonian liquids:

$$\frac{d^2w}{dr^2} + \frac{4dw}{rdr} + \frac{1}{r^2}\frac{d^2w}{d\theta^2} + \frac{3\cos\theta}{r^2}\frac{dw}{d\theta} = 0 \qquad (3.13)$$

where at the boundaries $w = 0$, for $\theta = (\pi/2) - \alpha$ $w = \Omega$ for $\theta = \pi/2$ and r, θ and ϕ are the spherical polar coordinates for the stationary state and α is the angle between the cone and plate.

Integrating the moment of the shear stress

$$\tau_{\theta\phi} = \eta \sin\theta \cdot dw/d\theta \qquad (3.14)$$

over the surface of the disk we obtain

$$M = \frac{2\pi a^3}{3}\eta\Omega\left(\int_{(\pi/2)-\alpha}^{\pi/2}\frac{d\theta}{\sin^3\theta}\right)^{-1} \qquad (3.15$$

where a = radius of the plate

therefore

CONE AND PLATE VISCOMETER

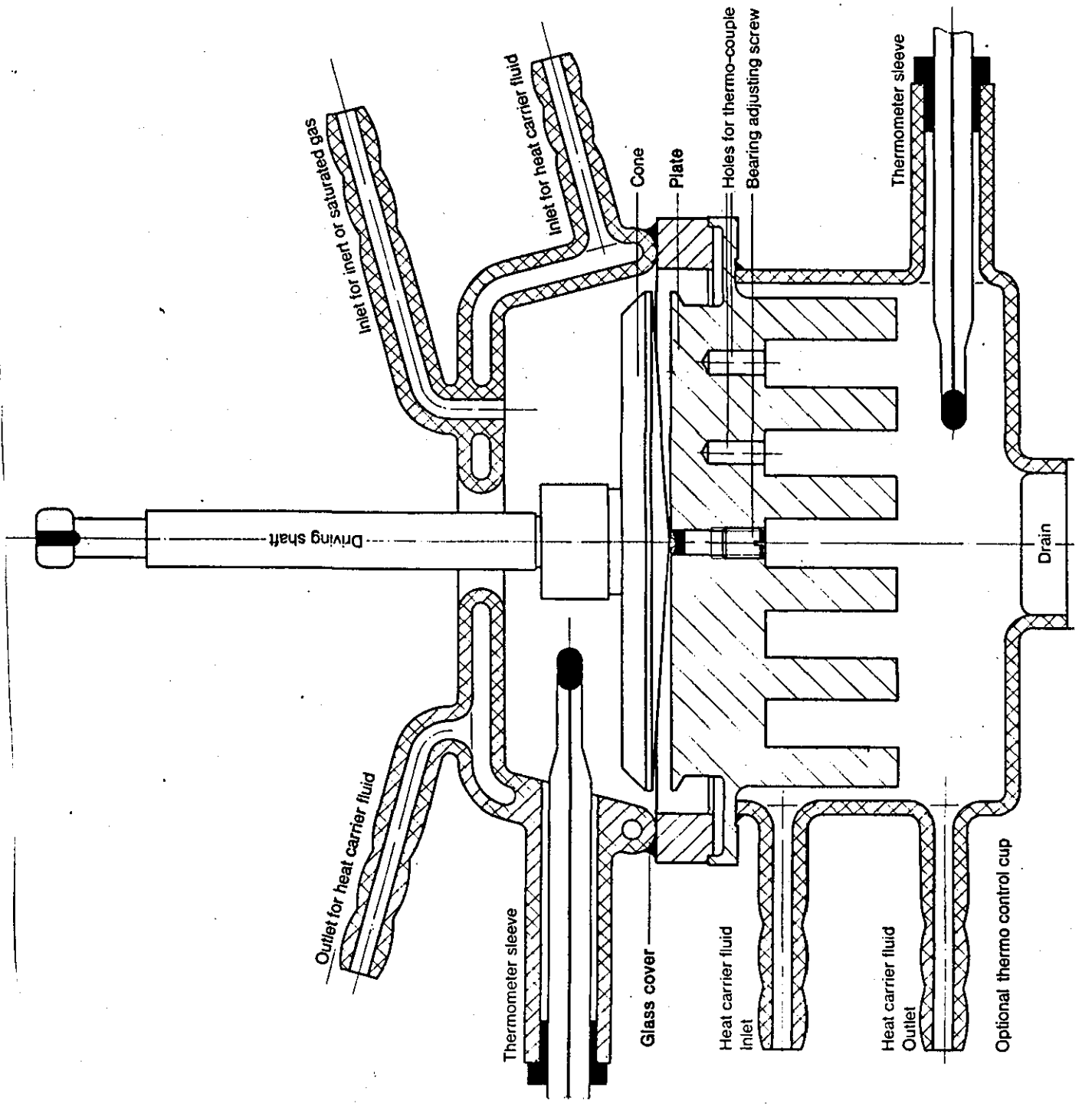

FIGURE 3·6

$$M = \frac{4\pi a^3}{3}\,\eta\,\Omega\left(\frac{\sin\alpha}{\cos^2\alpha} - \ln\tan\left(\frac{\pi}{4} - \frac{\alpha}{2}\right)\right)^{-1} \qquad (3.16)$$

which is valid for any value of α. For small values of α (3.16) abbreviates to

$$M = \frac{2\pi a^3}{3\alpha}\,\eta\,\Omega \qquad (3.17)$$

If one considers a point P on the rotating cone at a distance r from the centre of the plate. The velocity at P is $r\Omega$ the liquid thickness is approximately $r\alpha$ therefore the rate of shear $\dot{\gamma}$ is uniform and equal to Ω/α. Consequently shear stress τ is uniform and the torque M is given by

$$M = \int_0^{2\pi}\int_0^a r \cdot \tau r \; d\phi \; dr = \frac{2\pi a^3}{3}\,\tau \qquad (3.18)$$

for a linear viscoelastic liquid.

It is therefore reasonable to assume that if α is small the rate of shear and shear stress will be uniform for a Newtonian liquid.

The Rheomat facilitates measurement of shear stress and shear rates from 5.6 rpm to 352 rpm. However the torque produced limits the shear rate at high viscosities. At a given shear rate a shear stress is produced. The shear stress is read as a voltage output on a digital voltmeter. The viscosity is calculated as follows:

$$V \propto \tau \qquad (3.19)$$

$$R \propto D \qquad (3.20)$$

$$\tau = \eta D \qquad (3.21)$$

$$\therefore \quad V = K\eta R \qquad (3.22)$$

where V is the voltage output, R is the rpm, τ and D are the shear stress and strain respectively, η is the viscosity and K is a machine constant.

A plot of V versus R produces a straight line of slope $K\eta$. If a liquid of known viscosity is placed in the instrument K may be deduced.

It follows that viscosity of a liquid may be found by plotting V versus R for that system and calculating the subsequent slope of the graph, knowing K, η the viscosity may be calculated.

(b) Experimental Technique

Approximately 20 g of a polymer-salt complex was placed on the plate. The cone was then quickly placed on the sample and dry nitrogen passed over the cone and plate to maintain a dry atmosphere. Any excess polymer-salt complex flowed over the side of the plate onto the recess around the plate. Obviously for solutions of relatively high viscosity it was necessary to perform this operation at elevated temperatures. Values of V were taken for stepwise increases in R until the torque limit was reached. This procedure was repeated.

The temperature was increased by $10^{o}C$ from ambient up to $140^{o}C$ by placing the plate fins of the Rheomat in an oil bath. The fins ensured good thermal contact between the sample and the oil bath and thus the heating rate was $20^{o}C\ hr^{-1}$ in comparison to $10^{o}C\ hr^{-1}$ in the dielectric measurements. Time was allowed for the samples to reach thermal equilibrium as described previously.

It was not possible to measure the viscosities of the more viscous samples at room temperature by this process, thus values were only obtainable at the upper end of the temperature scale for these samples.

4.0 RESULTS

4.1 Characterisation of Polymers Studied

The molecular weights, glass transition temperatures, trade names and suppliers of the polymers studied are given in Table 4.1.

Table 4.1 also includes the melting points of poly(ethylene glycol) and poly(tetramethylene glycol).

4.2 Poly(propylene glycol) Containing Inorganic Salts

4.2.1 General Properties

The complexes were prepared in accordance with methods described in section 3.2. Table 4.2 illustrates the general properties of inorganic salt complexes of poly(propylene oxide). Two types of compounds are clearly discernible from this Table.

Compounds of the first type were formed from highly deliquescent salts. The resulting complexes were optically transparent and as will be shown later the glass transitions were shifted to higher temperatures in comparison to the original polymer. At ambient temperatures the majority of compounds prepared were above their glass transitions and were viscous liquids. The compounds were sensitive to water, which if present led to plasticisation and a subsequent reduction of Tg. The compounds were however pointedly less deliquescent than the parent salts. It was therefore obviously of prime importance that the compounds were maintained in an anhydrous environment from the period of manufacture to usage.

The second type of compounds were formed from strongly crystalline alkli chlorides and fluorides. They were opaque and distinctly two-phase. The compounds were very water sensitive and even at low salt

TABLE 4.1 Characterisation of the Polymers Studied

Polymer	Trade Name	Supplier	Tg(^{o}C)	Tm(^{o}C)	$\overline{M}_w$	$\overline{M}_n$	$\overline{M}_w/\overline{M}_n$	$\overline{M}_v$
Poly(ethylene glycol) (Semi-crystalline)	PEG 600	Shell Ltd.	-62.7	23.25	-	-	-	-
Poly(propylene glycol) (Amorphous)	PPG 2000	Shell Ltd.	-62	-	1990	1600	1.2	-
Poly(tetramethylene glycol) (Semi-crystalline)	Polymeg 1040	Quaker Oats Co.	-76	24	-	-	-	-
Poly(methyl vinyl ether) (Amorphous)	--	Polysciences Inc.	-24.5	-	-	-	-	4,800
Poly(ethyl vinyl ether) (Amorphous)	Lutonal A50	BASF (UK) Ltd.	-27.5	-	-	-	-	37,200
Poly(propylene glycol) (Amorphous)	P3	Lankro	-66	-	1500	-	-	-
Poly(propylene /Ethylene glycol) (Amorphous)	P317	Lankro	-68	-	1500	-	-	-

TABLE 4.2 Visual Properties of Inorganic Salt Complexes of Poly(propylene oxide)

Metal Salt	Colour of Complex	Optical Clarity	Comments
Lithium thiocyanate	Colourless	Transparent	Single phase, viscous liquids at room temperature. Viscosity was found to increase with increasing salt content. Less deliquescer than their constituent chemicals.
Sodium thiocyanate	"	"	
Potassium thiocyanate	"	"	
Ammonium thiocyanate	"	"	
Calcium thiocyanate	"	"	
Barium thiocyanate	"	"	
Lithium iodide	"	"	
Ammonium iodide	"	"	
Lithium trifluoro-methyl sulphonate	"	"	
Zinc chloride	"	"	
Zinc bromide	"	"	
Tin (II) chloride	"	"	
Lithium chloride	Colourless	Opaque	Hygroscopic two phase liquids
Sodium fluoride	"	"	

loadings blooming of the salt occurred.

Subsequent work in this thesis will confirm that compounds of the first type were true, single phase complexes and those of the second type were two phase compounds where the inorganic salt acts as a second phase filler with no significant chemical interaction taking place between the salt and the polymer.

4.2.2 Glass Transition Data for Inorganic Salt Complexes of Poly(propylene glycol)

Single glass transitions were observed for salt complexes of poly(propylene glycol). The glass transitions were well defined although at higher salt loadings a broadening was observed. Figures 4.1 and 4.2 illustrate the observations stated above.

The Tg of a salt complex varies with the mole percentage of inorganic salt incorporated and is illustrated in Figure 4.3. It is clearly discernible that a non-linear relationship exists between salt loading and the subsequent value of Tg. A maximum elevation of Tg appears to occur around 20 mole % salt loading. It is also clearly evident that different cations and anions elevate Tg with differing degrees of magnitude.

The size of the glass transition was empirically measured by calculating the step height(as shown below) per unit weight of material measured.

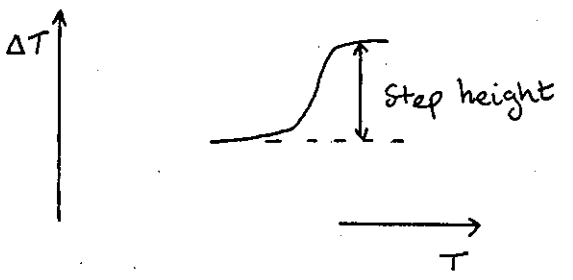

GLASS TRANSITIONS EXHIBITED BY SALT COMPLEXES OF POLY(PROPYLENE GLYCOL)

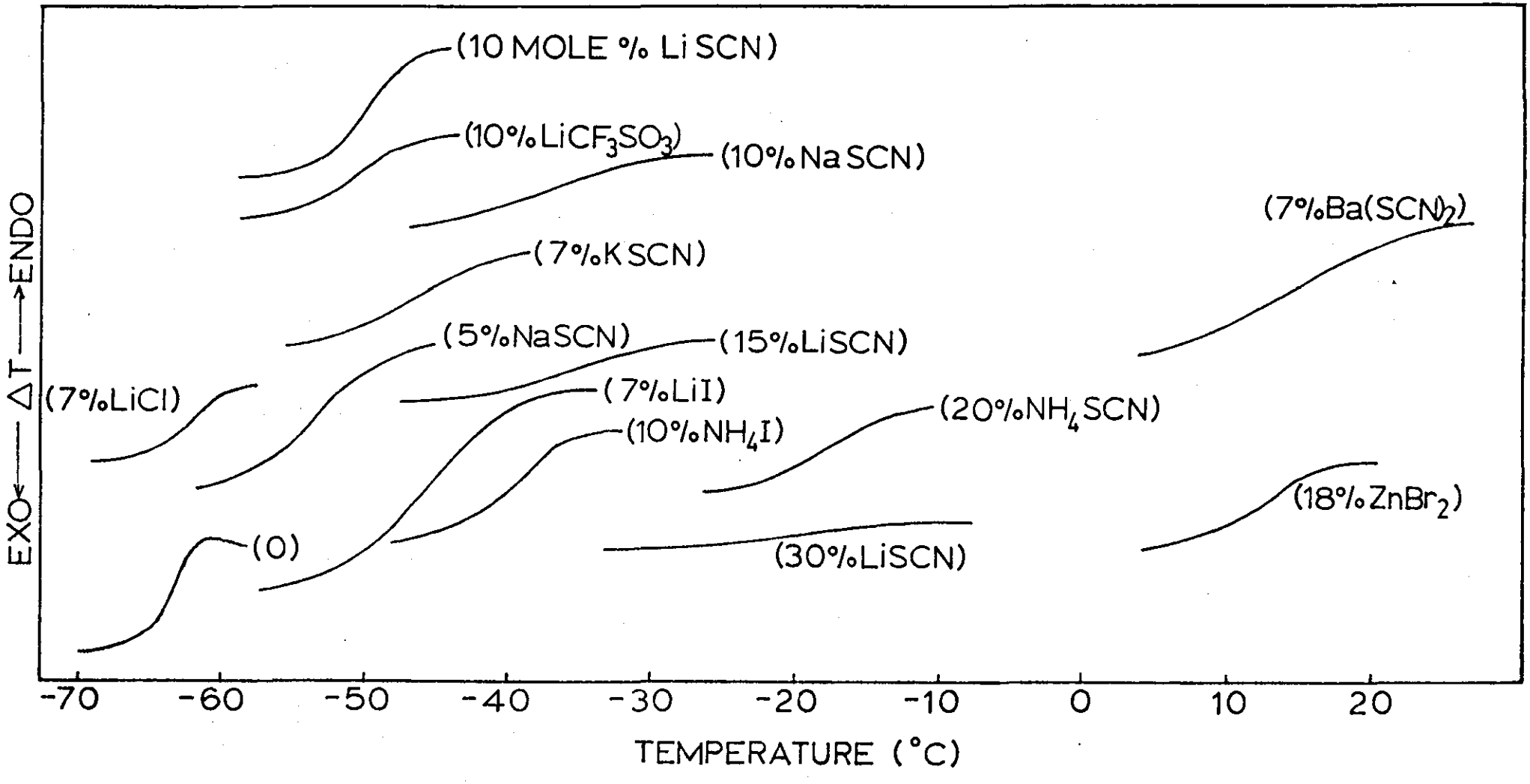

FIGURE 4.1

GLASS TRANSITIONS EXHIBITED BY SALT COMPLEXES OF POLY(PROPYLENE GLYCOL)

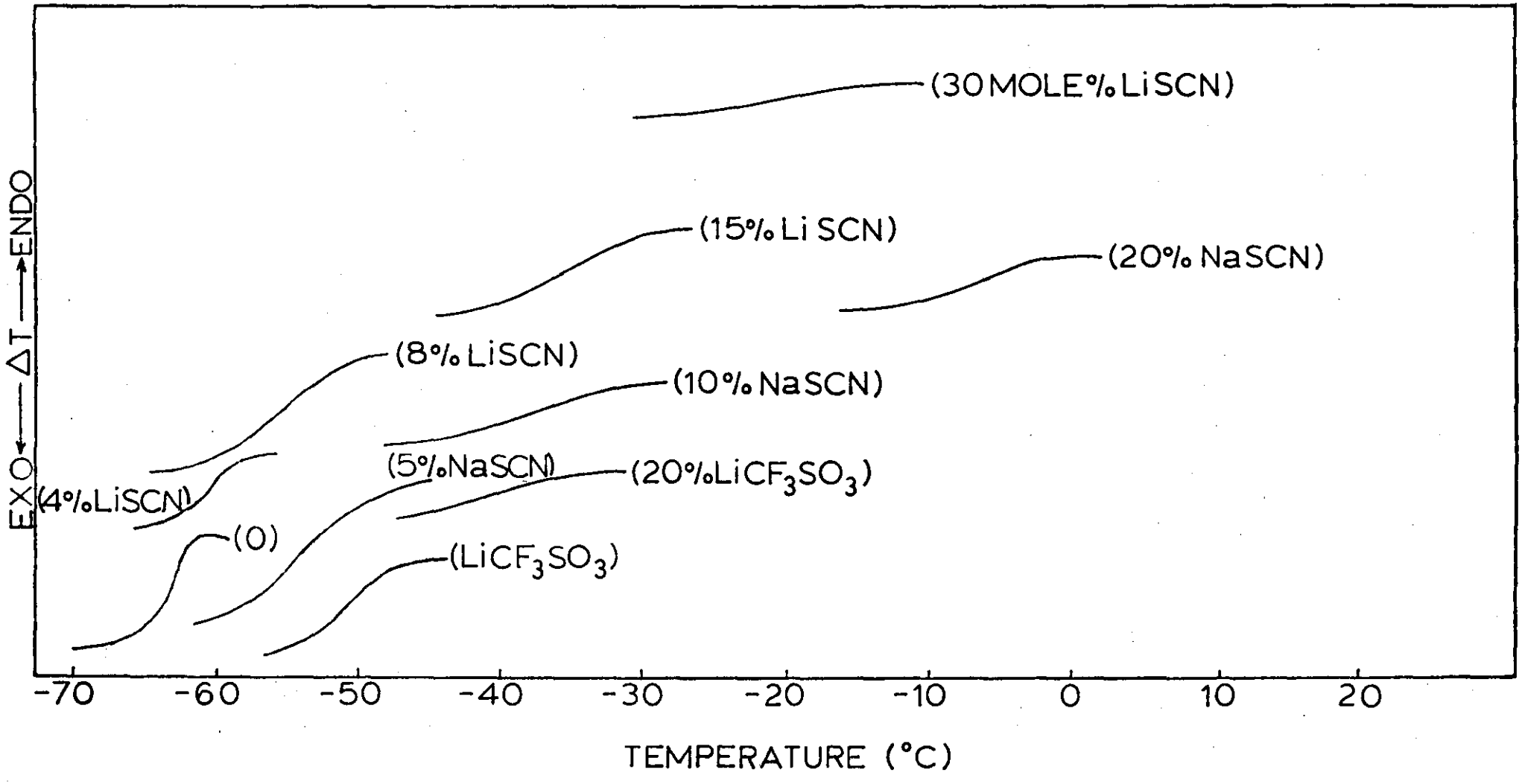

FIGURE 4.2

THE VARIATION OF GLASS TRANSITION TEMPERATURE WITH MOLE% OF INORGANIC SALT PRESENT IN POLY(PROPYLENE GLYCOL) COMPLEXES

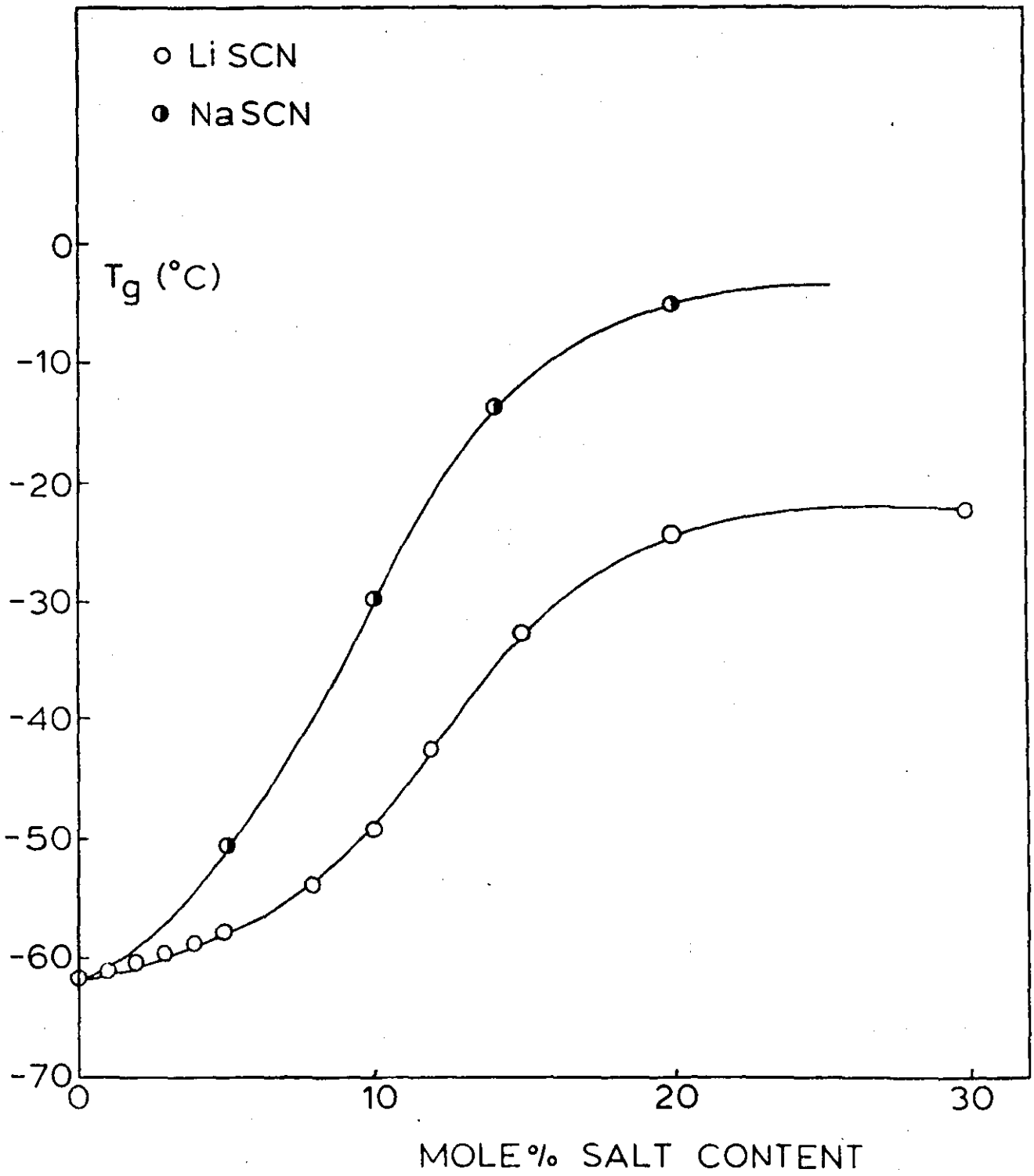

FIGURE 4·3

Figure 4.4 illustrates the magnitude of the glass transition, derived as above, of LiSCN and NaSCN complexed with poly(propylene glycol). Both salts show a decrease in the magnitude of the glass transition per unit weight of sample with increasing salt concentration. This need not however indicate that the transition is becoming any less energetic, the transitions are considerably broadened when salt is present in the form of a complex. If the transitions were a consequence of the polymer only (with no interaction from the salt) one would not expect to see any variation with increasing salt content (providing one first reduced the data to account for only the polymer present in the sample). Figure 4.4 illustrates this point succinctly, therefore it is possible to state that an interaction is taking place between the polymer and the salt and that the salt is not just acting as a filler. This therefore reinforces the visual observations already stated in section 4.2.1 that some salts were capable of forming complexes with poly(propylene glycol).

4.2.3 Viscosity Data for Inorganic Salt Complexes of Poly(propylene glycol)

The viscosities of three salt complexes above their glass transition regions were determined. Figure 4.5 illustrates the viscosity temperature profile for LiSCN poly(propylene glycol) complexes of various salt loadings. It is clearly evident that the viscosity at any given temperature increases with increasing salt content. This is to be expected because of the increase in Tg with increasing salt content.

The viscosities illustrated all decrease non-linearly with increasing temperature, tending toward a limiting value. Figure 4.6 shows the relationship between the increase in viscosity and the change in the glass transition. There is an initial large shift in

THE MAGNITUDE OF THE GLASS TRANSITION OF POLY(PROPYLENE GLYCOL) – INORGANIC SALT COMPLEXES

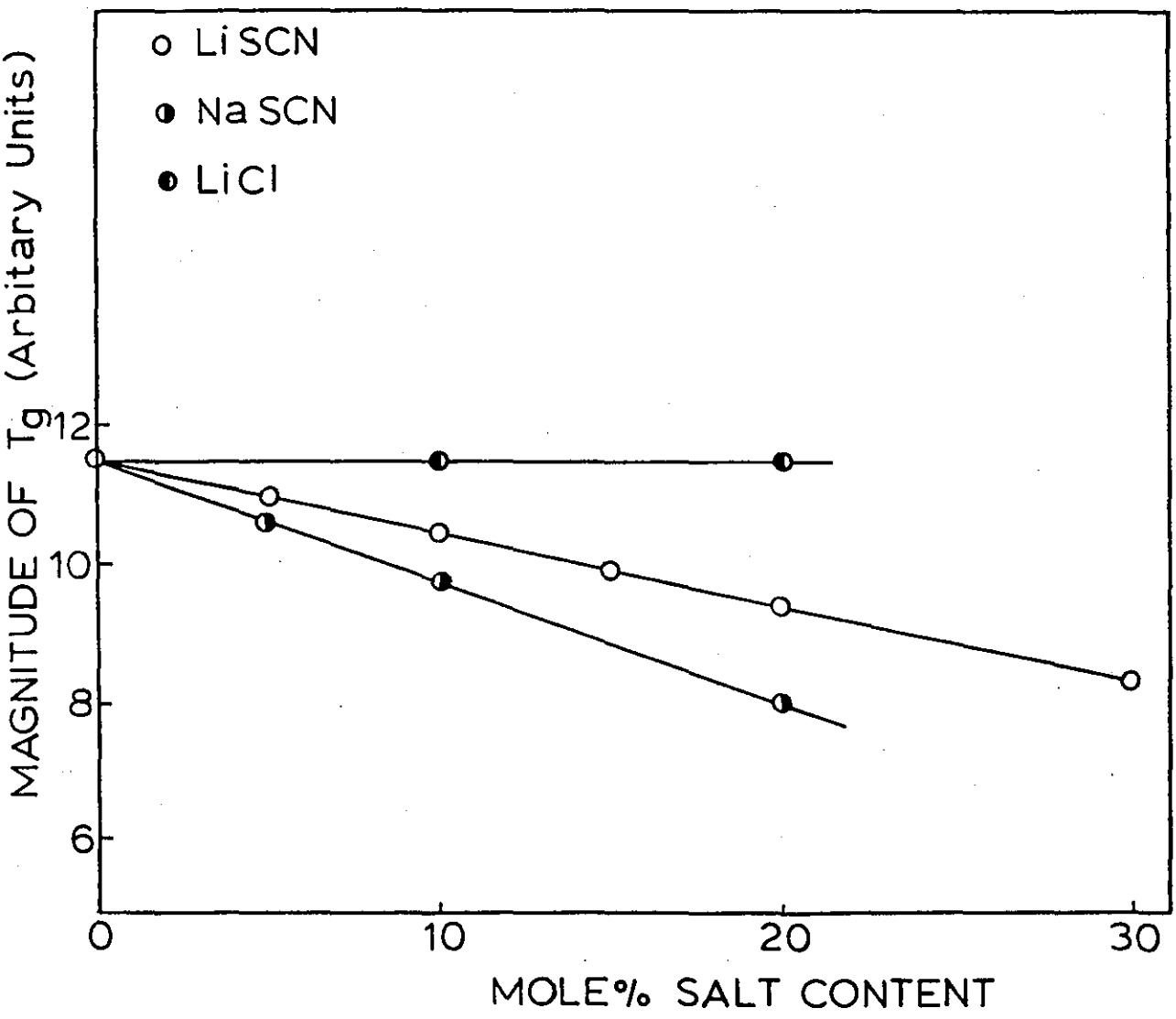

FIGURE 4·4

TEMPERATURE DEPENDENCE OF VISCOSITY FOR POLY(PROPYLENE GLYCOL) - LITHIUM THIOCYANATE COMPLEXES

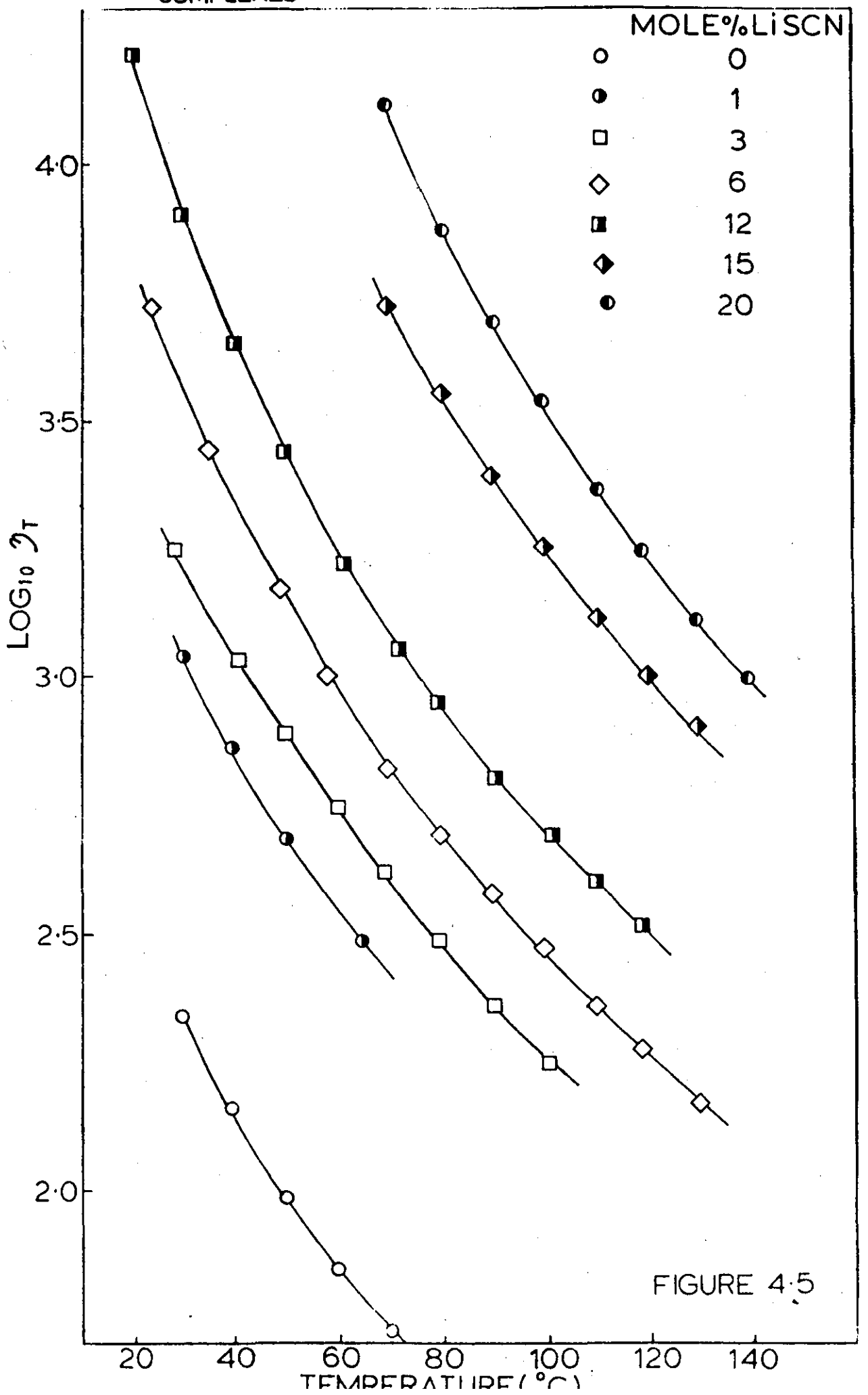

FIGURE 4·5

THE TEMPERATURE SHIFT OF VISCOSITY VERSUS THE SHIFT IN T_g FOR INORGANIC SALT COMPLEXES OF POLY(PROPYLENE GLYCOL)

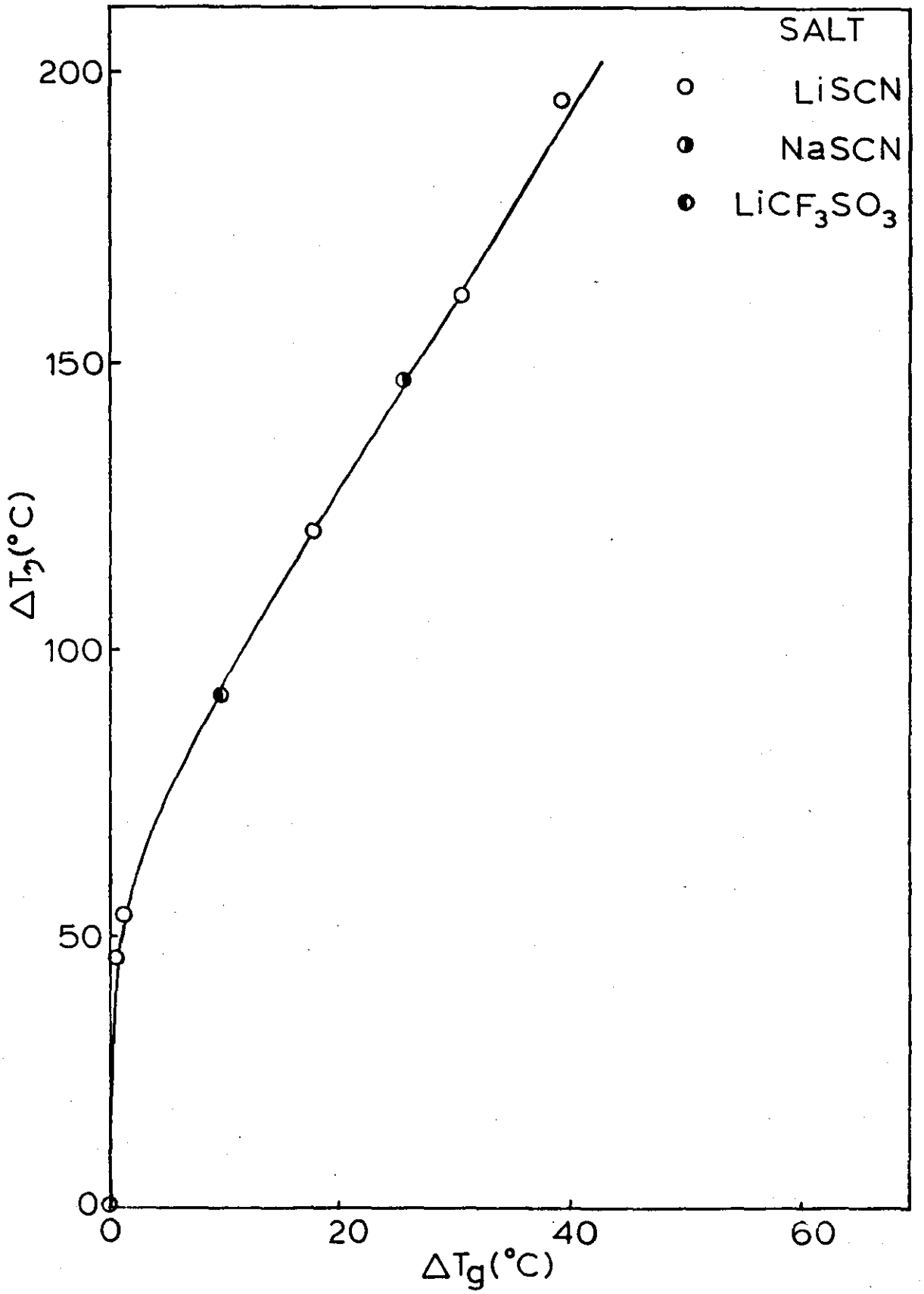

FIGURE 4·6

viscosity with only a small change in Tg. The relationship then becomes linear.

Figure 4.7 shows the viscosity temperature profile of NaSCN and $LiCF_3SO_3$ complexes of poly(propylene glycol). There is a large shift in viscosity as seen in Figure 4.5 on the addition of NaSCN and $LiCF_3SO_3$ to poly(propylene glycol). The $LiCF_3SO_3$ poly(propylene glycol) complex appears to have a similar profile to that of LiSCN complexes described above whereas NaSCN complexes appear to shift the viscosity to higher values than those for LiSCN complexes. In Figures 4.2 and 4.3 it is clearly evident that NaSCN shifts the Tg of poly(propylene glycol) to higher temperatures than does LiSCN for the same mole% salt content, this would appear to explain the higher values for viscosity. It is also suggested that the cation appears to have a more striking effect on the resulting properties so far discussed, of a polymer-salt complex than does the anion.

4.2.4 Dielectric Relaxations Shown by Poly(propylene glycol)-Inorganic Salt Complexes

Poly(propylene glycol) exhibits three molecular processes over the range of temperatures and frequencies studied. One can discern from Figure 4.8 the tail end of the α process followed by a liquid-liquid transition[207] involving the motion of the entire molecule. At still higher temperatures (at constant frequency) the onset of conductivity due to extrinsic impurities and an inherent mechanism involving the generation of protons[208] is observed.

Figures 4.8 and 4.9 are indicative of the relaxations observed upon addition and subsequent complex formation of inorganic salt to poly(propylene glycol). Figure 4.8 shows the temperature plane dielectric relaxation data for a series of poly(propylene glycol) lithium thiocyanate complexes of various salt loadings at 5 kHz

TEMPERATURE DEPENDENCE OF VISCOSITY FOR POLY(PROPYLENE GLYCOL)-INORGANIC SALT COMPLEXES

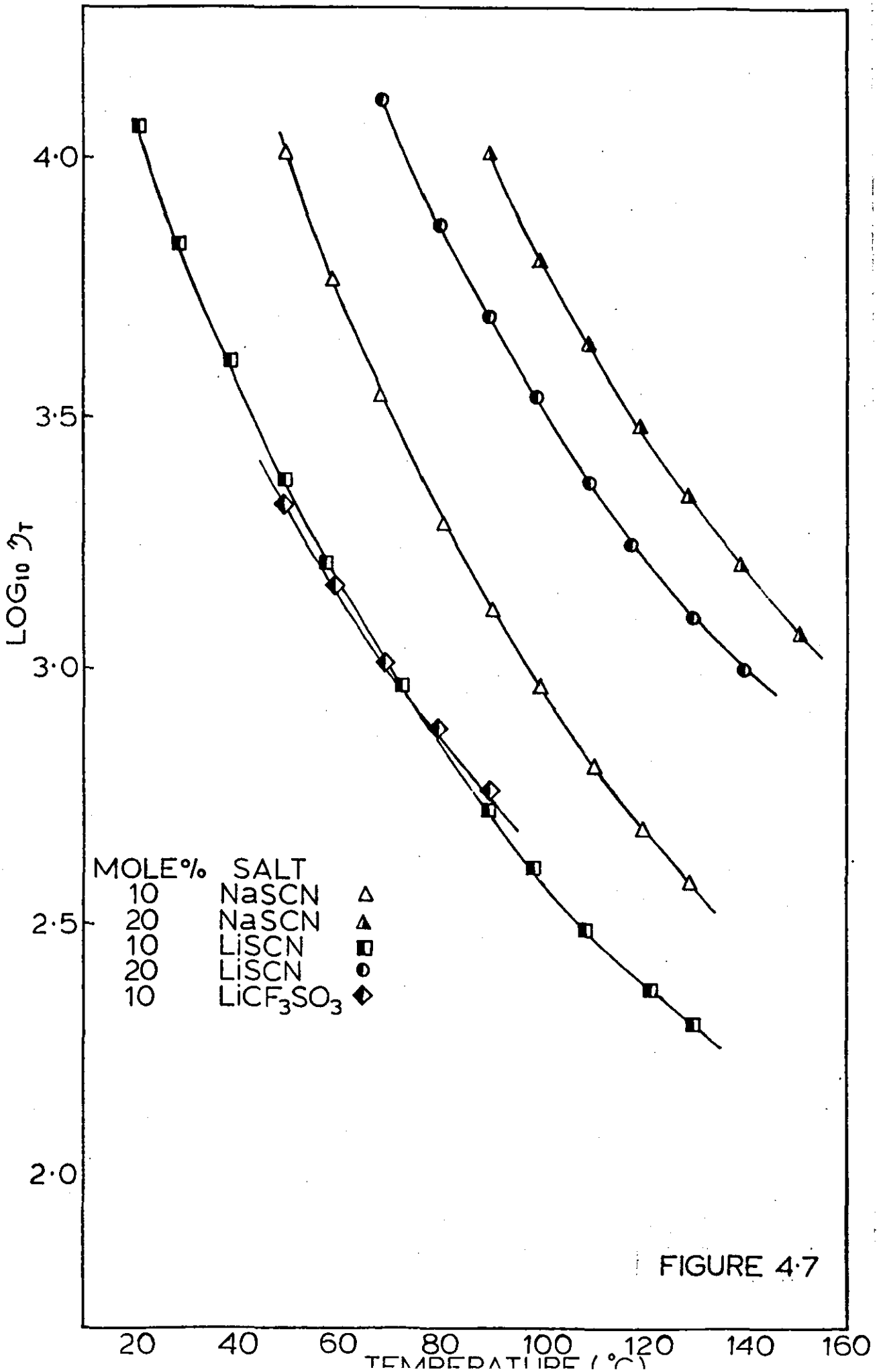

FIGURE 4·7

TEMPERATURE DEPENDENCE OF $LOG_{10}\varepsilon'$ AND $LOG_{10}\varepsilon''$ FOR POLY(PROPYLENE GLYCOL) LiSCN COMPLEXES AT 5kHz.

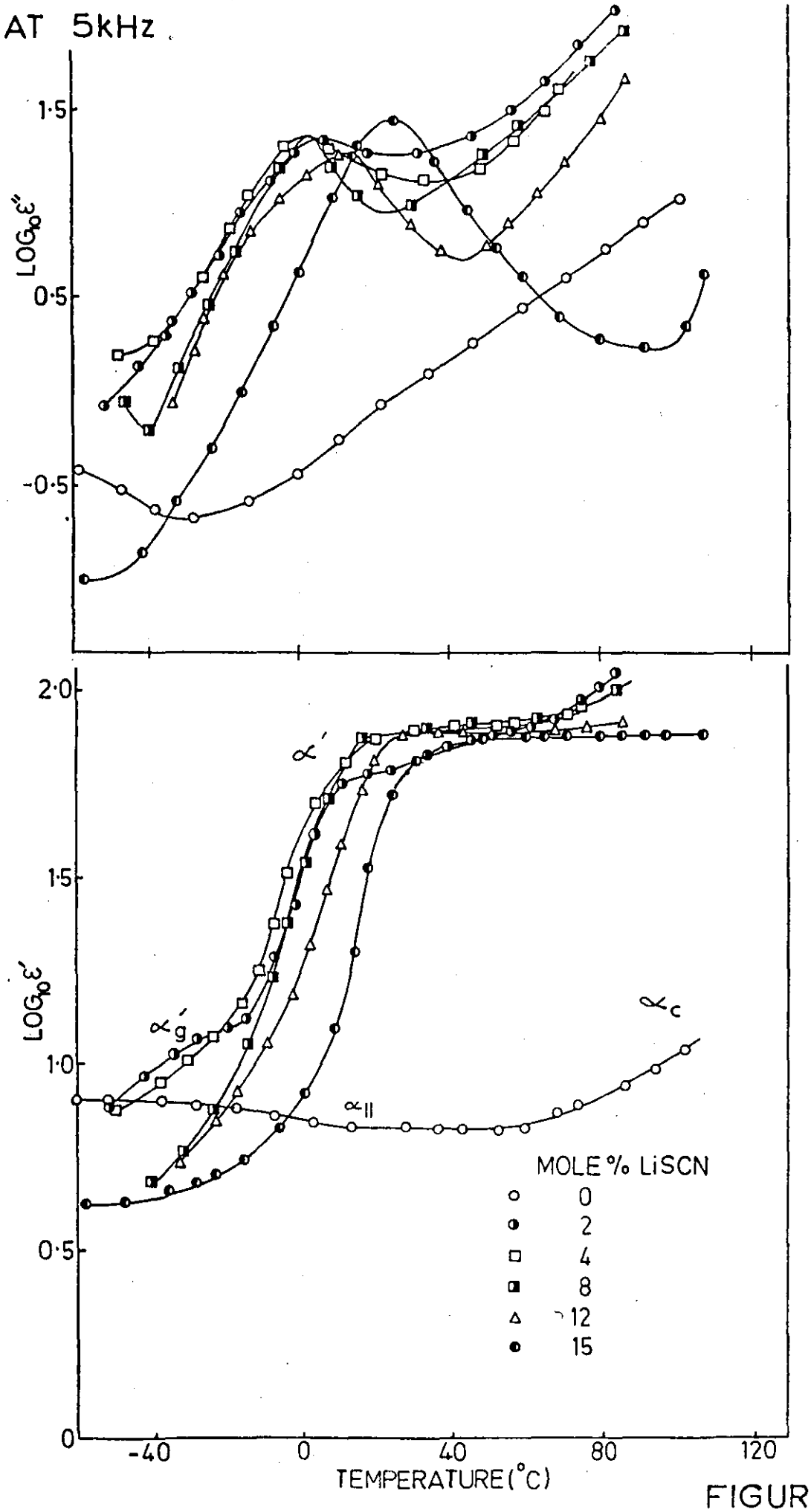

FIGURE 4·8

between -60 and 100°C. The original α relaxation as seen in the pure polymer is apparently reduced in stature. A second transition designated $\alpha g'$ is observed in low salt loaded complexes. The third transition observed designate α', is seen to be much greater in magnitude than the α and $\alpha' g$ process. This α' process is shifted to higher temperatures at constant frequency with increasing salt loading although the actual value for the relaxed dielectric constant (ε_r) appears to decrease slightly with increasing salt loading. It can be seen from the loss data that the relaxation is distorted by conductivity effects on the high temperature side of the relaxation. This distortion appears to lessen with increasing salt content.

Figure 4.9 shows the dielectric relxation data for two sodium thiocyanate poly(propylene glycol) complexes and a lithium trifluoromethyl sulphonate poly(propylene glycol) complex at 5 kHz. The same three processes as seen in Figure 4.8 are discernible in Figure 4.9, that of an $\alpha g'$, α' and α_c relaxations. The α' relaxation is considerably greater in magnitude than the $\alpha g'$ relaxation and as in Figure 4.8 appears at a higher temperature with increasing salt loading. The values for ε_r decrease with increasing salt content but is greater for a 20 mole% sodium thiocyanate poly(propylene glycol) complex than a 20 mole% lithium trifluoromethyl sulphonate complex.

Figure 4.10 summarises the temperature plane dielectric relaxation data of poly(propylene glycol)-lithium thiocyanate complexes measured at 10 MHz in the temperature range -40 to 120°C. The pure poly(propylene glycol) appears to show no change in dielectric constant and only a small decrease in the dielectric loss value over the temperature range covered. An enhancement upon the dielectric values of the original polymer are observed upon complex formation of poly(propylene glycol) with lithium thiocyanate at 10 MHz as was observed at 5 kHz. Obviously the relaxations observed at 10 MHz are shifted to higher

TEMPERATURE DEPENDENCE OF $LOG_{10}\varepsilon'$ AND $LOG_{10}\varepsilon''$ FOR POLY(PROPYLENE GLYCOL) INORGANIC SALT COMPLEXES AT 5kHz

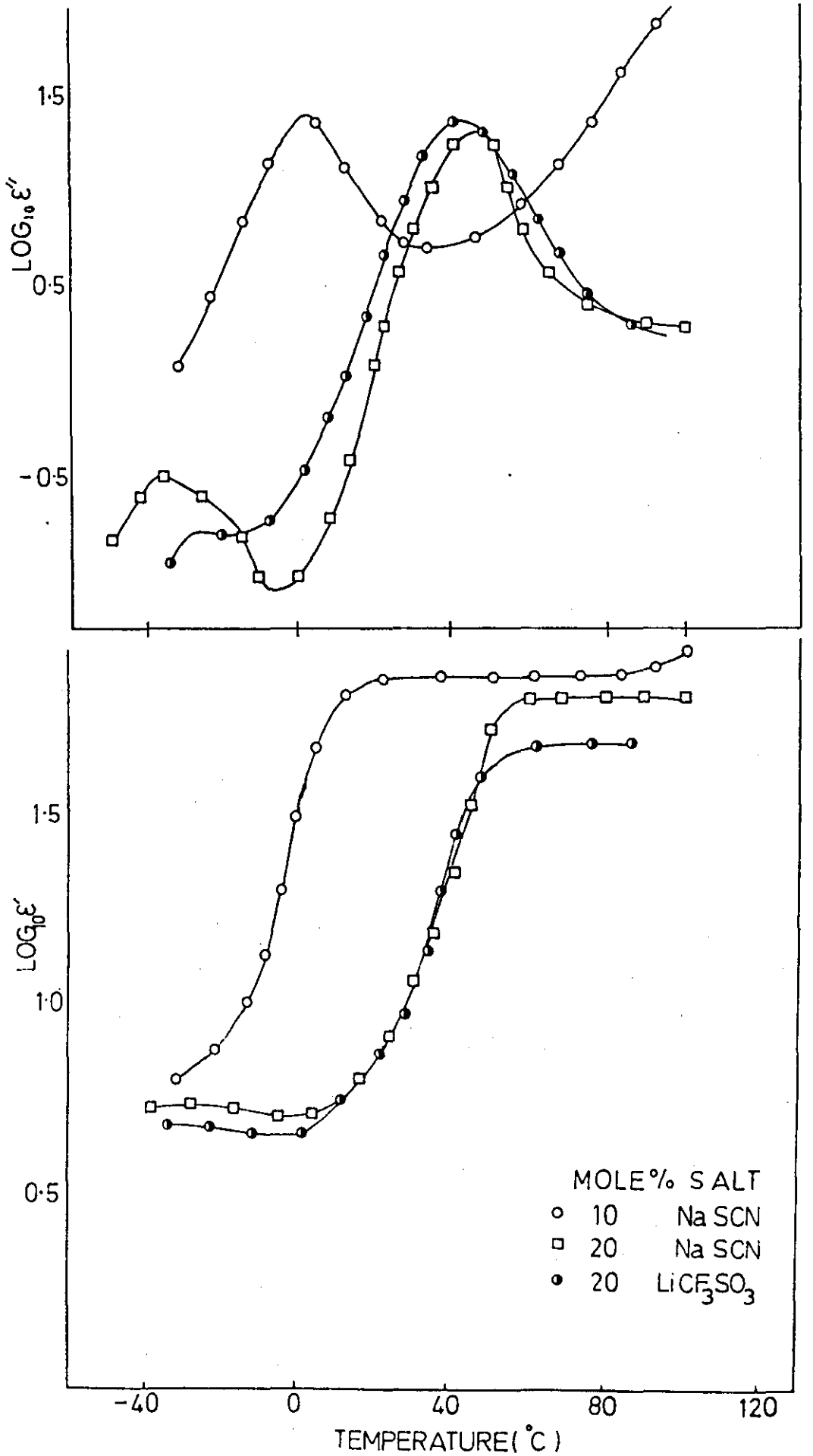

FIGURE 4·9

TEMPERATURE DEPENDENCE OF $LOG_{10}\varepsilon'$ AND $LOG_{10}\varepsilon''$ FOR POLY(PROPYLENE GLYCOL) INORGANIC SALT COMPLEXES AT 10MHz

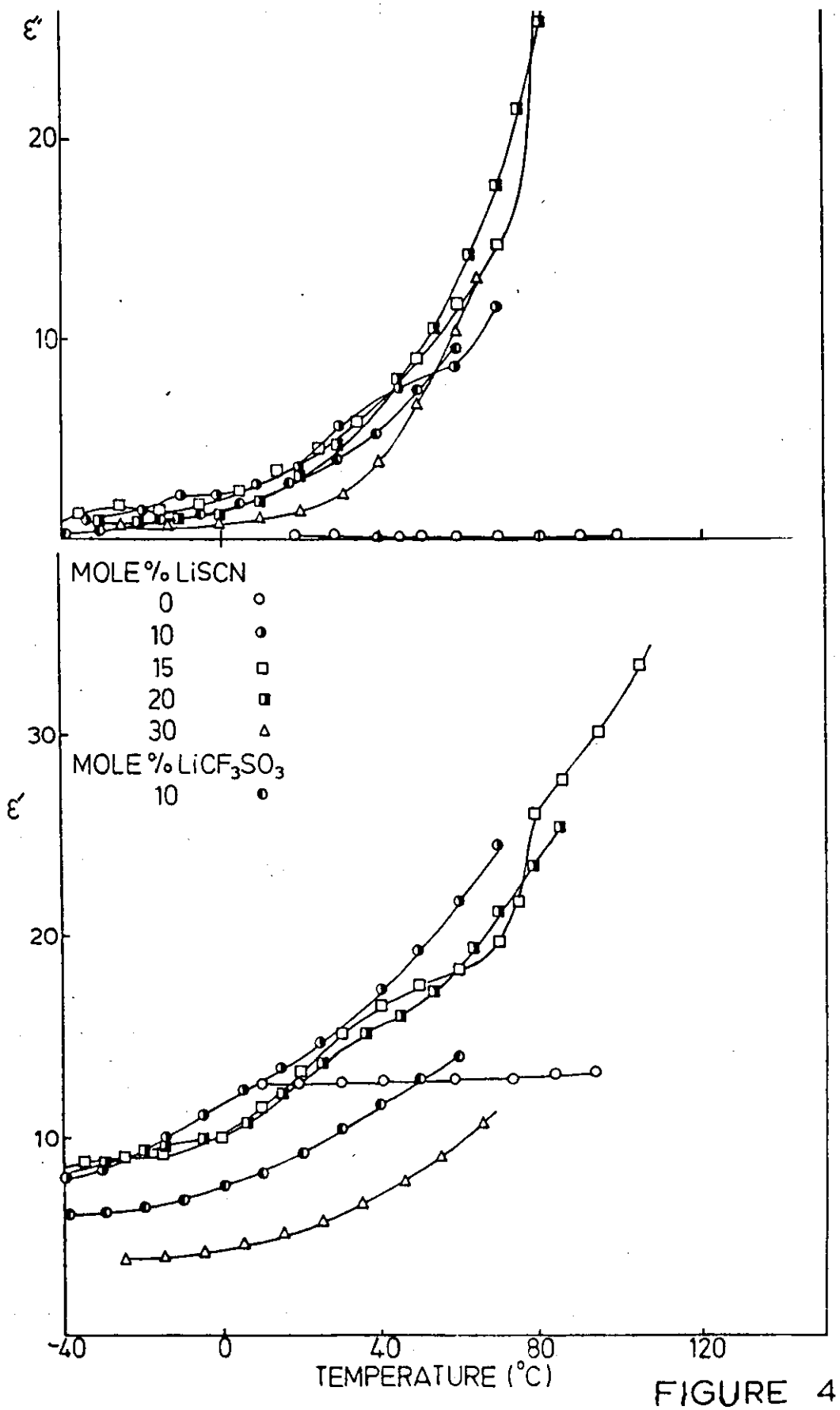

FIGURE 4·10

temperatures in comparison to those measured at 5 kHz.

The α' process is clearly discernible in the dielectric constant for salt loadings up to 20 mole%, the α' process being shifted to higher temperatures with increasing salt loading. The temperature range was not large enough to clearly see this process at 30 mole%. The α_g' process was however not visible in the dielectric loss data.

Included upon Figure 4.10 is the dielectric data for a 10 mole% poly(propylene glycol)-lithium trifluoromethyl sulphonate complex. Again the α_g' process is not visible and the values for dielectric constant and loss are less than those observed for a 10 mole% lithium thiocyanate complex.

Figure 4.11 shows the dielectric data for a series of complexes with P3 and P317 at 10 MHz. It can clearly be seen that different salts affect the dielectric properties markedly. The potassium thiocyanate complex with P3 shows the highest values for dielectric constant and loss at any given temperature and $Ba(SCN)_2$ - P3 and $ZnCl_2$ - P317 showing the lowest. The α_g' process appears at higher temperatures for the $Ba(SCN)_2$ - P3 and $ZnCl_2$ - P317 complex with respect to KSCN - P3. This is to be expected as the corresponding values for Tg for these complexes show the same trend. For all but the KSCN - P3 complex the dielectric loss shows an inflection for the α_g' process whilst the KSCN - P3 complex shows a clear loss peak. It is also worth noting that $Ba(SCN)_2$ - P3 appears to show a α' loss peak around 130°C even though the α_g' and α' processes are merged together in the dielectric constant data.

Both the NaSCN and KSCN complexes of P317 show a reduction in dielectric strength and occur at a lower temperature than their equivalent complexes with P3.

TEMPERATURE DEPENDENCE OF $LOG_{10}\varepsilon'$ AND $LOG_{10}\varepsilon''$ FOR P3 AND P317 INORGANIC SALT COMPLEXES AT 10MHz

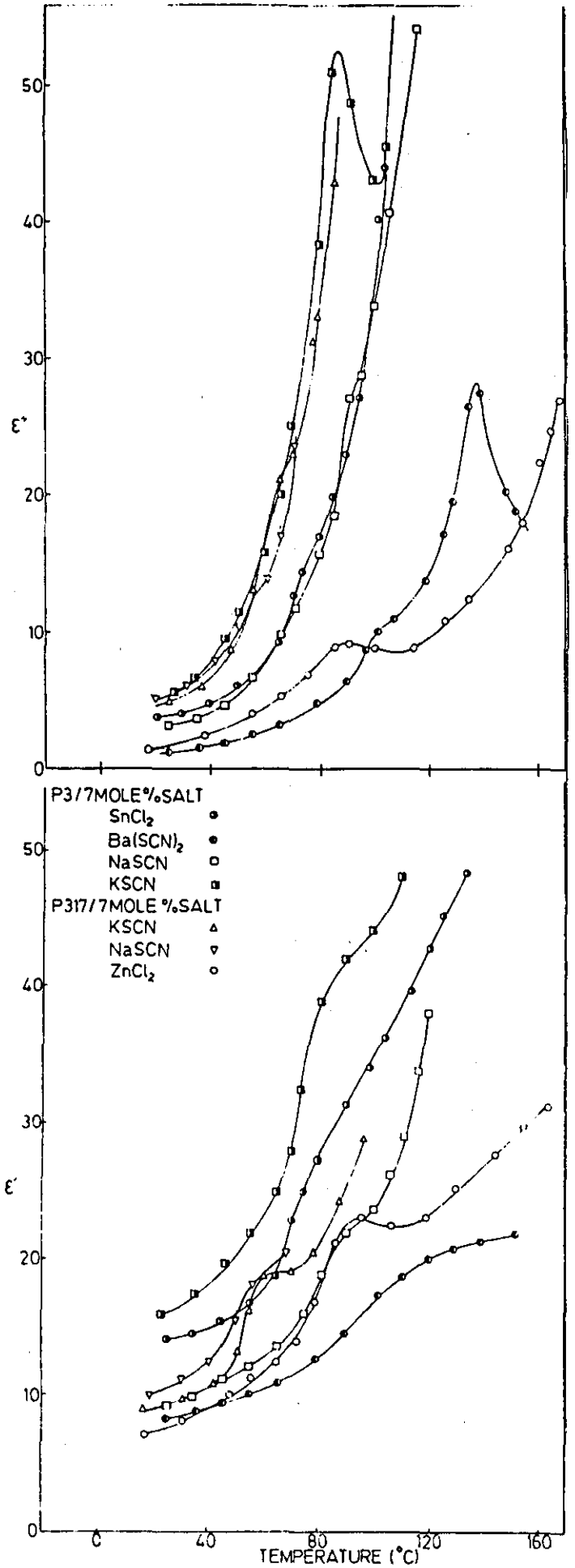

FIGURE 4·11

Figure 4.12 shows the logF versus 1/T plots of ε''_{max} for a series of lithium thiocyanate poly(propylene glycol) complexes and two sodium thiocyanate and a lithium trifluoromethyl sulphonate poly (propylene glycol) complexes. It is evident that the location of the α' relaxation and the mole% of lithium thiocyanate complex is not a straightforward relationship.

Figures 4.13 and 4.14 show the frequency dependencies of ε' and ε'' for a 15 mole% lithium thiocyanate poly(propylene glycol) complex. Although the range is somewhat limited a well defined set of curves is evident.

4.3 Poly(tetramethylene glycol) Containing Inorganic Salts

4.3.1 General Properties

Poly(tetramethylene glycol) complexes with inorganic salts were prepared as stated previously and their general properties are summarised in Table 4.3. It was clearly discernible that two different types of compound were formed as was shown for poly(propylene glycol). The first type behaved as complexes and the second type appeared as a polymer containing uncomplexed inorganic filler.

The complexes were all white solids at room temperature with the exception of the calcium thiocyanate complexes studied which were clear viscous liquids. The glass transition temperatures of the complexes were all higher than the parent polymer but it was found that a maximum transition temperature occurred;upon further addition of salt auto-plasticisation appeared to occur. The melting points of the complexes were depressed in comparison to the parent polymer and as stated previously was not observed at all in the calcium thiocyanate complexes. The complexes were deliquescent and therefore extreme care was taken

FREQUENCY TEMPERATURE LOCI (BASED ON $LOG_{10}\varepsilon''$ DATA) FOR INORGANIC SALT COMPLEXES OF POLY(PROPYLENE GLYCOL)

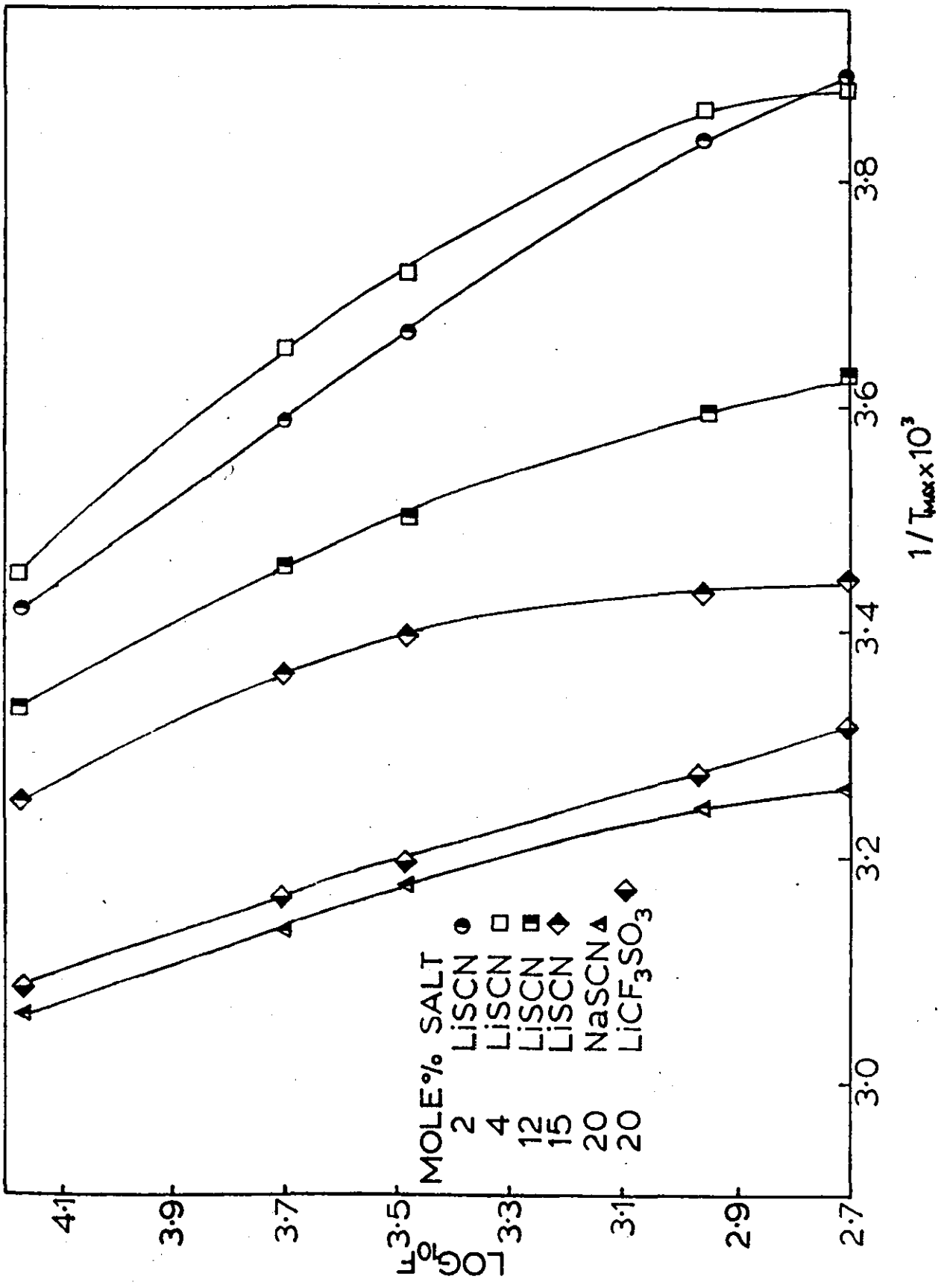

FIGURE 4·12

FREQUENCY DEPENDENCE OF ε AT VARIOUS TEMPERATURES FOR A 15 MOLE% LiSCN POLY(PROPYLENE GLYCOL) COMPLEX

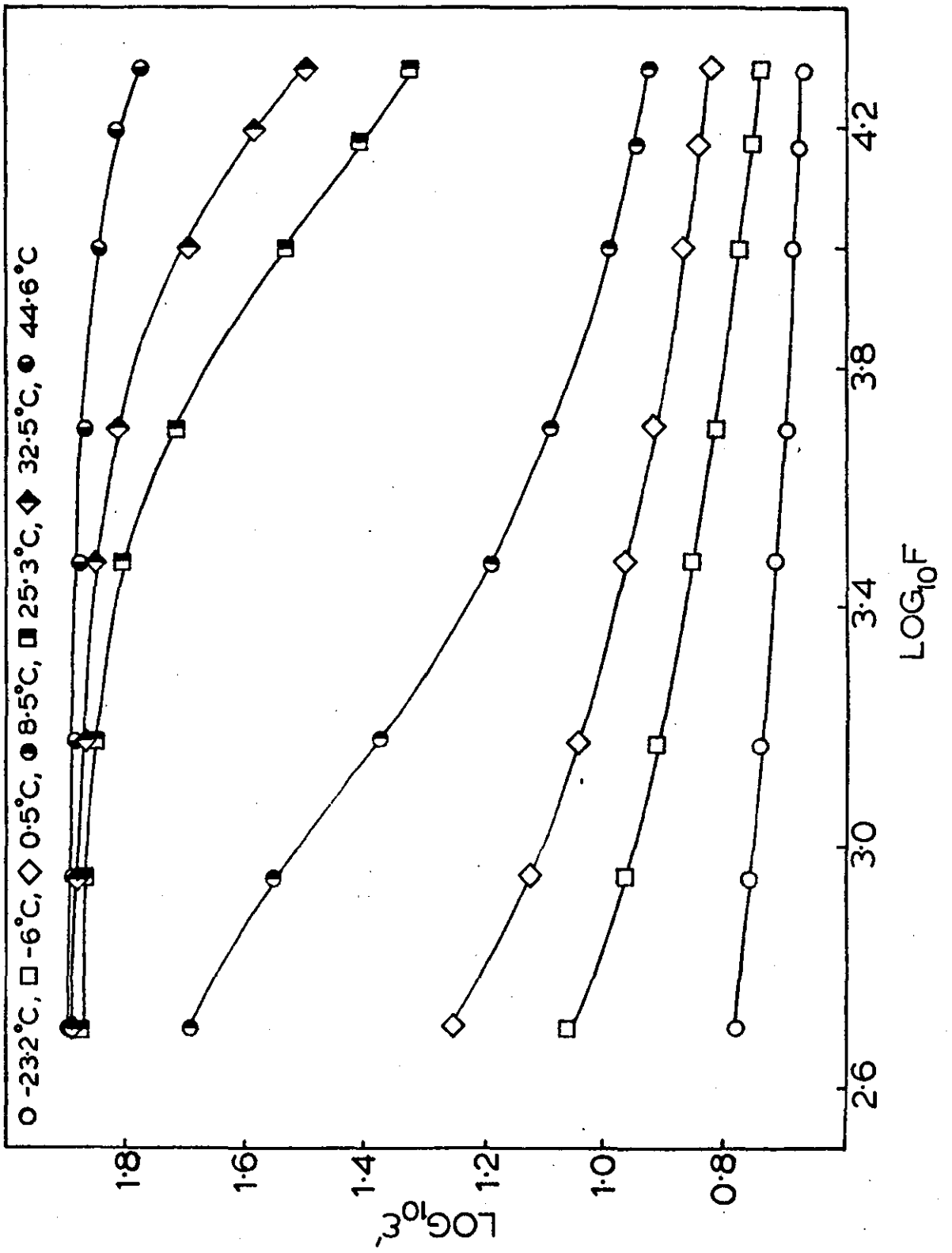

FIGURE 4·13

FREQUENCY DEPENDENCE OF ε'' AT VARIOUS TEMPERATURES FOR A 15 MOLE% LiSCN POLY(PROPYLENE GLYCOL) COMPLEX

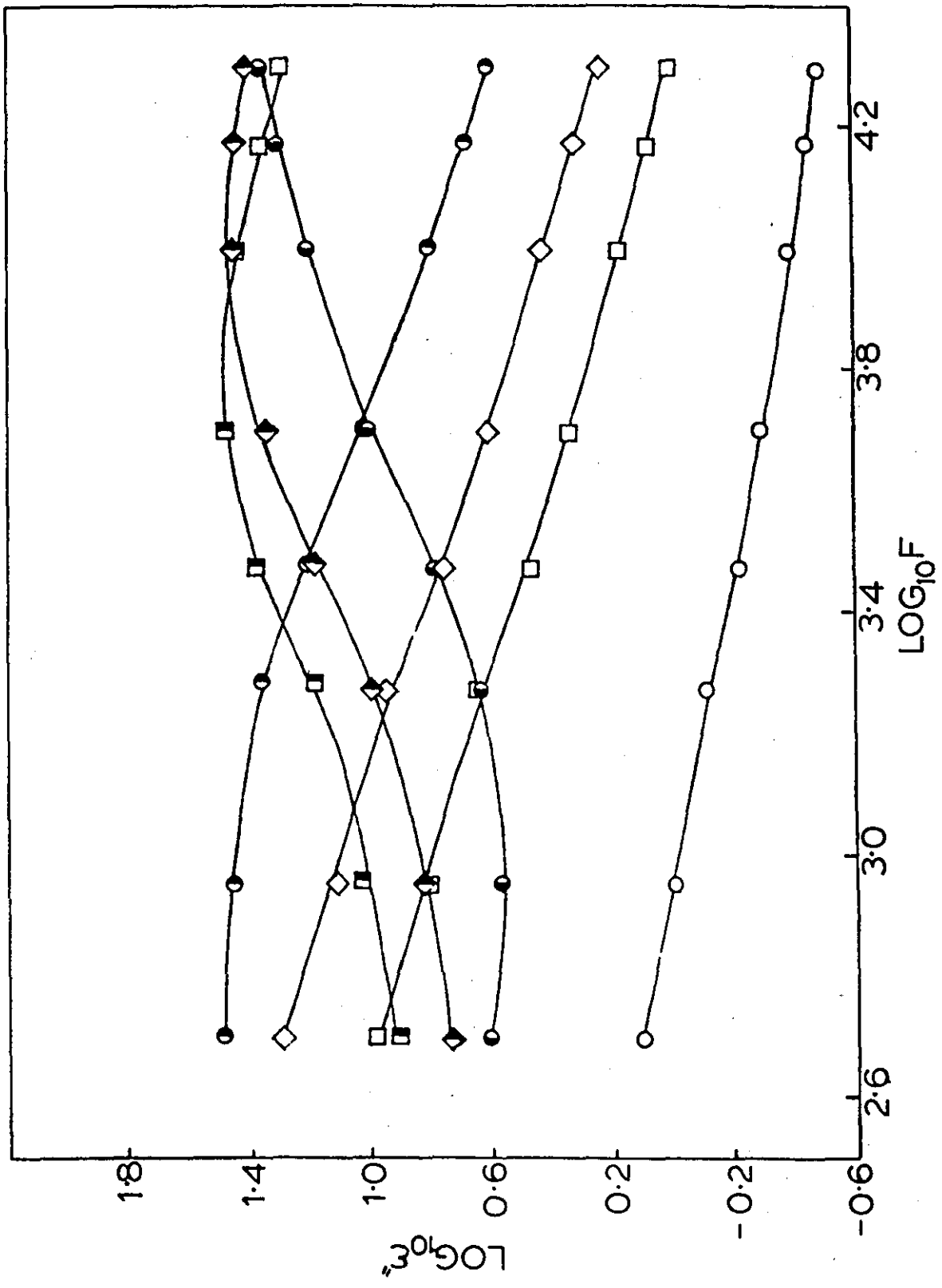

FIGURE 4·14

TABLE 4.3 Visual Properties of Inorganic Salt Complexes of Poly(tetramethylene glycol)

Metal Salt	Colour of Complex	Optical Clarity	Comments
Lithium thiocyanate	Colourless	Transparent	Single phase, white solids below their respective Tm's, viscous liquids above their respective Tm's. The viscosity was found to increase upon increasing salt content. Less deliquescent than their constituent chemicals.
Sodium thiocyanate	"	"	
Potassium thiocyanate	"	"	
Calcium thiocyanate	"	"	
Barium thiocyanate	"	"	
Ammonium thiocyanate	"	"	
Tin (II) chloride	"	"	
Lithium iodide	"	"	
Ammonium bromide	"	"	
Sodium chloride	White	Opaque	Two phase and hygroscopic

to ensure anhydrous conditions during measurement and storage.

4.3.2 Thermal Properties of Poly(tetramethylene glycol) Containing Inorganic Salts

Figure 4.15 illustrates the glass transition behaviour of poly (tetramethylene glycol) complexed to various inorganic salts. The glass transition temperature of poly(tetramethylene glycol) is broader than that observed for poly(propylene glycol) because of its inherent crystallinity the resulting complexes show a further broadening. The exception being 10 mole% $Ca(SCN)_2$ which appears to sharpen with respect to poly(tetramethylene glycol). This is a consequence of the suppresion in crystallinity but a further increase in salt content produces a broadening in Tg and reduction in the value of its Tg.

Upon addition of salt the Tg of the parent polymer was elevated up to a point whereupon further addition results in a reduction in the value for Tg towards its original value.

Table 4.4 shows the melting points for complexes of both poly (tetramethylene glycol) and poly(tetramethylene oxide), $\overline{Mn}$ 10,000. It is clearly evident that the melting behaviour is complex, resulting in some salts raising and some salts lowering the value of Tm. The complete suppression of Tm as observed for the calcium thiocyanate poly(tetramethylene glycol) system is not observed in the higher molecular weight polymer. On the contrary the higher molecular weight calcium thiocyanate complex produces one of the highest shifts in the value of Tm. It would appear that some salts cause a disruption in the crystallinity and are presumably not incorporated in the crystalline structure. Whilst others appear to be incorporated into or around the crystalline structure and thus elevate the value of Tm yet still reduce the overall crystallinity.

GLASS TRANSITIONS EXHIBITED BY SALT COMPLEXES OF POLY(TETRAMETHYLENE-GLYCOL

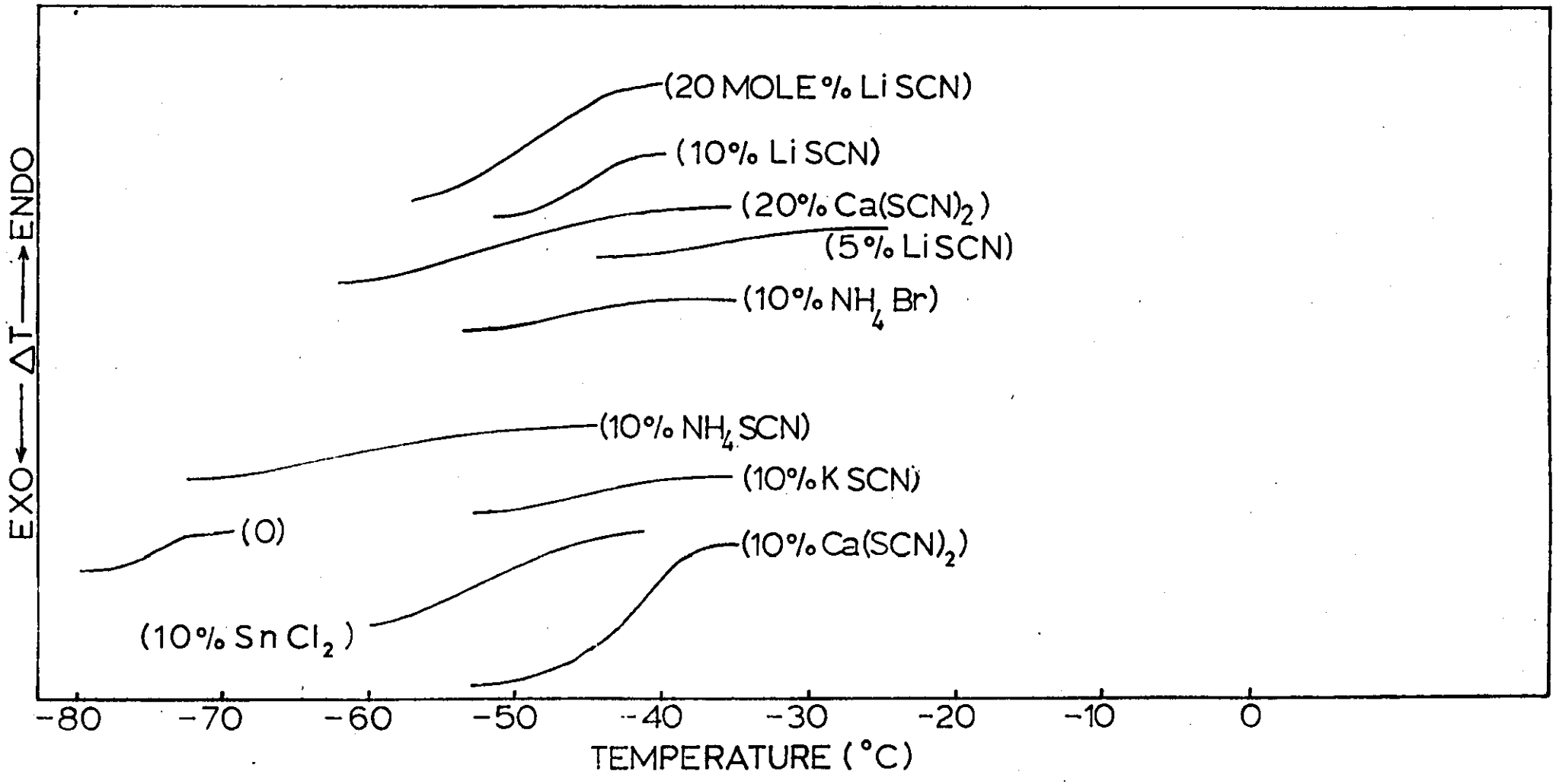

FIGURE 4·15

TABLE 4.4 Melting points (Tm's) of Inorganic Salt Complexes of Poly(tetramethylene glycol) and Poly(tetramethyl oxide)

Polymer	Salt	Mole%	Tm(^{o}C)
PTMG	-	-	24.9
PTMG	LiSCN	5	22.7
PTMG	LiSCN	20	22.6
PTMG	NH_4SCN	10	30.2
PTMG	KSCN	10	16.5
PTMG	NH_4Br	10	9.9
PTMG	$Ba(SCN)_2$	10	17.5
PTMG	$Ca(SCN)_2$	10	-
PTMG	$Ca(SCN)_2$	20	-
PTMG	$SnCl_2$	10	21.4
PTMG	NaSCN	10	21.0
PTMO	--	-	26.2
PTMO	LiSCN	15	41.0
PTMO	NaSCN	15	23.8
PTMO	$Ca(SCN)_2$	15	37.8

A transition near to the melting peak but lower in intensity and temperature was discernible in the parent polymer. This apparently smaller melting peak was also observed in the salt complexes often appearing much sharper than the original low temperature polymer melting peak. The main melting peak was often found to be split into two peaks, on subsequent melting and recrystallising the two peaks merged into one.

4.3.3 Dielectric Relaxations Exhibited by Inorganic Complexes of Poly(tetramethylene glycol)

Poly(tetramethylene glycol) exhibits three relaxation processes over the frequency and temperature range studied. One can discern the latter part of the α_g-process associated with the glass transition at low temperatures, the melting process α_c, and a small transition, α_i intermediate between the two. This process has been observed, amongst others, in dynamic mechanical measurements by Wetton and Allen[158]. Upon addition of lithium thiocyanate the α_g and α_i processes appear to merge and the α_c process is much more strongly defined.

Figure 4.16 summarises the temperature plane data for a poly (tetramethylene glycol) lithium cyanate complex at 5 kHz for various salt loadings in the temperature range -60 to +90°C. Close scrutiny of Figure 4.16 revealed, in accordance with the thermal measurements, the dielectric loss peak position of the melting process shown by DTA decreases with increasing salt content which will be a direct consequence of the suppression of crystallinity upon complexation. The values for ε_r, the relaxed storage component, above melting appear to be independent of salt loading being only slightly greater for 20 mole% LiSCN than for 10 or 15 mole%. The 20 mole% sample appeared to show an extra relaxation above melting between 0 and 20°C.

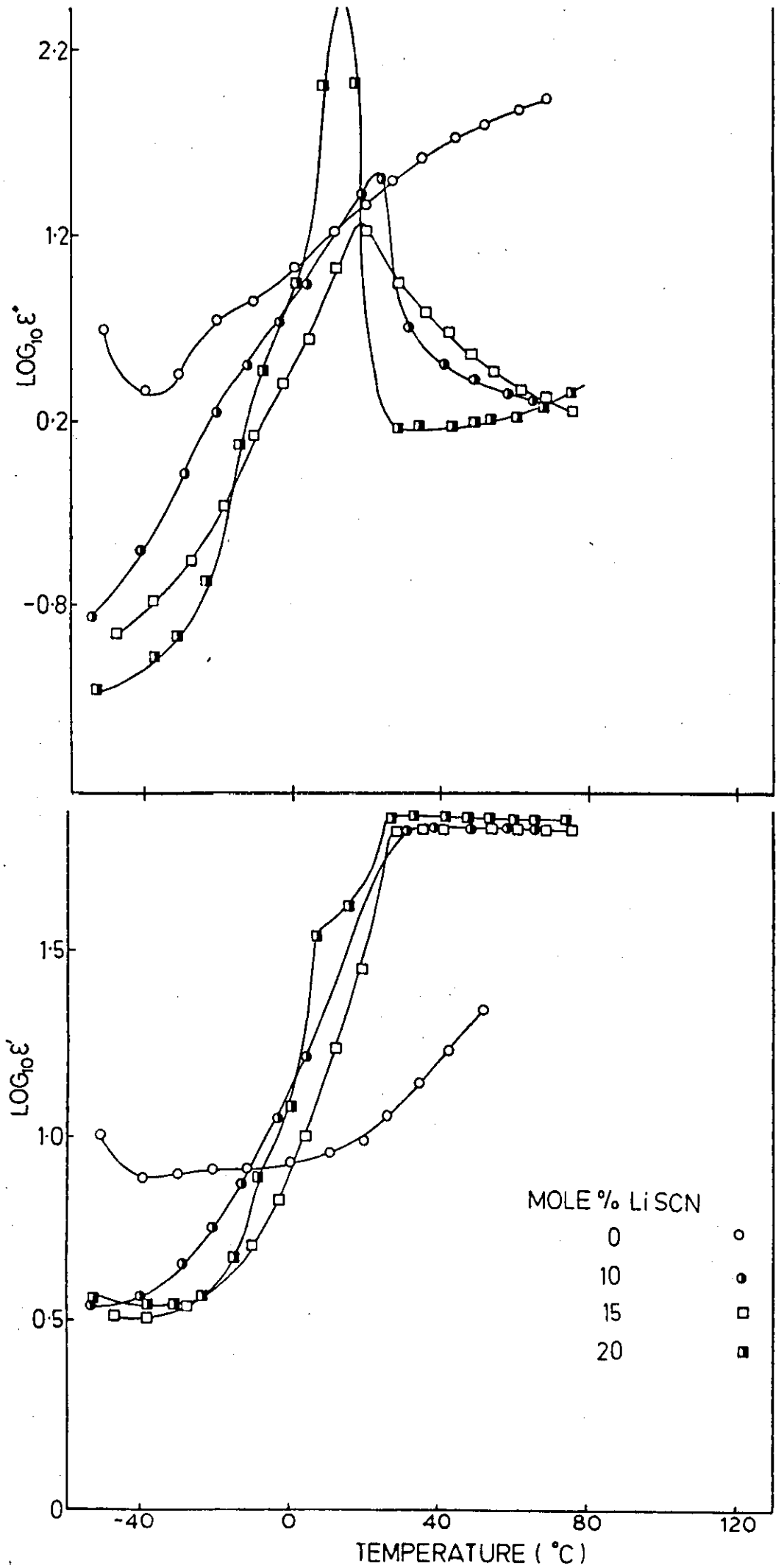

LiSCN COMPLEXES AT 5kHz

FIGURE 4·16

Figures 4.17 and 4.18 show the frequency dependence of dielectric storage and loss for 15 mole% respectively. Although the range is limited a well defined set of curves is indicated.

4.4 Poly(ethylene glycol) Containing Inorganic Salts

4.4.1 General Properties

Poly(ethylene glycol) complexes with lithium thiocyanate were prepared as stated previously and their general properties are summarised in Table 4.5.

Poly(ethylene glycol) is a semi-crystalline white solid at room temperature. Upon addition of lithium thiocyanate the degree of crystallinity is suppressed up to a critical point after which any further addition of salt prevents the polymer from crystallising.

The lithium thiocyanate was complexed to the polymer, the resulting adduct was deliquescent. Extreme care was therefore taken to ensure anhydrous conditions during storage and measurement.

4.4.2 Thermal Properties of Poly(ethylene glycol)-Lithium Thiocyanate Complexes

It was stated above that addition of lithium thiocyanate to poly(ethylene glycol) results in the suppression and eventual loss in crystallinity.

Single glass transitions were observed in lithium thiocyanate complexes of poly(ethylene glycol). The glass transitions were well defined and appeared to sharpen with increasing salt loading in accordance with the reduction and eventual loss in crystallinity. The above observations are illustrated in Figure 4.19.

Figure 4.20 illustrates the glass transition and melting point

FREQUENCY DEPENDENCE OF ε' AT VARIOUS TEMPERATURES FOR A 15 MOLE% LiSCN POLY(TETRAMETHYLENE GLYCOL) COMPLEX

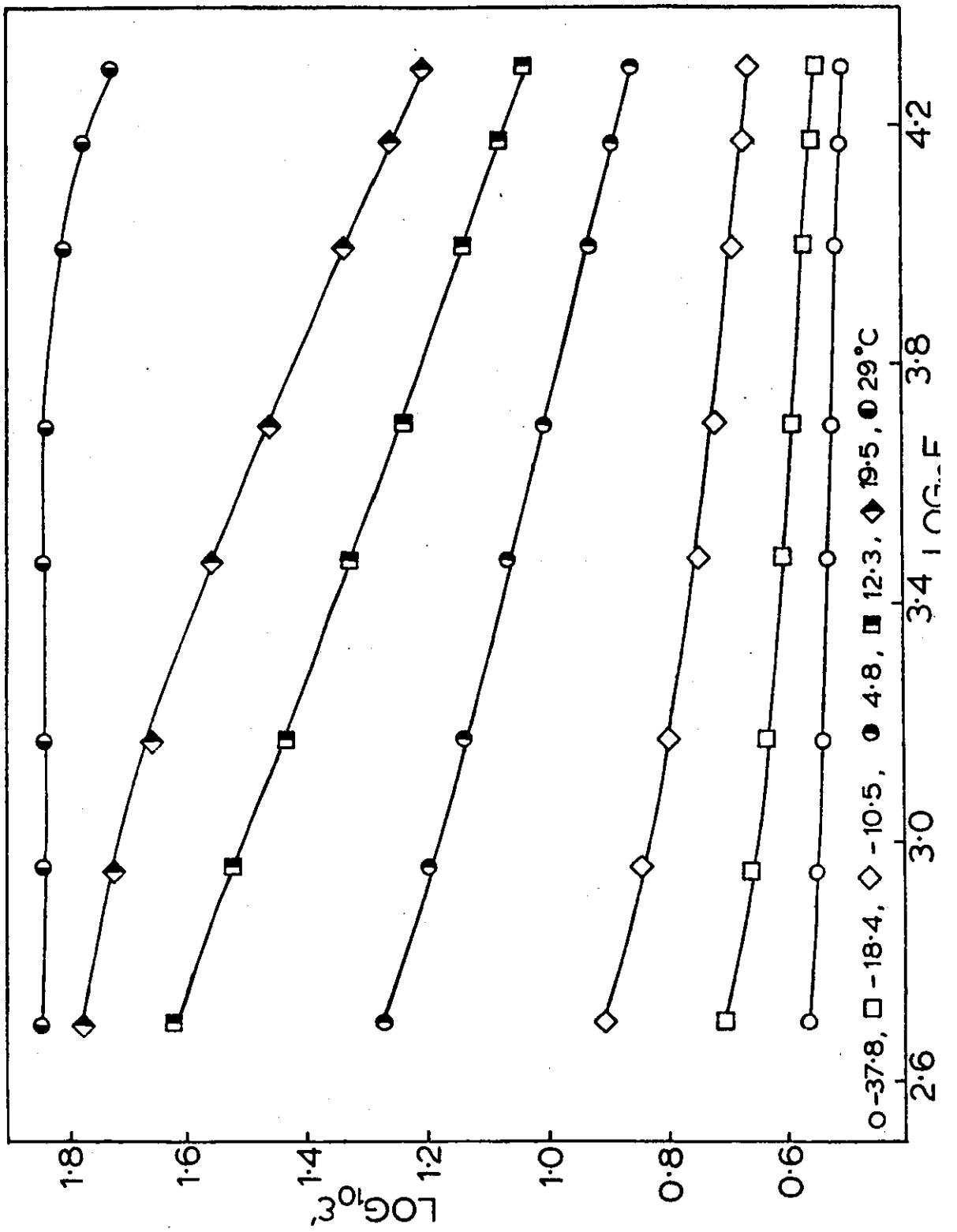

FIGURE 4·17

FREQUENCY DEPENDENCE OF ε'' AT VARIOUS TEMPERATURES FOR A 15 MOLE% LiSCN POLY(TETRAMETHYLENE GLYCOL) COMPLEX

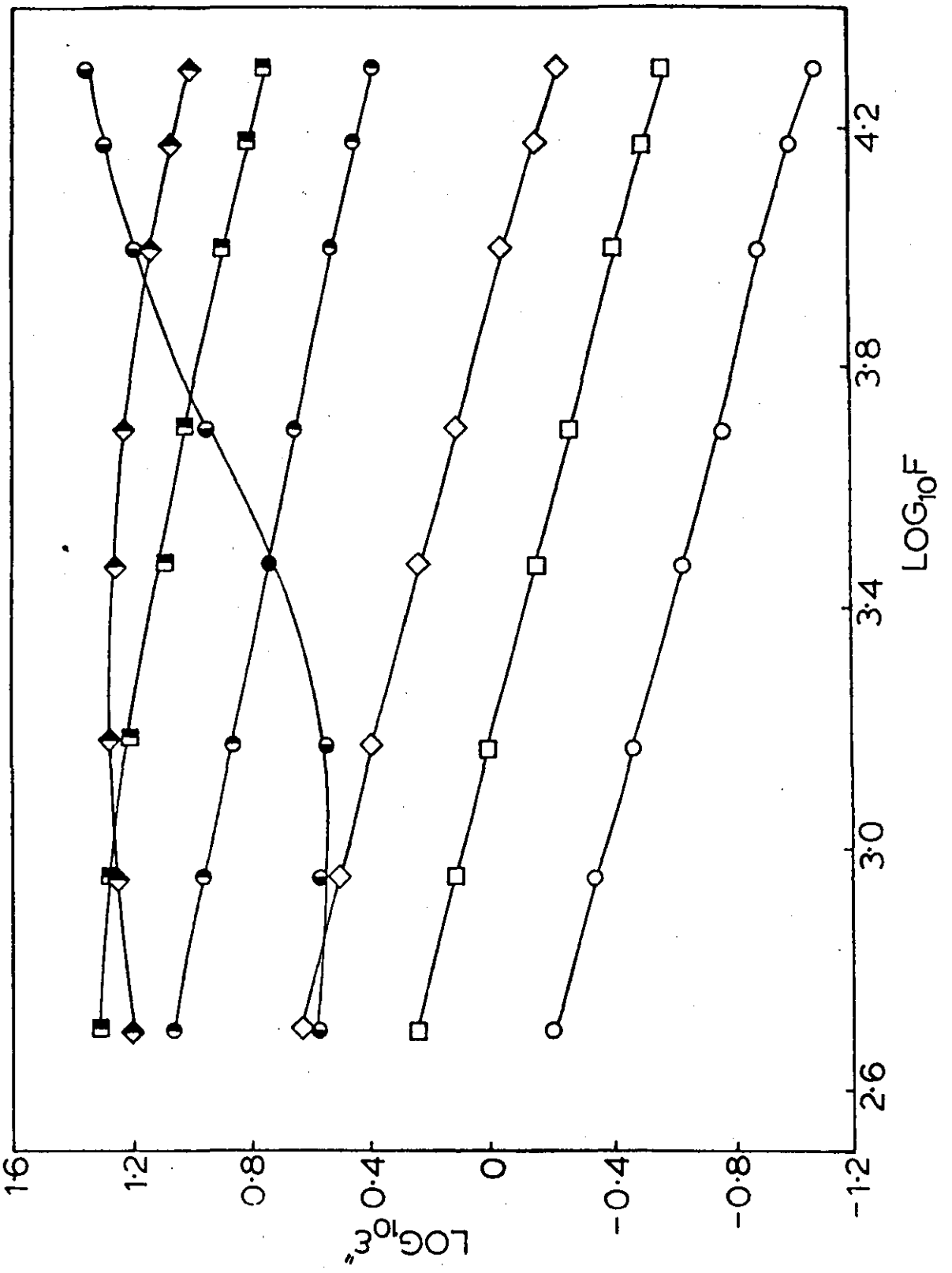

FIGURE 4·18

TABLE 4.5 Visual Properties of Poly(ethylene glycol) Complexes with Lithium Thiocyanate

Salt Loading	Nature of complex	Optical Clarity above Tm	Comments
0,5 and 10 mole%	Semi-crystalline	Transparent	Single phase, semi-crystalline below, viscous liquids above, a critical salt loading Less deliquescent than their constituent chemicals.
15 and 20 mole%	Amorphous	Transparent	

GLASS TRANSITIONS EXHIBITED BY LiSCN COMPLEXES OF POLY(ETHYLENE GLYCOL)

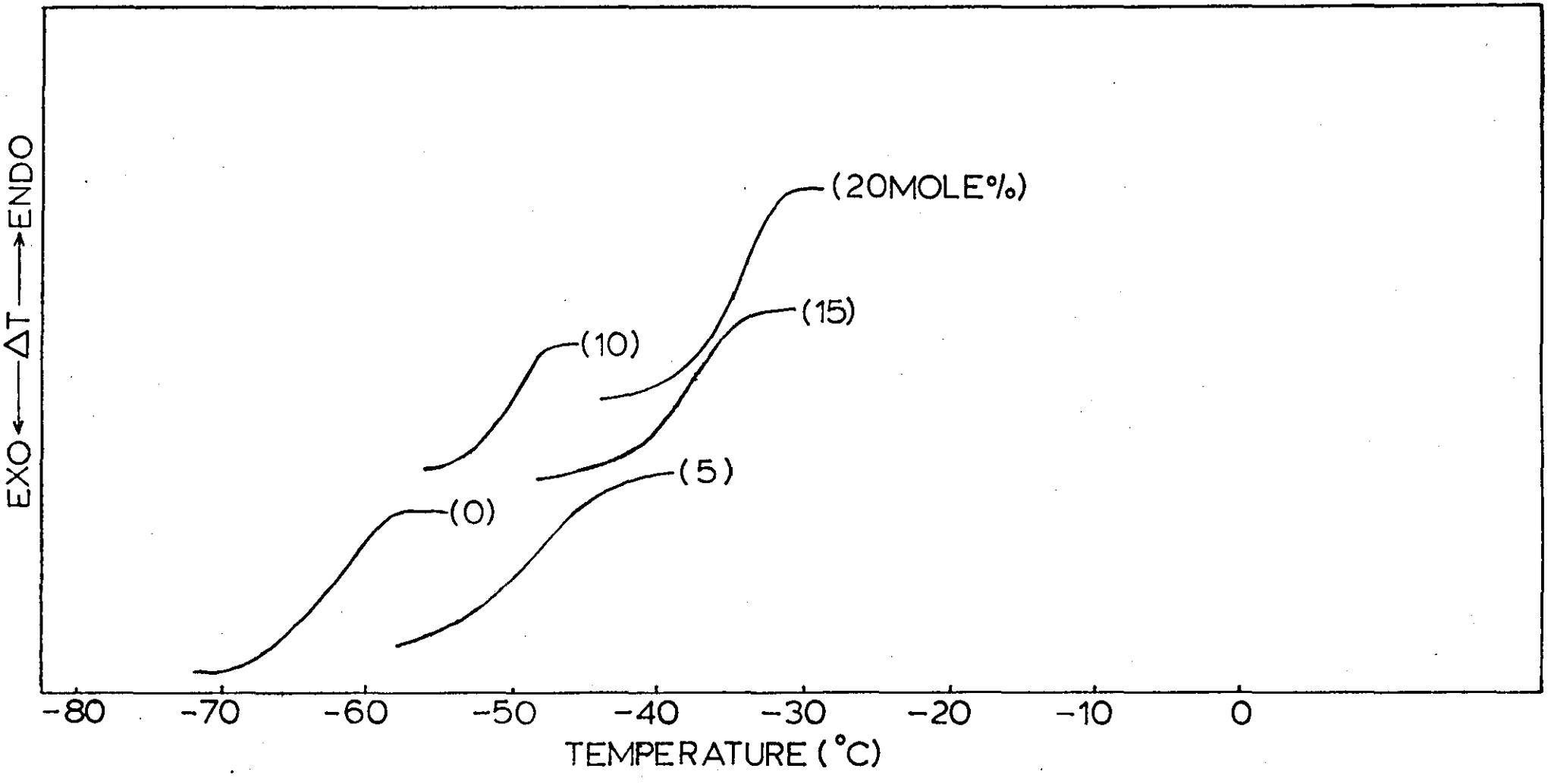

FIGURE 4.19.

THE VARIATION IN T_g AND T_m WITH MOLE% OF SALT CONTENT IN LiSCN POLY(ETHYLENE GLYCOL COMPLEXES

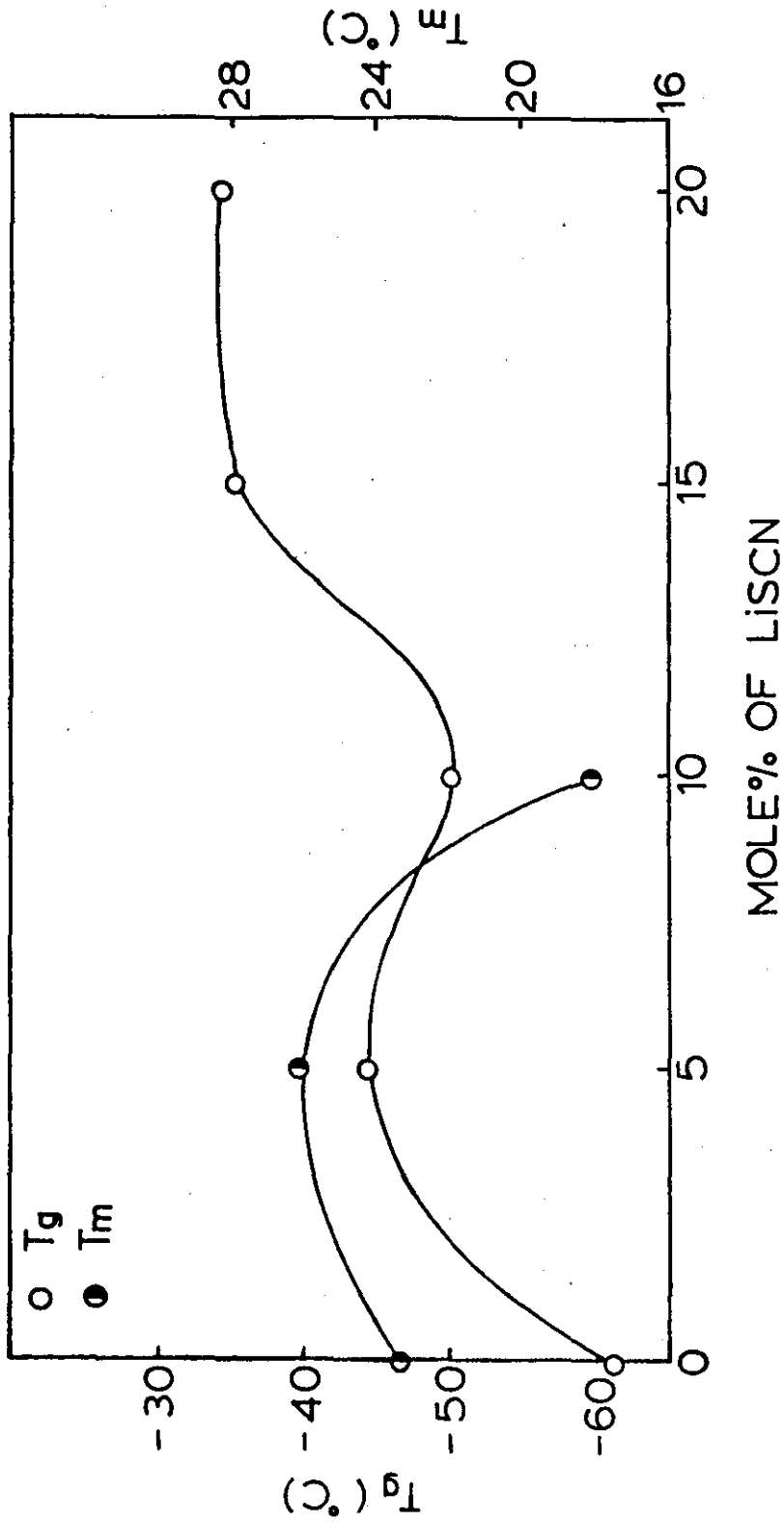

FIGURE 4·20

relationship between lithium thiocyanate and poly(ethylene glycol). The melting point increases to 5 mole% and then decreases to 10 mole% disappearing for 15 mole% and higher. The glass transition is seen to increase for 5 mole% decrease for 10 mole% and then increase to 15 mole% tending toward a limiting value of 20 mole%.

Upon addition of lithium thiocyanate to poly(ethylene glycol) at low concentrations, the lithium thiocyanate will be complexed with the hydroxyl groups at the end of the chain and in the amorphous regions of the polymer. Thus making the polymer chains stiffer and a subsequent increase in the value of Tm. Further addition of salt will cause a suppression in crystallinity, and a subsequent reduction in the value of Tm, thereby increasing the amorphous content of the sample. The reduction in the value of Tg of 10 mole% with respect to 5 mole% will therefore be as a result of a decrease in crystallinity and thus chain stiffness, and an increase in amorphous content and therefore an apparent dilution of the real salt content in the amorphous region. Further additions of salt completely suppress crystallinity and increase the value of Tg as the salt concentration in the now totally amorphous regions rises, as was seen in poly(ethylene glycol).

4.4.3 Viscosity Data for a Poly(ethylene glycol)-Lithium Thiocyanate Complex

Figure 4.21 shows the viscosity temperature profile for poly (ethylene glycol) and a 20 mole% poly(ethylene glycol) complex. The effects of crystallinity in the pure polymer are observed at the low temperature end of the viscosity profile. As the polymer melts the viscosity changes dramatically. This makes superposition difficult because as was shown earlier, the crystallinity is totally suppressed in the 20 mole% lithium thiocyanate complex. Despite the crystallinity

VISCOSITY TEMPERATURE PROFILE OF A LISCN POLY(ETHYLENE GLYCOL) c.f. THE HOMOPOLYMER COMPLEX

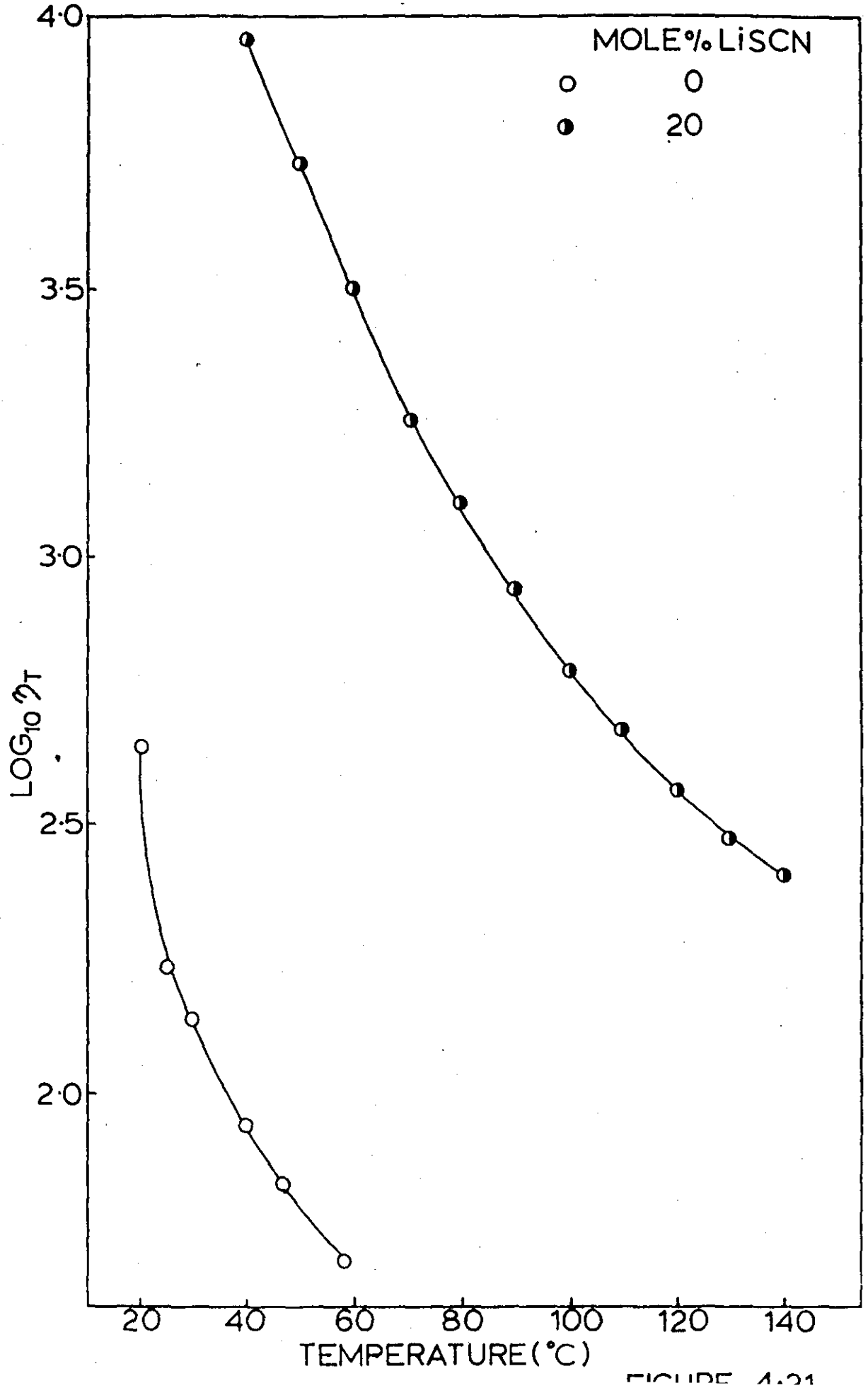

FIGURE 4·21

effects one can clearly discern a large positive temperature shift upon complexation.

4.4.4 Dielectric Relaxations Exhibited by Poly(ethylene glycol)-Lithium thiocyanate Complexes

Poly(ethylene glycol) shows three relaxations over the temperature and frequency range studied. The high temperature side of the α_g process is clearly discernible and the α_c process associated with crystal melting around 20°C and a process α_i intermediate between the two. The loss peak does not significantly fall above Tm due to the onset of conductivity. The dielectric data upon addition of lithium thiocyanate is somewhat more complex as shown in Figure 4.22. A single skewed loss peak due to the merging of the above processes is observed for 5 mole% salt loading. For 10 mole % salt loading two peaks are clearly discernible, a sharp peak of reduced area for the α'_c process and a merged α'_g and α'_i peak. At 15 mole% the α'_c process has disappeared completely and a single loss peak is observed. At 20 mole% this peak has reduced in height and shifted to higher temperatures in accordance with the shift in Tg.

The dielectric constant data tends toward a limiting value over the temperature range studied independent of salt content. For the 5 and 10 mole% a single step dielectric process is observed. However for 15 and 20 mole% (amorphous samples) two steps appear to occur. A lower temperature step associated with the α'_g process and a step occurring some degrees higher which may be similar to the α' seen in poly(propylene glycol), see Figure 4.8 2 mole% LiCNS/PPG.

The step process appears to be shifted to lower temperatures with the disappearance of the α_c process, but increases between 15 and 20 mole% as the Tg increases although the actual temperature

TEMPERATURE DEPENDENCE OF $LOG_{10}\varepsilon'$ AND $LOG_{10}\varepsilon''$ FOR POLY(ETHYLENE GLYCOL) LiSCN COMPLEXES AT 5kHz

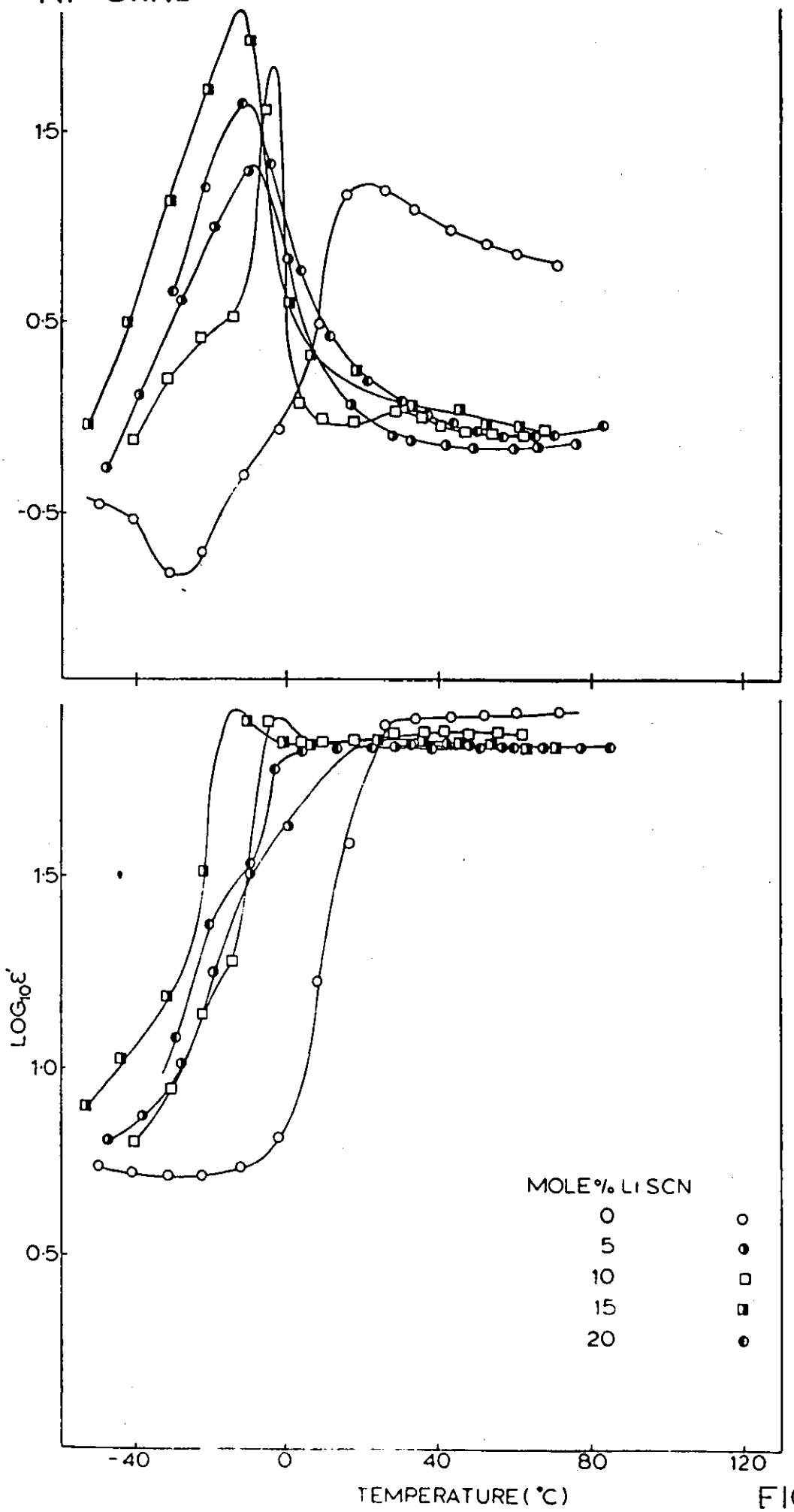

FIGURE 4·22

shift in the dielectric constant is greater than the Tg shift between 15 and 20 mole%.

The appearance of a peak in the dielectric constant with increasing temperature at constant frequency by some of the samples is not uncommon in oligomers of this molecular weight[207].

Figure 4.23 illustrates the frequency temperature plane location for the α'_c process in low salt loading poly(ethylene glycols) and the α'_g process for purely amorphous poly(ethylene glycol) salt complexes. The temperature shift with increasing frequency is seen to be small especially at low frequencies. The effect of such a low molecular weight with subsequently such a narrow distribution of relaxation times produces such a frequency temperature profile.

Figures 4.24 and 4.25 show the frequency dependence of $\log_{10}\varepsilon'$ and $\log_{10}\varepsilon''$ for a 15 mole% lithium thiocyanate-poly(ethylene glycol) complex at various temperatures respectively. As was seen for other polymer systems a well defined family of curves were observed. One can discern the tendency of low molecular weight oligomers to form a peak in the dielectric constant with increasing temperature at low frequency. The onset of a second process above α'_g is observed in Figure 4.25 at a temperature of -0.5°C at low frequencies.

4.5 Inorganic Salt Complexes Blended with Poly(ethylene vinyl acetate)

Inorganic salt complexes of poly(methyl vinyl ether) were blended with poly(ethylene vinyl acetate), (EVA), in various amounts. Figure 4.26 shows the dielectric relaxations observed for these blends. A single relaxation which appears as a peak in ε'' at -9°C at 5 kHz was observed for pure EVA. Upon blending with inorganic salts of poly (methyl vinyl ether) two relaxation peaks are discernible over the

FREQUENCY TEMPERATURE LOCI (BASED ON $LOG_{10}\varepsilon''$ DATA) FOR LiSCN COMPLEXES OF POLY(ETHYLENE GLYCOL)

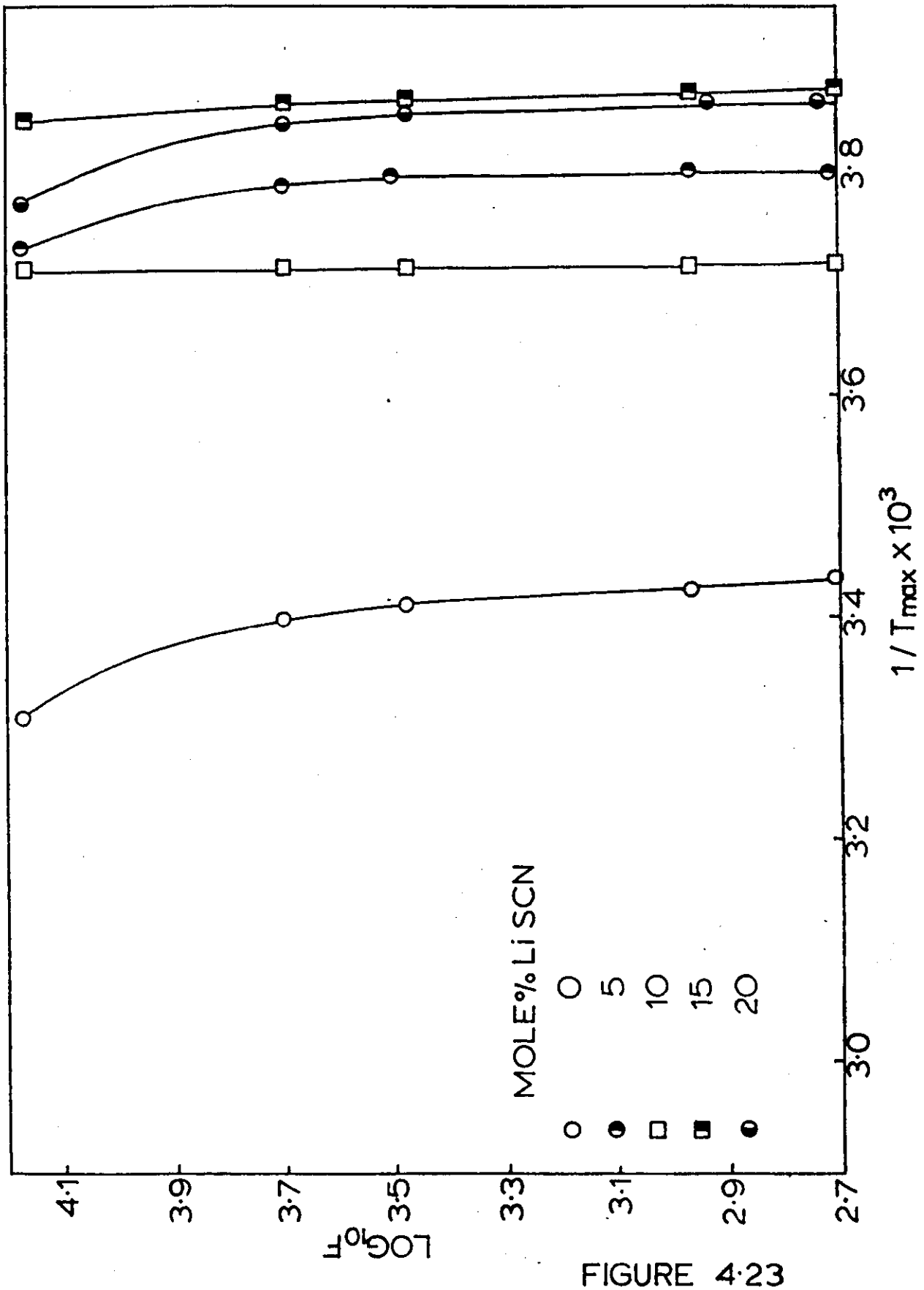

FIGURE 4·23

FREQUENCY DEPENDENCE OF ε' AT VARIOUS TEMPERATURES FOR A 15MOLE% LiSCN POLY(ETHYLENE GLYCOL) COMPLEX

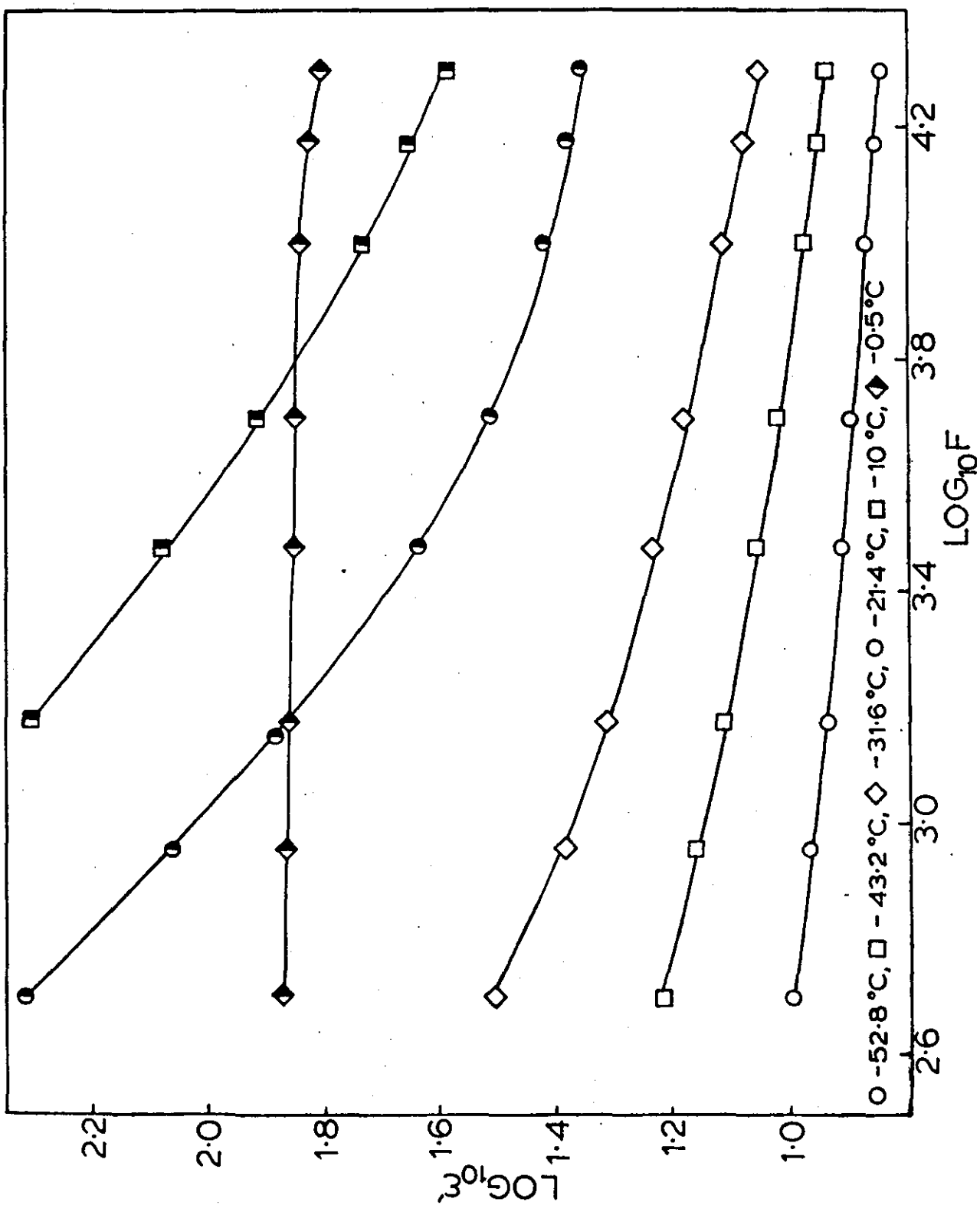

FIGURE 4·24

FREQUENCY DEPENDENCE OF ε'' AT VARIOUS TEMPERATURES FOR A 15MOLE% LiSCN POLY(ETHYLENE GLYCOL) COMPLEX

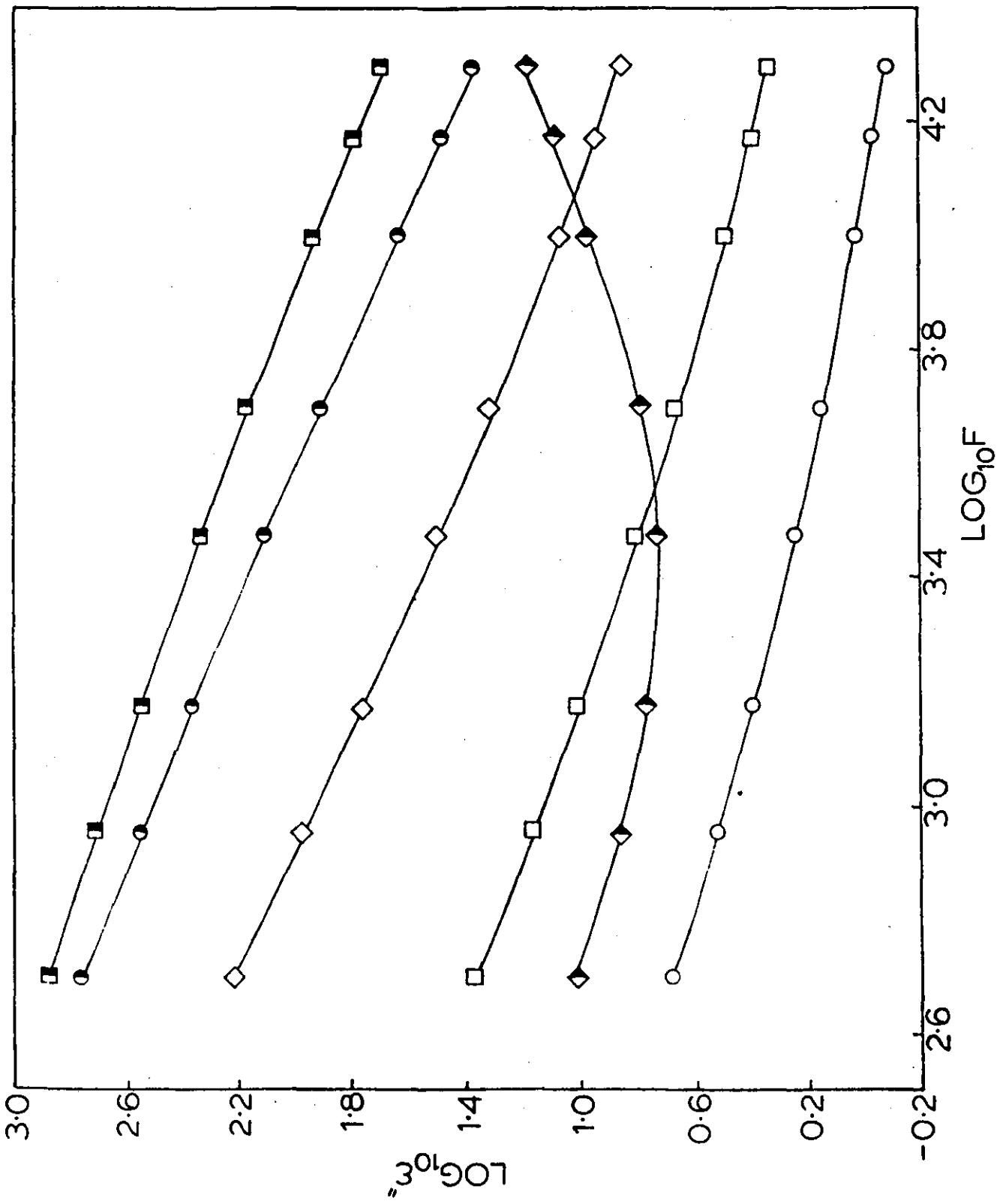

FIGURE 4·25

TEMPERATURE DEPENDENCE OF $LOG_{10}\varepsilon'$ AND $LOG_{10}\varepsilon''$ FOR BLENDS OF EVA / POLY. (ETHER) COMPLEXES AT 5kHz

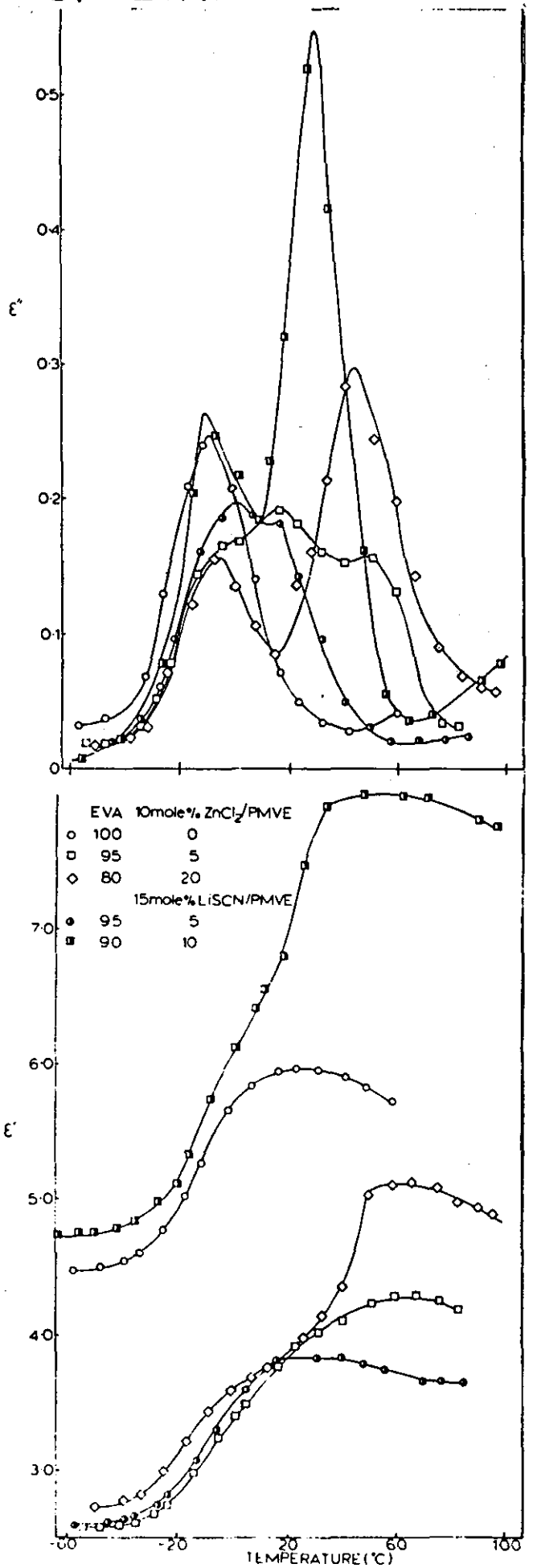

FIGURE 4·26

frequency and temperature range studied. A peak corresponding to EVA and one at a higher temperature corresponding to the salt complex. One can clearly see an increase in the dielectric loss peak upon increasing the amount of salt complex in the blend which is to be expected. It is pertinent to note that in a pure salt complex above the α' process, conductive processes are believed to occur. These conductive processes may override the α' process making it rather difficult to be able to discern between the two. In the above blends, if well blended, the salt complex will be dispersed throughout the sample. The resulting blend will thus comprise a relatively non-conductive matrix of EVA with the more conductive salt complex dispersed throughout the matrix. The α' process of the salt complex should therefore appear without the masking effect of the conducting process because of the EVA matrix preventing conductivity observed in Figure 4.26. In this way we have a method for studying the process without the interfering effects of conductivity.

4.6 Applications Testing

Figures 4.27 and 4.28 show the theoretical dielectric heating parameter ($\tan \delta / \varepsilon'$) for various salt complexes with temperature at 10 MHz and 20 MHz respectively. For all systems excluding a 7 mole% $ZnCl_2$ poly(propylene glycol) complex the dielectric heating parameter ($\tan \delta / \varepsilon'$) increases with increasing temperature. The 7 mole% $ZnCl_2$ poly(propylene glycol) complex is seen to decrease marginally with increasing temperature at 10 MHz.

Barium thiocyanate, lithium trifluoromethyl sulphonate and 30 mole% lithium thiocyanate poly(propylene glycols), showed markedly higher values for theoretical dielectric heating capability over the other systems.

TEMPERATURE DEPENDENCE OF THE DIELECTRIC HEATING PARAMETER FOR POLY(ETHER) SALT COMPLEXES AT 10MHz

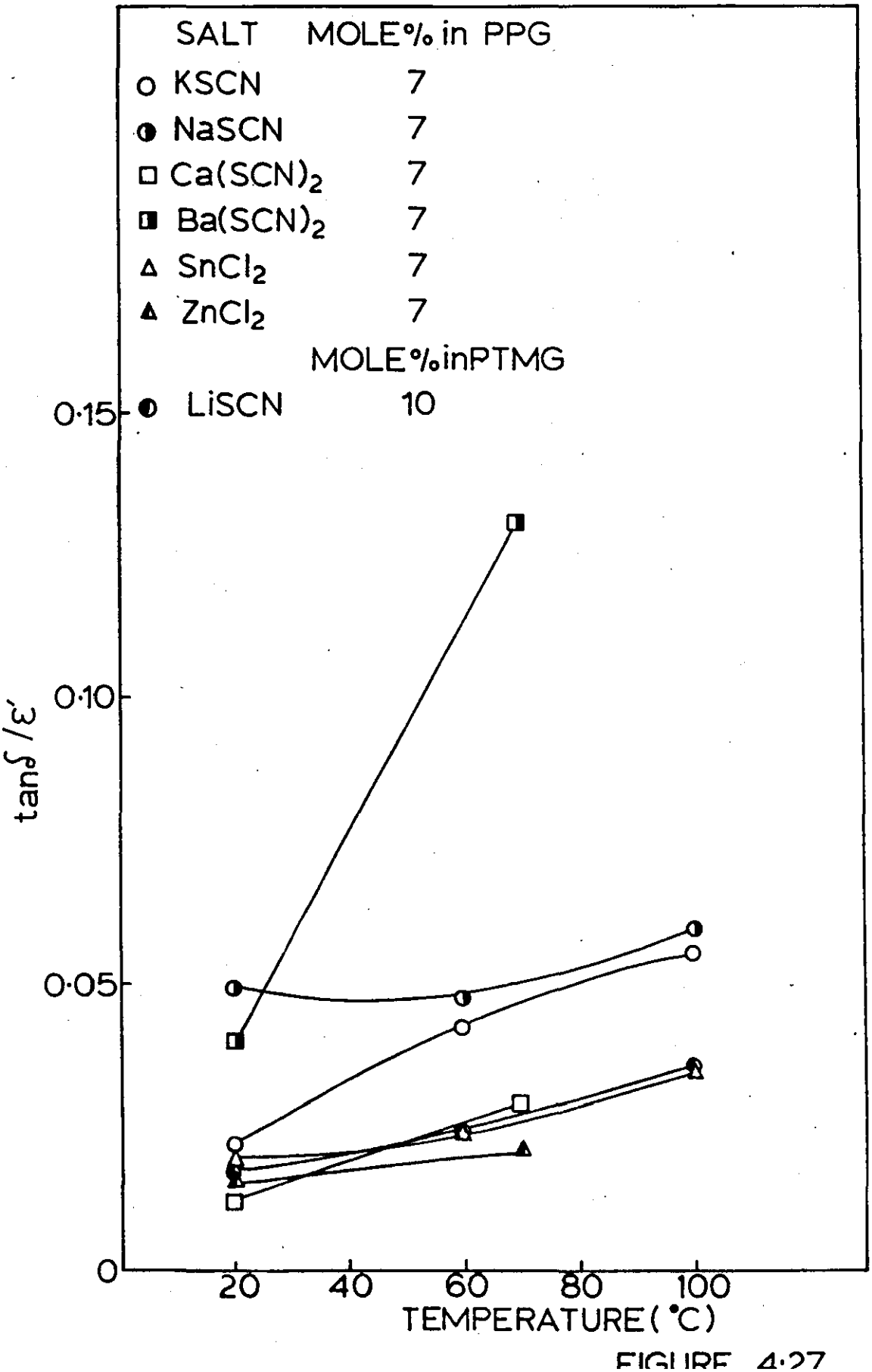

FIGURE 4·27

TEMPERATURE DEPENDENCE OF THE DIELECTRIC HEATING PARAMETER FOR POLY(ETHER) SALT COMPLEXES AT 10MHz

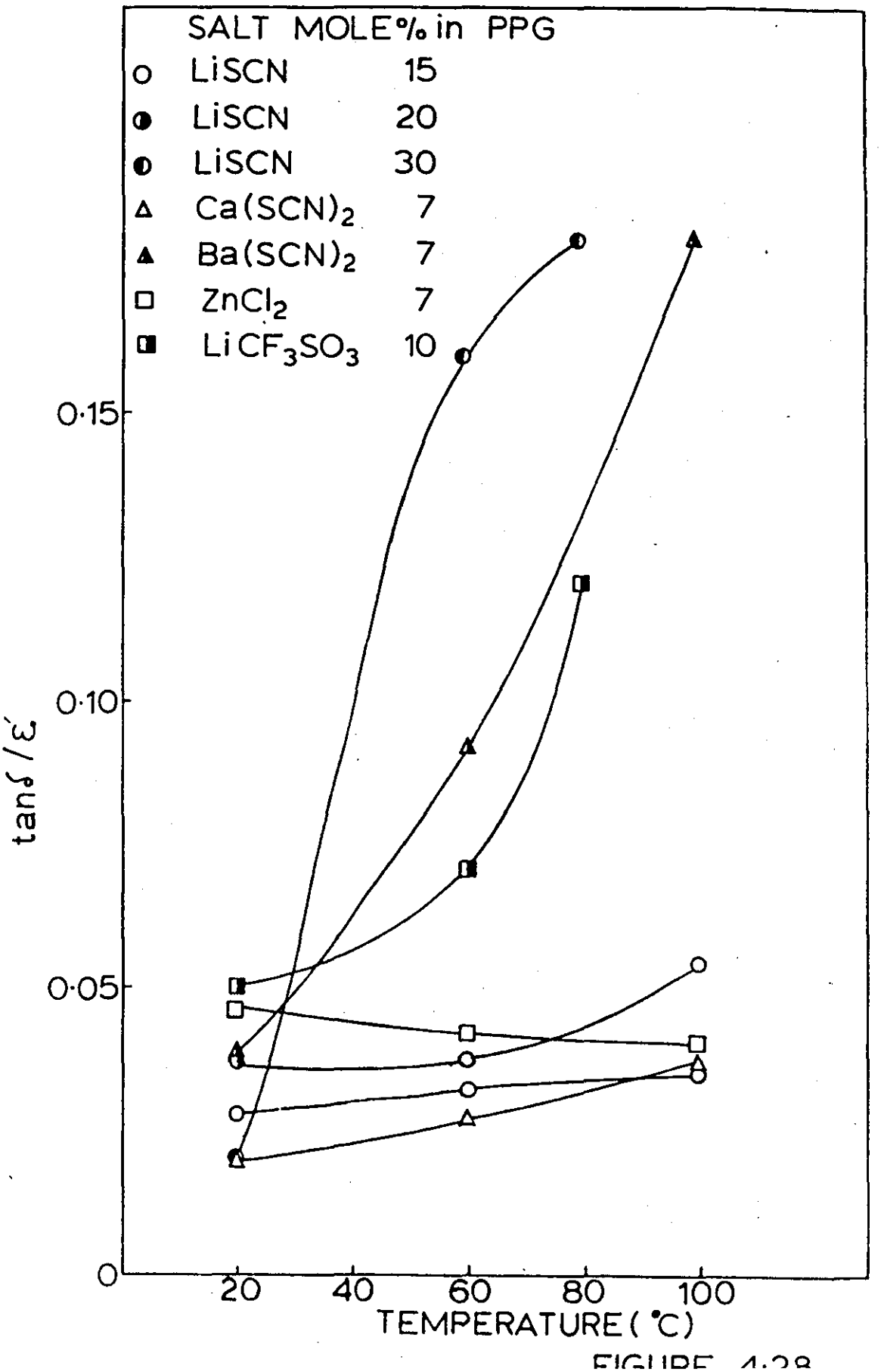

FIGURE 4.28

Increasing the salt loading appears to improve the theoretical dielectric heating capability in the lithium thiocyanate poly(propylene glycol) complex especially between 20 and 30 mole% salt content. Sodium thiocyanate shows higher values than potassium thiocyanate for theoretical dielectric heating capability especially at room temperature when complexed with poly(propylene glycol).

Replacing the thiocyanate anion with a trifluoromethyl sulphonate anion in a lithium cation results in a marked improvement in dielectric heating potential especially above ambient temperatures. A poly(tetramethylene glycol) lithium thiocyanate complex appears to give similar values for dielectric heating potential to its poly (propylene glycol) counterpart.

The salt complexes appear to compare favourably with dielectrically heat-sealable plasticised poly(vinyl chloride) which typically has a dielectric heating parameter of 0.0074 at 25^{o}C. A non-dielectrically heat-sealable dielectric like poly(styrene) has a correspondingly much lower tan δ / ε' value of 0.00015.

Table 4.6 lists examples of polymers that have been rendered heat-sealable upon blending with a poly(ether) salt complex. The salt complexes referred to as dielectric enhancers were blended in at levels between 10 and 20 weight %.

Table 4.7 shows some typical machine settings and times for salt complexes blended with usually non heat-sealable polymers. The dielectric machine settings, output and overload, refer to the amount of voltage applied to the system. The higher the value the more power input. The dielectric heating was performed on a Dynatherm Dielectric Welding Press.

TABLE 4.6 Examples of polymers that have been converted into dielectrically heat-sealable materials by salt complexes

Polymer	Dielectric Enhancer (DE)	Heating Time for seal (seconds)	Weight % DE
ABS	10 mole% NaSCN/PPG	-	20
ABS	10 mole% KSCN/PPG	3	20
HYTREL	15 mole% $Ba(SCN)_2$/PPG	-	15
HYTREL	10 mole% KSCN/PPG	-	10
HYTREL	15 mole% S_nCl_2/PPG	6	15
Poly(ethylene)	10 mole% KSCN/PPG	-	10
Poly(propylene)	10 mole% KSCN/PPG	20	10
Poly(styrene)	20 mole% LiSCN/PPG	10	10
SBS	10 mole% LiSCN/PPG	10	10

PPG = Poly(propylene glycol) M.W. 2000
ABS = Acrylonitrite-butadiene-styrene
HYTREL = A Dupont trade name for segmented poly(ether)-poly(ester)
SBS = Styrene-butadiene-styrene triblock copolymer

TABLE 4.7 Dielectric heating settings and time for dielectrically enhanced polymers

Polymer	Dielectric Enhancer (DE)	Weight % DE	Dielectric Machine Settings for Seal		
			Output	Overload	Time/seconds
ABS	10 mole% NaSCN/PPG	20	6.5	7	5
ABS	10 mole% KSCN/PPG	20	4.5	4.5	3
ABS	10 mole% LiSCN/PTMG	10	9	7	8
ABS	20 mole% $Ca(SCN)_2$/PTMG	10	9	6	10
HYTREL	15 mole% $Ba(SCN)_2$/PPO	15	9	7	10
HYTREL	15 mole% $SnCl_2$/PPO	15	8	7	6
HYTREL	20 mole% NaSCN/PTMG	10	9	6	10
SBS	10 mole% LiSCN/PPG	10	9	6	5
Poly(styrene)	20 mole% NaSCN/PTMG	10	9	6	10

PTMG = Poly(tetramethylene glycol) M.W. 1040
PPO = Poly(propylene oxide) M.W. 100,000

Figure 4.29 show typical examples of resistivities versus temperature for various salt complexes. One can discern a non-linear decrease in resistivity with increasing temperature. The resistivities appear to be lowest for lithium based complexes. The lowest resistivities shown correspond to complexes containing poly(propylene sulphide) and poly(propylene glycol). It is pertinent to note that the glass transition temperature of these low resistivity complexes lie considerably below those of the poly(vinyl alcohol) and poly (ethyl vinyl ether) complexes.

From the limited data shown, at ambient temperatures, the lithium based complex shows a resistivity of more than one and a half decades below that of an equivalent zinc based complex in poly(propylene sulphide).

Table 4.8 compares the charge stored and storage time of two uncomplexed polymers with those of complexed polymers. It can be seen that on increasing salt content from 18 mole% to 27 mole% $ZnCl_2$ in poly(propyelene oxide) the charge stored and the half life of storage is reduced. Complexation of poly(propylene oxide) appears to increase manifestly the half life of storage with comparison to uncomplexed poly(styrene) and poly(vinylidene fluoride). The actual charge stored however appears to be greatest for unmodified poly(vinylidene fluoride). The lower salt loading polymer appears to store more charge than poly(styrene) but the higher salt loaded polymer considerably less.

TEMPERATURE DEPENDENCE OF RESISTIVITIES FOR SALT COMPLEXES AT 500Hz

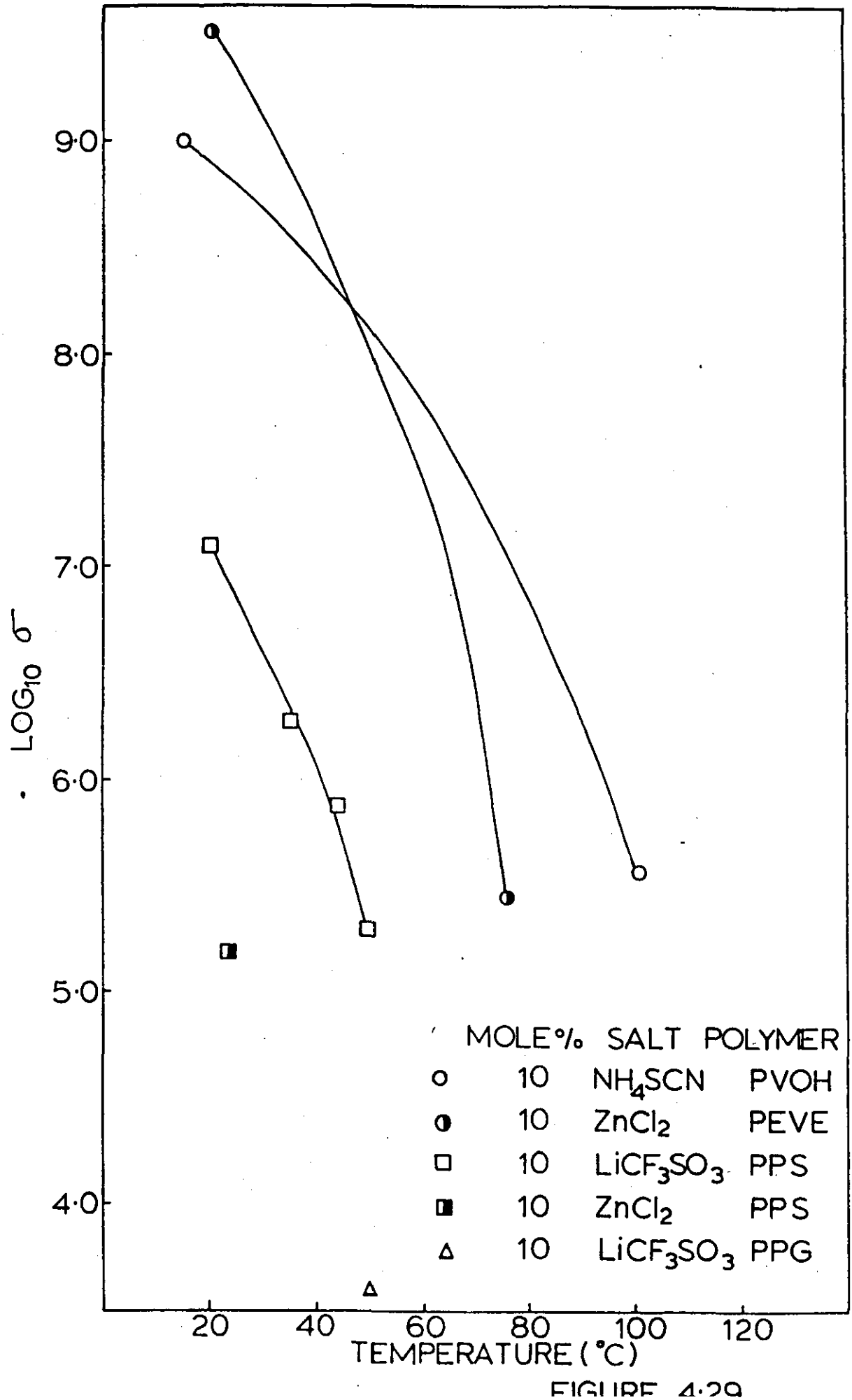

FIGURE 4·29

TABLE 4.8 Charge storage capacity of salt complexes

Polymer	Charge/μC	Half life 20°C) (minutes)
Poly(styrene)	0.029	33
Poly(vinylidene fluoride)	0.21	25
18 mole% $ZnCl_2$/PPO	0.072	10^5
27 mole% $ZnCl_2$/PPO	0.0029	1.3×10^4

5.0 DISCUSSION OF INORGANIC SALT COMPLEXES OF POLYETHERS

5.1 General Observations on Polyether Inorganic Salt Complexes

It was shown in chapter 4 that two types of system could be formed upon the addition of inorganic salts to polyethers. The general properties of the two types of system have been described previously but will be briefly clarified here.

Systems of type I were transparent viscous liquids, or were so above their Tm's when crystallinity was involved. Type II systems were opaque. Although transparency in itself is not an absolute measure for a single phase, because any heterogeneities smaller than 2000 Å would not be observable, the opacity of type II systems clearly indicated the presence of two phases. It was therefore optically apparent that the salt present was dispersed differently in the two types of systems.

The thermal properties of the two types of systems further illustrated their differences. An elevation in Tg and suppression of crystallinity where present with respect to their parent polymer characterised systems of the first type. Systems of the second type showed essentially no change in the observed thermal properties . A strong interaction between the salt and the polymer is therefore clearly indicated for polymers of the first type.

The water sensitivity of the two types of systems further illustrated their differences. Systems of the first type were in general derived from salts of a highly deliquescent nature, these salts often rapidly dissolved in their own water of crystallisation when exposed to the atmosphere. The resulting polymer salt complexes of type I systems were considerably less deliquescent than the uncomplexed salt with

only a slight water uptake upon prolonged exposure to a humid atmosphere. However it was found that systems of the second type absorbed water rapidly from the atmosphere.

From these basic observations systems of the first type may be regarded as complexes where the salt is molecularly distributed along the polymer chain. In contrast systems of the second type shared no or very weak interactions between the salt and the polymer, with the salt acting as a filler only.

5.2 Glass Transition Temperatures of Inorganic Salt Complexes of Polyethers

Eisenberg[17,21] has recently reviewed the effects of the elevation in the glass transition temperature by ions. He considered three models derived from a consideration of cross-linking, ion-clustering and copolymerisation effects all of which were capable of explaining the Tg elevation seen.

Otocka and Eirich[209] employed the first of these three models in their studies of copolymers of butadiene with ionic monomers. A linear relationship between Tg and the concentration of ionic groups was found. Furthermore the magnitude of the Tg was found to be dependent upon the nature of the ionic monomer. Viscoelastic studies of these systems showed a temperature much higher than Tg, below which the ions appeared to be acting as crosslinks. They concluded that the Tg was not due to ionic mobility but to other chain segments and that the ionic crosslinks increased Tg.

Studies by Otocka and Kwei[81] on the dynamic mechanical properties of ethylene-metal methacrylate copolymers showed a shift to higher temperatures of the glass transition with increasing salt content. They found that the system obeyed the basic copolymer equation

$$Tg = n_1 Tg_1 + n_2 Tg_2 \qquad (5.1)$$

A third mechanism for the elevation of Tg in ion containing polymers was proposed by Matsura and Eisenberg[208] involving the clustering of ions. The results obtained from an investigation of the glass transitions exhibited of various ethyl acrylate ionomers of various compositions found that the variation of Tg with ion content was uniquely sigmoidal. Furthermore that the steepest point on the curve concurred with the point in viscoelastic measurements when time-temperature superposition became ineffectual. The curves could be superimposed when the charge to ion separation (q/a) ratio was taken into consideration. They concluded that the results could be explained in terms of ion clustering[92] involving a subsequent decrease in segmental motion of sufficient magnitude to affect Tg.

More recently Tsutsui and Tanaka[211] were able to successfully correlate the glass transition temperature with the cohesive energy density for ionic polymers such as polyphosphates, polyacrylates and the ionenes. They proposed that the increases in intermolecular forces in ionomers as a consequence of the introduction of ionic structural units overpowered the normal Tg influences. They dominated to such an extent that at higher ion content Tg was solely a function of the electrostatic intermolecular forces and thus deducible from basic electrostatic theory in terms of cohesive energy density.

The theories stated above have been applied in the main to systems in which ionisable structural units have been copolymerised into the backbone. The elevation of Tg is however not solely restricted to these systems and it may be pertinent at this juncture to underline the work of Wetton and James[47], Moacanin and Cuddihy[49] and Hannon and Wissbrun[212]. The first two papers involved the incorporation

of zinc chloride and lithium perchorate respectively into poly(propylene oxide). They described the resulting elevation of Tg in terms of a strong electrostatic interaction between the cation and the ethereal oxygens. Hannon and Wissbrun[212] simply ascribed the elevation observed in Tg of a calcium thiocyanate-phenoxy system in terms of a reduction in free volume caused by the salt.

Several mechanisms have been proposed in this section for the elevation of Tg by the incorporation of ionic species into a polymer. Evidently the observed increase in Tg may be as a combination of any of the above models and before any definite assertion can be made supportive evidence would be required.

It is the intention over the next sections to apply the mechanisms discussed and present further evidence in support.

5.2.1 A Single Phase Model

In an earlier section it was stated that optical clarity in itself is not absolute evidence for a single phase. However the glass transition data obtained can give valuable support to this assumption.

It is well documented that block and graft copolymers[213] and blends[147,148] can clearly show two Tg's corresponding to the two polymer components separated into individual polymeric phase domains.

The appearance of a single glass transition process in the polyether inorganic salt complexes is indicative of the presence of a single polymeric phase.

MacKnight et al.[214] has estimated the degree of molecular compatibility of a series of compatible blends of poly(phenylene oxide)/poly (styrene) from the breadth of the glass transition. A single glass

transition was observed although somewhat broader than the glass transitions of the two homopolymers. In the case of a homogeneous blend a single glass transition of the same breadth as the homopolymers would be expected , any broadening therefore may be attributed to inhomogeneities.

Mason[215] has studied the effects of cross-linking in rubbers upon the thermal expansion, glass transition temperatures and imaginary shear modulus of rubbers. He noticed an increased broadening of all the above properties with increased degrees of crosslinking. This 'smearing out' of the transition was attributed to the existence of a distribution of the values of the fractional free volume.

A broadening of the glass transition accompanied by a reduction in magnitude of the glass transition was observed in poly(tetramethylene glycol) and poly(ethylene glycol) with respect to poly(propylene glycol). This is a consequence of the inherent crystallinity in the former two in comparison to the amorphous low molecular weight poly(propylene glycol). Thus prior to the complexation with salts there is a broader glass transition in the crystalline polyethers studied.

At low salt loadings, the glass transition data presented in Figure 4.1 for poly(propylene glycol) complexes indicates compatibility as described by MacKnight et al.[214] or lack of any significant cross-linking. As the salt loading increases and the glass transitions broaden inhomogeneities may occur, or as will be described in detail later, crosslinking between polymer chains by the salt will start to occur as the ether oxygens are progressively complexed in the chelate rings as described by Wetton and James[46].

Obviously the broadening observed in the crystalline polymers with respect to the amorphous poly(propylene glycol) undergo further

broadening upon salt complexation except where crystallinity has been totally suppressed as in poly(ethylene glycol). Figure 4.19 shows a sharpening of the glass transition corresponding to loss in crystallinity in poly(ethylene glycol) as salt loading increases. It would therefore appear that crystallinity has a marked effect upon the breadth of the glass transition. Reduction of crystallinity by the addition of salt to form polymer salt complexes appears to sharpen the glass transition in comparison to salt addition in amorphous polymers which broadens the glass transition.

Amorphous and crystalline phases in semi-crystalline polymers are obviously inhomogeneous. Reduction of this inhomogeneity should sharpen the glass transition as described by MacKnight et al.[214]. Total suppression of crystallinity (as observed for a 20 mole% calcium thiocyanate poly (tetramethylene glycol) complex) should therefore markedly sharpen the observed glass transition, because the inhomogeneous crystalline phase which is of the order of 20 to 30% in the pure polymer to 0% in the complexed polyether is a large change in inhomogeneous content. Only a relatively small sharpening of the complex however is observed. It would therefore appear that the breadth of a glass transition of a polyether inorganic salt complex is dependent upon both the degree of crosslinking caused by salt bridges between polyether chains and the degree of inhomogeneity introduced into the system upon complexation.

This interference with the breadth and the positioning of the glass transition in polyether salt complexes suggests that the salt is dispersed on a molecular level throughout the polymer. A single polymeric phase could be oberved if the salt was behaving like a conventional filler[213], However the positioning of the glass transition temperature would be expected to be close to the pure polymer glass

transition in direct contrast to that which is observed.

Visual evidence for a single phase system comes from a comparison between types I and II compounds. It was clearly obvious that in type II compounds that two phases existed as a consequence of their opaqueness in direct contrast to the transparent type I compounds. Furthermore type II compounds showed no appreciable change in their glass transition temperatures. The observed behaviours of type I and type II compounds was strongly indicative of a single phase in the former and a two-phased filled system in the latter.

Figure 4.4 revealed the variation in magnitude of the glass transition with the amount of salt present. It was self-evident that in the lithium chloride system the lithium chloride was acting as a filler and so no significant change in Tg was observed as seen in Figure 4.4. In these type II compounds only the polymer present underwent a glass transition whereas in the type I compounds the whole sample including the salt underwent a glass to rubber transition. Further indicating that the type I compounds were dispersed throughout the system on a molecular level.

5.2.2 The Elevation of the Glass Transition Temperature of Polyethers by Lithium Thiocyanate

Attempts were made without success to produce an inorganic salt complex of poly(methylene oxide). This was as a consequence of several problems. Poly(methylene oxide) is highly crystalline (circa 90%) and as a consequence is insoluble in many solvents. It is however soluble in dichlorobenzene if refluxed at 80°C for several hours. Addition of a salt solution and subsequent solvent removal did not however yield the desired polymer-salt complex. In fact in the case of the weak Lewis acid zinc chloride a black oil was produced presumably as a consequence of the depolymerisation reaction.

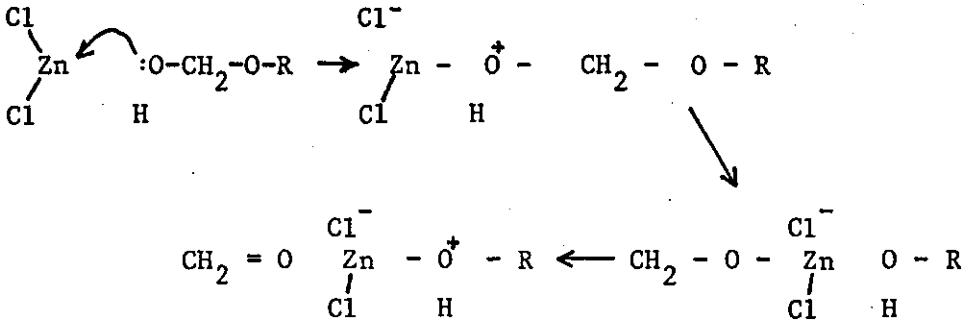

Poly(ethylene glycol), poly(propylene glycol) and poly(tetramethylene glycol) all showed elevation of their respective glass transitions upon complexation with lithium thiocyanate as shown in the previous chapter. It was shown previously that several factors influence the position of Tg but to produce the variations in Tg observed molecular complexation between the polymer and the salt, rather than the much weaker physical effects of a filler, must occur.

Essentially the most likely interactions for molecular complexation are those between the lone electron pairs of the end hydroxyl group and of the ether oxygens with the cation. Padova[216] claims that the anion thiocyanate has a zero solvation number. A coordinate bond would result as the consequence of such an interaction between the polymer chain and the cation. The lithium cation, like many other cations, is capable of accepting more than one lone pair of electrons and therefore more than one ether linkage is possible.

If two adjacent ether oxygens on the same chain were coordinated to the same cation a chelate ring would result. If, however, the oxygens were on different chains or were the terminal oxygens at the end of the chains a crosslink via the salt would be formed. The ultimate choice between intra and intermolecular coordination will be dependent on both the salt and the polymer and for some systems it is likely that both exist.

A coordination number of four is favoured by the lithium cation with the ligands arranged tetrahedrally around the central cation[17]. Figure 5.1 illustrates some of the possible interactions between poly(ethylene glycol) and poly(propylene glycol) with lithium thiocyanate. The simplest case for coordination occurs when only a single ether or hydroxyl oxygen is interacting with the lithium ion. When two oxygen atoms are involved there is the possibility for both intra and intermolecular coordination. It is however only until three oxygen atoms are involved in the coordination process that the lithium ion has fulfilled its coordination requirements. For the intramolecular case three adjacent oxygen atoms are required to interact with the cation. For intermolecular coordination it is possible that all three oxygen atoms belong to different chains. Alternatively that two adjacent oxygens form a five-membered chelate ring containing the lithium salt and a third oxygen from a different chain coordinates to the lithium.

If the thiocyanate anion is ionised it is possible for four oxygen atoms to be coordinated to the lithium cation. For the intramolecular situation this would require four adjacent oxygens to coordinate. For intermolecular coordination several possibilities may occur. Two adjacent oxygen atoms on different chains may all be coordinated to the same cation, or a three oxygen chelate ring and a fourth oxygen coming from a different chain. It is also possible for a two oxygen chelate ring and the remaining two oxygens from two different chains. Or, finally, all four oxygens could be coordinating from four different chains.

If the thiocyanate is covalently bound to the lithium cation then it is possible for a maximum of three oxygens to coordinate to the salt. In the situation where the thiocyanate is ionised a maximum of four oxygen atoms may be employed for coordination. Furthermore if the coordination was ion-dipolar rather than coordinate in nature it would

SCHEMATIC REPRESENTATION OF POSSIBLE POLY(ETHER) LITHIUM THIOCYANATE COMPLEX STRUCTURES

R = H FOR POLY(ETHYLENE GLYCOL)
R = CH_3 FOR POLY(PROPYLENE GLYCOL)

MODEL A 1 OXYGEN COORDINATION

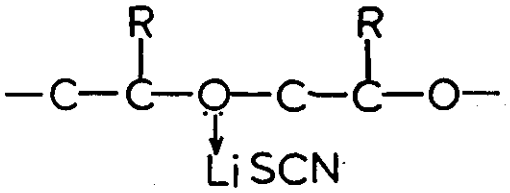

MODEL B 2 OXYGEN COORDINATION

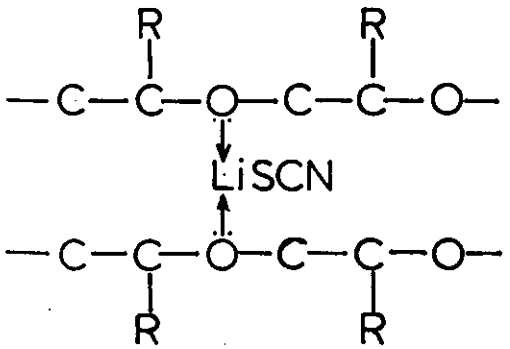

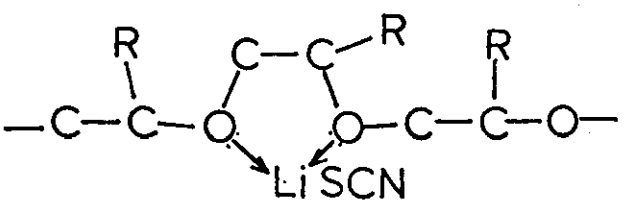

MODEL C 3 OXYGEN COORDINATION

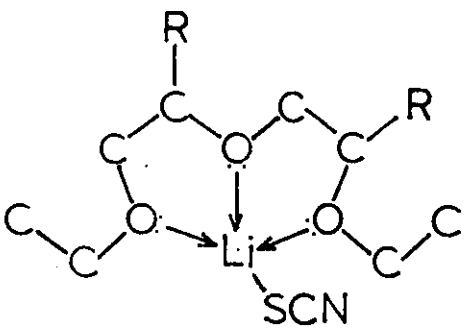

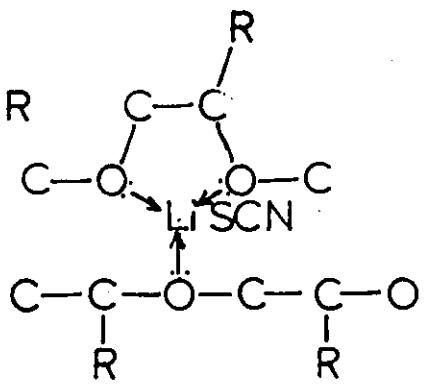

FIGURE 5·1

be possible for more than four atoms to be involved in the coordination. This situation has been observed for crown ethers and poly(ethylene oxide) containing alkali metal cations.

Poly(tetramethylene glycol) and poly(tetramethylene oxide) present a somewhat different situation. It is well known that the most stable ring structures involve either five or six members in the ring[17]. It is clearly evident that both poly(ethylene glycol) and poly(propylene glycol) can fulfil this requirement. However poly(tetramethylene glycol) or the high molecular weight polymer are only capable of forming an energetically unfavourable seven-membered chelate ring involving four carbons, two oxygens and the salt molecule. It therefore seems likely that low and high molecular weight poly(tetramethylene oxides) are not capable of forming intramolecular interactions with inorganic salts. The complexes of poly(tetramethylene oxides) must therefore be intermolecular to ensure full coordination of the lithium salt.

The solubility of an inorganic salt may reasonably be expected to reach a maximum when all the oxygen atoms available for coordination, have coordinated to the salt. The maximum mole% of inorganic salt incorporated into a polyether will depend upon the coordination number of the cation and will thus vary for the four schemes presented above. Table 5.1 gives the maximum value of salt in a polyether for a given coordination number.

Figures 4.2 and 4.19 show the elevation in Tg for lithium thiocyanate complexes of poly(ethylene glycol) and poly(propylene glycol). It can clearly be seen that the Tg elevation tended towards a limiting value close to 25 mole% salt loading, indicating on average a coordination of 3 oxygen atoms to every salt molecule. This corresponds to the model for 3 oxygen coordination described earlier. The relationship derived between the number of coordinating oxygens and the maximum mole percentage of salt incorporated does however present problems.

TABLE 5.1 The theoretical relationship between the solubility of an inorganic salt in a polyether and the coordination model

Number of coordinating oxygen atoms	Maximum mole% of inorganic salt soluble in polyether
1	0.5
2	0.33
3	0.25
4	0.20
5	0.17
6	0.14
7	0.12
8	0.11

TABLE 5.2 K-values and glass transition temperatures of the structures observed in poly(propylene glycol) salt complexes

Salt	3 Oxygen coordination		2 Oxygen coordination		1 Oxygen coordination	
	K	Tg_B	K'	Tg_C	K''	Tg_D
LiCNS	0.3	305	0.3	250	0.9	220
NaCNS	0.4	350	0.3	290	0.9	220

It assumes that the number of coordinating oxygens is independent of salt concentration up to the maximum mole% achieved. It may not be unreasonable to suppose that at low salt loadings more oxygen atoms are coordinated to the salt than at the maximum salt loading. The sigmoidal shape of the Tg versus mole% of inorganic salt present, coupled with the fact the salt complexes follow the basic copolymer equations, are evidence against greater coordination at low levels.

More importantly the assumption that all the oxygen atoms are freely available for coordination and that steric or conformational hindrances are negligible must be somewhat erroneous. Even in purely amorphous polymers some short term order exists.

It is therefore clear that the experimentally derived value for the maximum mole% will be below the theoretically permissible maximum value. It would therefore appear that the number of coordinating oxygens is close to three for the lithium thiocyanate complexes which in theory is the preferred coordination number for a simple lithium salt molecule.

5.2.3 Intramolecular versus Intermolecular Coordination

It has been shown in the previous section that in polyethers lithium thiocyanate is coordinated to three oxygens. For such a coordination number both intra and intermolecular coordination is possible in poly(ethylene glycol) and poly(propylene glycol). In poly(tetramethylene glycol) the energetically unfavourable seven-membered ring will result in the possibility of intermolecular coordination only.

In poly(ethylene glycol) and poly(propylene glycol) the existence of ringed chelate structures along the polymer chain would cause an

increase in chain stiffness and as a consequence increase the glass transition temperature. The resulting polymer may be considered as a random copolymer of coordinated and uncoordinated monomer units.

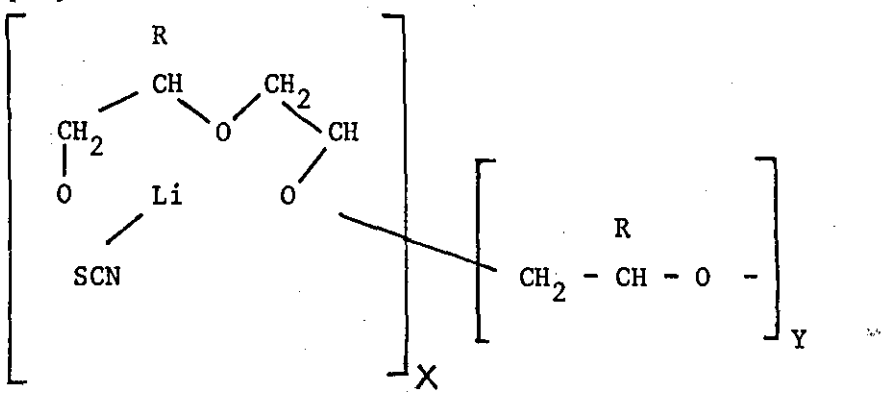

Figure 5.2 shows the Tg data for lithium thiocyanate complexes of poly (propylene glycol) as shown previously in Figure 4.3 replotted in terms of weight fraction. The Tg of the r esulting random copolymer may be predicted from the Gordon-Taylor-Wood equation

$$Tg = \frac{Tg + \left(KTg_B - Tg_A \right) W_B}{1 - \left(1-K \right) W_B} \qquad (2.13)$$

A reasonable fit up to a weight fraction of 0.60 was obtainable between experimental data and equation (2.1) by varying values of K and Tg_B. The solid line in Figure 5.2 represents the theoretical values of Tg corresponding to K = 0.3 and Tg_B = 305 . Above a weight fraction of 0.60 the experimental values appear higher than the theoretical values. The dashed line shows the Tg elevation resulting from cross-linking derived from the empirical relationship

$$Tg = \frac{3.9 \times 10^4}{M_c} \qquad (2.10)$$

It was assumed that the crosslinking involved a 5-membered chelate ring on one chain and an oxygen atom from another chain.

Above a weight fraction of 0.6 the experimentally obtained values for Tg became asymptotic whereas the theoretical values derived from the

A COMPARISON OF THE T_g DATA OF POLY(PROPYLENE GLYCOL) – ALKALI METAL THIOCYANATE COMPLEXES WITH A MODIFIED VERSION OF THE GTW EQUATION

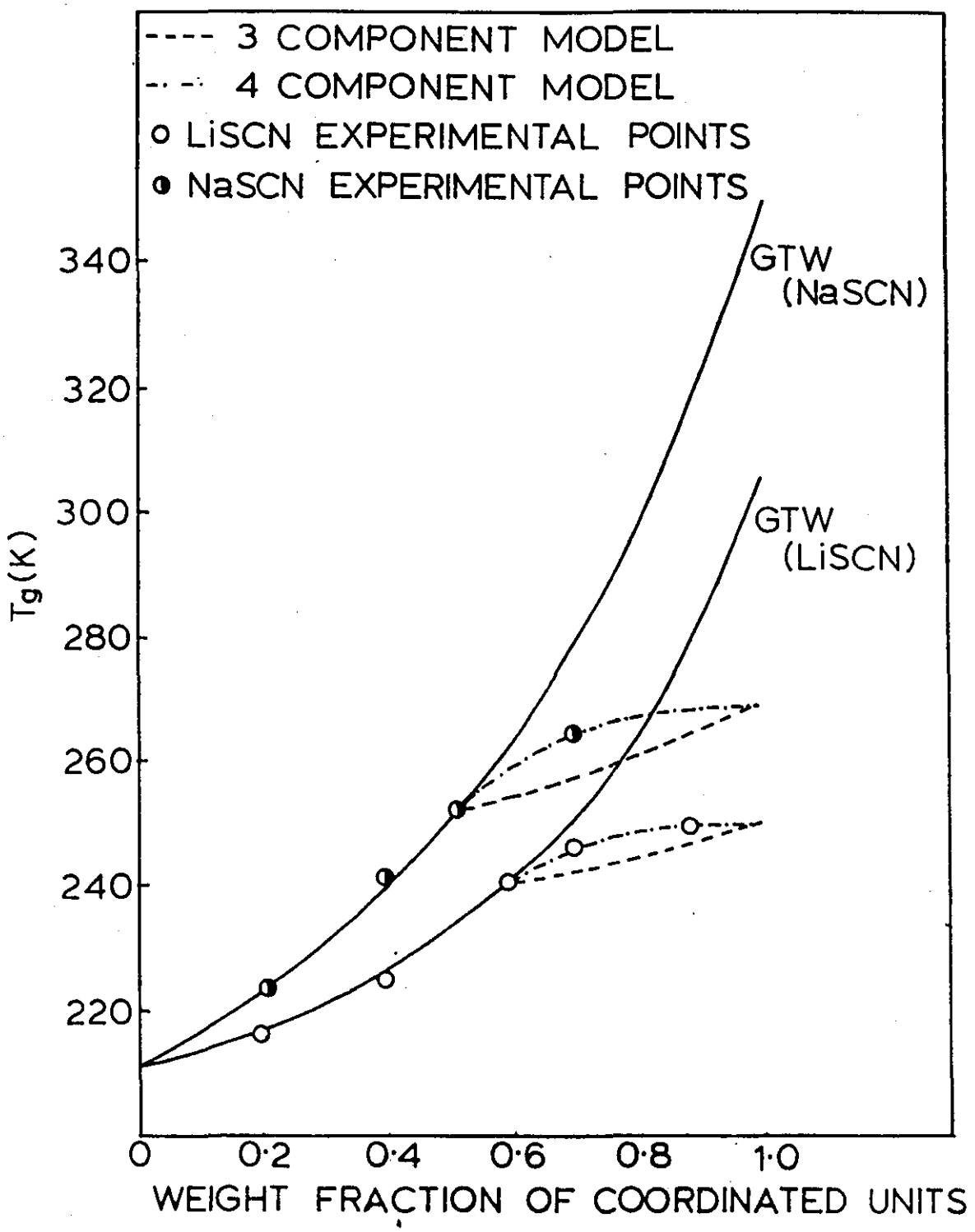

FIGURE 5·2

crosslinking and copolymer equations continued on to higher values.

It would therefore appear that at weight fractions up to 0.60 for a poly(propylene glycol)-lithium thiocyanate complex the salt is intramolecularly coordinated to the polyether. This as described earlier will involve 3 adjacent monomer units. Obviously as the number of monomer units complexed to the salt increases, the probability of three adjacent monomeric units being available for complexation reduces. Until a point is reached where three adjacent uncomplexed monomer units do not exist or that they are in conformations so situated that intramolecular complexation is not possible. This appears to correspond to a weight fraction of 0.60. Above this weight fraction, if all 3 coordinate bonds available to the lithium salt are to be employed, intermolecular bonding of some form must take place.

As the experimental values fall below the theoretical values incomplete chain chelation begins to occur. Uncomplexed oxygen atoms will arise as the number of oxygens available for complexation falls to such a level, that the possibility for 3 oxygen atoms being available in a given space for complexation is extremely low as salt loading reaches high levels. James[22] observed a deviation from the Gordon-Taylor-Wood equation above 70 weight % for a zinc chloride poly(propylene oxide) complex. They ascribed the slight elevation in Tg above this salt loading to coordination of only one ether oxygen to a salt molecule. Evans et al.[220] have considered the effects of competing irreversible cooperative reactions on polymeric chains. They applied this principle to the data of James et al.[47] and altered the Gordon-Taylor-Wood equation to account for the coordination of one oxygen to one molecule. From the modified equation

$$K W_B (Tg - Tg_B) + K' W_C (Tg - Tg_C) + W_A(Tg - Tg_A) = 0 \quad (5.2)$$

where subscripts A , B and C refer to poly(propylene oxide), chelate ring coordination to salt and single oxygen coordination respectively,

a better fit to experimental data was achieved. It was assumed that below a salt loading of 0.6 in lithium thiocyanate and 0.5 in sodium thiocyanate all the complexation was essentially intramolecular. Above these salt loadings it was assumed that complete coordination of the salt did not take place. From a consideration of the possible structures values for Tg, K and weight fraction have been successfully assigned to intramolecular structures containing both three and two oxygen atoms and a third structure where only one oxygen atom is assumed to be coordinated to the salt molecule. This may be described by a further modification of the Gordon-Taylor-Wood equation such that

$$K\, W_B(Tg - Tg_B) + K'\, W_C\, (Tg - Tg_C) + W_A\, (Tg - Tg_A) + K''\, W_D\, (Tg - Tg_D) = 0 \qquad (5.3)$$

where K, K' and K'' are the K-factors for three, two and one oxygen coordination respectively and Tg_B, Tg_C and Tg_D are the corresponding glass transitions of the three structures. Values for K, K' and K'' and their corresponding glass transitions for a lithium thiocyanate system and a sodium thiocyanate system are given in Table 5.2. The two structure and three structure modifications to the Gordon-Taylor-Wood equation are shown in Figure 5.2. One can discern a good fit of experimental and theoretical values upon consideration of the three structure model.

Flory[21] has studied the intramolecular reactions between neighbouring groups on vinyl polymers. Statistical analysis of the condensation of consecutive substituents, X, in the polymeric structure $-(CH_2CHX-)$. Even when these units (X's) were arranged regularly on alternate atoms along the chain, 13.5% of them did not react as a consequence of isolation effects. Analogies between the above system and the random formation of chelate rings can be made. Thus, from

a statistical viewpoint a maximum of 86.5% (corresponding to a maximum possible weight fraction of 0.94) of the available oxygen atoms can form chelate rings when a five-membered ring is involved. Obviously the value will be less as the size of the chelate ring increases. The number of oxygen atoms available, on a statistical basis, for complexation will thus decrease as the coordination number of the salt molecule increases.

The complexation of lithium thiocyanate with poly(ethylene glycol) cannot be treated in the same manner as for poly(propylene glycol) above, because of the inherent crystallinity at low salt loadings. The varying degrees of amorphous content as the salt loading increases and the inability to ascertain the degree of complexation in the crystalline regions render the applicability of the copolymer equation infeasible. Wright et al.[218, 39-42] have been consistent in producing alkali and ammonium thiocyanate complexes of poly(ethylene oxide) in which the cation is coordinated to four ether oxygens. They claim that the complex exists in both an amorphous and a double helical crystalline form. They also found that a reduction occurred in the melting points of sodium thiocyanate complexes when using poly(ethylene glycols), of molecular weights 6000 or less, when compared to higher molecular weight complexes. Also an amorphous poly(ethylene glycol) 600 maleate gel was found to show a crystalline peak upon complexation with a 1:6 sodium iodide to polymer ratio. It would therefore appear that salt complexes of poly(ethylene oxide) can form stable crystalline complexes. It is however pertinent to note that the crystalline structure for oligomers may be different to that of their high molecular weight counterparts[218]. It therefore seems likely that a less ordered crystalline structure results from low molecular weight poly(ethylene glycol) complexes and in the case of a lithium thiocyanate complex at high salt loading is suppressed completely.

It was observed in Figure 4.19 that the elevation in Tg levelled off at around 20 mole% which corresponds to the 1:4 salt to ether ratio observed by Wright et al.[39-42, 216]. Assuming the same considerations described earlier by Flory[217] that on a statistical basis at least 13.5% of available oxygens cannot coordinate in a two oxygen system and is likely to be higher for systems requiring more oxygens, it is likely that three oxygens only would be involved in the coordination of lithium thiocyanate to poly(ethylene glycol). It would therefore appear from the evidence that the bonding in lithium thiocyanate complexes of poly (ethylene glycol) is predominantly intramolecular as observed for poly(propylene glycol) complexes.

The observed variation of glass transition temperature with increasing mole percentage of salt content is complex for lithium thiocyanate poly(tetramethylene glycol) solutions as shown in Figure 4.15. It was observed in poly(ethylene glycol) complexes that a suppression of the degree of crystallinity is observed upon increasing salt content. This phenomenon was also observed in poly(tetramethylene glycol) systems culminating in a total suppression in crystallinity for calcium thiocyanate complexes of high salt loadings at all temperatures.

No large elevations for the value of Tm were observed in poly(tetramethylene glycol) complexes as were observed for poly(ethylene oxide) complexes[39-42,218] (in fact many salts appeared to reduce the value of Tm as shown in Table 4.4). It may therefore be assumed that the manner of incorporation of salt into the crystalline phase as observed for poly(ethylene glycol) complexes [39-42,218] does not occur in the poly (tetramethylene glycol) complexes. It is likely that lithium thiocyanate is excluded from the crystalline regions in poly(ethylene glycol) and poly(tetramethylene glycol) complexes or only partially incorporated in for example the chain ends inside the crystalline phase.

The elevation of Tm by some salts in poly(ethylene oxide) has been found to be more dependent upon the molecular weight of the polymer than the complexing salt[42]. Tm elevation was observed for the higher molecular weight poly(tetramethylene oxides) as shown in Table 4.4 but nothing like the Tm elevations observed in poly(ethylene oxides).

The weaker Tm and Tg elevation observed in poly(tetramethylene glycol) complexes in comparison to poly(ethylene glycol) complexes is therefore a consequence of the nature of the salt complex interaction. Poly(ethylene glycol) complexes are formed by intramolecular coordination of the cation to oxygen atoms. Strong intermolecular coordination would result in a greater elevation in Tg than observed. The inability of poly(tetramethylene glycol) to form intramolecular coordination to salts and the lack of strong intermolecular coordination indicate that the coordination of the ether oxygens is on a one cation to one ether oxygen basis. If this occurred however the Tg should be expected to continue rising up to a theoretically possible 50 mole% maximum salt loading. The observed Tg data appeared to indicate a maximum in the value of Tg with increased salt loading. It is therefore proposed that a weak ion-dipole interaction occurs involving more than one chain, in which the cation is surrounded by a cage structure of weakly coordinated ether oxygens. Each ion-dipole interaction is very weak and as a consequence any crosslinks formed are negligible. The ratio of coordinating oxygen atoms to the salt will necessarily be higher than that for intramolecular complexes. Therefore a maximum salt loading will occur at a much lower mole% in ion-dipole interactions than for intramolecular interactions. Any further coordination of salt to polymer above this maximum will necessitate the breaking of ion-dipole interactions and as a consequence a lowering of the value of Tg with respect to the maximum. It is clearly discernible that a maximum in Tg

is observed for poly(tetramethylene glycol) complexes with increasing salt loading, as shown in Figure 4.15 and further addition of salt results in a lowering of Tg.

Crystallinity has two effects on the glass transition of poly (tetramethylene glycol) complexes. If crystallinity were not present the value of Tg for the pure polymer would be expected to be lower in temperature. Therefore as salt is coordinated and crystallinity suppressed, the effective value of Tg_0' (the glass transition of pure polymer) would be expected to fall. Thus the combined effect of Tg_0' and the glass transition of fully coordinated polymer would appear to fall as Tg_0' decreased. Secondly a reduction in crystallinity would result in a narrowing of the glass transition due to reduced cross-linking effects.

5.2.4 Other Salt Complexes of Polyethers

In the previous section it was shown that lithium thiocyanate formed several structures with polyethers. The structure adopted for a particular lithium thiocyanate polyether complex has been shown to depend on the polymer involved. It was shown that for poly(ethylene glycol) and poly(propylene glycol) the complex formed with lithium thiocyanate was predominantly a chelate structure involving three adjacent oxygen atoms with intermolecular coordination occurring at high salt loadings. The coordination model proposed for poly(tetramethylene glycol) involved weak ion-dipole interactions.

Previously[47] it has been shown that the anion can have a significant effect upon the Tg of poly(propylene oxide) complexes of zinc halides.

Figure 5.3 illustrates the effect of cationic radius upon the glass

OBSERVED T_g ELEVATIONS FOR VARIOUS SALT COMPLEXES OF POLY(PROPYLENE GLYCOL) AT 7 MOLE% SALT LOADING

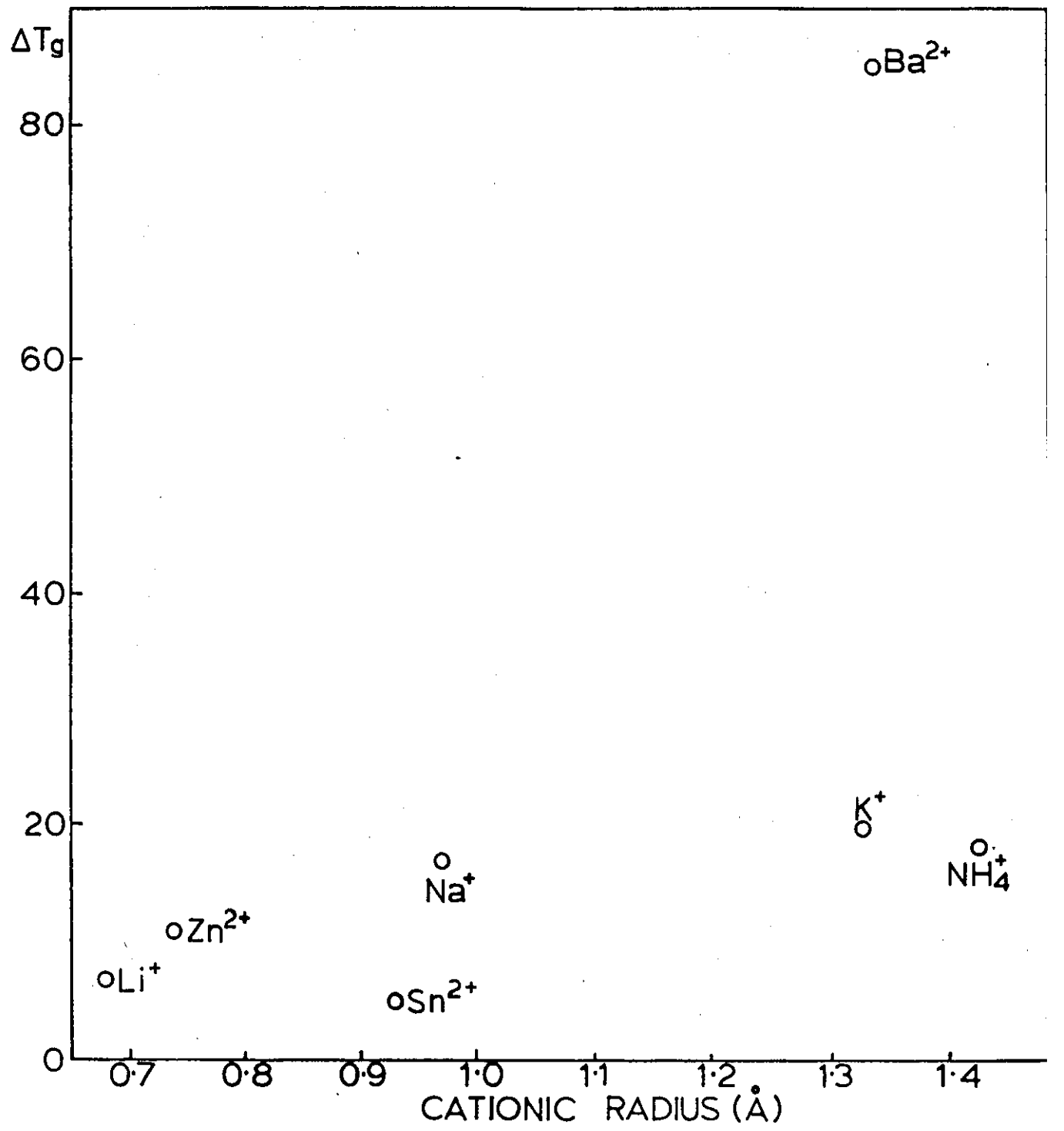

FIGURE 5·3

transition temperature of thiocyanate complexes of poly(propylene glycol). It is clearly evident that a simple relationship between ionic size and the elevation of Tg does not exist. For if cationic size were the sole governing factor in elevating Tg ammonium thiocyanate would be expected to have shown the greatest shifts in glass transition, due to increased flex energy, as it has the largest cationic radius.

Both James[22] and Rowe[23] concluded that the observed Tg elevation was a balance of both the ionic radius and the polarity of the cation-anion bond.

Table 5.3 shows ionic radii and typical coordination numbers of some cations. One would expect from a consideration of coordination numbers that the higher the coordination number the greater the elevation in the glass transition there would be. For the more ether oxygens bound to the cation the greater the increase in chain stiffness and thus increase the value for Tg. Lithium thiocyanate complexes have been shown to coordinate to three oxygen atoms. Sodium thiocyanate has been shown in Figure 4.3 to behave in a similar manner to lithium and is suggested to coordinate to three oxygen atoms. Even though the sodium cation is usually six-coordinated, sodium structures showing four coordination exist. The most widely known example being that of the salicylaldehyde complex $Na(OC_6H_4CHO)(HOC_6H_4CHO)$. As one continues down the alkali metal group the electron pair acceptor ability of the cation is increasingly impaired. As the charge density decreases with increasing ionic radius (the ratio of charge to ionic radius will be even less for NH_4^+ than K^+ because of the cationic size of NH_4^+) so the ligand binding becomes weaker.

It was observed that at temperatures above approximately 90°C the salt complexes of both potassium and ammonium with poly(propylene glycol)

TABLE 5.3 Ionic radii, ratio of the charge to ionic radii and coordination number of several cations

Cation	Ionic radii	Charge/Ionic radii	Coordination number
Li^+	0.68	1.47	4, 6
Na^+	0.97	1.03	6
K^+	1.33	0.75	6
NH_4^+	1.43	0.70	6
Ca^{2+}	0.99	2.02	6
Ba^{2+}	1.34	1.49	6
Zn^{2+}	0.74	2.70	4
Sn^{2+}	0.93	2.15	4

broke down and the salt came out of solution. Whereas the other complexes appeared stable to much higher temperatures. This was presumably due to the weaker interaction of these ions to the ether oxygen.

The complex stability for non-transition metal ions decreased with decreasing ratios of charge/ionic radius[18]. Thus the stability constants decrease in the order:

$$Li^+ > Na^+ > K^+ \qquad Ca^{2+} > Ba^{2+}$$

Also due to the higher charge density on the cations of the alkaline earth metals, these cations are more strongly hydrated[221]. It is found that calcium complexes are more stable than those of sodium[18].

Obviously as the coordination number increases the number of oxygens involved in coordination increases if complete coordination of a cation is to occur. Providing the anion remains attracted to the cation five oxygen atoms are required for complete coordination of the cation for both ammonium and potassium complexes. It is highly unlikely in this case that the coordination is intramolecular as this would involve the coordination of five adjacent oxygen atoms along the chain; thus forming a fourteen-membered chelate ring in either poly(ethylene glycol)or poly(propylene glycol). The coordination therefore is likely to involve both inter and intramolecular linkages. If strong intermolecular linkages occurred the resulting complex would be expected to show rubber-like behaviour. However it has been stated above that the complex stability of potassium and ammonium ions is low therefore any crosslinking linkages would be expected to be weak. These labile linkages may explain why potassium and ammonium complexes appear as viscous liquids at room temperature.

The ratio of the charge to ionic radius of both calcium and barium

cations is high. Therefore one would expect, and has been shown, that these cations would form very stable complexes, binding the oxygen atoms very tightly. From Table 5.2 it can be seen that both barium and calcium have a coodination number of six. If the anions remain bound to the cation, four oxygen atoms will be required for full coordination of the salt. As was shown for potassium and ammonium above the likelihood of an intramolecular structure is small as this would involve four adjacent oxygen atoms forming an eleven-membered ring. It therefore seems likely that both intra and intermolecular bonding occurs in barium and calcium complexes. It was observed that upon heating to high temperatures or if left for a considerable length of time, the viscous liquids produced by complexation of barium and calcium thiocyanate to poly(propylene glycol) converted into gels. This gelation was irreversible. It is therefore suggested that the final structure of a barium or calcium thiocyanate complex with poly(propylene glycol) is one involving two chelate rings, each involving two oxygen atoms, from neighbouring chains. The salt therefore acts like a strong crosslink between two chains. The crosslinks are stable whereas in potassium or ammonium they are not because of the greater strength of the coordinate bond in alkaline earth cations as shown earlier. It was shown earlier that the effect of crosslinking upon elevation of Tg is more marked than the elevation predicted by the Gordon-Taylor-Wood equation for copolymer behaviour. Figure 5.3 clearly shows the enhancement of Tg due to the crosslinked barium complex in comparison to the moderate enhancement of the mainly intramolecularly coordinated complexes. Further evidence for the crosslinking effect is given in Figure 4.1, from the breadth of the glass transition of the barium thiocyanate complex. It has been shown [213] that crosslinking results in a significant broadening of the glass transition. The glass transition of the barium thiocyanate complex appears much broader than for comparable mole percentages of other salts.

It is however possible for all four coordinating oxygens to originate from the same chain. In doing so it is not necessary for the four oxygen atoms to be adjacent to each other. It is possible that the cation may be coordinated to oxygen atoms from different parts of the same chain. As a consequence the structure would be the equivalent of a cyclisation process.

Both tin II and zinc cations have a coordination number of four and form tetrahedral complexes[18]. It would therefore be expected that these structures form five-membered chelate rings with poly(propylene glycol). James et al.[47] have also proposed this. The ratio of the charge to ionic radii of these cations is very high therefore one would expect these complexes to be very stable. Even to very high temperatures James[22] found the zinc chloride complexes to be very stable.

The anion appears to affect the glass transition by influencing both the intermolecular forces and the chain flexibility. The polarity of the molecule will obviously vary with the anion and as a consequence influence the intermolecular forces. The size of the anion will affect the chain flexibility.

An increase in anionic size would be expected to raise Tg by increasing the flex energy, however the amount of free volume associated with the anion will increase with increasing size of anion. This increase in free volume will cause a reduction in the value of Tg. Hence in Figure 4.1 the lithium complexes involving trifluoromethyl sulphonate, thiocyanate and iodide show increased glass transition elevations with reducing anionic size.

Figure 4.15 shows typical glass transitions observed in poly (tetramethylene glycol). The glass transition temperature of poly

(tetramethylene glycol) is lower in temperature than poly(propylene glycol) for two main reasons. Firstly the polarity is less in poly (tetramethylene glycol) and therefore intramolecular forces are reduced as a consequence of the number of dipoles per unit volume. Secondly there are no side groups to hinder rotation around a central axis which affect chain flexibility. The inherent crystallinity in poly(tetramethylene glycol) however acts to increase the value of Tg by in simple terms acting as crosslinks and causing chain stiffness. The resulting glass transition is a compromise between these three effects. The observed glass transition of poly(tetramethylene glycol) appears broader, reduced in height and at a lower temperature than poly(propylene glycol). The broadening of the glass transition has been stated earlier to be due to crosslinking effects[213], which in poly (tetramethylene glycol) are as a result of crystallinity. The reduction in height is partly a consequence of a lesser amount of material undergoing the glass transition as the weight fraction of amorphous material is reduced.

It was stated earlier that complexation resulted in a broadening of Tg. One can clearly see the broadening of Tg of poly(tetramethylene glycol) as a consequence of complexation with inorganic salts. The exception being calcium thiocyanate which appears to show a sharper Tg than equivalent mole% salt loaded complexes.

It was proposed for lithium thiocyanate complexes of poly(tetramethylene glycol) that the coordination involved consisted of weak ion-dipole interactions. A cage structure of oxygen atoms weakly interacting with the cation results. The strength of the ion-dipole interaction will obviously vary with the number of oxygens involved and the ratio of the charge to ionic radii. It was also shown for lithium thiocyanate that once a cage structure had formed any further

addition of salt would only act to disrupt this structure resulting in a reduction in Tg.

The sharpening of the temperature profile is indicative of a reduction in crystallinity. Thus 10 mole% of calcium thiocyanate has almost suppressed crystallinity appears as a relatively sharp transition. At 20 mole% calcium thiocyanate the transition has broadened again even though crystallinity has been totally suppressed presumably because of the array of structures present in a 20 mole% salt complex of poly (tetramethylene glycol).

For any given mole% of salt complexed to poly(tetramethylene glycol) the resulting Tg will depend upon the level of crystallinity and the degree of ion-dipole interaction.

Even though the ion-dipole interactions are relatively weak crosslinks, the crosslinking effect is evident in samples like 5 mole% lithium thiocyanate poly(tetramethylene glycol) where no large change in crystallinity has occurred. The breadth of the glass transition is extremely broad due to crosslinking effects from both crystallinity and the weaker ion-dipole interactions. The effect seems to be even larger for 10 mole% ammonium thiocyanate.

5.2.5 Molecular Weight Effects on Salt Complexes

Variations in molecular weight have been observed[45] for low and high molecular weight poly(propylene oxide) complexes of lithium perchlorate. Two glass transitions were observed in high molecular weight poly(propylene oxide) corresponding to pure polymer and the polymer complex. A single transition was observed in the low molecular weight complex.

James[22] however observed a single glass transition in zinc halide complexes of both high and low molecular weight poly(propylene oxide). He found that at low and high salt loadings the Tg was independent of molecular weight, but that the Tg between these extremes of the low molecular weight polymer complex always appeared at higher temperatures.

Single glass transitions were observed in both high and low molecular weight complexes of poly(tetramethylene oxide). Total suppression of the melting peak was observed in low molecular weight poly(tetramethylene oxide) but not in high molecular weight polymer. This is conceivable if one considers that a certain length of uncoordinated monomer units is required for crystallisation;if the chains are equally coordinated the probability for a given number of free units to be available for crystallisation must be less in the low molecular weight polymer.

5.3 Viscosity Studies of Polyether Complexes

Eisenberg et al.[24] observed a viscosity enhancement in low molecular weight poly(ethylene glycol) and poly(propylene glycol) upon complexation with lithium perchlorate. They were able to superimpose a log viscosity versus temperature plot for various salt loadings to form one master curve. Above a 3 mole% loading they observed a linear relationship between the increase in viscosity and the increase in the glass transition temperature. Below this salt loading a rapid increase in the viscosity was accompanied by only a small change in Tg.

It was observed in Figures 4.5, 4.7 and 4.21 that a large viscosity enhancement occurs upon addition of salt. It has been suggested in this thesis that the salt is coordinated to the oxygen atoms contained in the polyether. The large viscosity increases are indicative of a strong interaction between the polymer and the salt.

In Figure 4.6 the increase in viscosity was plotted against the increase in Tg. A similar shape to that observed by Eisenberg et al.[24] was recorded, that of an initial large increase in viscosity accompanied by a small increase in Tg at low salt loadings followed by a linear relationship between increases in viscosity and Tg.

It is feasible to suggest that the initial increase in viscosity may be associated with the joining together of hydroxyl chain ends. Two types of oxygen atoms are present in poly(propylene glycol), a hydroxy oxygen atom at the chain end and the ethereal oxygen atom in the backbone of the chain. The hydroxy oxygen atom will have a more strongly electron donating power than the ethereal oxygen atom. Therefore it is reasonable to suppose that the salt will be complexed with the hydroxy oxygen atoms in preference to the ethereal oxygen atoms. At low salt loadings the salt will complex with hydroxy oxygen atoms at the chain ends and may tie up several chain ends as a consequence, without complexing with any or few ethereal oxygen atoms. The apparent chain length will thus appear to increase as a consequence of these salt linkages and thus increase the viscosity markedly without affecting the glass transition temperature of the main chain significantly.

Once all the hydroxy oxygen atoms have been complexed further salt loadings will result in complexation with ethereal oxygen atoms. The resulting increase in viscosity appears to be as a consequence of the increase in the glass transition temperature.

The viscosity and Tg data for sodium thiocyanate complexes and lithium trifluoromethyl sulphonate complexes were transposed onto Figure 4.6 they were observed to lie upon the same line. This would suggest that the same structures produced in the lithium thiocyanate complexes are also prevalent for these other two complexes.

5.4 Dielectric Relaxation Studies of Polyether Salt Complexes

5.4.1 Dielectric Relaxation Studies of Poly(propylene glycol) Salt Complexes

Dielectric studies of oligomers of poly(propylene glycol) have been undertaken by several workers in the bulk[207]. Bauer and Stockmayer[222] observed a double dispersion in ε' and ε''. A high frequency process which did not vary with molecular weight was attributed to the glass transition. A low frequency process which shifted to lower frequency with increasing weight and became more diffuse. Varadarajan and Boyer[207] have studied this second relaxation dispersion at low frequencies designating it the T_{11} process, that of a liquid-liquid transition involving motion of the whole polymer. They calculated activation enthalpies for the Tg and T_{11} of 39 and 18 k Cal mol^{-1} respectively.

Figure 4.12 shows the frequency temperature locations for the relaxation of lithium thiocyanate complexes of poly(propylene glycol). It can be seen that the α'-process shifts to higher temperatures with increasing salt content in accordance with the observed glass transitions. The activation energies may be determined from equation (5.4)

$$\frac{d\ (\log f)}{d\ (1/T)} = \frac{-\Delta E}{2.303R} \qquad (5.4)$$

One can see that the slopes of the frequency temperature plots in Figure 4.12 increase with decreasing temperature, indicating an increase in activation energy with decreasing temperature. The activation energy at high temperatures appears to increase with increasing salt content. Typical values for the variation of activation energy with temperature are shown in Table 5.4. As stated above the activation energies are seen to increase with decreasing temperature.

TABLE 5.4 Temperature dependency of the activation energy of the α'-relaxation of inorganic salt complexes of poly(propylene glycol)

Mole%	Salt	$\frac{\Delta E}{KJ\ mol^{-1}}$	$\frac{T}{K}$
4	LiSCN	40.23 52.22 59.33 78.16	285.7 277.8 270.3 263.2
12	LiSCN	73.65 90.01 157.18	294.1 285.7 277.8
15	LiSCN	70.45 158.37	307.7 294.1
20	NaSCN	108.57 157.19 189.75	322.6 312.5 307.7
20	$LiCF_3SO_3$	96.22 120.43	322.6 312.5

The observed increase in activation energy with decreasing temperature is typical of a main chain relaxation in wholly amorphous polymers[223]. Williams[223] calculated the activation energy of the α -process and found it indicative of a cooperative process namely the glass transition. James observed a shift in temperature of the α -transition with increasing salt content at low salt loadings.

In section 5.2 an attempt was made to interpret salt complexes in terms of the Gordon-Taylor-Wood equation[143,144]. This copolymer model was found to be inappropriate for a copolymer of coordinated and uncoordinated structures because of the variety of coordination structures possible. By applying the modification described by Evans et al.[218] it was possible to achieve a good fit to experimental data. A single glass transition was observed by differential thermal analysis, it is however conceivable that each of the different coordinating units will exhibit a dielectric relaxation associated with that unit. MacKnight et al.[212] have observed this effect in a blend of poly(2,6-dimethyl-1,4, - phenylene ether) and poly(styrene). It was found from dynamic mechanical measurements that even though partial mixing had occurred two distinct phases existed in all the blends studied. However differential scanning calorimetry only gave a single Tg process for the blends. It therefore becomes obvious that the nature of the experiment and the size of the molecular process it represents will govern whether or not it is a viable test for homogeneity.

At relatively low lithium thiocyanate complexes two dielectric relaxations were observed, one associated with the glass transition of pure polymer and the other with the glass transition of coordinated units. It will be recalled that in the previous section the observed viscosity behaviour at low salt loadings was due to the coordination of hydroxyl oxygens at the chain ends. It is feasible to suppose that

such coordinated units will have a different glass transition to that of coordinated units on the main chain. Therefore further additions of salt will have dielectric relaxations at higher temperatures. It can be seen in Figures 4.8 and 4.12 that the α' relaxation is shifted to higher temperatures with increasing salt loading. It therefore seems likely that the coordination of ether oxygen atoms is dominating the dielectric response. The peaks are not separated in temperature by many degrees and therefore appear as one merged peak.

One can clearly discern two relaxation areas in Figure 4.9 for 20 mole% loadings of sodium thiocyanate and lithium trifluoromethyl sulphonate complexes of poly(propylene glycol). If the complexes can be described in terms of a three, two or one oxygen atom coordination then the low temperature relaxation will correspond to a one oxygen atom coordination model of low Tg merged with the shifted α-relaxation. The two and three oxygen atom coordination may not be separated in temperature extensively and appear as one merged peak. However the sodium thiocyanate complex appears to have a smaller shoulder on the low temperature side of the α' loss peak and this may correspond to two oxygen atom coordination.

It was stated earlier that the α-relaxation shifted to higher temperatures upon complexation with the salt molecules. This is indicative of a significant degree of molecular mixing between the coordinated and uncoordinated phases. It has been observed in polymer blends that the individual components of a blend may exhibit two Tg's corresponding to the individual phases that have broadened and moved closer together[148]. This would appear to explain the observed dielectric behaviour of salt complexes of poly(propylene glycol). As the salt loading of lithium thiocyanate increased the α-relaxation merged into the α'-relaxation peak.

Data from Figures 4.13 and 4.14 has been redrawn in the form of Cole-Cole plots [155] as shown in Figure 5.4. The theoretical implications have been discussed in chapter 2, but as previously described it is possible to derive values for ε_r, ε_u and α, the relaxed, unrelaxed dielectric constants and the distribution of relaxation times from such diagrams.

Table 5.5 shows the values of ε_r and ε_u at various temperatures over the α'-relaxation of a 15 mole% lithium thiocyanate poly(propylene glycol) complex. The values of ε_r and ε_u were derived as described in chapter 2 from a series of Cole-Cole plots at the corresponding temperatures. One can discern from Table 5.5 that ε_u was constant over the temperature range but that ε_r decreased slightly with increasing temperature. Hence, the magnitude of the dielectric relaxation, $(\varepsilon_r - \varepsilon_u)$ also decreased with increasing temperature.

It was shown in the Fröhlich-Kirkwood theory equation (2.67) that the temperature dependence of the magnitude of the dielectric relaxation is determined by the temperature dependence of ε_r, ε_u, μ_{eff} the effective dipole moment and g_r the reduction factor. It can be seen from this equation that if the molecular configuration μ_{eff} remains constant, the temperature dependence of $\varepsilon_r - \varepsilon_u$ will depend on the intramolecular interactions g_r and the $^1/T$ factor. Depending on which is the dominant factor will decide whether or not $\varepsilon_r - \varepsilon_u$, increases or decreases with temperature. The observed decrease in temperature indicates that the $^1/T$ factor is dominant.

Values of α, the distribution of relaxation times, from the Cole-Cole diagrams and β the Fuoss-Kirkwood [156] empirical distribution parameter were found to be independent of temperature. The parameter β was calculated from the data in 4.14 using equation (2.45). The

COLE-COLE PLOT FOR THE α' RELAXATION FOR A 15MOLE% LiSCN POLY(PROPYLENE GLYCOL) COMPLEX AT 25°C

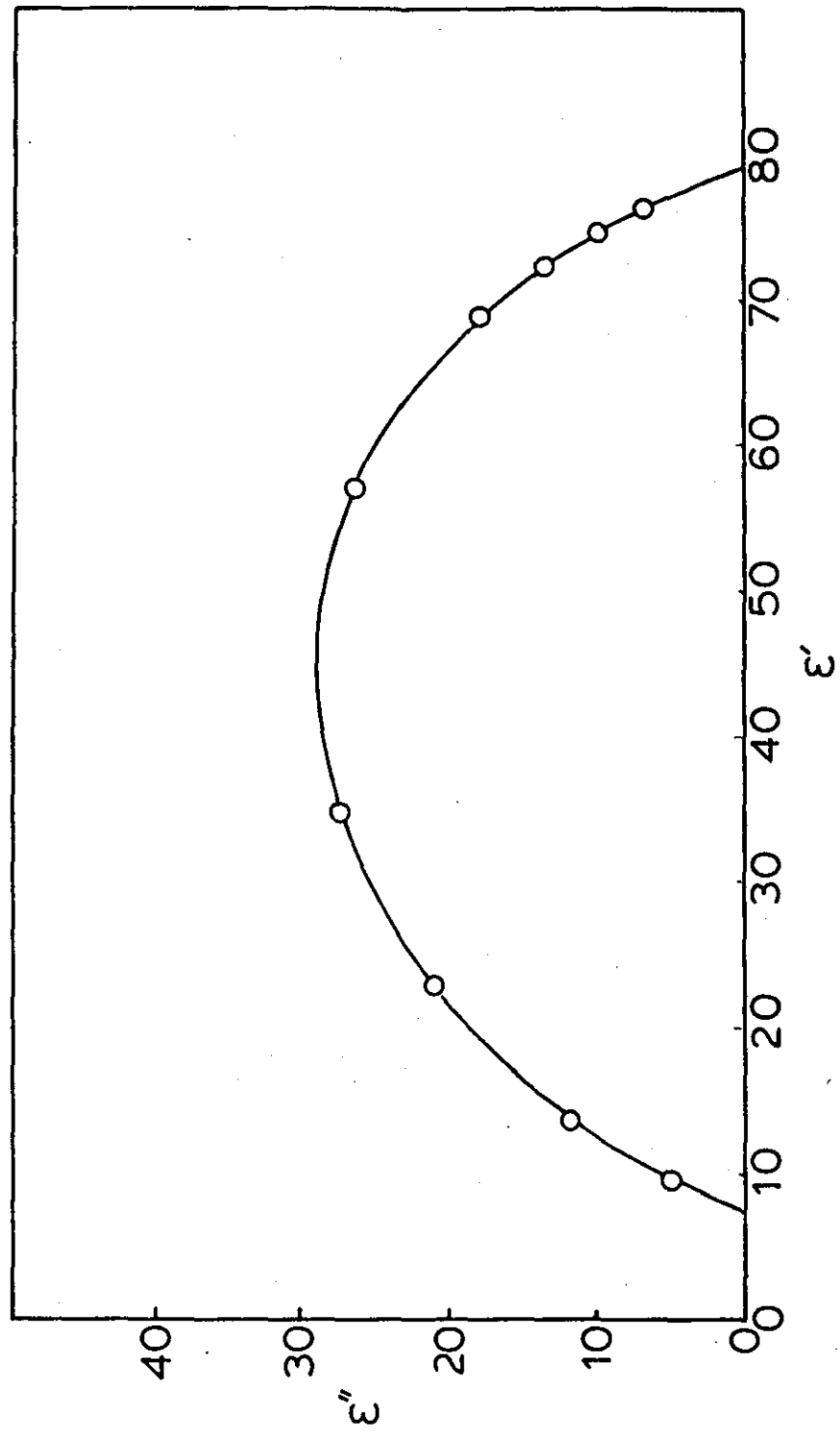

FIGURE 5·4

TABLE 5.5 Temperature dependence of ε_r and ε_u for the α'-relaxation of a 15 mole% poly(propylene glycol) lithium thiocyanate complex

Temperature (^{o}C)	ε_r	ε_u
8.5	79.0	7.5
25.0	79.0	7.5
32.5	78.5	7.5
40.0	77.4	7.5

isothermal values of α enabled a normalisation of the dielectric data in Figure 4.14 to form a master curve for the α'-relaxation shown in Figure 5.5. From this master curve it is evident that the $\varepsilon''/\varepsilon''_{max}$ curve was almost symmetrical about log f/fmax = 0. The full line represents the Debye curve calculated for a single relaxation time model[153] using equations (2.36) and (2.37).

The symmetry and breadth of the master curves of the α'-relaxation suggests that the relaxation may not be associated with the glass transition of the complex. The relative symmetry of the master curves of the α'-relaxation made it possible to apply the empirical Cole-Cole[155] distributions. A value for α = 0.14 was used for the Cole-Cole distributions. The distribution is represented by the dashed line. A good fit between experimental and theoretical values was obtained upon the high frequency scale of the distribution but at low frequencies deviations were observed. These deviations are believed to arise as a result of conductivity effects which tend to increase the value for the dielectric loss at low frequencies.

The dash dot line represents the Cole-Cole distribution of the α'-relaxation of an 18 mole% zinc chloride poly(propylene oxide) complex, as calculated by James[22]. It can be seen that the distribution is rather broader than the α'-relaxation of the 15 mole% lithium thiocyanate poly(propylene glycol) complex. This may well be as a consequence of the sizeable difference in the molecular weights of the two polymers. It was over 100,000 for poly(propylene oxide) in comparison to only 2000 for poly(propylene glycol). It is further noted that at low frequencies deviations occurred between the theoretical and experimental values in both the systems. The deviations were however more noticeable in the zinc chloride system. This may well reflect upon the ability to displace the cations in the two systems.

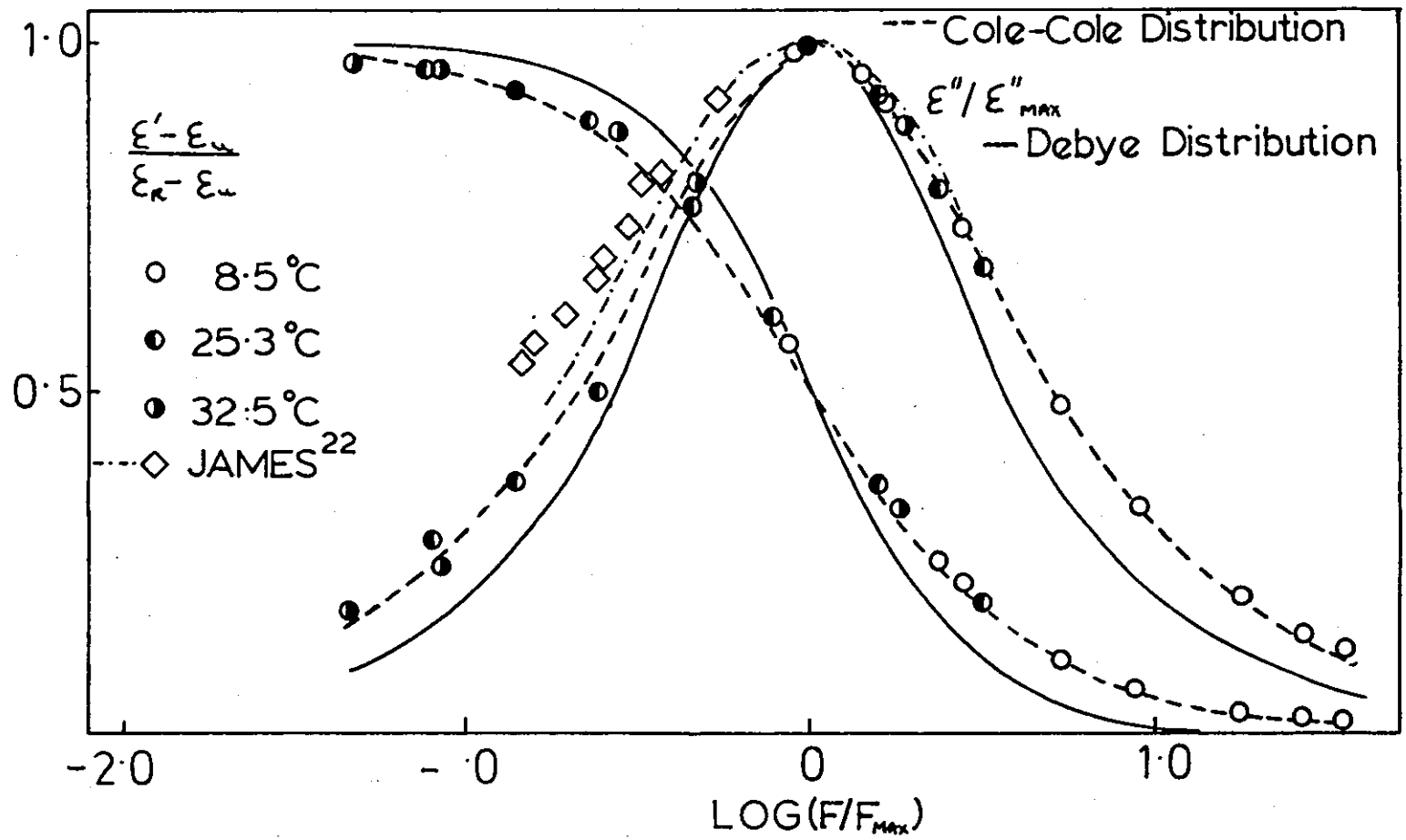

FIGURE 5·5

MASTER CURVES OF $\varepsilon''/\varepsilon''_{max}$ AND $(\varepsilon'-\varepsilon_\infty)/(\varepsilon_R-\varepsilon_\infty)$ AS A FUNCTION OF LOG(F/F_{max}) FOR 15 MOLE % Li CNS POLY(PROPYLENE GLYCOL) [α'-RELAXATION]

James[22] showed that the zinc chloride poly(propylene oxide) system involved coordination of the salt in a five-membered ring involving two adjacent ether oxygens. It is believed the lithium thiocyanate is coordinated to three adjacent oxygen atoms. Therefore the area of attack for the extra coordinating oxygen to displace the anion is much greater in the zinc chloride system with respect to the lithium thiocyanate system. Therefore the number of ions displaced could be expected to be less in the lithium thiocyanate system. This appears to be reflected in the magnitude of the relaxation which appears to be considerably greater in the zinc chloride system. Furthermore the high charge density of the lithium cation will make it considerably more difficult for the anion to be completely displaced from the vicinity of the cation with respect to the zinc system. Hence the number of ions likely to be involved in conduction would be expected to be greater in the zinc system. As a consequence the discrepancies between theory and experimental values of the Cole-Cole plots, as observed, would be more marked in the zinc system.

Activation energies of some complexes have been calculated from the slopes at high frequencies of the plots shown in Figure 4.12 using equation (5.4). Figure 5.6 shows the activation energies calculated from this method. One can discern a linear relationship between activation energy and lithium thiocyanate loading but it is not until high salt loadings that the activation energy approaches values that approximate to a cooperative motion. Also included are values for a different anion and a different cation.

Figure 4.9 shows the dielectric loss and constant for a poly(propylene glycol) complex containing lithium trifluoromethyl sulphonate and sodium thiocyanate complexes. Although there is a considerable difference in the glass transition temperatures the α'-relaxation

ACTIVATION ENERGIES OF THE α'-RELAXATION OBSERVED IN SALT COMPLEXES OF POLY(PROPYLENE GLYCOL)

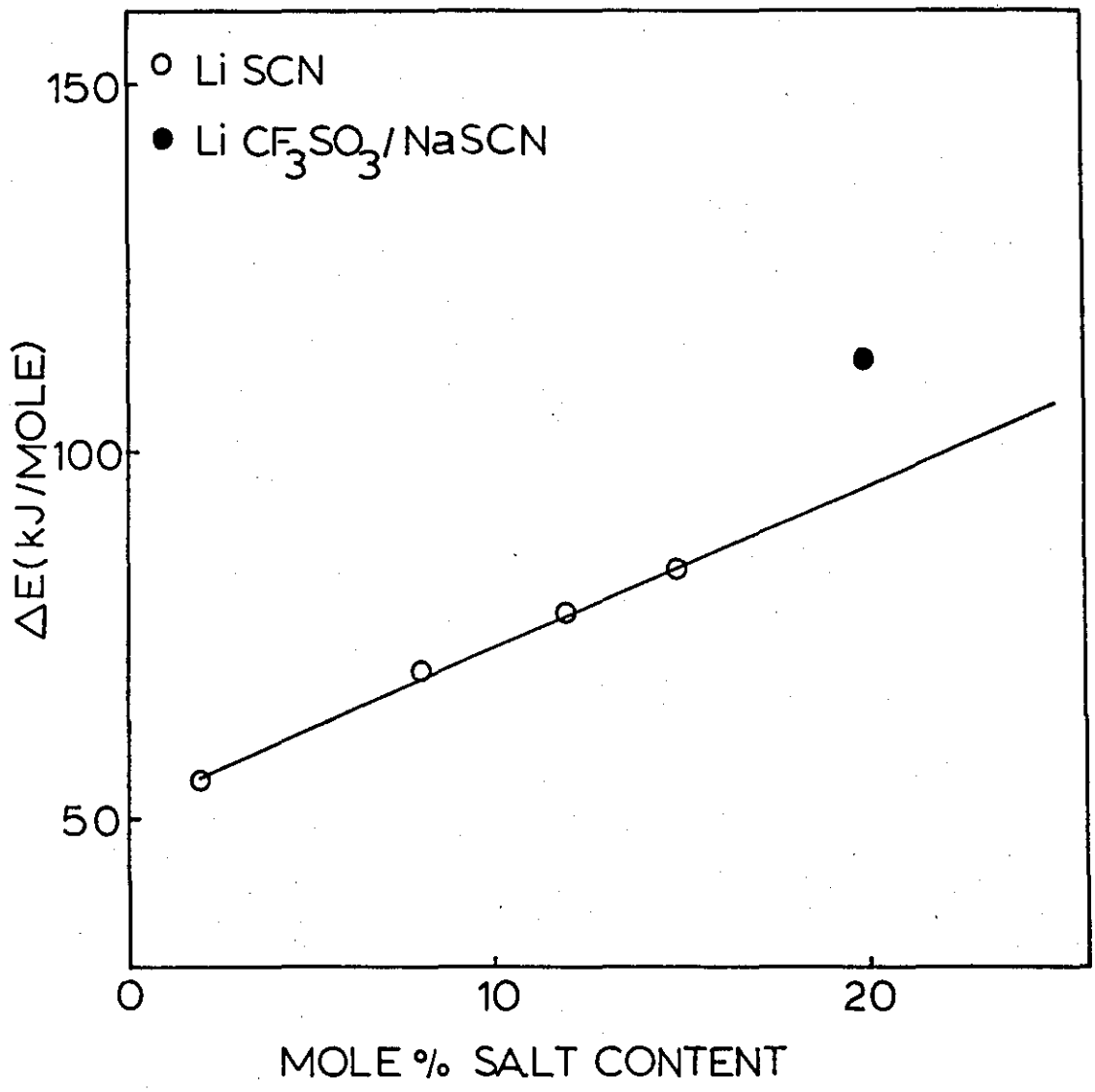

FIGURE 5·6

of these two systems at this mole% appear to be occurring at approximately the same temperature. This further supports the belief that the α'-relaxation is not associated primarily with the glass transition temperature.

5.4.2 A Molecular Model for the α'-Relaxation

Previous publications relating to the dielectric properties of ion-containing polymers have been mainly concerned with ionomeric systems [20,24] and in particular ethylene-methacrylic acid copolymers and their salts[87,90,224]. No relaxations akin to the α'-relaxation of poly(propylene glycol) inorganic salt complexes have been observed.

MacKnight et al.[224] studied the dielectric properties of poly (ethylene) modified by the addition of phosphoric acid side groups. They observed an additional dielectric dispersion at high phosphoric acid levels that increased in magnitude with increasing phosphoric acid content. It was further noted that the relaxation shifted to lower temperatures with increasing phosphoric acid content and that the activation energy was independent of the number of acid groups. A broadening of the distribution of relaxation times however did occur. This is in direct contrast to the observations for the α'-relaxation in salt complexes of poly(propylene glycol). These showed an increase in activation energy with increasing salt content, a shift to higher temperatures of the relaxation with increasing salt content and the distribution of relaxation times was seen to be independent of temperature.

MacKnight et al.[224] interpreted their observations upon the basis of a Maxwell-Wagner-Sillars[177-179] types of interfacial polarisation involving a separated system of microphases. They noted however that the relaxation could not be entirely a MWS-type polarisation, as this necessitates an unlimited increase in values of ε' and ε'', because

they observed a peak in ε'' and ε' approached an asymptotic value.

In section 2.2.7 Maxwell-Wagner-Sillars effects were discussed. A prerequisite for such a system was heterogeneous phases. Visual observations and thermal properties have indicated a single phase structure for inorganic salt poly(propylene glycol) complexes up to high salt loadings. Therefore conventional Maxwell-Wagner-Sillars would not be possible in these systems.

Pohl[186,187] observed high dielectric constants in macromolecules containing a high degree of conjugation; he ascribed the values to hyperelectronic polarisation as described in section 2.2.9. There is no evidence for unsaturation in poly(propylene glycol) or the complexes formed by coordination with inorganic salts. Therefore this effect appears to be inappropriate for salt complexes.

The existence of bound salt molecules on a polymer chain is akin to a model suggested by Schwarz[183,184] discussed previously in section 2.2.8. He described a system whereby mobile ions are electrostatically attached to stationary counterions but are isolated from other similar regions. It is clear that both crown ethers and salt complexes contain stationary ions that are segregated by virtue of their coordination along the polymer chain. If the α'-relaxation is analogous to the model described by Schwarz then the anion must be locally mobile around the cation. However the stereochemistry of the complexes and the steric restraints imposed by the anion preclude such mobility in the anions.

James[22] observed the disappearance of the α'-relaxation loss peak and a reduction of the dielectric constant upon absorption of water into zinc halide poly(propylene oxide) complexes. He concluded that since the α'-relaxation was observed for a salt bound to the polymer, the relaxation was associated with complex formation.

None of the above mechanisms were found adequate to describe the α'-relaxation in inorganic salt complexes of poly(propylene glycol). From the observations made it is believed that the α'-relaxation may result as a consequence of the type of equilibria shown in Figure 5.7. It is possible for these equilibria to occur because of the fast segmental motion of the polymer chain above Tg. The disrupting oxygen atom may come from either the next monomeric unit or from a different chain. The species designated B and C are representative of the type of interaction occurring although other structures are possible. Obviously such a process inevitably must lead to conduction as a result of ionic transport through the polymer. It is therefore suggested that the α'-relaxation occurs as a consequence of equilibria illustrated in Figure 5.7. The chemical interactions involved in such equilibria are clearly not complicated and therefore would be expected to have a narrow distribution of relaxation times.

As the salt loading increases the number of uncoordinated oxygen atoms available to undergo equilibrium reactions described above decreases. As a consequence it will become increasingly more difficult to form species such as B and C. The magnitude of the relaxation will therefore be seen to depend on not only the level of salt present but, above a definite concentration, will be dependent upon the number of uncoordinated oxygen atoms present. It can be shown that at low salt loadings, e.g. 10 mole%, if 3 ogygen atoms are coordinated to the salt the ratio of uncoordinated oxygen atoms to salt molecules will be approximately 6:1. However a doubling of the salt concentration to 20 mole% will reduce this ratio to 1:1. It is clear that a theoretical maximum must occur in the magnitude of the α'-relaxation with increasing salt content corresponding to 20 mole% in a chelated structure involving 3 oxygen atoms. However experimentally, the somewhat obscure maximum occurred around 10 mole%.

EQUILIBRIUM STRUCTURES POSSIBLY FORMED DURING THE α'- RELAXATION

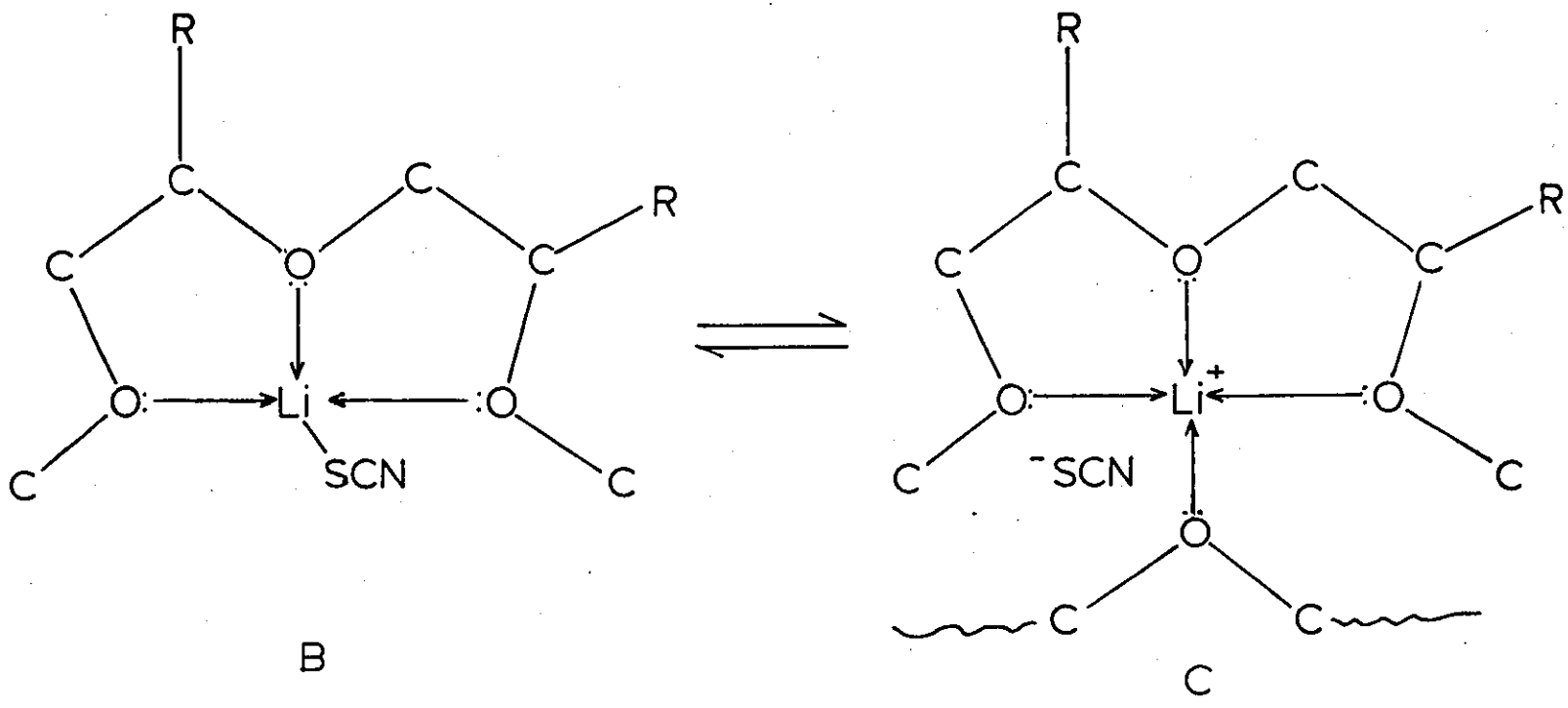

FIGURE 5·7

The activation of the α'-relaxation will be affected by the number of oxygen atoms available for equilibrium coordination. Figure 4.12 shows the frequency temperature plane loci of lithium thiocyanate complexes of poly(propylene glycol). It can be seen that the log f versus $^{1}/T$ plots are straight lines at higher frequencies similar to an Arrhenius-type rate constant[225], normally associated with the kinetics of chemical reactions. It would be expected that at low salt loadings the number of oxygen atoms available for coordination will be high ensuring a low activation energy. At high salt loadings the availability of oxygen atoms for equilibrium coordination will be significantly reduced resulting in a higher activation energy for these complexes as a consequence of the increased number of chain segments required to rearrange to instigate equilibrium coordination. This will result in the necessity for a more cooperative process and hence a higher activation energy. In Figure 5.6 one can clearly discern an increase in the activation energy with increasing salt loading.

Figure 4.12 also shows the frequency temperature plane loci of two salts other than lithium thiocyanate namely sodium thiocyanate and lithium trifluoromethyl sulphonate. The activation energies calculated from Figure 4.12 of these complexes lie on the same slope as the lithium thiocyanate complexes. It would therefore appear that the activation energy is independent of both cation and anion for a complex having the same structural arrangement. This is feasible if one considers that the activation energy will be determined more by the chain process rearrangement than by the energetically fairly simple ionisation of the cation-anion bond.

From Figure 4.12 one can see that the temperature location of the α'-relaxation is shifted to higher temperatures for sodium thiocyanate

and lithium trifluoromethyl sulphonate complexes with respect to the lithium thiocyanate complexes. It is believed that steric hindrance of the equilibrium coordinating oxygen by the larger anion, trifluoromethyl suphonate, necessitates a greater conformational freedom of the chain to allow the coordinating oxygen to approach the cation. This requires a higher temperature.

The temperature shift of the α' -relaxation in sodium thiocyanate complexes is believed to be a Tg effect. The conformational freedom of the chain at any temperature will depend on the position of Tg. For any complex a certain conformational freedom will be required for an equilibrium coordination to occur. The temperature at which this occurs for any system will be some definite temperature above Tg. If the complexes have the same anion, i.e. no added steric effects, the α'-relaxation will occur at this definite temperature above Tg. It has been shown previously in Figure 4.3 that for the same mole% sodium thiocyanate shifts the Tg more than lithium thiocyanate. Therefore one would expect the conformational freedom of the sodium thiocyanate complex to be less than a lithium thiocyanate complex at any temperature. As a consequence the α'-relaxation would be expected to occur at a higher temperature than lithium thiocyanate which is what is observed.

Above the α'-relaxation the dielectric constant comes to a limiting value before starting to rise again. The dielectric loss dips after the α'-relaxation and once again starts to rise. This high temperature process designated α'_c in Figure 4.8 is believed to be due to conductivity effects. The dielectric loss term, ε''_o, arising from d.c. conductivity[157] is given by equation (5.8)

$$\varepsilon''_o = \frac{K\ G_o}{f} \qquad (5.8)$$

where G_o is the d.c. conductivity of the sample. K is a proportionality constant and f is the frequency of measurement. A plot of log ε''_o

versus log f has a slope of -1 if conductivity is occurring. Figure 5.8 shows log ε''_o versus log f plots for three complexes in the α'_c region. Their slopes are all -1 therefore conductivity appears to be occurring in this region.

It is clear that at some point above the α'-relaxation the anion dislodged from the complex by the extra coordinating oxygen will start to migrate. From Figures 4.8 and 4.9 it is clear that the temperature at which this conductivity begins to occur increases with increasing mole% of salt present, except for 8 mole% lithium thiocyanate. This salt loading corresponds to the highest values of ε_r for the systems shown in Figure 4.8. It therefore seems likely that the onset of conductivity is dependent upon the number of anions available for conductivity which shows a maximum at around 10 mole% salt loading for a three coordinate oxygen system. Although the anion is displaced by the extra coordinating oxygen it will still be associated with the cation. It will therefore require an extra impetus of energy to remove the anion completely, i.e. the temperature has to increase. The onset of conductivity appears to be governed by whether or not there is sufficient energy available to remove the anion completely from the cation and the number of such anions present. It must also be recalled as shown in Figure 4.8 that poly(propylene glycol) also shows conductivity effects above its glass transition. Binks and Sharples[208] have described proton conductivity for several polyethers above their glass transitions.

5.4.3 Dielectric Relaxation Studies of Poly(tetramethylene glycol) Inorganic Salt Complexes

Wetton and Williams[226] have studied the dielectric properties of amorphous and crystalline poly(tetramethylene oxide). They observed a broadening of the loss curves with decreasing temperature in the frequency plane. They were able to resolve this data into two component

FREQUENCY / DIELECTRIC LOSS PROFILE ABOVE THE α'-RELAXATION

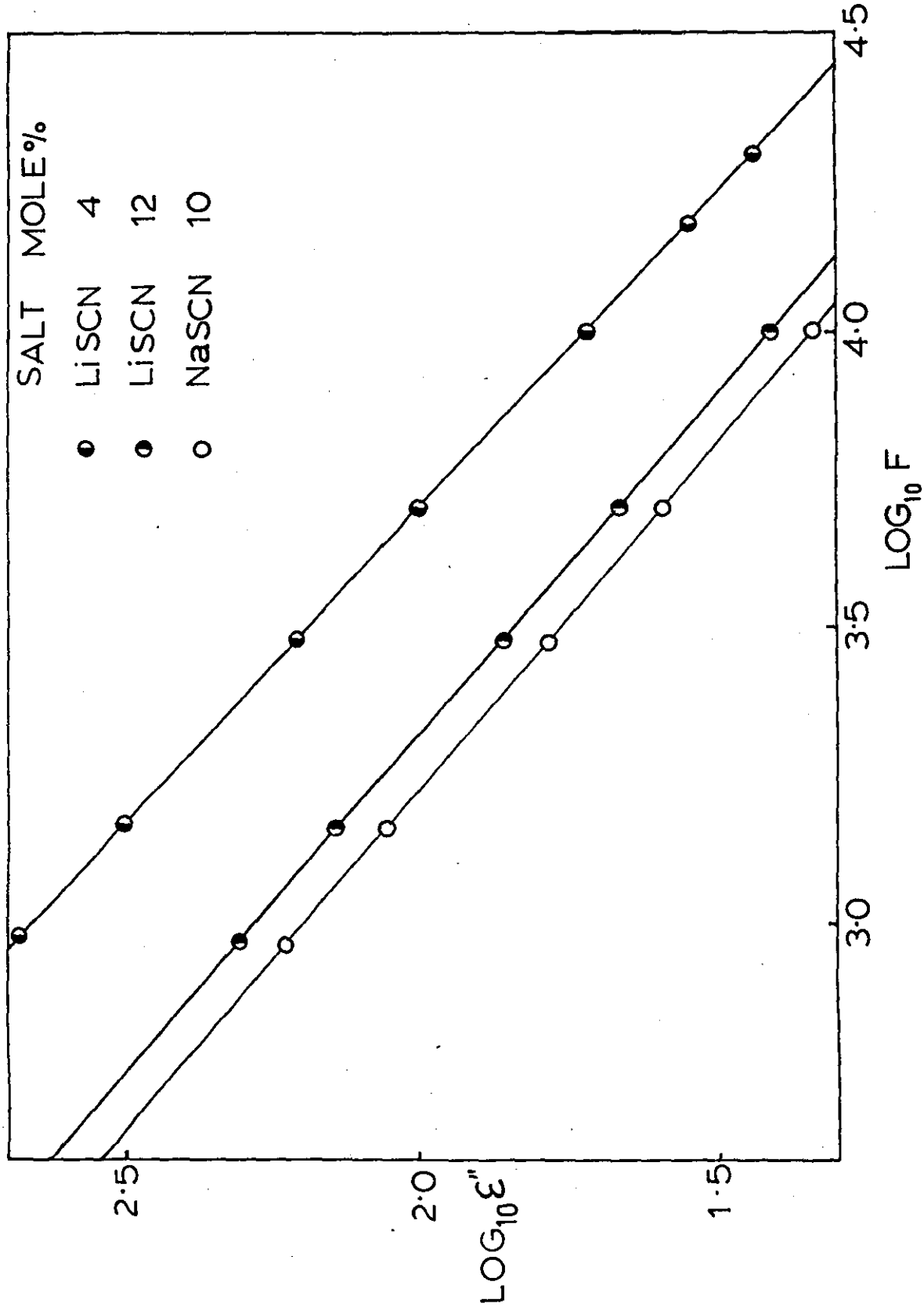

FIGURE 5·8

relaxations α and β . An increase in the loss peak of some 30% was observed in the amorphous polymer in comparison to a 33% crystalline polymer, supporting the belief the α -relaxation was associated with the glass transition in the amorphous regions of the polymer. The low temperature β -process was believed to occur as a result of local motions of the chain as proposed by Yamafugi and Ishida [227].

The dielectric relaxations over the temperature and frequency range studied were dominated by the crystallization process as can be seen in Figure 4.16. It is well known that interfacial polarisation of the type described by Maxwell[177], Wagner[178] and Sillars[179] may arise in crystalline polymers[188]. The polarisation arises as a result of charge conduction through the sample usually occurring at low frequencies or high temperatures. Additionally there will be a part of the loss factor arising from bulk conductivity rising steeply as the temperature is raised. Obviously as the heterogeneity disappears, i.e. the sample melts the effects described above will disappear, as seen in Figure 4.16.

The melting points of the lithium thiocyanate complexes are 34°C, 32°C, and 22.6°C for 10, 15 and 20 mole% lithium thiocyanate poly (tetramethylene glycol) complexes respectively. The positions of the α'_m-relaxation appears to follow this trend. The breadth of the α'_m-relaxation peaks are considerably narrower than the α'-relaxation peaks observed in poly(propylene glycol) complex peaks and so the relaxation times are narrower for this process. It was stated in section 4.3.3 that the melting peak as observed by DTA decreased with increasing salt content. The peak height of the dielectric loss α'_m-relaxation decreased between 10 and 15 mole% and increased again to 20 mole%. It therefore appears that the α'_m-relaxation is dependent

upon the crystalline content at whose boundaries the polarisation takes place and the salt content which generates the charges trapped at the boundaries.

It is pertinent to note that the final values for the dielectric constant did not fall as the heterogeneities were removed but continued to rise to a limiting value of similar magnitude to that observed for the α'-relaxation in poly(propylene glycol) complexes.

The interfacial polarisation process appears to be superimposed upon another process. Figures 4.17 and 4.18 show the frequency dependence of the dielectric constant and loss around the interfacial polarisation process. A very broad curve is observed in the loss data which is indicative of the presence of two processes[157]. It is tentatively suggested that the underlying process which the α'_m-process is superimposed upon is an α'-relaxation similar to that observed in poly(propylene glycol) complexes. It was not possible to segregate the peak heights and calculate the activation energy of this underlying process. However its temperature profile and magnitude are concurrent with the belief that this process is similar to the α'-relaxation in poly(propylene glycol) complexes. It is unfortunate that an extensive study of the dielectric properties of a poly(tetramethylene glycol) complex that had suppressed crystallinity completely had not transpired. For this would have allowed a more positive assessment of this underlying process. In the next section the dielectric properties of a polymer complex that has suppressed crystallinity completely is discussed.

5.4.4 Dielectric Relaxation Studies of Poly(ethylene glycol) Lithium Thiocyanate Complexes

Connors et al.[228] have studied the dielectric relaxations, shear

moduli and nuclear spin-lattice relaxation times of poly(ethylene oxides) of various molecular weights. They observed a strong influence in the dynamic properties upon varying molecular weight. Conductivity effects limited the frequency range studied in low molecular weight samples. The variation with molecular weight were believed to arise from the dependence of crystallinity upon molecular weight. It was suggested that the relaxations observed below the melting point were due to an overlapping mechanism involving motions of the chain backbone from within both the amorphous and crystalline phases.

Figure 4.22 shows the temperature plane dielectric relaxations for poly(ethylene glycol) and complexes with lithium thiocyanate. Three regions are discernible in the loss data, corresponding to the glass transition and melting of the polymer with a transition intermediate between the two. Lang et al.[229] has observed three transitions below the primary crystallization process two of which were related to glass transitions and a third appeared to be a secondary melting peak. It is suggested that the intermediary peak α_i, is related to the secondary melting peak. Above the melting peak the loss values decrease slowly, suggesting the presence of the onset of a further loss process. Arisawa et al.[230] plotted log ε'' versus log f for the above Tm region and calculated a slope of -1 indicative of conduction. As mentioned previously Binks and Sharples[208] explained this in terms of proton hopping in poly(ethers). A single broad relaxation step is observed in the dielectric constant at 5 kHz over the temperature range studied.

At 5 mole% salt loading the three relaxations observed in the dielectric loss of the uncomplexed polymer are replaced by a single asymmetric relaxation peak which is broader on the low temperature side of the relaxation. This is indicative of the presence of more than

one relaxation. From Figure 4.20 it is clear that the 5 mole% salt loaded polymer is semi-crystalline (although somewhat reduced in crystallinity). The melting point of the complex is seen to shift to higher temperatures but a much larger shift is observed in the glass transition temperature. The melting process and the glass transition are therefore closer together in temperature than for the pure polymer and may as a consequence appear as one asymmetric relaxation. The dielectric constant appears as one relaxation, which appears to broaden above $-20^{o}C$.

At 10 mole% salt loading three relaxations are observed in the loss data. A broad low temperature process associated with the glass transition, a narrow relaxation at approximately $-5^{o}C$ and a small process at around $22^{o}C$. At this salt loading the crystallinity is severely reduced. From Figure 4.20 one can see a reduction in the value of the melting point and a shift to lower temperatures of the glass transition. The reduction in crystallinity appears to be supported by the lower value of the glass transition and the sharpness of the transition as seen in Figure 4.19. The size of the loss process also appears to reflect the reduction in crystallinity. The reduction in crystallinity together with the lower value of the glass transition would indicate a greater degree of conformational freedom of the amorphous chains. In which case an α'-relaxation as observed above for poly(propylene glycol) salt complexes may be expected to occur. As the temperature is lowered the anions 'freed' by the α'-relaxation may become trapped at the interface of the crystals. If this occurred Maxwell-Wagner-Sillars effects may be expected to occur. The sharpness of the relaxation and the slope of the frequency temperature location as shown in Figure 4.23 are indicative of a Maxwell-Wagner-Sillars polarisation as observed around $-5^{o}C$.

The shift of the glass transition to lower temperatures for the

10 mole% sample with respect to the 5 mole% sample would appear to explain why this process is visible in the dielectric loss data in 10 mole% and not in 5 mole%. The low temperature process is likely therefore to be a merged α'_g and α'-process.

At 15 mole% salt loading no evidence for crystallinity was found. A single relaxation which appears broader on the low temperature side of the relaxation is observed in the dielectric loss as shown in Figure 4.22. The height of the loss peak is increased with respect to lower salt loadings. The loss peak appears at lower temperatures for 15 mole%, in comparison to 5 and 10 mole% salt loaded systems. The lack of a high temperature(crystallinity) process will cause a shift of the combined relaxation peak to lower temperatures.

At 20 mole% the loss peak shifts to a higher temperature presumably as a consequence of the increase in the glass transition as shown by Figure 4.19. The loss peak still appears slightly broader on the low temperature side indicating the presence of more than one process. The dielectric constant of 20 mole% clearly shows however two processes as seen in Figure 4.22. This splitting of the dielectric constant into two regions was observed in low salt loaded poly(propylene glycol) complexes. The two processes were designated α'_g and α' and it is believed the same process occurs in poly(ethylene glycol) complexes. That of a process associated with the cooperative motion of the polymer complex, α'_g, and a process occurring at higher temperatures involving the further coordination of an oxygen atom as subsequent ionisation of the cation-anion bond occurs.

Further evidence for the presence of more than one process is discernible in Figures 4.24 and 4.25. The breadth of the relaxation with frequency is indicative of the presence of more than one process[157].

6.0 APPLICATIONS OF INORGANIC SALT COMPLEXES

6.1 High Frequency Dielectric Relaxation Studies of Poly(ether) Salt Complexes

To ascertain the possible usage of salt complexes as dielectric enhancers it was necessary to measure the dielectric properties of the complexes at high frequencies. It will be recalled from section 2.4 that the theoretical heating ability is proportional to the frequency, therefore the higher the frequency the more heat generated by the system. Also from section 2.4 it will be recalled that all other factors being equal, the heating ability is proportional to $\tan\delta/\varepsilon'$ which more significantly may be written as $\varepsilon''/\varepsilon'^{2}$.

Figure 4.10 shows the dielectric loss and constant at 10 MHz for a series of lithium thiocyanate poly(propylene glycol) complexes of various salt loadings. For the pure polymer it can be seen that in the temperature range studied, from ambient temperatures up to 100°C, no significant variation in dielectric constant and only a small decrease in dielectric loss is observed. This indicates that over this temperature range the polymer is above the α -relaxation and no significant conduction is occurring as a consequence of insufficient ion-hopping. Hence the low values in the dielectric loss data.

As the frequency is increased the α -relaxation has been seen to broaden and shift to higher temperatures. Williams[231] observed a loss peak at approximately -20°C at 3.3 MHz. At low salt loadings (10 and 15 mole% lithium thiocyanate) a small relaxation is observed at approximately -20°C which may be attributable to the α-relaxation of poly(propylene glycol).

The loss curves for the remainder of the temperature profile

continue to increase with temperature without showing any further peaks. The dielectric constant however shows transitions for 10, 15 and 20 mole% lithium thiocyanate. Evidently these transitions are the α'-relaxations observed at low frequencies, as discussed in the previous chapter, obviously shifted to higher temperatures with increasing frequency.

It was shown in the last chapter that the dielectric strength, as measured from $\varepsilon_r - \varepsilon_u$, increased up to a maximum of 10 mole% and then decreased. Also the α'-relaxation shifted to higher temperatures at constant frequency with increasing salt content. It therefore becomes evident that the dielectric constant around the α'-relaxation and above, i.e. from approximately 20°C upwards, decreases with increasing salt content. It will be recalled that the dielectric heating factor is inversely proportional to the square of the dielectric constant. If this were the sole governing parameter then one would expect an increase in the theoretical dielectric heating capability with increasing salt content.

This however is not the case as the dielectric heating parameter is directly proportional to the dielectric loss also. However it can be seen in Figure 4.10 that there are only small differences in the dielectric loss below 50°C except for 30 mole% salt loading between the various salt loadings. Even though the 30 mole% salt loading has a lower dielectric loss at these temperatures the large difference in the square of the dielectric constant in comparison to the other systems more than compensates for this at higher temperatures (60°C upwards) as the dielectric loss nears the values for the other systems.

It was also shown in the previous chapter that upon increasing the size of the anion a shift to higher temperatures of the α'-relaxation resulted. This shift to higher temperatures will ensure that the

dielectric constant of the salt system containing the bulkier anion (assuming the same cation) will have a lower value than corresponding smaller anion systems. The dielectric loss values at this frequency are almost identical at room temperatures for salt loadings up to 20 mole% in the lithium thiocyanate system. The lithium trifluoromethyl sulphonate system has similar values also. Therefore as a consequence of the larger anion size of trifluoromethyl sulphonate with respect to thiocyanate a system containing the former has a higher theoretical dielectric heating capability than the latter, assuming all other parameters are the same.

Figure 4.11 showed the dielectric relaxations exhibited by salt complexes of P3, poly(propylene glycol) and P317, a poly(propylene glycol/poly (ethylene glycol) block copolymer. It can be seen that the α'-relaxation is strongly dependent on the type of salt present. With the exception of the potassium thiocyanate systems the positions of the α'-relaxations appear to reflect upon the glass transitions of the complexes. Namely an increase in temperature for the α'-relaxation with increasing glass transition temperature. It has been stated earlier that the α'-relaxation is not solely dependent upon the glass transition but is also influenced by the steric hindrance. However the degree of conformational freedom available at any temperature will be dependent upon the glass transition temperature.

The potassium thiocyanate system is the exception to the rule. It was observed that at approximately $80^{o}C$ that the complex began to break up. The salt became clearly visible and a two phase system formed. A similar complex breakdown was observed in ammonium complexes. It is believed that the inability to achieve adequately the desired coordination number of six, together with the high size/charge ratio results in a weaker complex structure for potassium and ammonium salts.

It can be seen that the α'-relaxation in P317 systems are shifted to lower temperatures with respect to equivalent P3 systems. It is also evident that the dielectric strengths of the α'-relaxation of P317 systems are somewhat reduced in magnitude, as measured by $\varepsilon_r - \varepsilon_u$, with respect to the equivalent P3 systems. It is obvious that the ethylene glycol units have a significant effect on the dielectric properties of these systems. A comparison of the α'-relaxations, as shown in Figures 4.8 and 4.22, for poly(propylene glycol) and poly(ethylene glycol) complexes show a sharper transition for the latter over the former. Also that the α'-relaxation of poly(propylene glycol) complexes occur some 40°C higher in temperature than poly(ethylene glycol) complexes. This obviously reflects upon the restriction of conformational freedom that is introduced by the larger molecular weight and the presence of methyl groups on the backbone in poly(propylene glycol).

It is likely that during the manufacture of P317 complexes competition exists between ethylene glycol units and propylene glycol units. Furthermore, that the slightly more polar ethylene glycol units may offer a more attractive site for coordination than the propylene glycol units. In either case the α'_g' and α'-relaxations of the two components will be separated in temperature. This will introduce additional freedom to the chain and the observed α'-relaxation for the propylene glycol units will occur at lower temperatures.

It is clear from the evidence presented in this thesis that the complex stability differs markedly for different salt systems. Ranging from weak complexes of potassium and ammonium salts to strong complexes involving barium and calcium salts. The dielectric properties of the complexes are markedly affected by the coordination strength of the various linkages. This is manifested in the α'-relaxation where the strength of the anion-cation bond will have some influence on the

ability of the extra coordinating oxygen atom to displace the anion. Although the overall activation energy is dependent upon the conformational freedom of the polymer complex it is evident in the potassium system, for instance, that this is not the only factor. Conversely in barium and calcium thiocyanate systems where some degree of crosslinking is believed to occur, the complexes are extremely stable. Furthermore it is evident from the size of the α' -relaxation that they do not readily loose the anion. In fact the size of the loss peak of barium thiocyanate would suggest that few anions are liberated. The anions that are liberated will also find it difficult to migrate through the crosslinked structure and hence shows less conductive effects than other systems.

An analysis of the dielectric heating parameter as shown in Figure 4.27 and 4.28 reveals superior dielectric heating capabilities in those complex systems which produce fewer anions as the consequence of the α'-relaxation. For although the dielectric loss increases markedly in the weaker complexed systems it is accompanied by a large increase in the dielectric constant. It will be recalled that the dielectric heating capability is inversely proportional to the square of the dielectric constant. Therefore it is necessary for the dielectric loss increase to be equal to the square of the dielectric constant to maintain the same heating capability. For the heating capability to further improve requires a dielectric loss increase of even greater proportions. It is evident that for the more weakly coordinated systems the dielectric loss does rise more than the square of the dielectric constant with increasing temperature, but not sufiiciently to raise the dielectric heating parameter markedly.

In the more tightly bound complexes it is evident that the dielectric loss and constant do not rise to the values observed for potassium and

ammonium complexes. However because the dielectric constant does not increase so much it is obvious that such a large increase in dielectric loss is not required to maintain the same heating capability. Hence in these systems the theoretical dielectric heating capability is manifestly increased with increasing temperature as shown in Figures 4.27 amd 4.28. For the relatively small increase in dielectric constant is more than offset by the increase in dielectric loss.

6.2 Use of Salt Complexes as Dielectric Enhancers

It was shown in section 2.4 that the rates of dielectric heating are proportional to $\tan\delta / \varepsilon'$. From a theoretical consideration if the salt complex is to act as a dielectric enhancer, at the required low concentrations, it is necessary for the salt complex to have a dielectric heating parameter greater than the matrix polymer. If the preferred concentration is < 10 pph then to have a significant effect upon the overall heating rate, the heating parameter must be at least an order of magnitude higher.

At room temperatures the inherent dielectric heating parameter of poly(vinyl chloride) is approximately 0.0074 and poly(styrene) is 0.00015 at 10 MHz. It can be seen from Figure 4.27 that at 20°C the dielectric heating parameters of salt complexes lie between 0.012 and 0.049. It is therefore clear that the salt complexes will enhance the dielectric heating capability of poly(styrene) manifestly but not poly (vinyl chloride) at low loadings. It is evident therefore to improve the dielectric heating capability of poly(vinyl chloride) a dielectric enhancer whose theoretical heating parameter is of the order of 0.10 or greater at room temperature is required. Furthermore, to improve the dielectric heating capability of poly(vinyl chloride) to commercially interesting levels it is likely that a dielectric heating parameter of

greater than 0.5 would be required. However it must be said that the dielectric heating characteristics of PVC are normally adequate for most applications.

It is clear therefore that in polymers that at present have very low or no dielectric heating capability, the incorporation of a salt complex renders these polymers capable of being heated dielectrically. However in systems like poly(vinyl chloride), which are already used commercially for dielectric heating, the salt complexes measured are at least an order of magnitude too low to be of commercial interest as dielectric enhancers. That is not to say that a salt complex may not be found,that may be of use in poly(vinyl chloride) systems. From the discussion in the previous section it is apparent that a high salt content complex which is bound strongly to the polymer, possibly a divalent cation, whose anion is bulky, may well prove to be of the order of magnitude required.

Similar problems were encountered with the dielectric enhancement of a poly(ethylene vinyl acetate), EVA, system. The dielectric heating parameter for this polymer is approximately 0.016 at 20^{o}C. A blend containing 10% of a potassium thiocyanate poly(propylene glycol) complex produced only a 25% improvement in heating rate. An improvement of the order of 100% is required to render the system commercially interesting. Figure 4.26 showed the dielectric properties of various blends of salt complexes with EVA. It is evident that the components of the blend are acting independently dielectrically speaking. Therefore it seems likely that two distinct phases of a matrix of EVA containing salt complex inclusions exists. However the values of the dielectric constant and loss normally associated with these complexes appears to be drastically reduced. Although the dielectric loss and constant appear to increase with increasing weight fraction of the more

conductive phase the numbers are some two to three orders of magnitude less. It appears therefore that at the interface between the salt complex and the EVA, the EVA is constraining the salt complex to such an extent that only polymer in the centre of the inclusions is capable of undergoing the α'-relaxation. As the inclusions will be relatively small a proportionally large reduction in the amount of salt complex capable of undergoing an α'-relaxation will result as a consequence of the restraining action of the matrix.

This effect obviously adds further problems to the ability of a salt complex to enhance the dielectric heating capability of a polymer like EVA. It is further worth noting that the long range conductive effects observed above the α'-relaxation are inhibited by the matrix. Hence the decrease on the high temperature side of the loss peak not usually observed in the pure complex. This will naturally result in a maximum value in the theoretical dielectric heating parameter in the blended system with increasing temperature. It will be recalled that in Figures 4.27 and 4.28, the dielectric heating parameter generally increased with increasing temperature.

6.3 Other Electrical Uses for Salt Complexes

Considerable interest worldwide has been shown in the development of a solid electrolyte system. Obviously salt complexes if of the order of magnitude required would be very promising materials for this end use. The resistivity of an electrolyte is dependent upon the film thickness. An estimate of the resistivity that would be required gives values of 10^5 (Ωcm) at 1μm and 10^4 (Ωcm) at 10μm. Figure 4.29 showed resistivities measured at 500 Hz (to avoid polarisation effects). It is evident that systems based on poly(propylene sulphide) and poly (propylene glycol) approximate to the order of magnitude required. Those

of poly(vinyl alcohol) and poly(ethyl vinyl ether) do so at elevated temperatures. This is to be expected as anions will not be released for conduction in the required numbers until the α' -relaxation has occurred. The α'-relaxation in poly (propylene glycol) and poly(propylene sulphide) have been shown to occur at temperatures much lower than the other two systems.

It is clear that for conductive effects to be maximised requires that the anion and, to a lesser extent, the cation are capable of moving. It is likely that the smaller the ion the greater will be its mobility in the viscous medium of the salt complex. Other factors including the electronegativity of the anion and hence the degree of ionic character of the cation-anion bond together with the degree of shielding of the cation by the anion will influence the ability of the anion to break free from the cation. It was also mentioned in the discussion of the α'-relaxation that a maximum occurred in the dielectric strength of the α'-relaxation. This maximum will vary in accordance with the number of oxygen atoms coordinated to the salt. It is obviously important to achieve the maximum dielectric relaxation strength possible as this corresponds to the maximum number of ions generated for the α'-relaxation of the system.

It will be further recalled that the conductive effects on the high temperature side of the α'-relaxation were more pronounced the lower the salt content. It therefore seems likely that the opposite of the effects desired for dielectric heating are required for an electrolyte.

Finally it is necessary to have a solid electrolyte. Therefore it is necessary to convert the normally viscous liquids into solids. This is achieved for poly(propylene glycol) complexes by incorporating

urethane chemistry and as a consequence converting the glycol complexes into crosslinked urethanes.

Further uses considered in the electrical field have concentrated on the ability of these systems to store charge. Table 4.8 has shown the half life storage times of some polymer electrets. It can be seen that good electrets could be formed from salt complexes but that the necessity to maintain an anhydrous environment severely limits the commercial potential of these compounds as electrets.

Possible uses as capacitors are limited because of the deliquescent nature of the complexes and also the necessity to maintain a steady value for the dielectric constant over the required temperature range from -20 to +80°C. This could be achieved if the α'-relaxation lay outside of this temperature range. Table 6.1 shows two possible systems that partly fulfil these requirements. The two complexes correspond to the pre - α'-relaxation (10 mole% NH_4SCN/PEVE) and the post- α'-relaxation (15 mole% LiSCN/PEG). There is always the possibility above the α'-relaxation for ion migration towards the electrodes which is particularly dangerous for a system containing thiocyanate as this is converted to cyanide and sulphur at the electrode.

TABLE 6.1

Frequency = 5 kHz

Salt Complex	Temperature (^{o}C)	Dielectric Constant
10 mole% NH_4SCN PEVE	0	7.5
	40	8.5
	60	10.0
15 mole% LiSCN PEG	0	71.0
	20	70.7
	40	70.85
	60	70.46
	70	70.21

7.0 CONCLUSIONS

7.1 Overall Features

In this thesis a series of poly(ether) inorganic salt complexes have been prepared, studied and assessed for commercial viability. The complexes prepared were generally optically transparent (above their melting points where appropriate) and to high temperatures remained thermoplastic. Complexes of poly(propylene glycol) were all amorphous but those of poly(ethylene glycol) and poly(tetramethylene glycol) showed varying degrees of crystallinity depending upon salt loading. All the evidence in this thesis is indicative of the formation of complexes between the salt and the polymer rather than the salt acting as a second phase filler. It has been apparent that a range of complex structures have been formed dependent upon the particular salt/polymer system involved.

7.2 Poly(propylene glycol) Complexes

The actual structure of the poly(propylene glycol) complexes was found to be strongly dependent upon the nature of the coordinating salt. In essence three types of structure were believed to form.

The first type exemplified by complexes with lithium thiocyanate and zinc chloride were believed to involve the formation of chelate rings involving three and two oxygen atoms respectively. A single Tg was observed for all the complexes formed and occurred at an elevated temperature with respect to the parent polymer.

The second type of complex formed was believed to involve more than three oxygen atoms. It is believed that these complexes involved relatively weak ion-dipole interactions. The complexes showed single glass transitions higher than the original polymer but were unstable

at higher temperatures breaking down into their constituent parts. This type of complex was exemplified by salts of ammonium and potassium.

The third type of complex involved elements of both intra- and intermolecular bonding. It was thought likely that the complex involved two separate five-membered chelate rings possibly from different chains but not necessarily coordinated to the same salt molecule. This resulted in a much larger shift in the glass transition temperature with respect to other complexes and a broadening of the glass transition which is indicative of crosslinking. This type of complex was exemplified by alkaline earth metal thiocyanate complexes.

Viscosity measurements showed a systematic increase with increasing shift in the glass transition as a consequence of increased salt loading except at low concentrations. It is believed that at low salt loadings the salt is mainly bound to the hydroxyl chain ends resulting in an apparent increase in molecular weight and hence a dramatic increase in viscosity with only a marginal elevation of Tg.

The observed viscosity increases and Tg elevations were found to vary with both the amount and type of salt added. It was evident from the above observations that the salt was molecularly dispersed throughout the polymer. It was therefore possible to consider the system as a copolymer of complexed and uncomplexed structural limits. A modification of the copolymer equation to allow for the different possible structures formed as the salt loading increased ensured a good fit to the experimentally observed glass transitions.

Dielectric studies revealed two new transitions not present in the original polymer. A transition associated with the glass transition of the complex and a transition higher in temperature designated the α'-relaxation. The α'-relaxation was not found to depend solely

upon the position of the glass transition although this obviously had some effect. Other steric factors were found to influence the position of the α'-relaxation. High values for both the dielectric loss and constant were observed for the α'-relaxation depending on salt concentration and the type of salt involved. A mechanism is proposed involving the displacement of the anion from the complex structure by an additional coordinating oxygen. Eventually the anion was totally displaced from the environment of the cation and ionic conductivity was observed.

7.3 Poly(ethylene glycol) Complexes

Complex structures similar to those observed in poly(propylene glycol) complexes were believed to exist in poly (ethylene glycol) complexes. Much of the behaviour was however dominated by the presence of crystallinity in these complexes. However at high salt loadings (from 15% lithium thiocyanate and higher) the crystallinity was found to be totally suppressed at all temperatures.

Elevation of the glass transition was observed upon complexation although the observed elevation with increasing salt content was more complicated than observed in poly(propylene glycol)complexes. This was believed to arise as a consequence of the suppression of crystallinity upon complexation.

Maxwell-Wagner-Sillars type polarisations dominated the dielectric relaxation studies in the low salt loaded complexes. The polarisation arising from the trapping of ions at the crystalline interface. However at high salt loadings, in the absence of crystallinity an α'-relaxation was observed similar to that seen in poly(propylene glycol) complexes.

7.4 Poly(tetramethylene glycol/oxide) Complexes

Both low and high molecular weight poly(tetramethylene oxide) complexes with inorganic salt complexes have been prepared. The degree of crystallinity was found to influence the properties of the complexes markedly. No crystallinity however was observed in a low molecular weight poly(tetramethylene glycol) calcium thiocyanate complex at high salt loading. The high molecular weight equivalent however did show the presence of a crystalline phase.

The relatively small shifts in glass transition temperature upon complexation with respect to poly(propylene glycol) and poly(ethylene glycol) complexes indicated a much weaker interaction between the salt and the coordinating polymer. It was suggested that a weak ion-dipole interaction and complexes involving single oxygen coordination were responsible for the formation of poly(tetramethylene glycol) inorganic salt complexes.

As was observed in poly(ethylene glycol)complexes Maxwell-Wagner-Sillars type polarisations were believed to dominate the dielectric relaxations observed in poly(tetramethylene glycol) complexes.

7.5 Commercial Uses of Salt Complexes

Although clearly at an early stage in their development, salt complexes appear to have varied applications. Clearly the most developed area is as dielectric enhancers. It has been shown that insufficient improvement in the dielectric heating capability occurs upon blending into polymers that already are used in dielectric welding. Although future salt complexes may be developed to overcome this problem. It is clear however that salt complexes can be used to render polymers that

at present are incapable of being dielectrically heated into dielectrically weldable materials. Several companies have shown interest and performed trials to this end.

Other less well developed areas have been explored and it is clear that in areas such as solid electrolytes, salt complexes have an interesting future. Further development work is clearly required if salt complexes are to find outlets as capacitors or electrets.

REFERENCES

1 R.H. Norman: 'Conductive Rubbers and Plastics', Elsevier, Amsterdam, 1970.

2 G.M. Gale: 'Anti-Static Agents', RAPRA, Tech. Rev. No.43, 1968.

3 A. Blythe: 'Electrical Properties of Polymers', Cambridge University Press, London, 1979.

4 H. Shirakawa and S. Ikeda: Polymer J., 2, 231, (1971).

5 H.A. Pohl and E.H. Engelhardt: J. Phys. Chem., 66, 2085, (1962).

6 R.D. Hartman and R.D. Pohl: J.Polym.Sci.,A1-6 , 1135, (1968).

7 A.V. Topchiev: J.Polym.Sci., A1, 591, (1963).

8 S.B. Mainthia, P.L. Kronik, H. Uhr, E.F. Chapman and M.M. Labes: 144th Meeting Am.Chem.Soc., 11Q, Los Angeles (April 1963).

9 H. Inoue, K.Noda, T.Takiuchi and E. Imoto: Kogyo Kagaku Zasshi, 65, 1286, (1962).

10 D.S. Acker, R.J. Harder, W.R. Hertler, W.Mahler, L.R. Melby, R.E. Benson and W.E. Mochel: J.Am.Chem.Soc., 82, 6408, (1960).

11 M. Hatano, H. Nomori and S.Kambara: Polym.Prep., 5(2), 849, (1964).

12 J.H. Lupinski and K.D. Kopple: Science, 146, 1038, (1964).

13 P. Kathirgamanathan, S.A. Mucklejohn and D.R. Rosseinsky: J. Chem. Soc., Chem. Commun., 86, (1979).

14 P. Kathirgamanathan and D.R. Rosseinsky: J.Chem.Soc., Chem.Commun., 356, (1980).

15 P. Kathirgamanathan and D.R. Rosseinsky: J.Chem.Soc., Chem. Commun., 839, (1980).

16 M.J.S. Dewar and A.M. Talata: J.Am.Chem.Soc., 86, 1592, (1964).

17 F.A. Cotton and G. Wilkinson: 'Advanced Inorganic Chemistry', 2nd Ed., Wiley Interscience, New York, 1967.

18 S.F.A. Kettle: 'Coordination Compounds', Nelson, London, 1969.

19 R.P. Houghton: 'Metal Complexes in Organic Chemistry', Cambridge University Press, London, 1979.

20 A. Eisenberg and M. King: 'Ion-Containing Polymers', Academic Press, New York, 1977.

21 S.L. Davydova and N.A. Plate: Coord.Chem. Rev., 16, 195, (1975).

22 D.B. James, Ph.D. thesis, Loughborough University, 1977.

23 A.M. Rowe: Ph.D. Thesis, Loughborough University, 1982.

24 A. Eisenberg: 'Ions in Polymers', Advances in Chemistry, 187, Am. Chem. Soc., Washington, 1980.

25 C.J. Pederson; J.Am. Chem.Soc., 89, 7017, (1967).

26 C.J. Pederson: J.Am. Chem. Soc., 92, 391, (1970).

27 S. Kopolow, T.E. Hogen-Esch and J. Smid: Macromolecules, 4, 359, (1971).

28 S. Kopolow, Z. Machacek, U. Takaki and J. Smid: J. Macromol. Sci., Chem. 7, 1015, (1973).

29 S. Kopolow, T.E. Hogen-Esch and J. Smid: Macromolecules, 6, 133, (1973).

30 J. Dale and P.O. Kristiansen: Acta Chem. Scand., 26, 1471, (1972).

31 S. Alev, F. Schue and B. Kaempf : J.Polym. Sci.,Polym. Lett. Ed., 13, 397, (1975).

32 F.A.L. Anet, J. Krane, J. Dale, K. Dacisvatn and P.O. Kristiansen: Acta Chem. Scand., 27, 3395, (1973).

33 R.M. Izatt, D.P. Nelson, J.H. Rytling, B.L. Haymore and J.J. Christensen: J. Am., Chem., Soc., 93, 1619, (1971).

34 A.A. Blumberg, S.S. Pollack and C.A.J. Hoeve: J. Polym. Sci.,A2, 2499, (1964).

35 A.A. Blumberg and J. Wyatt: J. Polym. Sci., B4, 653, (1966).

36 R. Iwamoto, Y. Saito, H. Ishihara and H. Tadokoro: J. Polym. Sci., A2, 1509, (1968).

37 N. Yokoyama, H. Ishihara, R. Iwamoto and H. Tadokoro: Macromolecules, 2, 184, (1969).

38 R. Iwamoto: Bull. Chem. Soc. Japan, 46,1114, (1973).

39 D.E. Fenton, J.M. Parker and P.V. Wright: Polymer, 14, 589, (1973).

40 P.J. Wright: Br. Polym. J., 7, 319, (1975).

41 P.V. Wright: J. Polym. Sci., Polym. Phys. Ed., 14, 955, (1976).

42 C.C. Lee and P.V. Wright: Polymer, 23, 681, (1982).

43 M.B. Armand, J.M. Chabagno and M.J. Duclot: 'Fast Ion Transport in Solids', 131, Elsevier - North Holland, 1979.

44 R.F. Lundberg, F.E. Bailey and R.W. Callard: J. Polym. Sci., A1, 1563, (1966).

45 J. Moacanin and E.F. Cuddihy: J. Polym., Sci., C(14), 313, (1966).

46 R.E. Wetton, D.B. James and W. Whiting: J. Polym. Sci., Polym. Lett. Ed., 14, 577, (1976).

47 D.B. James, R.E. Wetton and D.S. Brown: Polymer, 20, 187, (1979).

48 P.G. Delduca, A.M.Y. Jaber, G.J. Moody and J.D.R. Thomas: J.Inorg. Nucl. Chem., 40, 187, (1978).

49 H. Cheradame,J.L.Souquet and J.M. Latour: Mat. Res. Bull., 15, 1173, (1980).

50 K.F. Wissbrun and M.J. Hannon: J. Polym. Sci., Polym. Phys. Ed., 13, 223, (1975).

51 F. Higashi, C.S. Cho, H. Kakinoki and O. Sumita: J. Polym. Sci., Polym. Chem. Ed., 17(2), 313, (1979).

52 P. Dunn and G.F. Sansom: J. Appl. Polym. Sci., 13, 1641, (1969).

53 P. Dunn and G.F. Sansom: J. Appl. Polym. Sci., 13, 1657, (1969).

54 P. Dunn and G.F. Sansom: J. Appl. Polym. Sci., 13, 1673, (1969).

55 P. Dunn and G.F. Sansom: J. Appl. Polym. Sci., 14, 1799, (1970).

56 R.D. Andrews, 2nd International Conference on Yield, Deformation and Fracture of Polymers, Cambridge, 26-29 March, 1973.

57 R.D. Andrews, B.H. Jhaveri and P.J. Rubin: Polym. Prep., 14(2), 1265, (1973).

58 A Ciferri, E. Bianchi, F. Macchese and A. Tealdi: Makromol.Chem., 150, 265, (1971).

59 B. Valenti, E. Bianchi, G. Greppi, A.Tealdi and A. Ciferri: J.Phys. Chem., 77, 389, (1973).

60 E. Bianchi, A.Ciferri, A. Tealdi, A Torre and B. Valenti: Macromolecules, 7, 495, (1975).

61 A. Frasci, E. Martuscelli and V. Vittoria:J.Polym.Sci., Polym. Lett. Ed., 9, 561, (1971).

62 D. Acierno, E. Bianchi, A.Ciferri, E. de Giudio, C.Magliaresi and L.Nicolais: J. Polym. Sci., Symp., 54, 259, (1976).

63 H.G. Kim and P.J. Harget: J. Appl. Phys., 50(10), 6072, (1979).

64 A. Siegmann and Z. Baraam: Makromol. Chem., Rapid Comm., 1, 113, (1980).

65 H. Kakinoki: J. Polym. Sci., Polym. Lett. Ed., 14, 407, (1976).

66 S. Reich and I. Michaeli: J. Polym. Sci., Polym. Phys.Ed., 13(1), (1975).

67 S. Reich, S. Raziel and I. Michaeli: J. Phys. Chem., 77, 1378, (1973).

68 R. Dewsberry: J. Phys., D.9, 2049, (1976).

69 H.G. Biedermann, E. Griesel and K. Wichmann: Makromol.Chem., 172, 49, (1973).

70 Y. Yurima, E. Tsuchida and M. Kuneka: J. Polym. Sci., A1(2), 3511, (1971).

71 H.G. Biedermann and K. Wichmann: Z. Naturforsch., B28,182, (1973).

72 E. Tsuchida, Y. Karino, H. Nishide and Y. Yarimura: Makromol. Chem., 175, 171, (1964).

73 H.G. Biedermann and P. Seidl: Makromol. Chem., 177, 631, (1976).

74 V.D. Kopylova, V.B. Kargman, K.M. Saldadze, A.I.Kokonin and L.N. Swvorova: Polym. Sci. USSR, 15(4), (1973).

75 N.H. Agnew: J. Polym. Sci., Polym. Chem. Ed., 14, 2819, (1976).

76 E.P. Otocka: J. Macromol. Sci., Revs. Macromol. Chem., C5, 275, (1971).

77 A. Eisenberg: J. Polym. Sci., Symposia, 45, 99, (1974).

78 R. Longworth and D.J. Vaughan: Nature, 218, 85, (1968).

79 W.J. MacKnight, W.P. Taggart and R.S. Stein: J. Polym. Sci., Symposia, 45, 113, (1974).

80 E.P. Otocka and T.K. Kwei: Macromolecules, 1, 244, (1968).

81 E.P. Otocka and T.K. Kwei: Macromolecules, 1, 401, (1968).

82 E.P. Otocka and D.D. Davis: Macromolecules, 2, 437, (1969).

83 F.C. Wilson, R. Longworth and D.J. Vaughan: Polym. Prep., 9, 505, (1968).

84 B.W. Delf and W.J. MacKnight: Macromolecules, 2, 309, (1969).

85 H.A. Davies, R. Longworth and D.J. Vaughan: Polym. Prep., 9, 515, (1968).

86 C.L. Marx, J.A. Koutsky and S.L. Cooper: J. Polym. Sci.,B9, 167, (1971).

87 R. Longworth and D.J. Vaughan: Polym. Prep., 9, 525, (1968).

88 W.J. MacKnight, T. Kajiyama and L. McKenna: Polym. Eng. Sci., 8, 267, (1968).

89 A.V. Tobolsky, P.F. Lyons and N. Mata: Macromolecules, 1, 515, (1968).

90 B.E. Read, E.A. Carter, T.M. Conner and W.J. MacKnight: Br. Polym. J., 1, 123, (1969).

91 A. Eisenberg: Macromolecules, 3, 147, (1970).

92 A. Eisenberg and M. Navratil: Macromolecules, 6, 604, (1973).

93 A. Eisenberg and M. Navratil: Macromolecules, 7, 84, (1974).

94 A. Eisenberg and M. Navratil: Macromolecules, 7, 90, (1974).

95 German Pat. 1068115 (1957), H.Hoegl, O. Sus, W. Neugabauer (Chem. Abs., 55, 20742a, (1961).

96 U.S. Pat. 3 162532, (1957), H. Hoegl and W. Neugabauer.

97 German Pat. 1233265, (1967), P.M. Cassiers, J.M. Nyss, R.M. Hart and J.S. Williams.

98 Japan Pat. 4-17907, (1967), K. Morimoto and A. Inami.

99 R.M. Schaffert: IBM J. Res. Develop., 43, 4108, (1971).

100 S.E. Cummins and T.E. Luke: I.E.E.E. Trans. Electron. Devices, E918, 761, (1971).

101 K. Shigahara, M. Nishimura and E.Tsuchida: Bull. Chem. Soc. Japan, 50, 3397, (1977).

102 M. Yoshida and I. Oshida: Oyobutsuri, 33, 34, (1964).

103 G. van der Veen and W.Prins : Nat. Phys. Sci., 70, 230, (1971).

104 C.K. Chiang, S.C. Gau, C.R. Fincher Jr., Y.W. Park, A.G. Macdiarmid and A.J. Heeger: Appl. Phys. Lett., 33, 18, (1978).

105 H. Shirakawa and S. Ikeda: Kobunshi, 28, 369, (1979).

106 E. Berman and P. Wildes, 4th Internat. Conf. Photochem. Conversion and Storage of Solar Energy, p. 43, (1982).

107 M. Kaneko, A. Yamada and A. Kurimura: Inorg. Chim. Acta, 44, L289, (1980) and Inorg. Chim. Acta, 45, L73, (1980).

108 M. Kaneko, M. Ochiai and A. Yamada: Makromol. Chem., Rapid Commun., 3, 299, (1982).

109 N. Oyama, S. Yamaguchi, M. Kaneko and A. Yamada: J. Electroanal. Chem., 139, 215, (1982).

110 I. Litant: Design and Compts. in Eng., 22, 10, (1966).

111 British Plastics, 37, 673, (1964).

112 Netherlands Pat. 6, 510, 986, (1966), General Electric Co. (Chem. Abs. 65, 7382e, (1966)).

113 D.Macinnes Jr., M.A. Druy, P.S. Nigrey, D.P. Nairns, A.G.Macdiarmid and A.J. Heeger: J. Chem. Soc., Chem. Commun., 317, (1981).

114 C.A. Vincent: New Scientist, 1403, 36, (1984).

115 Japan Pat. 7427, 570, (1974), S. Suzuki, H. Iwabori and F. Tamura, (Chem. Abs., 81, 128771s, (1974)).

116 F. Higashi, C.S. Cho and H. Kakinoki: ibid 15, 2303, (1977).

117 F. Higashi, C.S. Cho and H. Kakinoki: J. Polym. Sci., Polym. Chem. Ed., 17, 313, (1979).

118 M. Mutter and E. Bayer: Chem. Technol., C, (1981).

119 H.S. Makowski and R.D. Lundberg: 'Ions in Polymers', Ed. A. Eisenberg, Am. Chem. Soc., 37, (1980).

120 R.D. Lundberg: Polym. Prep., Am. Chem. Soc. Div. Polym. Chem., 19(1), 455, (1978).

121 H.S. Makowski, R.D. Lundberg and G.S. Singhal: U.S. Patent 3870841, 1975 to Exxon Research and Eng. Co.

122 F. Bueche:'Physical Properties of Polymers', Interscience, New York, 1962.

123 P.J. Flory: 'Principles of Polymer Chemistry', Cornell University Press, Ithaca, 1953.

124 V.A. Kargin, A.I. Kitaigorodskii and G.L. Slonomskii: Kolloid Z, 19, 131, (1957).

125 G.S. Yeh: J. Macromol. Sci. Phys., B6, 465, (1972).

126 G. Allen, S.E.B. Petrie, Eds.: J. Macromol. Sci. Phys., B12, 1 and 2, (1972)'Symposium on the Physical Structure of the Amorphous State'.

127 W. Kauzman: Chem. Revs., 43, 219, (1948).

128 T.G. Fox and P.J. Flory: J. Appl. Phys., 21, 581, (1950).

129 J.H. Gibbs: J. Chem. Phys., 25, 185, (1956).

130 J.H. Gibbs and E.A. di Marzio: J. Chem. Phys., 28, 373, (1958).

131 E.A. di Marzio and J.H. Gibbs: J. Chem. Phys., 28, 807, (1958).

132 E.A. di Marzio and J.H. Gibbs: J. Polym. Sci., 40, 121, (1959).

133 E.A. di Marzio and J.H. Gibbs: J. Polym. Sci., A1, 1417, (1963).

134 E.A. di Marzio: J. Res. Nat. Bur. Std. U.S., 68A, 611, (1964).

135 G. Adam and J.H. Gibbs: J. Chem. Phys., 43, 139, (1965).

136 E.A. di Marzio, J.H. Gibbs, P.D. Fleming (III) and I.C. Sanchez: Macromolecules, 9, 763, (1976).

137 A.K. Doolittle: J. Appl. Phys., 22(12), 1471, (1951).

138 A.K. Doolittle: J. Appl. Phys., 23(2), 236, (1952).

139 M.L. Williams, R.F. Landel and J.D. Ferry: J. Am. Chem. Soc., 77, 3701, (1955).

140 L.E. Nielson: J. Macromol. Sci. Revs., Macromol. Chem., C3(1), 69, (1969).

141 L.E. Nielsen: 'Mechanical Properties of Polymers and Composites', Vol. 1, Marcel Dekker, New York, 1974.

142 T.G. Fox: Bull. Am. Phys. Soc., 1, 123, (1956).

143 M. Gordon and J.S. Taylor: J. Appl. Chem., 2, 493, (1952).

144 L.A. Wood: J. Polym. Sci., 28, 319, (1958).

145 K.A. Illers: Kolloid Z., 190, 16, (1963).

146 G. Kanig: Kolloid Z., 190, 1, (1963).

147 N.W. Johnson: J. Macromol. Sci.,Rev. Macromol. Chem., C14(2), 215, (1976).

148 J.A. Manson and L.H. Sperling: 'Polymer Blends and Composites', Plenum Press, New York, 1976.

149 R.F. Landel: Trans. Soc. Rheology, 2, 53, (1958).

150 C.A. Kumins and J. Roteman: J. Polym. Sci., A1, 527, (1963).

151 C.T. Moynihan, L.P. Boesch and N.L. Laberge: Phys. Chem. Glasses, 14(6), 122, (1973).

152 A.A. Bakr and A.M. North: Eur. Polym. J., 13, 799, (1977).

153 P. Debye: 'Polar Molecules', The Chemical Catalog Co. Inc., Dover Publications, 1929.

154 R.A. Davies and J. Lamb: Quart. Revs., 11, 134, (1957).

155 K.S. Cole and R.H. Cole: J. Chem. Phys., 9, 341, (1941).

156 R.M. Fuoss and J.G. Kirkwood: J. Am. Chem. Soc., 63, 385, (1941).

157 N.G. McCrum, B.E. Read and G. Williams: 'Anelastic and Dielectric Effects in Polymeric Solids', Wiley, London, 1967.

158 R.E.,Wetton and G. Allen: Polymer, 7, 331, (1966).

159 D.W. Davidson and R.H. Cole: J. Chem. Phys., 18, 1417, (1950).

160 D.W. Davidson and R.H. Cole: J. Chem. Phys., 19, 1484, (1951).

161 D.W. Davidson: Can. J. Chem., 39, 571, (1961).

162 G. Williams and D.C. Watts: Trans. Faraday Soc., 66, 80, (1970).

163 G. Williams, D.C. Watts, S.B. Dev and A.M. North: Trans. Faraday Soc., 67, 1323, (1971).

164 F.A. Grant: J. Appl. Phys., 29(1), 76, (1958).

165 S. Glasstone, K.J. Laidler and H. Eyring: 'Theory of Rate Processes', McGraw-Hill, New York, (1941).

166 J.J. Aklonis, W.J. MacKnight and M. Shen: 'Introduction to Polymer Viscoelasticity', Wiley-Interscience, New York, 1972.

167 H. Leaderman: 'Elastic and Creep Properties of Filamentous Materials and Other High Polymers', Textile Foundation, Washington.

168 K.C. Rusch: J. Macromol. Sci, Phys., B2(2), 179, (1968).

169 N.G. McCrum and E.L. Morris: Proc. Roy. Soc., A281, 258, (1964).

170 L. Onsager: J. Am. Chem. Soc., 58, 1486, (1936).

171 J.G. Kirkwood: J. Chem. Phys., 7, 911, (1939).

172 H. Fröhlich: 'Theory of Dielectrics', Oxford University Press, London, 1958.

173 K. Deutsch, A.W. Hoff and W. Reddish: J. Polym. Sci., 13, 565, (1954).

174 T. Schatzki: J. Polym. Sci., 57, 496, (1962).

175 N. Saito, K. Okano, S. Iwayangi and T. Hideshema, in 'Solid State Physics', Eds. F. Seitz and D. Turnbull, 14, 343, Academic Press, New York, 1963.

176 E.A.W. Hoff, D.W. Robinson and A.H. Willbourn: J. Polym. Sci., 18, 161, (1955).

177 J.C. Maxwell: 'Electricity and Magnetism', Clarendon Press, Oxford, 1892.

178 K.W. Wagner: Arch. Elektrotechn., 2, 271, (1914).

179 R.W. Sillars: Proc. Roy. Soc., A169, 66, (1939).

180 L.K.H. Van Beek: Prog. Dielectrics, 7, 69, (1967).

181 B.V. Hamon: Aust. J. Phys., 6, 304, (1953).

182 M.R. Wertheimer, L. Paquin and H.P. Schreiber: J. Appl. Polym. Sci., 20, 2675, (1976).

183 H.P. Schwan, G. Schwarz, J. Maczuk and H. Pauly; J. Phys. Chem., 66, 2626, (1962).

184 G. Schwarz: J. Phys. Chem., 66, 2636, (1962).

185 A.S. Michael, G.L. Falkenstein and N.S. Schneider: J. Phys. Chem., 69(6), 1456, (1965).

186 P. Rosen and H.A. Pohl: J. Polym. Sci., A1 4, 1135, (1966).

187 C.J. Norrell, H.A. Pohl, M Thomas and K. Berlin: J. Polym. Sci., Polym. Phys. Ed., 12, 913, (1974).

188 M.E. Baird: 'Electrical Properties of Polymeric Materials', The Plastics Institute, London, 1973.

189 F. Gutman and L.E. Lyons: 'Organic Semi-Conductors', Wiley, London, 1967.

190 N.F. Mott: Adv. Phys., 16, 49, (1967).

191 M. Pollack: Proc. Int. Conf. Phys. Semiconductors, 86, I.P.P.S., London, 1962.

192 D.A. Seanor: J. Polym. Sci., A2 6, 463, (1968).

193 A. Reiser, M.W.B. Lock and J. Knight: Trans. Faraday Soc., 65, 2168, (1964).

194 J.F. Fowler: Proc. Roy. Soc., A236, 464, (1956).

195 L.F. Amborski: J. Polym. Sci., 62, 331, (1962).

196 F.S. Smith and C. Scott: Brit. J. Appl. Phys., 17, 1149, (1966).

197 M. Hatano, S. Kambra and S. Okamato: J. Polym. Sci., 51, 26, (1961).

198 R.W. Warfield and M.C. Petree: Die Macromol. Chem., 58, 139, (1962).

199 R.M. Black and A. Charlesby: 'Progress in Dielectrics', 2, 77, Heywood, London, 1960.

200 J.F. Fowler and F.T. Farmer: Nature, 171, 1020, (1953).

201 R.E. Barker and C.R. Thomas: J. Appl. Phys., 35, 3203, (1964).

202 B. Rosenberg: J. Chem. Phys., 36, 816, (1962).

203 D.D. Eley and R.B. Leslie: Adv. Chem. Phys., 7, 238, (1964).

204 G.S. Fielding-Russell: Ph.D. thesis, Loughborough University, 1967.

205 L. Hartshorn and W.H. Ward: J. Inst.Elec.Eng., 79, 597, (1936).

206a M. Navier: Mem. de l'Aced.de Sci., 6, 389, (1827).

206b G.G. Stokes: Trans. Cambr. Phil. Soc., 8, 287, (1845).

207 K. Varadarajan and F. Boyer: Polymer, 23, 314, (1982).

208 A.E. Binks and A. Sharples: J. Polym. Sci., A2(6), 407, (1968).

209 E.P. Otocka and F.R. Eirich: J. Polym. Sci., A-2, 6, 921, (1968).

210 H. Matsuura and A. Eisenberg: J. Polym. Sci., Polym. Phys. Ed., 14, 1201, (1976).

211 T. Tsutsui and T. Tanaka: Polymer, 18, 817, (1977).

212 M.J. Hannon and K.F. Wissbrun: J. Polym. Sci., Polym. Phys. Ed., 13, 113, (1975).

213 J.J. Aklonis, W.J. MacKnight and M. Shen: 'Introduction to Polymer Viscoelasticity', Wiley-Interscience, New York, 1972.

214 J.R. Fried, F.E. Karasz and W.J. MacKnight: Macromolecules, 11, 150, (1978).

215 P. Mason: Polymer, 5, 625, (1964).

216 J. Padova: Bull. Res. Counc. Lsr, A10, 63, (1961).

217 P.J. Flory: J. Am. Chem. Soc., 61, 1518, (1939).

218 J.M. Parker, P.V. Wright and C.C. Lee: Polymer, 22, 1305, (1981).

219 G. Weber, W. Saenger, F. Vogtle and H. Sieger: Angew. Chem., 18, 226, (1979).

220 J.W. Evans, D.K. Hoffman and D.R. Burgess: J. Chem. Phys., 80(2), 936, (1984).

221 K.M. Mackay and R.A. Mackay: 'Introduction to Modern Inorganic Chemistry', Intertext Books, London, 1968.

222 M.E. Bauer and W.H. Stockmayer: J. Chem. Phys., 43, 4319, (1965).

223 G. Williams: Trans. Faraday Soc., 62, 2091, (1966).

224 P.J. Phillips and W.J. MacKnight: J. Polym. Sci., A2, 8, 727, (1970).

225 S. Glasstone and K.J. Laidler: 'The Theory of Rate Processes', McGraw-Hill, New York, 1941.

226 R.E. Wetton and G. Williams: Trans. Faraday Soc., 61, 2132, (1965).

227 K. Yamafugi and Y. Ishida: Kolloid Z., 183, 15, (1962).

228 T.M. Conner, B.E. Read and G. Williams: J. Appl. Chem., 14, 74, (1964).

229 M.C. Lang, C. Noel and A.P. Legrand: J. Polym. Sci., Polym. Phys. Ed., 15, 1319, (1977).

230 K. Arisawa, K. Tsuge and Y. Wada: Jap. J. Appl. Phys., 4, 138, (1965).

231 G. Williams: Trans. Faraday Soc., 61, 1564, (1965).